UNIVERSITY OF SOUTHAMPTON

Faculty of Engineering and Physical Sciences

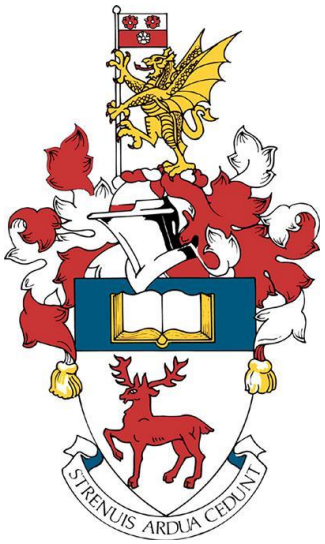

INVESTIGATION INTO DYNAMIC MEMBRANES AND INTEGRATION WITH ANAEROBIC BIOREACTORS

by

Aminu Yakubu

Thesis submitted for the degree of Doctor of Philosophy

September 2019

Supervisors: Prof. Sonia Heaven & Prof. Charles Banks

UNIVERSITY OF SOUTHAMPTON

ABSTRACT

FACULTY OF ENGINEERING AND PHYSICAL SCIENCES

Water and Environmental Engineering Research Group

Doctor of Philosophy

INVESTIGATION INTO DYNAMIC MEMBRANES AND INTEGRATION WITH ANAEROBIC BIOREACTORS

Aminu Yakubu

Dynamic Membranes (DM) are considered as low-cost alternatives to conventional membranes and offer the possibility of higher flux and lower resistance when carefully applied. The development of this technique was investigated under batch, semi-continuous and continuous studies. Given the variety of materials that could form the support for DM, three potential materials of same pore size but different make were trialled.

Batch trials was set up to test the materials before selection of the nylon mesh as the material of choice based on resistance and permeate turbidity.

Subsequent investigations on nylon mesh established the limit for substrate TSS concentration (< 5g TSS L^{-1}), below which changes in TMP could be kept low. Tests were carried out using the two modes of operation: Constant flux and constant pressure (gravity - induced flow). In constant flux operation, the TMP rose significantly when the substrate TSS reached 5 g L^{-1}. For constant TMP operation, the flux level did not significantly improve with increased head, indicating that cake layer resistance was the dominant mechanism for DM filtration.

Semi-continuous tests explored the possibility of pre-forming the DM under set conditions using a range of flux from 5 to 15 L m^{-2} h^{-1}, and despite the longer time it took for the DM to form at the lowest flux, it was observed that lower formation flux resulted in stable filtration performance and solids retention, and permeate turbidity was similar in all cases.

Long term studies for the integration of DM with functional anaerobic digesters was carried out by setting up AF digesters and granular digesters for the treatment of tomato wastewater and an external DM for the polishing of the effluent solids. Flux values of around 20 L m^{-2} h^{-1} was achieved, whereas the permeate turbidity was generally less than 40 NTU although periods of instability resulted in higher permeate turbidities. The digestate type was shown to influence on DM structure and performance even in an external configuration.

Keywords: Dynamic Membranes, Flux, Transmembrane Pressure, Turbidity, tomatoes wastewater.

List of figures

List of Tables

DECLARATION OF AUTHORSHIP

I, Aminu Yakubu, declare that this thesis and the work presented in it are my own and have been generated by me as the result of my own original research.

'Investigation into Dynamic Membranes and Integration with Anaerobic Bioreactors'

I confirm that:

1. This work was done wholly or mainly while in candidature for a research degree at this University;
2. Where any part of this thesis has previously been submitted for a degree or any other qualification at this University or any other institution, this has been clearly stated;
3. Where I have consulted the published work of others, this is always clearly attributed;
4. Where I have quoted from the work of others, the source is always given. With the exception of such quotations, this thesis is entirely my own work;
5. I have acknowledged all main sources of help;
6. Where the thesis is based on work done by myself jointly with others, I have made clear exactly what was done by others and what I have contributed myself;
7. Parts of this work have been presented as:

    - BBSRC AD-Net. Early Career Researcher Conference (29th June 2015) – Poster Presentation

    - BBSRC AD-Net. Early Career Researcher Conference (05th July 2016) – Oral Presentation

    - BBSRC AD-Net. Early Career Researcher Conference (03rd July 2017) – Oral Presentation

    - BBSRC AD-Net. Early Career Researcher Conference (16th July 2018) – Poster presentation

Signed:

Date: 16th September 2019

Acknowledgement

I will like to express my sincere gratitude to my supervisors: Professor Sonia Heaven and Professor Charles Bank for their support, advice and constructive feedback. I am especially thankful to Professor Sonia Heaven for her constant encouragement and for her support during trying times.

I will like to thank the laboratory support of Dr Dominic Mann and Pilar Pascual-Hidalgo who were always available to advice and help on numerous occasions when things appeared to be falling apart in the laboratory.

I am especially grateful to my sponsors; the Petroleum Technology Development Fund, Nigeria for providing me with scholarship and financial support to enable me carry out this PhD research.

I thank members of the research group of Water and Environmental Engineering Group for the sense of camaraderie- special mention to Alba Serna-Maza, Dhivya Puri, Simone Cinquepalmi, Santiago Pacheco Ruiz and Pakpong Sriprasert.

Thanks also to Angie Bywater and Dr Louise Byfield of ADNet for their support with research workshops and conferences.

Finally, my appreciation to my family and friends in Nigeria and beyond, and especially Salmah, for all the love and support.

Definitions and Abbreviations

AF	Anaerobic Filter
AF-DM	Anaerobic Filter-Dynamic Membrane
AnDMBR	Anaerobic Dynamic Membrane Bioreactor
AnMBR	Anaerobic Membrane Bioreactor
COD	Chemical Oxygen Demand
CSTR	Continuously Stirred Tank Reactor
DM	Dynamic Membrane
DMBR	Dynamic Membrane Bioreactor
EGSB	Expanded Granular Suspended Bed
EPS	Extracellular Polymeric Substances
GD-DM	Granular Digester-Dynamic Membrane
IA	Intermediate Alkalinity
MCRT	Mean Cell Residence Time
MF	Microfiltration
MLSS	Mixed Liquor Suspended Solids
NTU	Nephelometric Turbidity Unit
OLR	Organic Loading Rate
PA	Partial Alkalinity
PSA	Particle Size Analysis
PSD	Particle Size Distribution
SEM	Scanning Electron Microscopy
SFDM	Self-forming Dynamic Membrane

TA	Total Alkalinity
TAN	Total Ammonia Nitrogen
TMP	Transmembrane Pressure
TOC	Total Organic Carbon
TS	Total Solids
TSS	Total Suspended Solids
UASB	Upflow Anaerobic Sludge Blanket
VFA	Volatile Fatty Acids
VS	Volatile Solids
VMP	Volumetric Methane Production

Chapter 1: Introduction

The treatment and re-use of wastewaters from all sources presents a critical task for Engineers and Scientists seeking to apply novel concepts to alleviate cost and carbon foot print. This research interest is driven by increased pressure on freshwater sources and concerns on public health and aquatic life, due to discharge from industrial sources.

Water, as a critical resource, requires a significant amount of global energy demand for its production, discharge, treatment and reuse, with electricity demand for wastewater treatment predicted to reach 60% in 2040 compared to 2014 (OECD/IEA, 2016). Therefore, effective management is a key element towards preserving this important resource. The concept of the 'water-energy nexus' has gained attention in recent times due to the increased usage related to population growth and industrial activity. The interdependence between water resources and the industrial activity required for societal growth and development places pressure on the environment. Thus, there is a need to strike a balance between sustainable industrial development and the cost of its application.

The re-use of treated wastewater (via its direct application or discharge to receiving bodies) offers a very attractive option for sustainable resource management. This is because treated wastewater is a resource that is less dependent than freshwater supplies are upon seasonable variation or climatic anomalies, and could alleviate the pressure on natural water bodies, leading to improved environmental conditions. For instance, the EU uses only 2.4% of its treated effluents and less than 0.5% of annual freshwater withdrawals (EC, 2018)

Application of filtration technologies for water treatment offers the chance for lower footprints per unit of product, based on the pore size of the filter media, with the target contaminant size being the deciding factor. For wastewater treatment and discharge, conventional microporous membranes of pore sizes less than 0.1 µm are widely applied and research has largely focused on improving performance and reducing the energy demand required to drive the filtration process.

The main challenge involved in applying membranes in wastewater treatment is due to the impact of fouling, which even in the most efficient systems, necessitates an increased energy cost of at least 1 kWh m^{-3} of treated product, and rising in some cases to 10 kWh m^{-3}. This is significantly higher than the typical energy cost of between 0.3 and 0.6 kWh m^{-3} required by

conventional activated sludge treatment systems (Le-Clech et al., 2006, Tchobanoglous et al., 2003). It must be noted that a wide range of values of energy demand for membrane applications have been estimated by researchers (Liao et al., 2006, Martin et al., 2011) depending on the mode and conditions of operation employed. Given recent advances in materials and process technologies, there is a consensus that despite inherent benefits, it is still higher than treatment methods using other high rate reactors. Therefore, new materials, efficient means of controlling fouling, while achieving reasonable effluent quality, are required in order to realise the full potential that application of filtration technologies to wastewater treatment provides.

Since its first successful trial in 1978 by Grethlein and subsequent commercialisation by Dorr-Oliver (Stazi and Tomei, 2018), the use of membrane technology has proven to be a significant advancement in the treatment of wastewaters from municipal and industrial sources. The underlying principle for this and other ''high rate digesters'' is the formation and retention of the slow-growing biomass in the digester enabling increased biological activity; improved treatment quality given small footprint is also a major benefit (Stephenson, 2000, Liao et al., 2006). When used in an anaerobic system, the ability to generate energy while meeting the increasingly strict discharge standards required remains a key attraction. The conventional concept is to use microfiltration materials of pore sizes less than 0.5 μm, but while these have proven to be useful, the capital and recurrent cost of maintenance is a cause for concern (Chang et al., 2001). This is due to the propensity for fouling and the need for cleaning, maintenance, and replacement, which has led to much research in this area. Though there are several methods of cleaning membranes, there is little doubt that this contributes significantly to the overall cost of the membrane filtration process. This has made the application of membrane filtration for wastewater treatment challenging.

Anaerobic Membrane Reactors (AnMBR) incorporate membrane technology into the anaerobic digestion process. The replacement of a clarification tank with a membrane separation unit offers distinct advantages in space requirements and better effluent quality (van 't Oever, 2005). High rate bioreactors such as the Upflow Anaerobic Sludge Blanket (UASB), Expanded Granular Sludge Blanket (EGSB), Anaerobic Filter (AF) and Fluidised Bed (FB) reactors promote biomass retention by encouraging granulation of the biomass or attachment to support surfaces (Liao et al., 2006, Beaubien et al., 1996). Even though these

approaches prevent washout of biomass, complete separation and retention is not guaranteed. The AnMBR prevents the loss of biomass by ensuring complete decoupling of the Solids Retention Time (SRT) and the Hydraulic Retention Time (HRT), necessary for enhanced biodegradation of organic matter by typically slow-growing microbes thereby shortening the HRT. While this offers better performance in terms of quality of effluent, the cost of cleaning and energy demands must be taken into account. A recent survey carried out by Judd (2015) in respect of industrial membrane applications stated that the biggest technical challenges faced by suppliers and academic researchers alike were membrane surface fouling (16%) and screening/pre-treatment (16%). To give a specific example, the cost of cleaning (via aeration alone) for a pilot membrane bioreactor (MBR) plant contributed around 50% of the total operational cost (Gil et al., 2010).

The Dynamic Membrane (DM) employs the use of a more porous support with nominal pore size greater than 10 µm, such as a mesh of suitable fabric (e.g. nylon, polyester; woven, non-woven) for building a secondary layer which serves as a filter for the wastewater prior to the primary membrane (Kiso et al., 2000, Kuberkar and Davis, 2000). In this way the support material will be preserved. The secondary layer, also referred to as the cake layer, is of critical importance for the formation of the DM as it contributes to the filtration capability, resistance and hence energy required for filtration. In terms of cost and availability, the DM can be significantly less than conventional membranes and rather than depending on specialist companies for the membrane filtration equipment, the support meshes, and frames can be assembled using locally available materials. In addition, maintenance and cleaning of the mesh can be easily achieved, making its use and re-use more feasible.

Microfiltration has found successful applications in several industrial and domestic processes including wastewater treatment, from sources as diverse as food industry (Katayon et al., 2004), petrochemicals (Khaing et al., 2010), textiles (Badani et al., 2005), pharmaceuticals (Shariati et al., 2010) and landfill leachate (Alvarez-Vazquez et al., 2004).

1.1 Industrial wastewater characteristics and treatment

Industrial processes such as food processing, textile, pulp and paper processing, chemical processing, and other manufacturing processes require copious amounts of water and generate almost equally large quantities of effluents containing organic matter and other pollutants measurable by parameters such as Chemical Oxygen Demand (COD), Biochemical

Oxygen Demand (BOD), Suspended solids (SS), Turbidity, Colour, etc. Depending on the process, industrial wastewaters may contain more than 1000 mg COD L^{-1}. This is higher than municipal wastewaters that generally present around 200-800 mg COD L^{-1} (Lin et al., 2012). The implication is that industrial wastewaters provide a higher potential for energy recovery and if left untreated have a greater impact on the environment. For food processing wastewaters, AnMBRs have been have been successfully applied for such processes as dairy production (Farizoglu and Uzuner, 2011), brewery wastewater (Chen et al., 2016) and meat processing (Galib et al., 2016).

1.2 Treatment of tomato-based wastewaters

Tomato is grown almost worldwide and, in economic terms, is considered to be the fourth most viable food crop in low and middle income economies-with the top three being rice, sugarcane and wheat (Schreinemachers et al., 2018)

A large proportion of produced tomatoes are further processed into tomato juice and other useful tomato-based products such as paste, ketchup, soups and sauces (Gould, 1992). Tomato juices can be produced via thermal or non-thermal processing. One of the targets during production of tomato juice is to keep the organic contents in suspension for the shelf life of the products to ensure consistency in colour (Hsu, 2008). These organic contents are largely derived from intact and broken or crushed cells, cell fragments, and long-chain polymers of lignin, cellulose, hemicellulose, and water-insoluble pectic materials (Barrett et al., 1998, Jabbari et al., 2018).

Production of such items results in the generation of copious amounts of highly polluting and brightly-coloured wastewaters (Iaquinta et al., 2009, Iaquinta et al., 2006). A significant contribution to the wastewater is due to the washing and juicing process with typical strength of between 1200 to 1500 g COD L^{-1}. The treatment of tomato-based wastewater is particularly challenging as it is acidic (pH around 4-5) and of low alkalinity (Gohil and Nakhla, 2006) and contains high particulate and colloidal fractions. In addition, wastewaters derived from tomato processing are deficient in soluble nutrients, and they also have very poor settling properties (Xu et al., 2006)

Despite the economic importance of the industry, studies on treatment options for wastewaters derived from tomato-processing are very limited and have been restricted to

some physical treatments, e.g. nanofiltration (Iaquinta et.al, 2008), or biological treatment (combination of UASB-aerobic treatment (Xu and Nahla, 2006). It is therefore essential to seek a method for treating such wastewaters while exploring the potential for treatment technologies that offer robust and simplified application at a relatively lower cost.

The applicability of such process (anaerobic digester combined with DM) for the treatment of tomato-based wastewater shows that the scope of such treatment process can be expanded to treat other types of wastewaters that usually pose challenges using stand-alone anaerobic processes. Such types of wastewaters include fruit processing, tannery and brewery wastewaters for which conventional membranes were applied (Batstone and Keller, 2001). In conclusion, the incorporated DM can be applied to any biological wastewater treatment handling flocculant biomass or high TSS substrate aiding in there capture and reducing the otherwise long HRT required for improved performance, while also improving the quality of the effluent generated.

1.3 Schematic of the overall contents of this study

A graphical abstract of the basis and contents of this research thesis is presented in Figure 1.1. This is to serve as a representative guide to the structure of the thesis. Chapters 1 and 3 which provide a general introduction to the subject and a detailed methodology respectively, are not captured in this abstract.

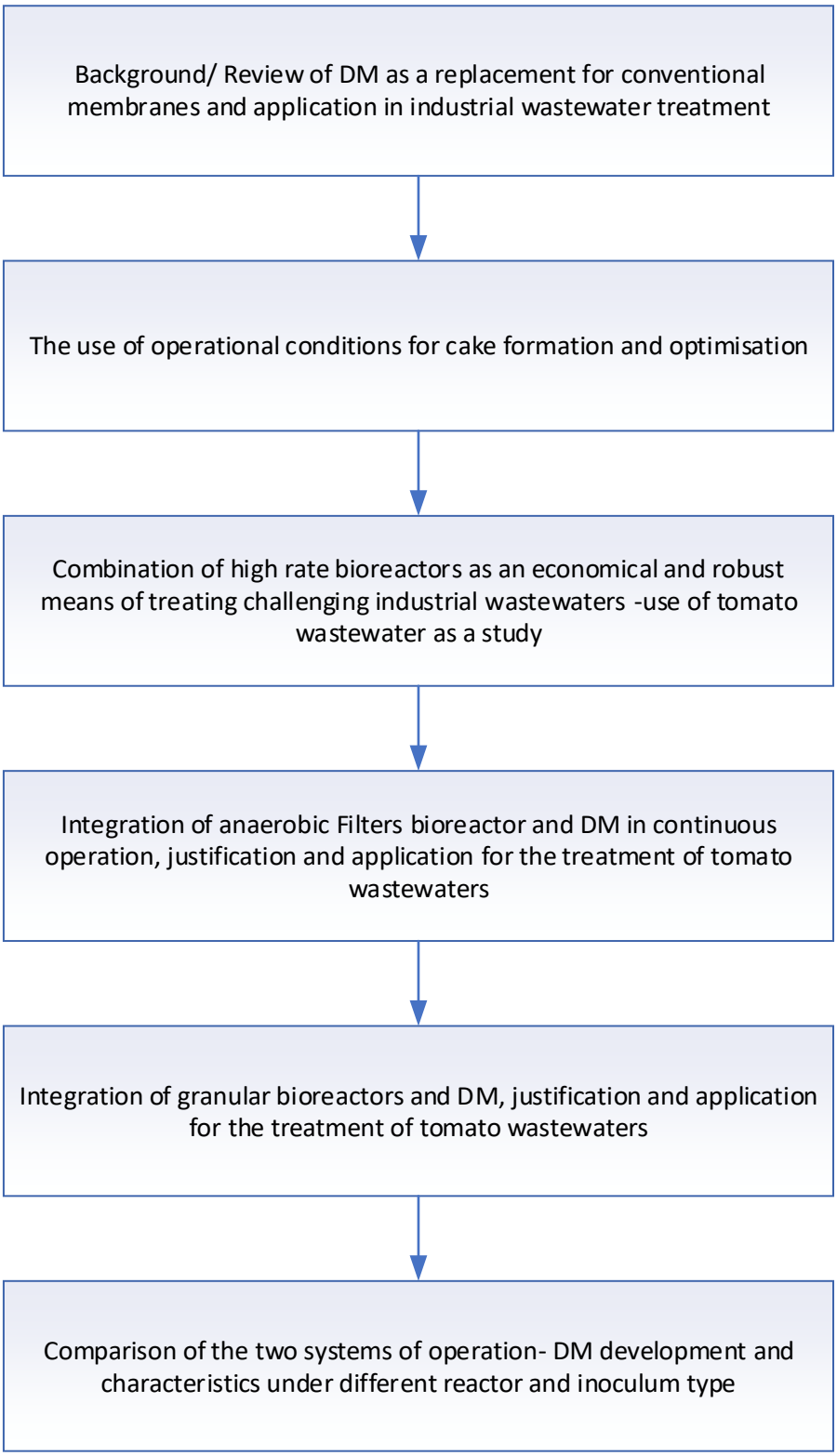

Figure 1-1: Schematic representation of the contents of this thesis

(Chapters 1 and 3 are excluded as they deal with general introduction and methods respectively)

1.4 Application of filtration techniques in wastewater treatment

Many factors affect fouling in membranes and while these factors are connected, an understanding of individual contributions is hard to establish due to the complexity of the substrates and processes involved. Fouling is attributable to a combination of soluble organics, colloidal particles, cell matter and inorganic precipitates (Stuckey, 2012). Pore plugging, which is fouling that occurs within the pores of membrane structures, and blinding or deposition of substances on the surface of the membrane are distinguishable from the clogging of the membrane cause by poor hydrodynamic condition (Judd, 2010). According to Zhang et al. (2006), fouling as indicated by rise in transmembrane pressure (TMP) occurs in three stages: an abrupt TMP rise, prolonged slow rise TMP and finally a sudden TMP rise. In industrial and municipal wastewater applications, membrane fouling is inevitable, but with the right approach and consideration for the maintenance, it can be minimised and coped with. Several research articles have explored different means of reducing fouling in membrane processes ranging from hydrodynamics (Tardieu et al., 1998, Böhm et al., 2012) to using additives and enhancers (Iversen et al., 2009, Ji et al., 2008, Iorhemen et al., 2017).

Efficient use of energy is also critical to improve the overall energy balance of the system because the applied energy required to control membrane fouling is usually not well utilised. For example Drews (2010), discovered that only about 10% of the energy used for the mitigation of fouling is used optimally in a pilot plant analysed. Therefore, it is necessary to investigate the means to bridge the gap between energy utilisation and efficiency.

Chapter 2: Literature Review

2.1 Anaerobic wastewater treatment

Anaerobic treatment of wastewaters from domestic, municipal and industrial sources enables the degradation of organic contents and offers several benefits: production of energy in the form of methane-rich biogas, low sludge production and potential for deployment within reasonably low footprints (Lettinga, 1995). The challenge of seeking ways to enhance the retention and conditions of the slow-growing biomass has led to an evolution of research and design applications. Anaerobic digestion consists of four identifiable phases namely hydrolysis, acidogenesis, acetogenesis and methanogenesis (Figure 2-1) which can be engineered for the treatment of various types of wastewaters. Also, the increasingly stringent discharge qualities required by state regulations as well as ever-present space and time constraints impose an additional treatment cost on new and available treatment technologies capable of achieving target objectives. Membranes generally ensure that these constraints are ameliorated by ensuring the retention of biomass and improving discharge standards compared to other treatment processes. Although the capital cost of membranes has been decreasing over the past decades (Le-Clech et al., 2006), this still represents a major investment cost, while the operational expenses also remain a cause for concern.

These concerns lead to the application of membranes to anaerobic wastewater treatment in order to improve, amongst other things, the concentration of the sensitive biomass and the quality of the discharge to the environment.

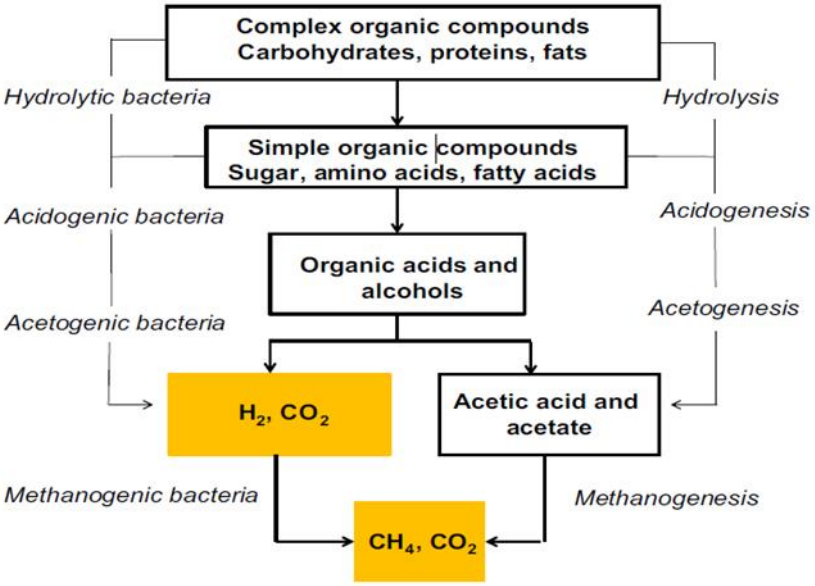

Figure 2-1: Anaerobic degradation of organic matter showing the stages/products of conversion adapted from Buonomenna and Bae (2015)

2.2 Membrane filtration and the critical flux concept

Filtration is the separation of a mixture of solid particles in a liquid medium across an interface based on size exclusion. This is driven by a pressure difference across both sides of the membrane filter. This pressure difference forces liquid across the membrane and the cake layer, if formed (Foley, 2006). There is a direct correlation between the increase in thickness of the cake layer and the required pressure for a given volume of filtrate. Field et al. (1995) put forward the concept of critical flux is such that there is a value of flux below which a reduction in flux with time does not occur and above this level, fouling will occur. The relationship between flux and pressure in terms of modelling filtration resistance is as shown in Equation 2.1:

$$J = \frac{\Delta P}{\mu(Rm+\alpha m)} \qquad \text{(Equation 2.1)}$$

Where J is the membrane flux in L m^{-2} h^{-1}, ΔP is change in pressure (Pa), μ is the viscosity of the fluid (Pa s), Rm is the membrane resistance (m^{-1}), α is the specific cake resistance (m kg^{-1}) and m is the mass of cake per unit membrane area (kg m^{-2}).

For the filtration process, a resistance in series model approach is required to understand the contribution of the various components to the filtration process. This resistance in series model can be represented by equation 2.2

$$R_m + R_c + R_g = \frac{\Delta P}{\mu J} \qquad \text{(Equation 2.2)}$$

Where R_m is the intrinsic resistance of the membrane, R_c is the cake layer resistance and R_g is the resistance due to pore blocking or gel layer.

Flux plays a critical role in membrane filtration performance and has a great influence on the economic feasibility of the treatment process. As such, critical flux is dependent on particle size, system hydrodynamics and membrane-particle interactions (Howell, 1995). For any given hydraulic treatment capacity, a higher membrane flux results in a smaller membrane area; therefore, an ideal situation is such that the membrane is operated just below the critical flux (referred to as sub critical flux) allowing the TMP to be maintained at a constant level. Yet, this is not entirely feasible as a non-fouling operation is not achievable (Liao et al., 2006).

The strong form of the critical flux concept is that a sub-critical flux is attained which is equal to clean water flux when operated under same conditions; while in its weak form, sub-critical flux does not equate to the clean water flux but rather is defined by constant permeability over a long period of time (Howell, 1995) as illustrated in Figure 2.2 . Several methods for determination of the critical flux have been applied (Howell, 1995, Bouhabila et al., 1998, Kwon and Vigneswaran, 1998, Cho and Fane, 2002, Defrance and Jaffrin, 1999), with varying degrees of reliability due to the difficulty of accommodating changes caused by cake deposition and consolidation (Le Clech et al., 2003). Another drawback in determining and subsequent application of the critical flux lies in the inability to predict permeability for long term membrane operations (Le-Clech et al., 2006). Therefore, experimental determination offers a better guide and is done by plotting the flux against TMP and observing the changes that occur from constant permeability to non-constant permeability which is indicative of fouling, although the value of critical flux obtained depends on the rate of flux with time and the method employed (Le Clech et al., 2003). This transition is indicative of the commencement of fouling and as such it is referred to as 'secondary critical flux' (Bouhabila et al., 1998, Le Clech et al., 2003). When evaluating this, Cho and Fane (2002) observed a two- stage transition of TMP when operating an Membrane bioreactor (MBR) below the

nominal critical flux which they attributed to Extracellular Polymeric Substances (EPS) and biomass fouling.

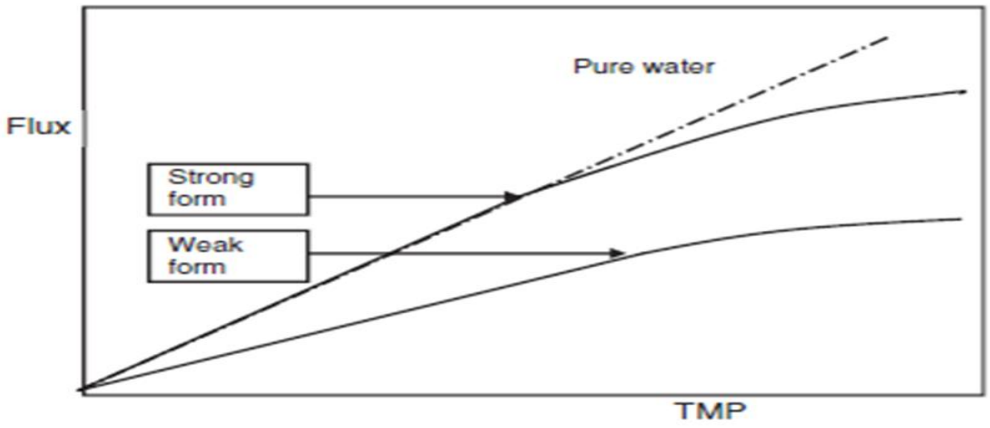

Figure 2-2: The two forms of critical flux (Field et al., 1995, Field and Pearce, 2011)

Therefore, it is more realistic to apply the design or sustainable flux when considering the long-term performance of the membrane bioreactor. Studies have shown that design fluxes applied in long-term operation are much lower than the critical flux. For example, the critical flux for a mesh filter used in a study by Satyawali and Balakrishnan (2008) was 3.9 L m^{-2} h^{-1} for a 30 µm nylon mesh, with the applied flux set at <1 L m^{-2} h^{-1} in order to achieve relatively stable performance. (Chu et al., 2014) determined the critical flux in an aerobic system as 75 L m^{-2} h^{-1} and found that operating at values below this showed lower flux declines over longer periods of operation. There is an advantage to be gained from applying very low fluxes, (even at the expense of time of DM formation) as this causes the slow build-up of the DM with the TMP kept stable and low compared to when higher flux is applied even under subcritical flux (Saleem et al., 2016). The fouling process in membranes is usually complicated and is not easily defined but a schematic of the stages involved proposes three stages (Cho and Fane, 2002, Meng et al., 2009):

- Initial, short term rise in TMP (attributed to fouling by EPS)
- Long term gradual increase in TMP
- Rapid increase in TMP with respect to time (dTMP/dt) (caused by biomass deposition)

2.2.1 Sustainable flux

Field and Pearce (2011) described sustainable flux as that flux which is attainable while applying cleaning and fouling control strategies with the aim of achieving operational cost objectives for the duration of the membrane life. From this description, it can be inferred that the main goal of membrane performance is not to push the limit of filtration by applying a rather high nominal or critical flux and attempting to maintain it. Rather, operators should focus on preserving membrane performance. To this end, the sustainable flux is employed with the long-term operation of the membrane in mind, i.e. economic cost required for maintenance and replacement being at the forefront of its application. This sustainable flux is highly dependent on the other contributing factors of the membrane operation, such as feed type, control mechanism and hydrodynamics. This differentiates it from the critical flux concept which is based on specific operating conditions and which usually serves as a general guide (Field and Pearce, 2011)

A more effective way to assess membrane performance is not to single out flux as the overriding factor in choice of application. The appropriate approach is to consider the pressure change for different values of flux and, with the aid of the fluid properties, plot the development of resistance of the membrane. The time and the energy expended in maintaining the level of flux may be a more accurate justification of the sustainable flux. If all the parameters related to biological function (COD/BOD conversion) are kept constant, the focus on membrane performance should be on whether the selected flux can be applied with consideration for the lowest energy consumption. This is central to the concept of sustainable flux. Hwang et al. (2008a) compared contributors to TMP for three different fluxes of 13, 20 and 27 L m^{-2} h^{-1} and found a marked difference by comparing the live/dead ratio (describes the activity of the bio-cake layer) and its spatial distribution. Although resistance built up more quickly with higher fluxes, it allowed more uniform distribution of this along the depth of the cake layer with a clearer non-uniform layer forming under low flux. This phenomenon caused the initial gradual rise in TMP for low flux, followed by an abrupt rise in TMP. This is in contrast to the rise in TMP at higher flux, which was much more rapid. They further explained that the behaviour of TMP at higher flux is attributable to factors such as the compression of the cake layer and reduction in porosity, increase in cake layer caused by bacterial deposition and EPS produced.

2.2.2 Operational flux

A study on the effect of the mode of operation on performance showed a direct influence of the initial imposed flux on the rate of membrane fouling: the higher the initial imposed flux the faster the fouling and hence DM formation (Cho and Fane, 2002). In addition, the mode of operation has a major impact on the consolidation of the cake layer as illustrated in the measured TMP or flux profile. There is a marked difference, for example, when a certain flux is imposed at the start compared to when the flux was imposed incrementally up to a specific value. In the former case, even though the critical flux was exceeded, a significantly lower TMP is observed compared to the latter. A rapid decline in flux, due to the consolidation and aggregation of the cake layer is observed with initial imposition of a higher flux compared to less consolidation if the flux is increased gradually. At higher flux, increased convection towards the membrane leads to the aggregation of colloids and deposits (Chen et al., 1997, Kim et al., 1993b, Kim et al., 1993a).

In early applications of the MBR process, the MLSS and SRT were usually applied at higher rates than is usually the case at present. It was not uncommon to see values of 30 g L^{-1} and 100 days in order to minimise sludge production and space constraints. This has not proven to give optimal performance and most recent operations are carried out at a manageable concentration of mixed liquor suspended solids (MLSS) and SRT of around 10-15 g L^{-1} and 20-30 days respectively (Hai et al., 2013). Practical reasons dictate that the operational flux and the feed type should be carefully studied. This will inform an appropriate selection of the best manner of operation rather than subjecting the membrane to higher flux at the beginning as was the norm in the early applications of the MBR.

2.3 Submerged or external configuration membrane bioreactors

Membranes can be operated in either submerged, sidestream or external configuration (Figure 2-3). Submerged membranes are popular as they offer lower energy requirements (Ndinisa et al, 2009), at the expense of lower flux and productivity. The argument for external configuration is that because the filtration chamber is separate from the reactor, cleaning and replacement of membranes can be carried out without affecting the anaerobic conditions of the bioreactor (Smith et al., 2012). There are a few concerns that are more specific to submerged than external configurations. Submerged MBRs typically use bubble

scouring as a means of alleviating fouling, although it has its own challenges too. For example, consideration must be given to the effective distribution of bubbles as they tend to be a critical factor affecting performance, particularly for flat sheet membranes (Drews, 2010).

Although reactors used are mostly CSTRs e.g. (Martinez-Sosa et al., 2011, Hu and Stuckey, 2006, Fuchs et al., 2003), EGSB (Chu et al., 2005) and UASBs (Cho and Fane, 2002) have also been studied. Regardless of the reactor configuration, it is helpful to target minimum contact between the biomass and the membrane to reduce the potential for fouling.

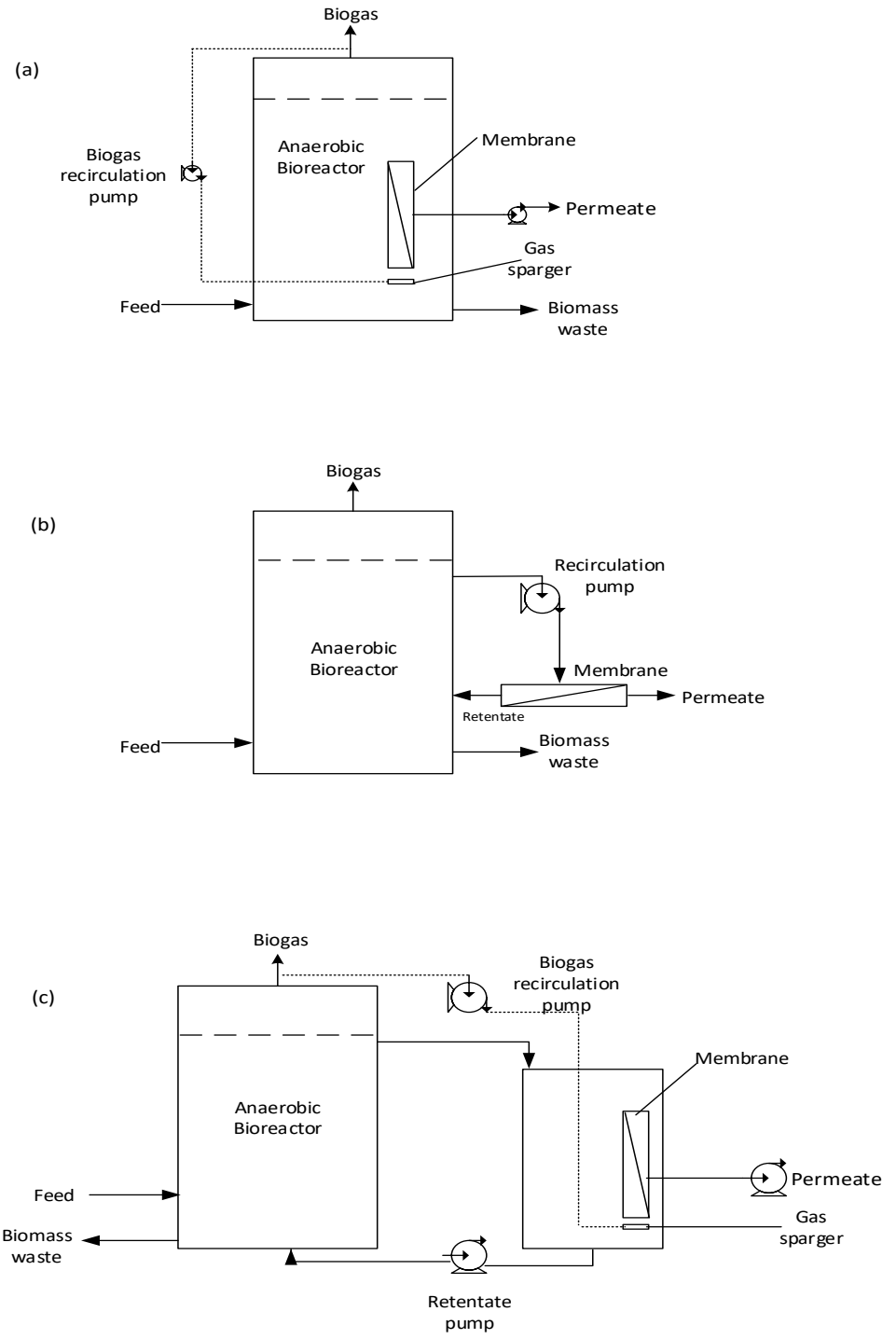

Figure 2-3: Types of AnMBR configurations a) submerged b) sidestream c) external(ly) immersed

2.4 Dynamic Membranes- background and applications

The Dynamic Membrane (DM) is an application that seeks to address some of the issues associated with use of microfiltration membranes in reactors; namely cost (both capital and operational) and maintenance, with the potential for providing higher flux and/or lower resistance (Fan and Huang, 2002).

In this application, a secondary membrane is formed on a support material, usually meshes or filter fabric material, resulting in an extra layer of filtration, especially for wastewaters containing significant suspended solids. In this manner, particulates and colloids form a ''dynamic membrane'' layer and the fouling of the support media is reduced (Ersahin et al., 2012, Chu and Li, 2006, Kuberkar and Davis, 2000). The major difference between the microfiltration membranes and support meshes/fabric is in in terms of pore size with the cut-off size between microfiltration and DM support materials widely considered to be 10 µm (Hai et al., 2013, Wakeman and Williams, 2002).

To better illustrate the concept of DM formation, **Error! Reference source not found.**.4 adapted from Lee et al. (2001) shows how the DM layer is formed on the support material and how it is able to reject some of the particulate suspended solids preventing them from fouling the membrane material itself. This DM layer now serves as a secondary membrane to provide some filtration and prevents direct fouling of the primary membrane, which is the support mesh (Fuchs et al., 2005, Jeison et al., 2008, Chu et al., 2008). The characteristics of the wastewater (mainly its suspended solids content) influence the development of this DM making it easy to create in situ in a repeatable manner (Fan and Huang, 2002). While the performance is expected to decrease over time, simple cleaning techniques such as backwashing with water or air or simply brushing off the surface layer can be applied without the need for chemical agents (Chu et al., 2008).

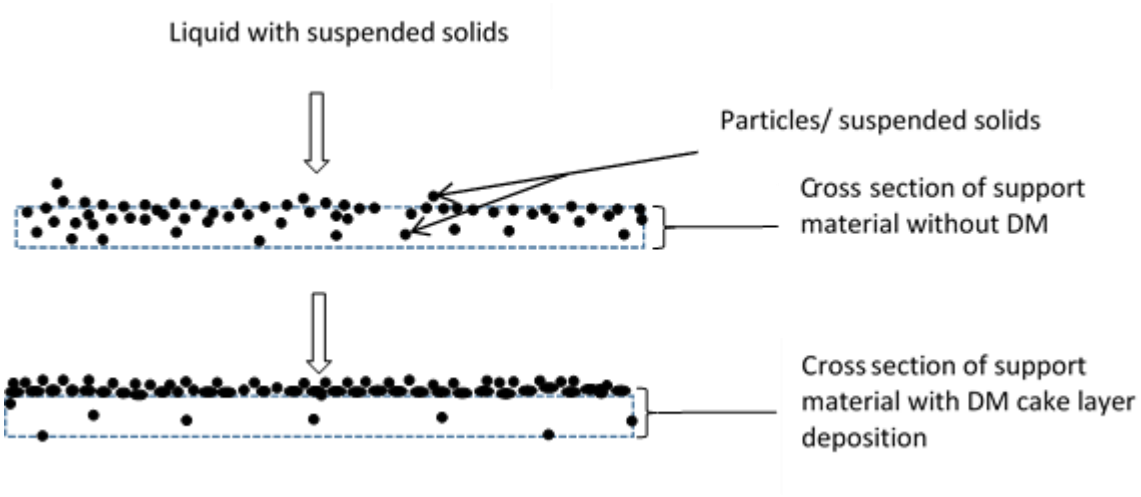

Figure 2-4: In -situ DM formation

2.4.1 DM formation process

The SFDM filtration operation is based on the principle that there exists an equilibrium between the rate of convection towards the surface of the membrane and the rate of back transport. This equilibrium state is determined and influenced by the hydrodynamic properties of the reactor as well as by fluid characteristics. A major aspect of performance is dependent upon the characteristics of the cake layer formed with distribution, porosity and consolidation being some of the key elements (Meng et al., 2009). For the development of the DM, there are three identifiable stages: the pre-coating (or DM formation or reformation stage (depending on whether a new membrane or a cleaned membrane is being used), filtration phase and backwash, with the changes in flux signifying the transition between the processes (Chu et al., 2008).

The formation of the cake layer is done by the contents (colloids, particulates, suspended solids) in the wastewater. Although the contents of wastewater are site and industry – specific, an attempt at classification according to size was made by Levine et al. (1991). The contents were classified according to particle size as dissolved (<0.001 µm), colloidal (0.001 – 1 µm), supracolloidal (1-100 µm) and settleable (>100 µm). Other factors that influence the size and distribution of organic matter in wastewater are treatment processes due to removal and solubilisation, which shows a decrease in size from the settleable (>100 µm) range to the supracolloidal range (1-100 µm) before and after treatment respectively (Levine et al., 1991). Studies show that the deposition of the particles starts with the formation of a

thin layer (a resistant biofilm) followed by the formation and growth of a thicker, less resistant (cake) layer (Mendret et al., 2009).

As might be expected, the most critical phase is the filtration phase, in which the effluent quality is much higher compared to the formation and backwashing stages. As such it is better to recycle the permeate during the DM formation phase. The process then proceeds to the filtration phase where the flux is generally stable and effluent is of better quality, and culminates in a significant drop in flux or consequent increase in TMP indicating that clogging has occurred and cleaning is required (Chu et al., 2008, Fan and Huang, 2002).

In order to understand the principle of particle deposition which governs the DM forming process, some equations, developed by Hermia (1982) and adapted from Ye et al. (2005) are presented in Table 2-1

Table 2-1: Dead-end filtration equations adapted from Ye et al. (2005)

Cake filtration	**Description**	**Equation**
Cake filtration	Deposition of particles larger than the membrane pore size onto the membrane surface	$t/V=aV + b$
Complete blocking	Occlusion of pores by particles with no particle superimposition	$-ln(J/J_0) = at + b$
Intermediate blocking	Occlusion of pores by particles with particle superimposition	$1/J = at + b$
Standard blocking	Deposit of particles smaller than the membrane pore size onto the pore walls, reducing the pore size	$t/V = at + b$

Where V is the cumulative volume of permeate at time t; J is the flux; J_0 = *initial flux;* a and b represent model parameters that can be related to physical quantities by equations 2.3 and 2.4 below

$$a = \frac{\mu C_b * \alpha c}{2 * A^2 * TMP} \qquad \text{(Equation 2.3)}$$

$$b = \frac{\mu R_m}{TMP * A} \quad \text{(Equation 2.4)}$$

Where μ is permeate viscosity, C_b is the concentration of the bulk solution; α_c is the specific cake resistance; A is membrane surface area; Rm is the hydraulic resistance of the membrane. Indeed Liu et al. (2009) was able to test the formation characteristics of DM and found good agreement with the filtration equations stated above.

For a better understanding of the pore blocking/deposition/membrane fouling process, Wakeman (1994) conducted a study to visualise the phenomena of membrane fouling and suggests the existence of an equilibrium region in the crossflow microfiltration channel that extends from the beginning to the end of the channel. The DM layer composes of two sub layers: a cake layer and a gel layer. The cake layer is loosely attached and is made of the sludge flocs and the microbes, while the gel layer is found underlying the cake layer and is made up mainly of EPS. The gel layer is much thinner, attaches to the support mesh and is not as easily removed as the cake layer. For these reasons, the gel layer is considered important in rejecting finer particles, although it takes longer to be formed than the cake layer.

The characteristics of these two layers differ in some respects, with the gel layer being more porous than the cake layer, which depends on the properties of the formation medium. Fan and Huang (2002) observed that the gel layer formed in a SFDM was made of hair-like and web-like structures and was able to reject finer particles. Additionally, the cake layer is weakly attached and easily sloughs off the surface of the support material. Furthermore, the phenomenon of pore blocking and cake formation which is central to the formation of the DM is initiated when the required filtration pressure is much greater than the pressure that can be absorbed by the membrane layer causing a non-equilibrium of pressure across the boundary (Song, 1998). The equilibrium thickness of the cake layer increases with the applied pressure because a thicker cake layer is needed to absorb higher pressure.

2.4.2 Types of DM

There are two types of DMs based on their formation process: the self-forming dynamic membrane (SFDM) and the pre-coated membrane. The SFDM is formed by the action of the contents (suspended solids, colloids, flocs) in the wastewater being filtered. While this method of formation may appear straightforward and simple, the successful application and

sustainability of the process is influenced by other parameters including wastewater characteristics and operational conditions. The earliest study of DMs was done by Marcinkowsky et al. (1966), although this was carried out using Hydrous Zr (IV) oxide as the formation material in a reverse osmosis process.

Several studies have been conducted on the application of SFDM in treatment of wastewater and the results have been encouraging (Ersahin et al., 2012, Zhang et al., 2010, Saleem et al., 2016, Chang et al., 2001). These studies have been carried out using a variety of different support materials and were able to obtain fluxes higher than conventional membranes and at low TMP: detailed discussions are provided in sections 2.4.4 and 2.8

Alternatively, the pre-coated dynamic membrane is formed by the use of a chemical solution or a composition of specific external materials and for this type, Zr (IV) oxide has proven to be the most popular chemical component used on the surface of the porous material for DM formation (Johnson et al., 1972, Groves et al., 1983, Chen and Chiang, 1998, Altman et al., 1999, Wang et al., 1999, Nakao et al., 1986), compared to oxides of Al and Fe (Nakao et al., 1986). The major drawback of pre-coating is that external additive(s) are required for formation with the potential for increased cost, inhibition of the performance of microbes in a biological system and the likelihood of chemicals manifesting in filtered permeate. For these stated reasons, this study focuses on the use of SFDM in an anaerobic bioreactor.

2.4.3 Support materials for DM formation

For the SFDM, the support materials used are mainly meshes or fabrics (woven or non-woven). These possess different characteristics, with meshes offering resilience but at a higher cost since there is a tendency for indiscriminate sludge accumulation because of the flat structure, making cleaning harder (Fuchs et al., 2005). It is desirable for the support material to be hydrophilic, due to the obvious advantage of increased permeability, and such membranes are generally referred to as 'low fouling', because of higher resistance to attachment by organics (Judd, 2010). Woven filters are generally made from polyester, while non-woven filters which can be made from polypropylene are produced as discontinuous filaments of 0.5 – 3 μm diameter in an amorphous felt, with the pore size and permeability depending on the filament diameter and the degree of compression. The hydrophobicity of the materials or fabrics can be overcome by surface modification and graft co-polymerisation (Chuang et al., 2011, Wang et al., 2009). While the woven and non-woven support meshes

have been applied in biological wastewater treatment, other support materials such as ceramic tubes (Yang et al., 2011) stainless steel (Wang et al., 1999), polymers, microfiltration (MF) and ultrafiltration (UF) membranes have been utilised in physical application processes. Support material types made of nylon have shown greater flux performance per unit time compared to woven, non-woven and even steel meshes (Li et al., 2011).

In practice, support material should possess some inherent qualities including toughness and suitable pore size to achieve formation of the DM, and should be readily available at a reasonably low price as this will increase the potential for their use in wastewater treatment (Johnson et al., 1968)

2.4.4 DM applications in aerobic wastewater treatment systems

DM were initially applied in aerobic systems rather than anaerobic, due to the need for removal for regular operational maintenance. The predominant type were flat sheet modules (Ersahin et al., 2012) although few cases of tubular DM have also been tested, usually in activated sludge systems (Table 2-2 provides more details).

Activated sludge is an aggregate of suspended solids and microorganisms, connected in a polymeric network made up of polysaccharides, proteins, lipids and organic acids, which significantly influence its biological and physical (morphological) characteristics (Jin et al., 2003) (Örmeci and Vesilind, 2000). These morphological properties in turn affect the separation qualities of the sludge i.e. its filtration and/or settleability.

The floc size distribution in activated sludge is dominated by particles greater than 100 μm (Jin et al., 2004, Meng et al., 2007) , indicating the potential for cake layer formation on coarser meshes, with decreasing mean particle size causing higher cake resistance in conventional membrane filtration (Meng et al., 2006). A few factors have been attributed to the influence of aerobic floc to membrane filtration properties. Some of these have direct correlation in the physical sense (floc size and distribution); others are based on indirect factors such as zeta potential and osmotic pressure of the flocs and the cake layer (Nakamura et al., 2012, Espinasse et al., 2008). (Lim and Bai, 2003) showed that granular sludge maintained significantly higher flux compared to bulking sludge due to larger floc distribution of the granular sludge

Kiso et al. (2000) tested the performance of a 100 μm nylon mesh in a submerged bioreactor driven by water head difference, under intermittent and continuous aeration. Regardless of operating mode they obtained an effluent BOD and SS of less than 5 mg L^{-1} and 1.5 mg L^{-1} respectively, even at a relatively high filtration flux between 21 and 29 L m^{-2} h^{-1}. The OLR was low at around 0.7 g BOD L^{-1} day^{-1}, due to the maximum allowable water head difference of 45mm (corresponding to an average TMP of 0.4 kPa). Intermittent aeration led to frequent clogging of the meshes, requiring 1 or 2 weeks between cleaning episodes compared to 150 days when subjected to continuous aeration.

Fan and Huang (2002) used 100 μm dacron mesh in a submerged aerobic bioreactor treating municipal wastewater of varying influent COD between 97 and 372 mg L^{-1}, averaging around 250 mg L^{-1}. They achieved a variable flux between 14 and 33 L m^{-2} h^{-1} and total COD removal of over 84% of which they deduced that around 9% was contributed by the DM. The operational period without cleaning was 90 days, partly due to the effect of bottom and lateral aeration applied to the SFDM. When comparing the resistance of new and used modules, the authors also found that although the resistance of the new naked module was higher than the used module, due to a reduction in hydrophobicity of the material, as the biofilm formed it became more hydrophilic reducing the dead water zones present in the new naked modules.

(Fuchs et al., 2005) tested a nylon mesh with pore size of 30 μm in a submerged reactor with aeration for mixing and activated sludge, under ambient conditions. They achieved effluent COD concentrations of less than 40 mg L able to meet the EU discharge standard. Flux varied between 50 and 150 L m^{-2} h^{-1} but the interval between start of filtration and blocking of the mesh was one week or less and the organic loading rate was less than 0.35 g BOD L^{-1} day^{-1}

Irrespective of the configuration applied, as seen in the cases above, encouraging performance was observed as flux was consistently higher compared to anaerobic reactors. Apart from differences in floc morphology of aerobic and anaerobic floc particles, the presence of aerators providing dissolved oxygen in the aerobic system significantly increases the porosity of the cake layer and reduces its resistance. This was observed by Kiso et al. (2005) when applying a sequencing batch reactor equipped with a 100 μm mesh for the treatment of very low strength synthetic wastewater (BOD = 200 mg L^{-1}). Under intermittent aeration the system showed haphazard performance with significantly longer filtration time needed to filter equal volume compared to continuous aeration.

In conclusion, unlike anaerobic systems, in aerobic system there is no need to control exposure to oxygen, making regular maintenance simpler. In addition, as air circulation has the dual function of providing aeration and scouring the surface of the membrane / support material there is less emphasis on the need to minimise gas sparging. More research is required to understand why aerobic digestate offers lower specific resistance than anaerobic digestate; and instead of attempting to mimic the relatively high flux performance of aerobic DM, it is more feasible to focus on exploiting the unique characteristics of anaerobic DM at the expense of lower resistance.

Table 2-2: Studies on DM conducted using activated sludge/aerobic conditions (partially adapted from (Ersahin et al., 2012)

Support material used/pore size (µm)	**Formation material**	**Configuration**	**Flux (L m^{-2} h^{-1})/Pressure (kPa)**	**Cleaning method**	**Temp control**	**Reference**
Nylon mesh /100	Activated sludge/ synthetic WW	FS/ submerged	21-32/ driven by water level difference	Aeration	none	(Kiso et al., 2000)
Dacron mesh/100	Activated sludge/municipal WW	FS/ submerged	14.8-33.3/ driven by water level difference	Aeration	27 ºC	(Fan and Huang, 2002)
Non-woven polyester filter/50-200	Activated sludge/ synthetic WW	n.a/submerged	42-125/3-6	Aeration	20 ºC	(Alavi Moghaddam et al., 2002)
Fabric Filter/na	Activated sludge/domestic WW (supplemented with nutrients)	n.a/submerged	16.7/ driven by water level difference	Aeration	n.a	(Seo et al., 2003)
Mesh/100, 200, 500	Activated sludge	FS/submerged	n.a	none	n.a	(Park et al., 2004)
Non-woven/ n.a	Activated sludge/(synthetic	FS/ submerged	50-80/driven by water	Aeration/tap water	n.a	(Wu et al., 2005)

	+ domestic wastewater		level difference			
Woven nylon fabric/ 30	Activated sludge/municipal WW	FS / submerged	0.3-1/150	Aeration	ambient	(Fuchs et al., 2005)
Mesh/100	Activated sludge/ synthetic WW	FS /submerged	42-625/driven by water level difference	Aeration	n.a	(Kiso et al., 2005)
Filter cloth/n.a	Activated sludge/municipal WW	FS /submerged	17–21/150	Aeration	ambient	(Chu and Li, 2006)
Terylene filter cloth/56	Pre-coated PAC[a] /synthetic	FS /submerged	18.6/100	Brushing	25 ºC	(Ye et al., 2006)
Nylon/100	Activated sludge	FS /submerged	9.7-31.3/n.a	Aeration	ambient	(Wang et al., 2006)
Non-woven fabric/ n.a	Activated sludge	FS, tubular/submerged	20/72	physical cleaning	20 ºC	(Seo et al., 2007)
Nylon/30	Activated sludge/synthetic WW	n.a/submerged	0.8-0.9/0.6-8.8	Aeration/tap water	n.a	(Satyawali and Balakrishnan, 2008)
Stainless steel/74	Activated sludge + biodiatomite /municipal WW	Plate - frame/submerged	8.8-130/40	Air backwash	ambient	(Chu et al., 2008)
Silk/100	Municipal raw sewage	Plate - frame/submerged	4-20/n.a	Aeration	n.a	(Liu et al., 2009)
Non-woven polyester/100	Activated sludge/household WW	Filter bag/submerged	5/driven by water level difference	None	n.a	(Ren et al., 2010)

2.4.5 Essential difference between aerobic and anaerobic systems in terms of application of DM

The sludge type and characteristics affect the rate of membrane fouling, which in turn influences cake formation and membrane performance. EPS extracted from the cake layer in membranes treating wastewaters showed mainly protein-like and humic-acid substances (An et al., 2009, Zhang et al., 2011, Meng et al., 2007). Substances such as dissolved proteins and polysaccharides, produced during degradation of organic matter, were more abundant and showed greater accumulation under anaerobic conditions compared to aerobic conditions (Novak et al., 2003, Tomei et al., 2011). This difference is attributable to the higher fraction of colloidal COD produced in anaerobic digestion, which is efficiently removed in aerobic digestion.

These differences contribute to the rate of dewatering expected: a higher concentration of proteins and polysaccharides results in lower dewatering potential. Therefore, it is harder to filter anerobically-treated sludge compared to aerobically-treated sludge. Since cake formation is the major driver of the DM process and significantly influences the achievable flux, it is expected that these dissolved substances –EPS and proteins- cause the binding of small flocs, humic and inorganic substances to the surface of the support material improving the formation of the DM.

Wu et al. (2005) observed that the DM layer in an aerobic configuration rejected some high molecular weight organic matter, which they attributed to the degradation of the soluble microbial products in the reactor over its long-term acclimation and operation, rather than solely due to physical rejection. In addition, (Wu et al., 2005), found higher levels of ammonia in the permeate compared to the bulk phase of a DMBR which shows the organic nitrogen was degraded to ammonia while passing through the cake layer of the DM.

In terms of resistance, Ramesh et al. (2007) showed that the resistance from anaerobically-digested sludge was 4 times higher than the resistance of aerobically digested sludge (1 x 10^{13} m^{-1} as compared to 4 x 10^{13} m^{-1}) when subjected to similar filtration tests. This was more specific to the reversible resistance for which the significant contributor is attributable to the increased soluble microbial products in the anaerobic sludge compared to the aerobic sludge. This is in agreement with Jeison et al. (2008) who found that the anaerobic mesophilic and thermophilic digestate presented specific resistances of 6.3 X 10^{14} m kg-TSS^{-1} and 3.7 X

10^{14} m kg-TSS^{-1} respectively, which were higher than 1.2 X 10^{12} m kg-TSS $^{-1}$ (Ahmed et al., 2007) and 8.4 X 10^{12} m kg-TSS $^{-1}$ (Wang et al., 2007).

2.4.6 Performance of DM in removing organic materials from wastewater

For biological processes, meshes, filters (woven and non-woven) and fabrics have found popular use as support media. Even though the use of membranes in biological systems has mostly been in aerobic systems, the challenges encountered are similar for both systems (Cho and Fane, 2002). Through incorporating membrane filtration into biological systems, the optimisation of two separate activities is targeted: biological degradation and physical separation. The biological activity is dependent upon the mass loading while the physical separation is influenced by such parameters as concentration of SS, cross-flow velocity, pressure and the hydrodynamic conditions in the reactor (Beaubien et al., 1996). The overall biological performance of DM is influenced by the ability to achieve and enhance the retention of solids in the bioreactor leading to increased degradation of organic matter under aerobic or anaerobic conditions.

Kiso et al. (2005) achieved 99% suspended solids (SS) retention at a flux rate of 20 L m^{-2} h^{-1} while treating synthetic wastewater of 6.5 g MLSS L^{-1} using a nylon mesh of 100 µm pore size. Although influent COD concentrations are dependent on wastewater types, typical removal rates between 80% and 99% were achieved using DMs (Alibardi et al., 2016, Liu et al., 2009, Ersahin et al., 2014, Loderer et al., 2012). Long term operation has been shown to deteriorate permeate quality as observed by Guan et al. (2018) in which they found that the particles in the permeate was similar in size to the pore size and this is irrespective of the operational TMP in long term operation. For more specific toxicant removal, Jung et al. (2015) used a 100 µm nylon mesh as a media for treating a wastewater containing phenol and achieved removal efficiencies of 99.9%, 98% and 96% for phenol, NH_4-N, and dissolved TN even though the performance was influenced by the feeding mode employed. Although this cannot be strictly attributed to the DM itself as the porous material also serves as a filter.

2.4.7 Comparison of MBRs with DMBRs

Membrane bioreactors due to their characteristic ability to retain slow-growing biomass appear suitable for treating wastewater under hitherto challenging conditions, e.g. at ambient or low temperatures, without requiring long HRTs. Industrial wastewaters are

usually high in organic strength and therefore the energy balance is positive, even allowing for the energy requirement for controlling fouling to maintain membrane flux. On the other hand, domestic wastewaters characteristically have low organic strength, and in low temperature conditions, biomass growth rates remain very low; therefore, successful operation of the MBR will depend on ensuring long-term application with minimal need for cleaning. This will compensate for and reduce the additional energy required for operational maintenance. Any technique that seeks to improve such drawbacks requires deeper investigation. These improvements can be achieved in terms of cost and energy use while considering the capability for the retention of the viable biomass in the reactor and excellent utilisation of the reactor capacity through improved contact (Lettinga et al., 2001).

In theory, the application of conventional membrane filtration is similar to dynamic filtration; the major difference is in the pore size of the material and the filtration mechanism. Table 2-3 shows a compilation of similarities and differences between conventional MBRs and DMs.

Table 2-3: Comparison of DM to Conventional microfiltration membranes (partly adapted from Hu et al. (2018).

Parameter	**Dynamic Membranes**	**Conventional microfiltration membranes**
Pore size (um)	Between 10 μm and 200 μm	Less than 0.5 μm
Configuration	Mostly flat sheet (tubular also available)	Flat sheet, hollow fibre, tubular
Flow rate/flux (m^3 m^{-2} h^{-1})	2-65 (Anaerobic systems)	2-30 (anaerobic)
Transmembrane pressure (kPa)	Low (0.1 – 80)	High
Cost (capital and operational expenses)	Low	High

Solids retention capacity	High	Very high
Effluent quality	Good (but variable)	Excellent
Operation	Pump or gravity-driven	Pump or gravity-driven
Cleaning	Easy	Specialised
Organic loading rate	High	High
Temperature sensitivity	Low/moderate	Low/moderate

Compared to the use of microporous membranes for filtration, DM offer benefits such as lower filtration resistance, higher flux at low TMPs and low cost of operation and maintenance (Ersahin et al., 2012). It is only logical that in order to reduce energy use with increased flux, large pore membranes capable of achieving the required filtration should be employed (Liao et al., 2006). In summary, DM offer advantages in that they are easy to build and deploy to fit specific needs, with materials readily available and at a relatively lower expense. The major drawback is the comparatively lower permeate quality, and current lack of large-scale industrial applications.

2.5 Membrane configuration

Several types of membrane configurations are available based on differences in geometry, but the most important ones in MBR use remain plate and frame/flat sheet, hollow fibre, and tubular (Judd**,** 2010)**.** These geometrical and configuration differences influence properties and performance during operation. The flat sheet membrane offers the advantage of low manufacturing costs and higher resistance to clogging compared to the hollow fibre and tubular membranes. Its major disadvantage is low packing density and higher air use for cleaning causing higher opex costs (Hai et al., 2013). For the laboratory scale tests, flat sheets have been selected more often (Zhang et al., 2011, Xie et al., 2014, Ersahin et al., 2014, Yu et al., 2014, Jeison et al., 2008, Alibardi et al., 2016) than other tubular configurations (An et al., 2009), although Loderer et al. (2012) and Pillay et al. (1994) operated tubular membranes in aerobic systems. Overall, the use of flat sheet can be attributed to its ease of application and suitability for cake filtrations. In the past, most cases

of membrane filtration were in aerobic systems (Hu and Stuckey, 2006), but recent advances have indicated increased interest in applications in anaerobic conditions (Stuckey, 2012) due to the advantages stated previously.

2.6 Membrane location – submerged or external

Submerged DM systems were previously seen as better than side stream configuration because a) research has shown that external shear induced by pumping has a deleterious effect on biomass viability and b) it requires higher energy use (Buonomenna and Bae, 2015, Ghyoot and Verstraete, 1997). Alternatively, cleaning episodes and essential maintenance and replacement are far easier to handle with externally configured/ sidestream membranes. For example, Ersahin et al. (2017) tested the impact of external and submerged DM in an AD system and discovered that although submerged DM offered shorter start up time, the external configuration offered 28% lower resistance compared to the submerged configuration. When the ease of maintenance required for DM is considered, then the benefits of external configuration become even more apparent. Maintenance can be carried out in the form of cleaning or replacement without the need to pause the entire system- which can negatively affect its overall performance. Also, the external configuration can be more readily integrated to an existing treatment system without the need for major alterations. Side-stream systems have been successfully combined with other treatment processes including continuous stirred tank reactors (CSTR), upflow anaerobic sludge blanket (UASB) and expanded granular sludge blankets (EGSB). Apart from helping to retain the biomass, which may be in the form of aggregated micro particles, it also guarantees that the effluent is suitable for discharge, -essentially performing the duties of a post treatment option. In a pilot-scale application with the MBR external to the main digester, as investigated by (Dong et al., 2016), the results showed that reduced exposure of the membrane unit to the suspended solids and colloids helped to achieve long-term performance (178 days) without the need for cleaning.

More such cases are further discussed in detail below:

UASB + Membrane filtration: the combination of a UASB reactor with membrane filtration typically involves the placement of the membrane outside of the UASB, which serves as the main biological treatment unit. Some configurations used were straightforward: for example, Gao et al. (2010) coupled a flat sheet membrane unit to a UASB reactor treating

synthetic wastewater. Rapid flux decline from 12 to 9 L m^{-2} h^{-1} was observed in the first five days of operation before stabilisation at 8 L m^{-2} h^{-1} after 62 days of operation. Effluent quality was less than 20 mg COD L^{-1} and flux decline was attributed to fouling caused by production of EPS and other soluble microbial products. Ozgun et al. (2015) investigated the impact of adding a hollow fibre membrane to an existing UASB unit. Although there was a decline in sludge settleability, treatment efficiency increased by 20% and the effluent was free of particulates. Jeison et al. (2009) compared the long-term operation of a stand-alone UASB and a UASB plus sidestream MBR. They found a 10% decrease in biomass and a decrease in particle size in the UASB due to gradual biomass wash out, with a concomitant decrease in performance. In comparison, for the UASB + MBR an increase in sludge necessitated periodic wastage to control sludge age. For the UASB + MBR, an OLR of around 25-30 g COD L^{-1} day^{-1} was achieved in half the time taken to reach the same value in the UASB-only reactor. The authors concluded that under given conditions, the estimated cost of operation could be lower than for submerged configurations.

Zhang et al. (2010) and Xie et al. (2014) combined a UASB with DM filtration by placing the DM with support material pore size of 61 µm and 40 µm respectively, in the upper settling zone of the UASB, i.e. away from the mixed liquor. In the first case, a low TMP rise was observed over 90 days of operation at a high flux of 65 L m^{-2} h^{-1}, although the DM was unable to remove dissolved organic matter and in the later stages, even larger particles were present in the effluent. Xie et al. (2014) applied a similar set-up of a UASB in combination with a DM located in the upper settling zone, to treat landfill leachate, with the notable difference being the pore size of the support material used. Even though a low flux of 6 L m^{-2} h^{-1} was applied, frequent cleaning was required particularly during the start-up stage. Although the support material pore size was the notable difference, this implies the wastewater type has an effect on DM performance. Quek et al. (2017) applied a DM to a UASB for short-term tests in an external configuration and showed that mesh size had little contribution to resistance, although a rather narrow pore size range (28 µm and 46 µm) was tested.

To compensate for the energy demands associated with external/sidestream AnMBR configurations, (Lew et al., 2009) set up a system where the head difference provided the required TMP for the operation of a dead end membrane unit attached to a bioreactor inoculated with anaerobic granules. Even though the flux was maintained at 7.5 L m^{-2} h^{-1} (well

below the nominal membrane critical flux of 500 L m^{-2} h^{-1}), it required much more frequent backwash to compensate for the restriction in transmembrane pressure.

AF + MBR : Thus far, only one case of a combination of AF with DM has been reported (Li et al., 2017), wherein the DM (steel mesh of pore size 40 µm) was placed in the upper part of the reactor above carbon fibre which was used as a support medium for biomass attachment. No noticeable TMP increase was observed until after 90 days of operation at 20 L m^{-2} h^{-1}, when TMP rose to 15 kPa before cleaning was carried out to recover the flux set at 20 L m^{-2} h^{-1}. This indicated that a biofilm support could well mitigate the rate of fouling during mesh filtration. Subsequent use and cleaning reduced the duration between cleaning episodes, showing that even though the cleaning was reversible in the early stages, it could not entirely prevent the build-up of irreversible fouling in the latter stages of reuse.

In an effort to mitigate fouling and promote long-term stable operation, two main techniques are employed: intermittent operation (for which the filtration is paused/relaxed in between cycles of operation; and backwashing (reversal of flow-direction in order to remove some of the deposited matter on the membrane, although this is not applicable to flat sheet membranes (Zsirai et al., 2012)

2.7 Factors affecting DM formation and performance

An understanding of factors that affect DM formation and sustainability is necessary to improve performance and stability. Such factors include type and pore size of support material used, sludge properties, operational conditions and membrane configuration. In a study by Hernandez et al. (2002), the filtration performance of 10 µm and 100 µm material under a wide range of OLR (0.3 - 13.0 kg COD m^{-3} day^{-1}) was investigated. It was found that higher OLRs resulted in decrease in flux and that the 100-µm material had a higher tolerance for OLR increase compared to the 10 µm material. Jeison et al. (2008) using tubular membranes in both submerged and side stream configurations for treatment of acidified wastewater, noted that cake formation is the limiting factor for applicable flux under all conditions tested, and higher fluxes were achieved under mesophilic conditions compared to thermophilic conditions. They also observed a high cleaning efficiency, which indicated that the cake layer is the main source of the filtration resistance rather than internal fouling, as the temperature and configuration for the reactors were different.

Ho et al. (2007) evaluated the performance of an AnMBR using both polytetrafluoroethylene (PTFE) filter material and non-woven filter of 10 µm and 12 µm pore size respectively at 25 ºC. The flux varied between 4 L m^{-2} h^{-1} and 12 L m^{-2} h^{-1} suggesting that cake resistance is the key issue for controlling flux and TMP. The authors advised that the cake density should be controlled at a given value of 12 g m^{-2}, which may be done by regular backwashing, while also concluding that having a stable flux is more important than the initial flux value.

For a given range of wastewater characteristics, there is an ideal pore size and material type that suits the wastewater being treated as these properties affect the formation and retention capacity of the DM. There is no unanimous agreement on a direct relationship between pore size and performance. Kiso et al. (2000) tested meshes of sizes 100 µm, 200 µm and 500 µm. As expected, the 100 µm had the best retention capacity to form a sludge layer and hence better SS removal under aerobic conditions. Jeison et al. (2008) conducted a series of batch tests and, interestingly, was unable to build a DM layer on pore sizes greater than 60 – 70 µm in an anaerobic system. These differences maybe be due to operational and rheological conditions. When considering the impact of different materials of similar pore sizes, Ersahin et al. (2013) tested three sets of materials (mono-monofilament, mono-multi filament and staple (i.e. spun yarn) of pore sizes 10 µm and 40 µm. The highest flux was achieved with the staple yarn. In addition, there was little difference between different sizes of the same material compared to that for same pore sizes with different materials.

With these factors in mind and since the DM is formed by SS or colloids, a study of the effect of floc size distribution in relation to the material pore size and the material properties may be valuable to enhancing the design and application of DM in wastewater treatment. For the particle size distribution, a reduction in particle sizes increases back transport and consequently leads to higher solids deposition on the membrane surface (Jeison and van Lier, 2007). To achieve stable performance, it may be helpful to start with a higher sludge concentration, followed by a reduction in concentration once the DM formation is complete. This is effective because higher sludge concentration seems to favour faster DM formation but results in lower flux and higher permeate SS concentration (Chu and Li, 2006, Pillay and Buckley, 1992).

Physical conditions such as temperature and SRT also affect cake resistance and flux. For example, Jeison et al. (2008) observed that the specific cake resistance for a DM formed from mesophilic condition was almost twice that of a thermophilic condition. Ersahin et al. (2014)

tested the performance of a submerged Anaerobic Dynamic Membrane Reactor (AnDMBR) under SRTs of 20 and 40 days. During stable performance, the TMP and filtration resistance were both higher for a 40-day SRT compared to the 20-day SRT, which may be attributed to the lower metabolic rate and less degradation at longer SRTs. A similar observation was made by Pacheco-Ruiz et al. (2017) in which shorter mean cell resident time (MCRT) resulted in better flux performance in conventional submerged AnMBRs. A lack of understanding of the interdependence of these factors could lead to unstable and unsustainable performance as discovered by Jeison et al. (2008) who employed woven and non-woven membranes in mesophilic and thermophilic conditions resulting in a very low flux and unstable performance. This was attributable to higher specific cake resistance, and the authors concluded that control of cake thickness is required to achieve reasonable TMPs.

2.7.1 Mode of operation: constant flux vs constant TMP operation

Membrane reactors can be operated based on constant flux, constant pressure or variable flux and pressure. For constant flux as shown in (Fig 2-5a), the flux remains fixed while the pressure varies according to increase in resistance. In the constant pressure mode of operation, the pressure is kept constant and the flux is allowed to vary according to the change in pressure (Fig 2-5b). For most industrial plant operations, the constant flux method (usually operated below the nominal critical flux) is favoured as it reduces the propensity for fouling and there is an overarching need to establish guaranteed flowrates (Decloux and Tatoud, 2000, Marshall et al., 1996).

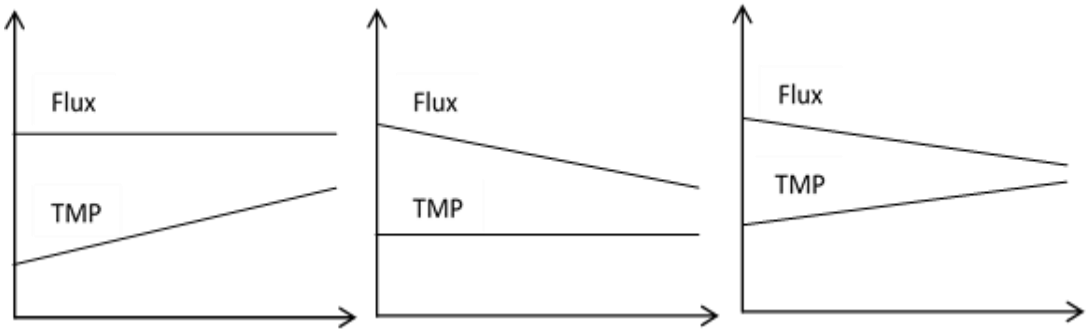

Figure 2-5: Modes of operation for filtration (a) Constant flux b) Constant pressure c) non-restricted flux and pressure (Tchobanoglous et al., 2003)

A third mode of operation (Fig 2-5c) allows the pressure and flux to vary according to changes in resistance (Tchobanoglous et al., 2003). When all other hydrodynamic conditions are the same, membrane performance shows a slight difference depending on whether flux or pressure is kept constant. In a study by Miller et al. (2014) a comparison of the two modes of operation was made for ultrafiltration. Resistances were similar for both constant flux and constant pressure operations below the critical flux (which is the flux at which a rapid increase in TMP is noticeable), and dissimilar when the operation was conducted above it. With constant pressure, when the system is operated above the critical flux, the resistance increases rapidly and then plateaus after 'peaking': this is due to the fall in the flux and in the rate of fouling. On the other hand, the constant flux operation shows a rapid increase even after reaching the same peak as the constant pressure operation.

Although less studied than the other two modes, there is a difference when the TMP and flux are both allowed to vary during operation, as observed in a study conducted by Bourgeous et al. (2001) using tubular membranes. They found that operating at constant flux shortened the period between cleaning episodes compared to allowing the flux and TMP to reach a predetermined value. This mode of operation is rarely applied in practical situations and the authors concluded that it is better to allow the flux to drop to pre-determined value or the pressure to exceed a set point before backwashing. This is in contrast to the results of a study by Vyas et al. (2002) which compared the two operating modes using tubular membranes. They observed that resistance caused by irreversible fouling was greater under constant flux compared to constant TMP operation. At the same time, the resistance caused by reversible fouling under constant TMP was higher than that caused by reversible fouling under constant flux. They also combined the two modes of operation in alternate runs, starting with constant flux-constant pressure mode and then reversing the order. For the constant flux-constant pressure mode, the operation started with a fixed flux and switched to a variable flux when the TMP reached a pre-determined value (in this case 100 kPa). This flux was allowed to decline freely until steady state was reached, although the flux at steady state was much lower than that obtained under constant flux mode. They also observed that the flux decline occurred at a slower rate compared to flux decline in strictly constant TMP mode. In the alternate run (constant TMP-constant flux mode), dropping the flux after operating at a fixed TMP did not have any significant effect on fouling resistance. This was attributed to the action of the strong adhesive forces on the particles. In another study carried out by (Defrance and Jaffrin, 1999), the filtration performance under stabilised operating conditions

for both constant TMP and constant flux was compared. The results showed that the TMP was always higher at a given flux under constant TMP compared to under constant flux. They attributed this to difference in the initial formation process before stabilisation, during which the decline in flux at constant TMP is induced by the drag of large particles to the surface of the membrane causing more blockage / more significant fouling compared to the constant flux operation.

Given that the flux is driven by the pressure gradient, similarity in filtration may be expected irrespective of the mode in which pressure is applied. Practical tests of this hypothesis revealed, however, that this is not necessarily the case in practice. For instance, in another study conducted by (Carrère et al., 2002), the effect of constant TMP and constant flux operating modes were evaluated for the microfiltration of lactic fermentation broth using tubular membranes. They concluded that when the membrane was operated above the critical flux, the constant flux gave a linear relationship between permeate produced and time; but the constant TMP was more productive in terms of time required to produce the same volume of permeate. In a review of biological wastewater treatment (both aerobic and anaerobic) using DM, a majority of the processes used the water head difference to control TMP (Ersahin et al., 2012). In terms of removal, the performance of the two systems was basically the same with only slight differences recorded at very high flux (Miller et al., 2014). In an ideal situation, a combination of the two may be useful in the sense that the operation starts with constant pressure to favour rapid formation of the DM and then switches to constant flux to maintain its sustainability. Nevertheless, this may prove too difficult in practice. In conclusion, the main criterion for which mode of operation to select depend on the relative importance of rate of evolution of DM versus resistance during operation; and since cake formation is critical to the development and performance of the DM, whichever mode is applied, it is useful to target the overall performance optimisation of the DM

2.7.2 Solids concentration

As the MLSS concentration affects the filterability of the mixed liquor, the expected solids content must be taken into account when designing and operating the Dynamic Membrane Bioreactor (DMBR). Higher sludge concentrations have been shown to result in higher solids in the effluent if all other hydrodynamic factors are maintained (Kiso et al., 2000, Fuchs et al., 2005), and ultimately affect the filtration process (Lee et al., 2001). Chu and Li (2006)

investigated the effect of MLSS concentration between 3 g L^{-1} and 10 g L^{-1} on formation of DM on porous media and suggested an inverse correlation between the MLSS and the permeate flux and turbidity, implying that higher MLSS concentration resulted in lower flux and effluent turbidity. In addition, there was a marked difference in flux between operation at 5 and 8 g MLSS L^{-1}, suggesting that the relationship between MLSS and flux decline is not exactly linear. The flux decline for elevated sludge concentrations can be attributed to higher blocking behaviour of solids on the porous media, although the rheological properties of the solids also play a part. During the formation stage, higher MLSS concentration resulted in lower effluent turbidity but was this reversed in the stable stage. Hu et al. (2017) showed that formation of DM using PAC took place in under 20 minutes for domestic wastewater treatment, with higher PAC dosage resulting in stable flux compared to without PAC addition.

In continuous bioreactors, changes in SS concentration are to be expected, and provided these changes are small and transient, they can be well managed by the DM and performance will not be adversely affected (Saleem et al., 2016, Ersahin et al., 2014).

2.7.3 Effect of pH on DM formation

During the filtration of a liquid medium, the pH is a correlative factor that directly or indirectly influences other contributory factors affecting the filterability of the liquid and filter media. A small number of studies have looked at the influence of pH on DM formation and performance (Cai et al., 2000, Nakao et al., 1986, Wang et al., 1999). Most of these have focused on pre-coated membranes, as expected given their dependence on chemical components. As for SFDMs in biological processes whether aerobic or anaerobic, the pH is normally accepted or conditioned to reflect the optimum for biological processes, with little regard to the effect on the DM in such conditions. pH and ionic strength strongly influence the structure of proteins and by implication the rate of fouling during membrane filtration. For example, Fane et al. (1983) reported that for short term tests, there was evidence of flux drop at pH 2 and pH 10 and an increase in produced flux at pH 5 when salt was added; while the flux was at minimum at pH 5 when salt was not added. This was attributed to the maximum adsorption of proteins occurring at the isoionic/isoelectric point of Bovine Serum albumin (BSA), when salt was added. Despite the adsorptive properties of the solids, the effect of pH on formation and performance of DM is illustrated in the observed impact on

the flux and morphological properties of the cake layer, leading to changes in the permeability of the DM.

2.7.4 Influence of pore size on DM formation and performance

Membranes and support materials are available in a range of pore sizes and this can have significant influence on the ability to retain solids in suspension. Ideally, the pore size of membranes should be small enough to prevent the passage of particles and suspended solids while being large enough to ensure passage of the liquid medium with 'acceptable' resistance. Typical contaminant particle sizes in wastewater are in the range of 0.001 to 100 µm, although most materials that contribute to the BOD and SS in municipal wastewater are less than 50 µm in size (Levine et al., 1985). The relationship between target contaminant size and membrane pore size exerts significant influence on membrane filtration in general and DM formation in particular. As expected, larger pore sizes should result in higher fluxes during operation for the same membrane materials. It has been observed that a smaller pore size in relation to the particle size favours cake layer formation through deposition above the surface of the membrane rather than the particles causing pore-plugging. For a given particle size distribution, the pore size of the membrane determines the pore blocking intensity. The particles that form the cake layer either attach to the membrane surface or are returned to the bulk suspension depending on the hydrodynamic conditions arising from forces due to flux, crossflow velocity and surface friction (Broeckmann et al., 2006).

For biological wastewater treatment, DM formation has been trialled on a wide range of pore sizes typically ranging between 10 µm and 500 µm (Ersahin et al., 2013, Park et al., 2004, Chu et al., 2014, Zhang et al., 2010, Fuchs et al., 2005). A much lower pore size could favour the development of DMs such that the cake layer could be formed quicker. This is in direct contrast to other studies in which DMs were formed on materials of larger pore sizes as stated above.

These differences may be assumed to depend on the operating conditions applied. The Carmen-Kozeny equation (equation 2.5) shows a correlation between specific resistance (α) with particle size diameter (dp), porosity (ε) and density (ρ).

$$\alpha = \frac{180\ dp\ (1-\varepsilon)}{\rho\ dp^2 \varepsilon^3} \qquad \text{(Equation 2.5)}$$

The correlation between MLSS concentration and specific cake resistance as given by the conventional cake filtration theory, can be expressed as equation 2.6 (Shimizu et al 1993)

$$R_c = \alpha\ v\ C_b \qquad \text{(Equation 2.6)}$$

Where R_c is the Cake Resistance, α is specific cake resistance, v is the volume of permeate per unit area ($m^3\ m^{-2}$) and C_b is the bulk concentration of the mixed liquor ($kg\ m^{-3}$).

A combination of equations (2.5) and (2.6) above yields equation 2.7:

$$R_c = \frac{180\ dp\ (1-\varepsilon)}{\rho\ dp^2\ \varepsilon^3} v\ C_b \qquad \text{(Equation 2.7)}$$

From equation 2.7, we can conclude that a relationship exists between particle size and cake resistance such that the smaller the particle size, the greater the resistance.

Particle size changes according to the mode of operation. For a side stream system, the effect of pump shear results in reduction in particle size (7-8 µm), compared to submerged system (20-40 µm)

2.8 Prospects and limitations of DM applications to wastewater treatment

Previous research focused on the properties of materials and conditions of formation as the main influences on the performance of DM: by adjusting these factors, filtration performance similar to microfiltration can be achieved (Ersahin et al., 2012, Ersahin et al., 2013, Loderer et al., 2012). Pre-coated DMs were mostly formed by either inert materials or precipitation of hydrous material such as Zr (IV) Oxide, Al (III), Fe (III), $Mg(OH)_2$ and Kaolin. For example, Al-Malack and Anderson (1996) showed that the DM layer formed by MnO_2 on a porous support had a 2 µm pore size which is less than ten times the pore size of the support layer. Also, Yang et al. (2011) were able to achieve a sustainable flux greater than 120 L m^{-2} h^{-1} using a combination of Kaolin and MnO_2 as formation materials to treat oily wastewater, although performance was affected by temperature. Noor et al. (2002) compared the performance of inert materials such as heavy and light kaolin, diatomite and Fuller's earth and concluded that Kaolin is the most effective in terms of performance. While DMs were created in such cases, the major disadvantage is the need to use external additives for its formation.

The application of Self-Forming Dynamic Membrane (SFDM) to municipal and domestic wastewaters, while promising, has been very limited. SFDM offers the benefit of using the intrinsic suspended solids organics in the wastewater to form the DM, avoiding the need for additives. Fuchs et al. (2005) attained a sustained flux between 50 and 150 L m^{-2} h^{-1} with a mesh filter treating activated sludge/raw wastewater at low pressures (between 3-10 mbar), even though the wastewater SS concentration was very low (112- 234 mg L^{-1}). In another study by Kiso et al. (2000), flux rates between 20-30 L m^{-2} h^{-1} were achieved using 100 µm mesh at TMPs of 10 mm head loss, although for very short operation cycles. In a longer test period of 120 days Satoh and Mino (2002) were able to achieve a flux rate of between 42 – 125 L m^{-2} h^{-1} using a coarse filter to produce good quality effluent without clogging.

Despite high flux and cleaner permeate, flux performance is varying and can be irregular. Cases of stable flux performance are rare but not impossible. Fan and Huang (2002) showed that stable flux of around 15 L m^{-2} h^{-1} was achievable after formation of DM in the treatment of municipal wastewater. It is interesting that the flux rates achieved were far higher than typical design flux rates expected for submerged membrane filtration systems (Fuchs et al., 2005).

The fluctuations in flux and effluent quality for SFDM is not unrelated to the uneven formation of the cake layer, as such the stability and porosity of the DM can be affected (Ping Chu and Li, 2005). Given the potential for achieving high flux with lower resistance in an anaerobic reactor, the major criteria for the application of DM is its stability, sustainability and removal efficiency over an extended period as most studies only focus on short term use and the effects of cleaning /regeneration are not well evaluated.

For aerobic systems, increase in the thickness of the cake layer results in the starvation of oxygen to the inner region of the cake resulting in death of bacterial cells and increased release of biopolymers (Meng et al., 2009). Consequently, control of the cake layer is one of the most critical aspects in membrane filtration. For most constant flux operations, a form of control or indication that cleaning is required is when the TMP reaches a certain pre-determined value, usually 0.6 bar (Zsirai et al., 2012), although (Alibardi et al., 2016, Zhang et al., 2010, Ersahin et al., 2014) had much lower values of around 20-25 kPa when the DM was operated away from the mixed liquor. At this point, the operation cycle is complete, and cleaning is required before the start of another filtration cycle. Several proposals have been made for either elimination of the fouling layer or control (of the cake layer) during filtration.

Though the two are linked, this section focuses on the control of the cake layer rather than elimination since the target is DM filtration and hence the cake layer is desirable, given certain conditions. This is because it is necessary to understand and target the optimum conditions under which the cake layer could provide the required filter while maintaining an acceptable pressure drop. The increase in flux results in a sharp decrease in the permeability of the cake layer due to its increased compression (Le-Clech et al., 2006), as the permeability of the cake layer is affected by flux, electrostatic interactions and particle size. Of particular interest with respect to cake aggregation, the presence of salt in the feed causes an increase in permeability due to higher electrolyte concentration.

To control the cake layer, shear is usually generated either by aeration in aerobic systems or by recirculating the biogas produced in an anaerobic bioreactor. These methods can reasonably be applied to the control of the cake layer in the DM. In most anaerobic DM systems surveyed, physical cleaning and gas recirculation were used as a control measure in submerged system and cross flow recirculation in side-stream membrane reactor system (Table 2.4). A study by Hong et al. (2002) showed that increasing the air flow rate in a submerged MBR lead to an increase in the permeate flux but only up to a critical point. High aeration or gas sparging rates can have a deleterious effect on the biomass in the reactor, however, causing breakage of flocs and increased soluble microbial products while also reducing the retention capacity of the DM (Fan and Zhou, 2007, Kiso et al., 2000). A comparison of several filtration modes (continuous, backwash and mixed) conducted by Wu et al. (2008) showed the mixed mode of operation lead to a low TMP and hydraulic resistance without affecting permeate productivity. A further analysis by the authors showed that applying a high flux (60 L m^{-2} h^{-1}) for short duration followed by low flux for a longer duration resulted in significantly lower resistance. A comparison of different filtration modes (continuous vs intermittent) by McAdam et al. (2005) showed that introducing a relaxation (off) time of two minutes to a 12-minute cycle improved the TMP by 80%. For DM formation, care must be taken when shear is applied as it could affect permeate quality. Sabaghian et al. (2018) found that the elevation of shear by aeration shear resulted in pore blocking/fouling rather than DM formation.

Table 2-4: Studies of Anaerobic Dynamic Membrane Bioreactors (AnDMBR) properties and control measures

Membrane configuration (sidestream or submerged	**Membrane configuration (Flat sheet, hollow fibre or tubular/ Pore size**	**Flux (L m^{-2} h^{-1})**	**Threshold TMP (kPa)**	**Constant Pressure or constant flux**	**Mode of filtration**	**Control measure**	**Ref.**
Sidestream/ External	Flat sheet	1.4-28	20	Constant flux	Continuous	Crossflow	(Alibardi et al., 2016)
Submerged/ Coupled to UASB	Flat sheet	65	25	Constant flux	Continuous	Physical cleaning	(Zhang et al., 2011)
Submerged/ Coupled to UASB	Flat sheet	6	40	Constant flux	Continuous	Physical cleaning	(Xie et al., 2014)
Submerged	Flat sheet	2.6	50	Constant flux	Filtration + backwash	Backwash and biogas recirculation	(Ersahin et al., 2014)
Submerged	Flat sheet/ 39µm	15	30	Constant flux	Filtration + Relaxation	Biogas recirculation/physical cleaning	(Yu et al., 2014)
Submerged	Flat sheet	3	n.a	Constant flux	Intermittent	Physical cleaning	(Jeison et al., 2008)
External	Flat sheet	0.5 - 3	n.a	varied	Intermittent	Physical cleaning	(Jeison et al., 2008)
Submerged/ Coupled to a UASB	Flat sheet/ 61µm	60	35	Constant flux	Continuous	Physical cleaning	(Ma et al., 2013a)
Submerged/	Flat sheet /75 µm	22..5	15-18	Constant flux	Continuous	Physical cleaning	(Hu et al., 2018)

2.9 Differences between municipal wastewater and industrial wastewaters and potential influence for dynamic membranes applications

Wastewater in general is classified according to its originating source. Municipal wastewaters are derived from residences, businesses and public facilities and as such represent a significant volume of the wastewater produced in a community. and fluctuates in both contents and volume due to changes in climate, seasonal variations and human activities (Metcalf & Eddy, 2013) . Municipal wastewater (without industrial sources) usually has a low concentration of organics due to higher dilution from domestic processes - bathing, washing, cooking etc., and is reflected in COD/TOC contents between 300/100 and 1100/330 mg L^{-1} (Metcalf & Eddy, 2013) . Industrial wastewaters or effluents are much more specific to the unit industrial processes present within the catchment area and although some variation is expected, are often less susceptible to changes. Due to the specificity of such activities, industrial wastewaters are further characterised according to the range of industries such as food processing, pulp and paper processes, produced water (oil and gas process), textile industries etc. Industrial wastewaters can contain recalcitrant compounds and the degree of treatment required is largely influenced by the target contaminants and expected treatment outcome. This makes industrial wastewaters some of the most challenging waters, for which its treatment requires careful consideration (Raper et al., 2018).

Due their potentially high organic contents (COD greater than 1000 mg L^{-1}), industrial wastewaters usually require characterisation and pre-treatment prior to discharge to either municipal wastewater treatment plants or receiving water bodies. Membranes have been applied to industrial wastewaters to remove target contaminants as they can enhance the ability of the biomass to acclimate to the specific characteristic of the wastewater, improving biological treatment (Dereli et al., 2012). Anaerobic membrane treatment of industrial wastewaters is characterised by fouling issues (compared to municipal wastewaters), and are due to the higher concentrations of organic and inorganic elements in their production process, increased loading rate and fluctuations in operational conditions (Dereli et al., 2012)

2.10 Conclusions and justification for this research study

In early studies on the application of DM to Reverse Osmosis (RO), the major problems encountered were mainly low and unstable flux and difficulties in controlling the DM-forming conditions. Recently, these problems have persisted (Ersahin et al., 2012). Whereas DM has been applied with much more success in aerobic systems (Kiso et al., 2000, Ren et al., 2010, Seo et al., 2007, Fan and Huang, 2002), due to the characteristic nature of aerobic biomass and operational conditions that allowed aeration of the bioreactor –aiding in maintenance of the DM. The major concerns about applying DM to anaerobic digesters are stability and sustainability due in part to very limited research. Failing this, unstable flux and high resistances are expected. The difficulties encountered in controlling the DM and lack of understanding of the formation and control of the cake layer are central to these challenges. Attempts at control of cake layer to improve resistance have been made using recirculation of biogas but have yielded little result, as evidenced by the persistent low operational flux (usually less than 3 L m^{-2} h^{-1}) and the need for frequent physical cleaning which can be a challenge when operated in submerged reactor configurations (Ersahin et al., 2014, Akram and Stuckey, 2008, Jeison et al., 2008). This implies that using the DM in a submerged application may not be optimal. Also, the few studies available on anaerobic DM reactors have focused on treatment of low strength municipal or domestic wastewater, with very little research carried out on its application to medium to high strength industrial wastewaters (Ersahin et al., 2012). That the DM can be used to mimic the use of conventional microfiltration membranes process through improved flux and reduced resistance is not in doubt. It can be suggested that the limitations observed in the use of DM in municipal wastewaters, can be attributed to its characteristic variability and low organic content. As such, these limitations can be overcome by applying DM to treat industrial waters capable of providing higher organic matter favourable for cake formation. In addition, there could be some benefit in purposefully pre-forming the DM in a controlled manner before deploying in treatment operations. There is also the possibility of integration of the DM with other digesters, as a post treatment in a low cost, robust and simplified approach that could be readily deployed for handling challenging food-processing wastewaters. The relatively high organic strength and lower volume of industrial wastewater compared to municipal wastewaters, offers the potential for small scale deployment which can be designed for specific industrial processes. Given the extent of research that has been carried out on high

rate digesters, this study proposes to build upon the existing knowledge of DM application, by investigating operational conditions central to the performance of DM, with the overall aim of combining this with functional anaerobic digesters for industrial wastewater treatment.

2.11 Research aim

The aim of this research is to investigate the potential of a low-cost anaerobic integrated system for the treatment of industrial wastewaters with low solids contents.

2.12 Objectives

- To investigate the impact of different operational conditions on cake formation and performance for dynamic membranes
- To assess the impact of solids concentration, initial imposed flux, TMP and induced mixing on DM formation and performance
- To test the influence of either gravity-driven filtration or pump-driven filtration on DM
- To investigate the potential for pre-formed DM- as an 'offline' conditioning as a filtration option of wastewaters of low TSS concentration
- To investigate the capacity of Anaerobic Filter (AF) and granular reactors (GD) and DM as an integrated process for the treatment of tomato-based wastewaters: In particular the impact of bioreactor and digestate type on the formed cake layer of the DM

Chapter 3: Methodology

3.1 General

Note: some of the following descriptions are based on standard methods used in the Environmental Engineering Laboratories at the University of Southampton and are therefore similar to parts of other theses from this group.

3.2 Reagents

Except where otherwise stated, all chemicals used were of laboratory grade and obtained from Fisher Scientific (Loughborough, UK)

3.3 Water

Unless stated, solutions and standards were prepared using ultra-pure deionised (DI) water obtained from a Barnstead Nanopure ultrapure water purification system (Thermo Scientific, UK)

3.4 Laboratory practice

All laboratory operations were conducted using good laboratory practice, having first carried out the appropriate risk assessments and, where necessary, COSSH assessments. All equipment, laboratory apparatus, and analytical instruments were operated in accordance with the manufacturer's instructions unless noted. All glassware was washed using washing detergent followed by rinsing with tap water and deionised water. The glassware used for the acid digestion was soaked in a 10% nitric acid bath for a 24 hour period after which the glassware was rinsed with Milli-Q water.

3.5 Monitoring and analytical methods

3.5.1 Total Solids (TS) and Volatile Solids (VS)

TS and VS determination were based on Standard Method 2540 G (APHA, 2005). After thorough agitation, approximately 10 g of sample was transferred into a weighed crucible by pipetting (digestate samples and substrate samples). Samples were weighed to an accuracy of ± 0.001 g (Sartorius LC6215 balance, Sartorius AG, Gottingen Germany) and placed in an oven (LTE Scientific Ltd., Oldham UK / Heraeus Function Line series, UK) for drying overnight at 105 ± 1 °C. After drying the samples were transferred to a desiccator to cool for at least 40 minutes. Samples were then weighed again with the same balance, transferred to a muffle furnace (Carbolite Furnace 201, Carbolite, UK) and heated to 550 ± 10 °C for two hours. After this ashing step, samples were again cooled in a desiccator for at least one hour before weighing a third time.

After all analyses, crucibles were washed with detergent, rinsed with deionised water, and stored in an oven until required for the next analysis. Crucibles were transferred from the oven to a desiccator for cooling to room temperature before each analysis. Total and volatile solids were calculated according to equations 3.1 and 3.2:

$$\%\ \mathrm{TS}\ = \frac{W_3 - W_1}{W_2 - W_1} \mathrm{x}\ 100$$

$$\%\ \mathrm{VS\ (on\ a\ wet\ weight\ basis)} = \frac{W_3 - W_4}{W_2 - W_1} \mathrm{x}\ 100 \qquad (3.1)$$

$$\%\ \mathrm{VS\ (on\ a\ TS\ basis)} = \frac{W_3 - W_4}{W_3 - W_1} \mathrm{x}\ 100 \qquad (3.2)$$

Where:

- W_1 = weight of empty crucible (g)
- W_2 = weight of crucible containing fresh sample (g)
- W_3 = weight of crucible and sample after drying at 105 °C (g)
- W_4 = weight of crucible and sample after heating to 550 °C (g)

3.5.2 Total and Volatile Suspended Solids

Total suspended solids (TSS) content was measured by passing a sample of known volume through a 0.4 µm pore size glass fibre filter paper (GF/C, Whatman, UK) of known dry weight (± 0.1 mg). After drying at 105 ^{o}C for 24 hours the paper was again weighed and the difference determined according to equation 3.3. For the Volatile Suspended Solids (VSS), the sample was further placed in a furnace operating at 550 ^{o}C for 2 Hours. After igniting for 2 hours, the sample was allowed to cool for at least half an hour before weighing and the VSS was calculated according to equation 3.4

$$\mathrm{TSS} = \frac{(\mathrm{W_2} - \mathrm{W_1})\ \mathrm{x}\ 1000}{\mathrm{V_s}} \qquad (3.3)$$

$$\mathrm{VSS} = \frac{(\mathrm{W_2} - \mathrm{W_3})\ \mathrm{x}\ 1000}{\mathrm{V_s}} \qquad (3.4)$$

Where:

VSS = Volatile suspended solids (mg L^{-1})

W_1 = weight of clean filter paper (mg)

W_2 = weight of filter paper + sample (mg)

W_1 = weight of clean filter paper (mg)

W_3 = weight of filter paper + sample after igniting at 550 C (mg)

Vs = sample volume (mL)

3.5.3 pH

pH was measured using a Jenway 3010 meter (Bibby Scientific Ltd, UK) with a combination glass electrode, calibrated in buffers at pH 4, 7 and 9.2. The pH meter was temperature compensated and had a sensitivity of ±0.01 pH unit and accuracy of 0.01±0.005 pH units. Buffer solution used for calibration was prepared from buffer tablets (Fisher Scientific, UK) prepared according to the supplier's instructions. During measurements, the sample was stirred to ensure homogeneity. In addition, the pH probe was rinsed with DI water in between measurements and placed into a mild acid solution to avoid cross-contamination.

Digestate samples were measured immediately after sampling to prevent changes in pH due to the loss of dissolved CO_2.

3.5.4 Turbidity

Turbidity was measured using a HI 93703 Turbidimeter (Hanna Instruments, UK). The Turbidimeter was calibrated with DI water as zero turbidity and turbidity standards of 10 and 500 NTU standard obtained from the same company. Measured turbidity was expressed in Nephelometric Turbidity Units (NTU) (APHA, 2005). For samples exceeding 40 NTU, a dilution with DI water was done according to equation 3.5

$$V_oS = \frac{3000}{T} \qquad \text{(Equation 3.5)}$$

Where:

- V_oS = volume of sample (mL) to be added to DI water to obtain the final value of 100 mL
- T = the Turbidity reading exceeding 40 NTU.

A portion of this diluted sample was then used for measuring the turbidity, and the actual turbidity reading was calculated from the obtained reading and converted using equation 3.6

$$T_a = \frac{T_n * 100\ \text{mL}}{VoS} \qquad \text{(Equation 3.6)}$$

Where T_n is the dilute turbidity reading and T_a = actual turbidity reading

3.5.5 Alkalinity

Alkalinity was measured by titration based on Standard Method 2320B (APHA, 2005). Digestate was sieved to obtain a homogenous sample and 5 ml of this was added to make up 50 mL of DI water. Titration was done using a Schott Titroline Easy automatic digital titration burette system (Schott, Mainz, Germany), with the samples being magnetically stirred while the titration was carried out. A 0.25 N H_2SO_4 titrant was used to determine endpoints of pH 5.7 and 4.3 allowing calculation of total (TA), partial (PA) and intermediate alkalinity (IA) (Ripley et al., 1986). PA is a measurement of bicarbonate buffering while IA is attributed to the buffering capacity of Volatile Fatty Acids (VFA).

The pH probe was calibrated before titration using buffers as described above and washed with DI water between subsequent samples to avoid cross contamination. Alkalinity was calculated according to the following equations 3.7-3.9:

$$TA = \frac{(V_{4.0} + V_{4.3} + V_{5.7}) \text{ x N x } 50000}{V} \quad \text{Equation 3.7}$$

$$PA = \frac{V_{5.7} \text{ x N x } 50000}{V} \quad \text{Equation 3.8}$$

$$IA = \frac{V_{4.3} \text{ x N x } 50000}{V_s} \quad \text{Equation 3.9}$$

Where:

TA = total alkalinity (mg $CaCO_3$ kg^{-1} WW)*

PA = partial or bicarbonate alkalinity (mg $CaCO_3$ kg^{-1} WW)

IA = intermediate or volatile fatty acid alkalinity (mg $CaCO_3$ kg^{-1} WW)

Vs = volume of sample (mL)

V_s = volume of titrant required to reach the pH value indicated in the subscript (mL)

N = normality of the H_2SO_4 titrant, or the theoretical normality multiplied by a correction factor for the specific batch of titrant

(- Samples were weighed and recorded as* mg $CaCO_3$ $kg^{-1,}$ wet weight (WW) *And in view of the high water content of the samples, it was assumed that the 1kg WW = 1L and was subsequently reported as* mg $CaCO_3$ L^{-1} *throughout the rest of this thesis)*

3.5.6 Total Ammonia Nitrogen

Total ammonia nitrogen (TAN) analysis was based on Standard Method 4500-NH_3 B and C (APHA, 2005). A sample aliquot of between 5 ml was weighed (i201, My Weigh Europe, Huckelhoven Germany) into a digestion tube and 50 mL of DI water added. Blanks (50 mL DI water). 5 mL of 10 M sodium hydroxide (NaOH) was added to each digestion tube to raise the pH above 9.5 and the samples were distilled using either a Foss Tecator Kjeltec system 1002 distillation unit (Foss Tecator A-B, Hoganas, Sweden) or a Büchi K-350 Distillation Unit (Büchi, UK). Erlenmeyer flasks previously filled with 25 mL of boric acid as an indicator were

used to collect the distillate and progress of the distillation was indicated by a colour change from purple to green. The distillate was titrated manually with 0.25N H_2SO_4 using a digital titration system (Schott Titroline, Gerhardt UK Ltd) until an endpoint was reached as indicated by a colour change to purple at which point the volume of titrant added was recorded. Standards and blanks were distilled in the same way. The TAN concentration was calculated according to the following equation 3.10:

$$\mathrm{TAN} = \frac{(\mathrm{A} - \mathrm{B}) \text{ x } 14.0 \text{ x N x } 1000}{\mathrm{V_s}} \qquad \text{(Equation 3.10)}$$

Where:

TAN = total ammonia nitrogen (mg L^{-1})

A = volume of titrant used to titrate the sample (mL)

B = volume of titrant used to titrate the blank (mL)

N = normality of the H_2SO_4 titrant, or the theoretical normality multiplied by a correction factor for the specific batch of titrant

V_s = volume of sample (ml)

3.5.7 Total Kjeldhal Nitrogen

Total Kjeldhal Nitrogen (TKN) analysis was carried out on duplicate samples alongside blanks and controls as follows: 5 mL was added to make up 50 mL sample and was placed in a glass digestion tube. Two Kjeltab Cu 3.5 catalyst tablets were added to facilitate acid digestion by lowering the activation energy of the reaction. 12 mL of low nitrogen concentrated H_2SO_4 was added carefully to each digestion tube and agitated gently to ensure that the entire sample was completely exposed to acid. The digestion tubes were then placed into the heating block with exhaust system using either a Foss Tecator 1007 Digestion System 6 (Foss Analytical, Hoganas Sweden) or a Büchi K-435 Digestion Unit (Büchi, UK) for approximately two hours until the solution colour became a clear blue-green. Both systems operated at 420 ± 5 ºC and once the reaction was completed the tubes were cooled to around 50 ºC and 40 ml of DI water slowly added to the digestion tube to prevent later crystallisation on further

cooling. Samples, blanks and standards were then distilled and titrated as for Total ammonia nitrogen.

$$\mathrm{TKN} = \frac{(\mathrm{A} - \mathrm{B})\ \mathrm{x}\ 14.0\ \mathrm{x}\ \mathrm{N}\ \mathrm{x}\ 1000}{\mathrm{W_s}} \qquad \text{Equation 3.11}$$

Where:

TAN = total ammonia nitrogen (mg kg^{-1} wet weight)

A = volume of titrant used to titrate the sample (ml)

B = volume of titrant used to titrate the blank (ml)

N = normality of the H_2SO_4 titrant, or the theoretical normality multiplied by a correction factor for the specific batch of titrant

W_s = wet weight of sample (kg)

3.5.8 Chemical Oxygen Demand

Chemical Oxygen Demand (COD) was measured by the closed tube reflux method with titrimetric determination of the end point (Environment Agency, 2007). If the sample COD was more than 400 mg L^{-1} pre-dilution was carried out. 2 mL of sample (or 2 mL DI water for blanks) was placed into the reflux tubes followed by the addition of 3.8 ml of FICODOX-plus reagent (Fisher Scientific Ltd, UK), the composition of which is shown in Table 3-1. The tube was sealed with a PTFE screw cap and the mixture refluxed at 150 ^{o}C for 2 hours. After cooling, a few drops of ferroin indicator (Fisher Scientific Ltd, UK) (Table 3-2) were added and the mixture titrated with acidified (2% Sulphuric acid) 0.025N ferrous ammonium sulphate (FAS) solution, the Molarity of which was calculated using equation 3.23. The end point was a colour change from blue to red. Although the salt content of the concentrated tomato juice was 4.7 g L^{-1} and since the samples tested was very dilute, therefore silver nitrate was the not used. COD values were calculated according to the equations 3.12 and 3.13:

$$\mathrm{M} = \frac{0.625}{\mathrm{V}} \qquad \text{Equation 3.12}$$

$$\mathrm{COD} = \frac{(\mathrm{A} - \mathrm{B})\ \mathrm{x}\ \mathrm{M}\ \mathrm{x}\ 4000}{\mathrm{dilution}} \qquad \text{Equation 3.13}$$

Where:

M = molarity of FAS

V = volume of FAS titrated in molarity measurement (ml)

COD = Chemical oxygen demand of sample (mg O_2 L^{-1})

A = average volume of FAS used for blank (mL)

B = volume of FAS used for sample (mL)

Table 3-1 : Ficodox-plus composition

Chemical	Concentration
Potassium di-chromate	1.7 g L^{-1}
Silver sulphate	8.1 g L^{-1}
Sulphuric acid	81.1%

Table 3-2: Ferroin indicator composition

Chemical	Concentration
1,10-phenantroline monohydrate	14.85 g L^{-1}
Iron (II) sulphate heptahydrate	6.95 g L^{-1}

3.5.9 Total Organic Carbon

Total Organic Carbon (TOC) was measured by Dohrmann TOC Analyser (DC-190), USA following the manufacturer's manual and method which is based on Standard Method 5310 (APHA, 2005). In all analytical runs, the linearity of the instrument was checked using standard solutions of 50, 500 and 1000 mg L^{-1} of potassium hydrogen phthalate (KHP) and Sodium Carbonate (Na_2CO_3) previously dried at 105 ^oC. Soluble TOC was centrifuged at 5000 *g* prior to filtration through a 0.45 µm syringe filter before measurement.

3.5.10 **Volatile fatty acids**

The method used was based on SCA (1979): Determination of Volatile Fatty Acids in Sewage sludge (1979). Samples were prepared for analysis by centrifugation at 13,000 rpm (micro-centrifuge, various manufacturers) for 15 minutes. The supernatant was diluted with deionised water as appropriate to obtain a maximum acetic, propionic, iso-butyric, n-butyric, iso-valeric, valeric, hexanoic and heptanoic concentration of 500 mg L-1 and the final formic acid composition was adjusted to 10 % vol. The diluted sample was filtered with a 0.45µm syringe filter to obtain a clearer sample. The supernatant after acidification and filtration was transferred into the vials and loaded onto the GC auto-sampler ready for the VFA measurement.

A standard solution containing acetic, propionic, iso-butyric, n-butyric, iso-valeric, valeric, hexanoic and heptanoic acids, at three dilutions to give individual acid concentrations of 50, 250 and 500 mg L^{-1} respectively, was used for calibration and also loaded onto the GC.

Quantification of the VFA was by a Shimazdu GC-2010 gas chromatograph (Shimadzu, Milton Keynes, UK), using a flame ionization detector and a capillary column type SGE BP-21. The carrier gas was helium at a flow of 190.8 mL min^{-1} and a split ratio of 100 to give a flow rate of 1.86 mL min^{-1} in the column and a 3.0 mL min-1 purge. The GC oven temperature was programmed to increase from 60 to 210 ^{o}C in 15 minutes with a final hold time of 3 minutes. The temperatures of injector and detector were 200 and 250 ^{o}C, respectively.

Total VFA concentration is reported as sum of the single compounds (acetic, propionic, iso-butyric, n-butyric, iso-valeric, valeric, hexanoic and heptanoic acids).

3.5.11 **Elemental Composition**

Carbon, Hydrogen and Nitrogen contents of samples were determined using a Flash EA 1112 Elemental Analyser (Thermo Finnigan, Italy). Samples were air dried in a freeze drier and milled to obtain a homogenous sample. Sub-samples of approximately 0.3-0.4 mg were weighed into standard weight tin disks using a five-decimal place analytical scale (Radwig, XA110/X, Poland). These were placed in a combustion/reduction reactor held at 900°C then flash combusted in a gas flow temporarily enriched with oxygen resulting in a temperature greater than 1700 ^{o}C and the release of N_xO_x, CO_2, H_2O and SO_2 (depending on the composition of the sample). The gas mixture was then analysed by GC with the different

components measured by appropriate detectors. The working conditions of the elemental analyser were as described in the manufacturer's technical literature and method sheets. The standard used in this analysis was birch leaf.

3.5.12 Methane and Carbon dioxide

Biogas composition was quantified using a Varian Star 3400 CX gas chromatograph (Varian Ltd, Oxford, UK). The GC was fitted with a Hayesep C column and used argon as the carrier gas at a flow of 50 mL min^{-1} with a thermal conductivity detector. The biogas composition was compared with a standard gas containing 65 % CH_4 and 35% CO_2 (v/v) for calibration (BOC, UK). A sample of 10 mL was taken from a gas-impermeable bag used for sample collection and was injected into a gas-sampling loop.

3.5.13 Gas volume

Biogas was collected in gas-impermeable sampling bags affixed to each reactor. Gasbag volumes were measured using a weight-type water displacement gasometer Walker et al. (2009) (The measurement procedure was as follows: the initial height of solution in the gasometer (h1) was recorded before the collected gas was introduced into the column through the top valve. After the bag was empty, the final height (h2) and the weight of water (m) were recorded, as well as the temperature (T) and pressure (P) in the room. All gas volumes reported are corrected to standard temperature and pressure of 0^{o}C, 101.325 kPa as described by Walker et al. (2009) according to the following equations 3.25 and 3.26. The weight method was adopted for all gas measurements, and the height method was used only as a check on gross measurement errors

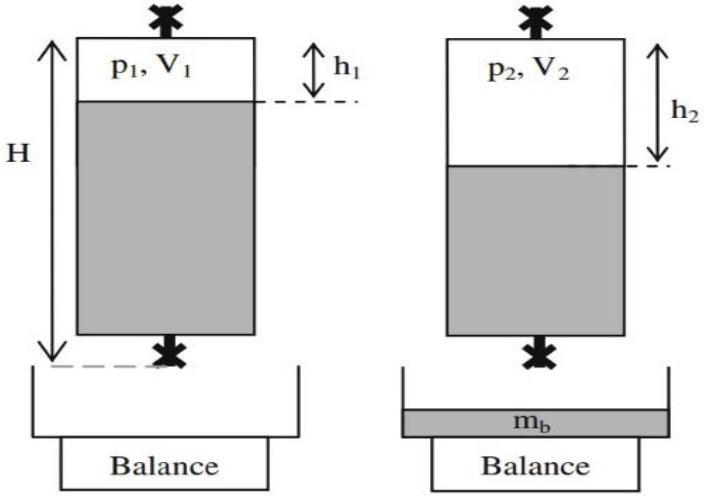

Figure 3-1: Diagram of set-up for weight-type gas measurement using liquid displacement

- Height Gasometer Governing Equation Equation 3.25

$$V_{stp} = \frac{T_{stp}A}{T_{atm}p_{stp}}\left(\left(p_{atm} - p_{H_2O}(T_{atm}) - \rho_b g\left(h_{t2} - h_{c2}\right)\right)h_{c2} - \left(p_{atm} - p_{H_2O}(T_{atm}) - \rho_b g\left(h_{t1} - h_{c1}\right)\right)h_{c1}\right)$$

- Weight Gasometer Governing Equation Equation 3.26

$$V_{stp} = \frac{T_{stp}A}{T_{atm}p_{stp}}\left[\left(\left(P_{atn} - p_{H_2O}(T_{atm}) + \rho_b g\left(H - h_1 - \frac{m_b}{A\rho_b}\right)\right)\left(h_1 + \frac{m_b}{A\rho_b}\right)\right) - \left(p_{atn} - p_{H_2O}(T_{atm}) + \rho_b g(H - h_1)\right)h_1\right]$$

Where:

V = gas volume (m^3)

P = pressure (Pa)

T = temperature (K)

H = total height of column (m)

h = distance to liquid surface from a datum (m)

A = cross-sectional area of gasometer (m2)

M_b = mass of barrier solution (kg)

ρ = density of barrier solution (kg m^{-3})

g = gravitational acceleration (m s^{-2})

1, 2, stp, atm, b, t, c subscripts refer to condition 1 (before addition of gas to column), condition 2 (after gas addition to column), standard temperature and pressure, atmospheric, barrier solution, collection trough and column respectively.

3.5.14 Biogas volumetric production

The biogas volumetric production was determined using **Error! Reference source not found.**

$$B_{vol} = \frac{(Biogas\ V_{stp})(\tau)}{V_R} \qquad \text{Equation 3.25}$$

Where:

B_{vol} = daily biogas production per litre of reactor (L L^{-1} day^{-1})

$Biogas\ V_{stp}$= measured biogas volume (L day^{-1}) from ***Error! Reference source not found.*** *

τ = percentage of CH_4 plus CO_2 of the gas composition (%); not normalised

*The biogas quantification method used the gas volume **Error! Reference source not found.** without the correction factor for water vapour as when the measured volume of biogas is multiplied by the not-normalised CO2 and CH4 fraction of the biogas composition the volume of other gases, including the dissolved air introduced through the influent and the water in form of vapour, is automatically taken into account.

3.5.15 Contact angle measurement

Contact angle analysis was carried out using the DSA100 Drop shape analyser. A single water droplet (around 1 µL) was applied to the material surface using a 500 µL PTFE-lined syringe (Kruss Ltd, UK). Several measurements were made and the average of three values was read as the contact angle for the material.

3.5.16 Particle Size Analysis (PSA)

Particle Size Analysis was carried out using a Mastersizer 2000 (Malvern, UK) equipped with an auto-sampler and connected to a dedicated computer. A well-mixed, representative sample volume of 10-20ml (depending on the signal obscuration range reading on the computer) is gently poured into the auto-sampler receptacle. The autosampler receptacle contains deionised water as the liquid dispersant and is equipped with a stirrer. The volume of the liquid dispersant is automatically set by the equipment. The autosampler disperses

the sample in suspension before delivering it to the optical bench. The optical bench provides the laser beam and captures the scattering pattern initiated by the optical beam. Malvern software installed in the computer retrieves and processes the data, reporting particles in size range of 0.02 to 2000 µm in terms of percentage volume per size class which is saved on the computer.

3.5.17 **Imaging-Fixing and Scanning Electron Microscopy (SEM)**

The samples were carefully cut from the membrane and immersed in a primary fixative comprising 3% glutaraldehyde, 4% formaldehyde in 0.1 M Piperazine-NN'-bis-2-ethanesulphonic acid (PIPES; Fisher Scientific, UK) buffer, held at pH 7.2. at room temperature for 30 mins and then stored at 4 ºC for up to five days prior to further processing. Specimens were then rinsed in 0.1M PIPES buffer, postfixed in 1 % osmium tetroxide (Oxkem, Oxford, England) in 0.1 M PIPES for one hour, rinsed in two changes of buffer and dehydrated in an ethanol series, critical point dried and mounted on stubs. These were then sputter coated in gold palladium and viewed on a FEI Quanta 250 scanning electron microscope (Eindhoven, Netherlands) in high vacuum mode situated at the Biomedical Imaging Centre, Southampton General Hospital, UK.

3.6 **Materials**

3.6.1 Membrane materials

Nylon mesh, and woven and non-woven polypropylene meshes (Cadisch, UK) of nominal pore sizes 20 µm were used as DM support materials.

3.6.2 Anaerobic filter support media

The media used for the AF digester were the K1 plastic wheel type carriers originally developed by Kaldnes Miljoteknolog, Norway (Figure 3-2), with the properties shown in Table 3-3.

Figure 3-2: Plastic K1 biofilm support carriers used in the digesters

Table 3-3: Properties of filter media for biofilm support

Characteristics	**Value/description**
Material	High Density polyethylene (HDPE)
Void ratio (%)	80 -85
Specific Surface area (m^{-2} m^{-3})	500
Specific gravity	0.96

3.6.3 Digestate and inoculum

Digestate from a mesophilic anaerobic digestion plant treating municipal wastewater biosolids in at Millbrook Wastewater Treatment Plant (WWTP) operated by Southern Water Ltd in Southampton, UK was used to represent digester contents in batch experiments and as inoculum for anaerobic filter experiments. Before use, in batch tests and as inoculum, the digestate was screened through a 1 mm sieve to remove larger particles. The digestate was diluted with tap water to the required TSS concentration before use in batch tests. The properties of the digestate as supplied, and after screening with 1mm sieve are presented in Table 3.4

Table 3-4: Typical properties of Millbrook digestate after screening with 1mm sieve

Parameter	Value
pH	7.3 ± 3
TS (g L^{-1})	40.5 ± 0.01
VS (% TS)	69.4 ± 0.14
TSS (g L^{-1})	38.2 ± 0.28

3.6.4 UASB inoculum

The granular digestate used as inoculum for the UASB -type digester was obtained from a wastewater treatment plant for processing pulp and paper wastewater (Kent, UK). The anaerobic granules (Figure 3-3) were first rinsed under running tap water and to remove fines and had TS and VS values of 145 ± 0.2 g L^{-1} and 116 g L^{-1} respectively.

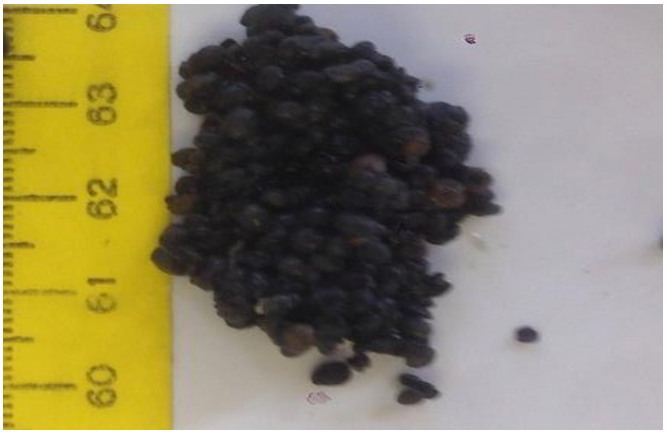

Figure 3-3: Granular digestate used as inoculum for the UASB-type digesters

3.6.5 Feedstock

Tomato juice used to simulate tomato-processing wastewater was bought from Aldi, UK made from concentrate in 1 L boxes. Figure 3-4 shows a photo of the label with the typical nutritional values. Depending on the OLR, the weekly concentrate was prepared by pouring out the required volume of concentrated juice, stirring for several minutes with a magnetic stirrer and then storing in a fridge at 4 ºC. This concentrated juice was used to prepare the required daily feed.

Figure 3-4: Tomato juice used as substrate, showing nutritional information.

3.7 Equipment

3.7.1 Membrane module

DM support material carrier cartridges were purpose-designed and 3-D printed (Duplicator 4S, Wanhao Ltd) for this work. The membrane module was produced from plastic PLA material as a flat sheet plate with features and dimensions presented in Figure 3.5. The main section was 3-D printed whereas the flanges used to hold the material in place were cut out of thin film PVC plastic (thickness = 2 mm) and used to hold the support material in place, attached with the aid of screws. The effective membrane surface filtration area of the membrane module was 0.0096 m^2. A 6 mm diameter hole was bored on the top side to provide a connection to a tube through which suction was applied and the permeate was drawn during operation.

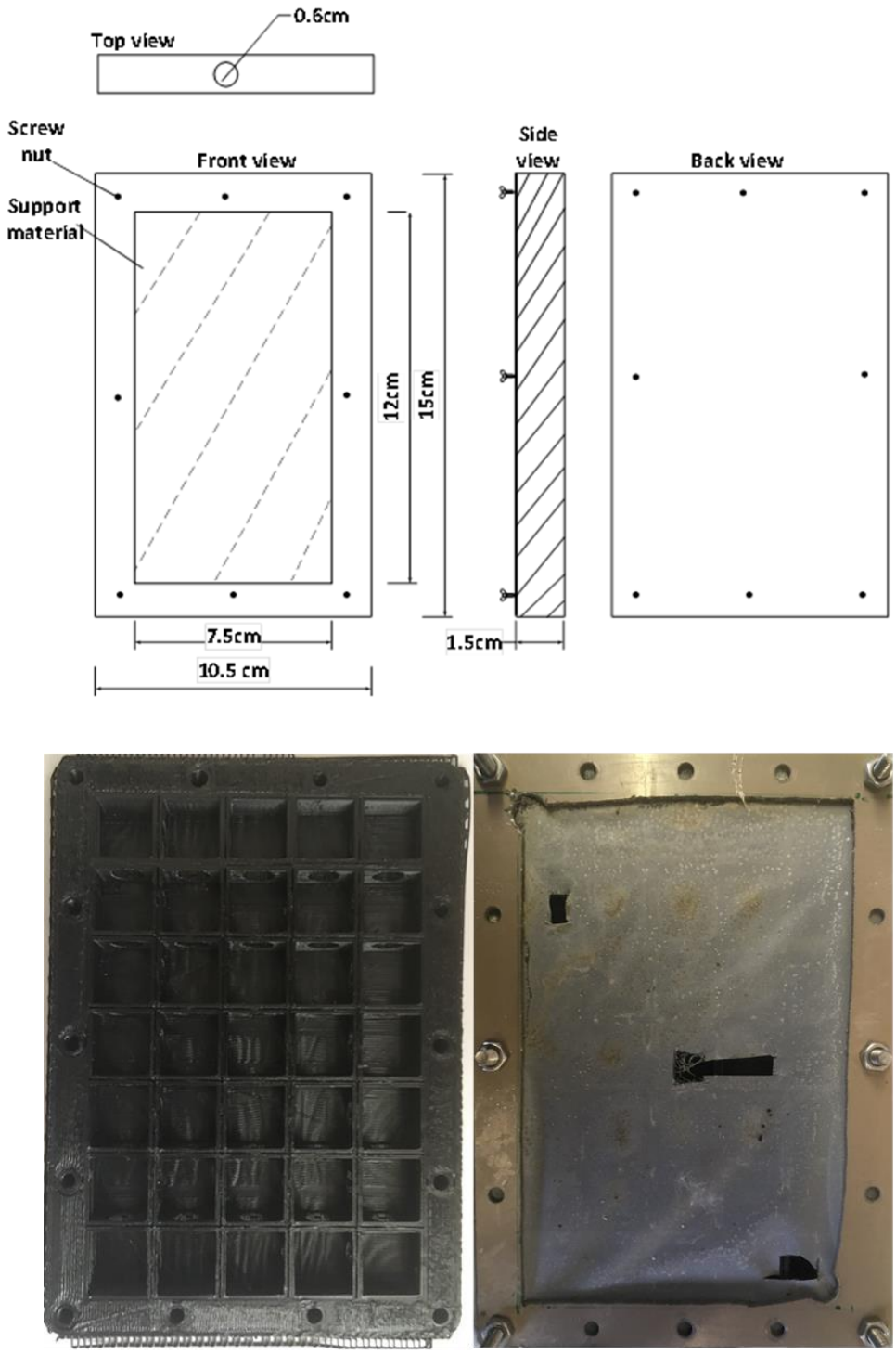

Figure 3-5: Top - DM module dimensions and photos of sample the DM carrier module main frame after 3D printing. Bottom – assembled, used DM with nylon mesh (with pieces sampled for analysis)

3.7.2 Cold batch test rig

The sketch and photos of experimental set-up for cold batch testing of DM formation is shown in Figure 3-6 and Figure 3-7 respectively and consisted of three parallel systems. In each case, a membrane module was submerged into a 4-L PVC tank which was continuously mixed by a stirrer with adjustable speed controlled by a voltage regulator. Filtration was driven by a peristaltic pump (Watson Marlow 323, UK). A pressure sensor (-1 to +6 bar, Hydrotechnik, UK) connected to a data acquisition system (Labjack, U3-LV) was used to measure the suction pressure which was recorded on a computer. The values of suction pressure and TMP are reported as positive quantities in relation to local atmospheric pressure (i.e. gauge pressure). An electronic balance (Adam Equipment, UK) recorded the accumulated weight of permeate every minute. A liquid level sensor on the permeate collector activated a return pump (12V DC, diaphragm pump) to return the filter contents into the main tank in order to maintain constant concentration and volume. Tests were carried out under ambient temperature which ranged from 12-20 ^{o}C without temperature control.

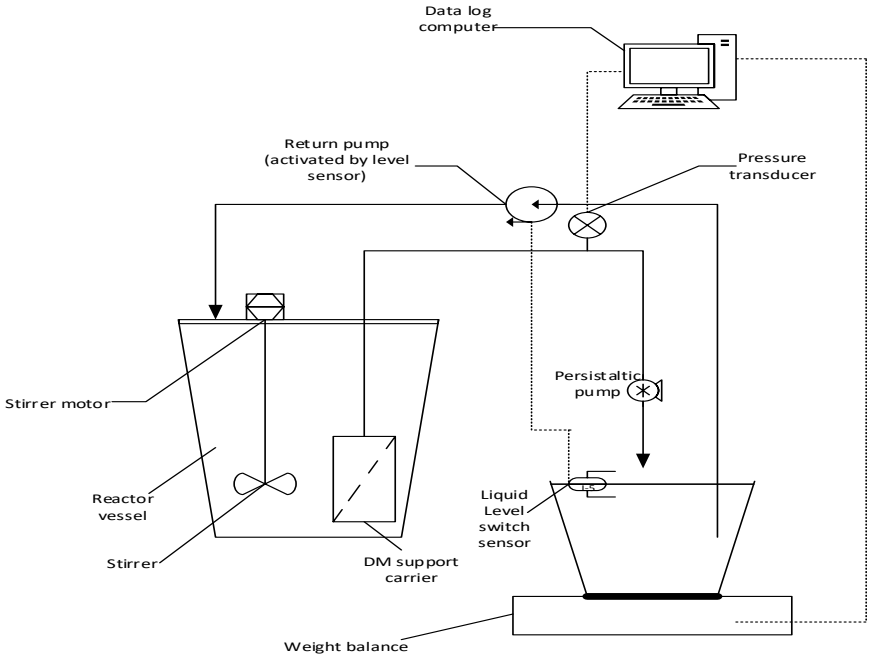

Figure 3-6: Schematic of batch test set-up

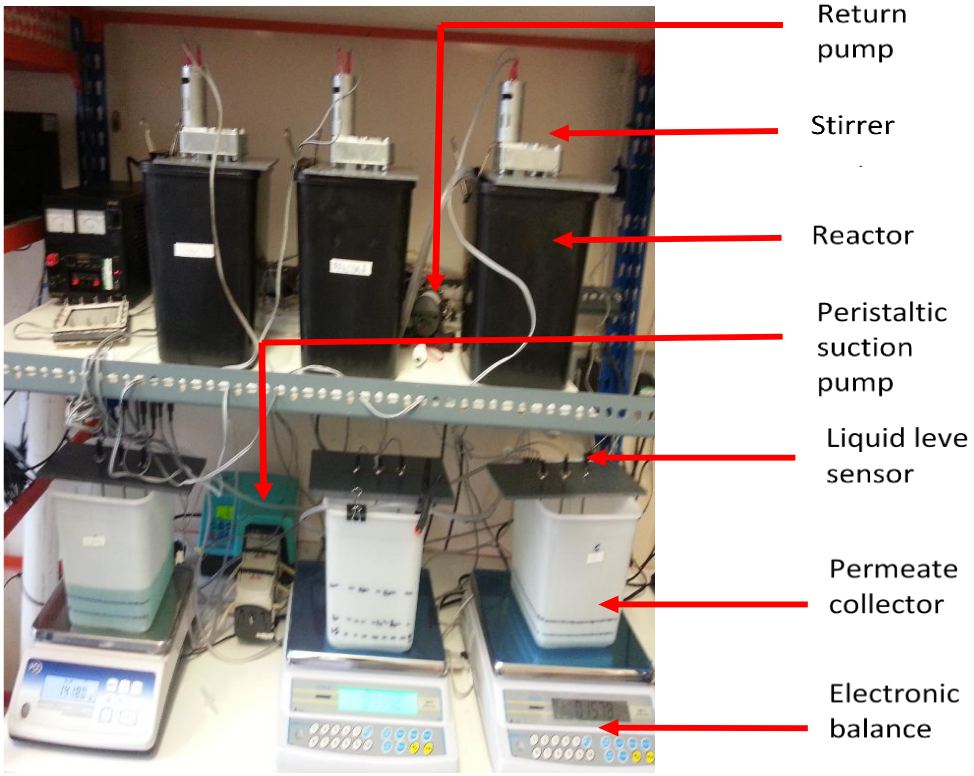

Figure 3-7: Photo of experimental set-up for batch tests

3.7.3 Semi-continuous Anaerobic Filters and Upflow Anaerobic Sludge Blanket Reactors

Anaerobic filters: Two anaerobic filters (AF) were used, each with a total volume of 4.5L litres and a working volume of 2.6 litres. A schematic drawing of a digester is shown in Figure 3-8. The AF were constructed from uPVC pipe with a nominal internal diameter of 10 cm, and a top flange to which a top plate was secured using stainless steel bolts and wing nuts. A gas-tight seal between the top plate and the digester flange was maintained using closed pore neoprene gasket. The top plate was fitted with a gas outlet connector and a feed port sealed with a rubber bung. Effluent was removed via a 15 mm diameter outlet port at the base of the AF. Temperature was maintained at 30 ± 2 ºC by water from a thermostatically controlled water-bath (set at a slightly higher 33 ºC to compensate for heat losses), circulating through an internal heating coil inside the digester. The reactors were also fitted with an IC temperature probe connected to a data logging device (U3-LV, LabJack USA) for continuous recording.

When assembled, and before filling, each AF was tested for gas leaks by applying a small positive pressure to the digester and submerging in water to ensure there was no gas escape when all ports were sealed. The digesters were connected to gas-impermeable bags which continuously collected biogas produced throughout the digestion period. Effluent was collected via an internal tube of 2 cm diameter working to drain the liquid from the top level of the tube.

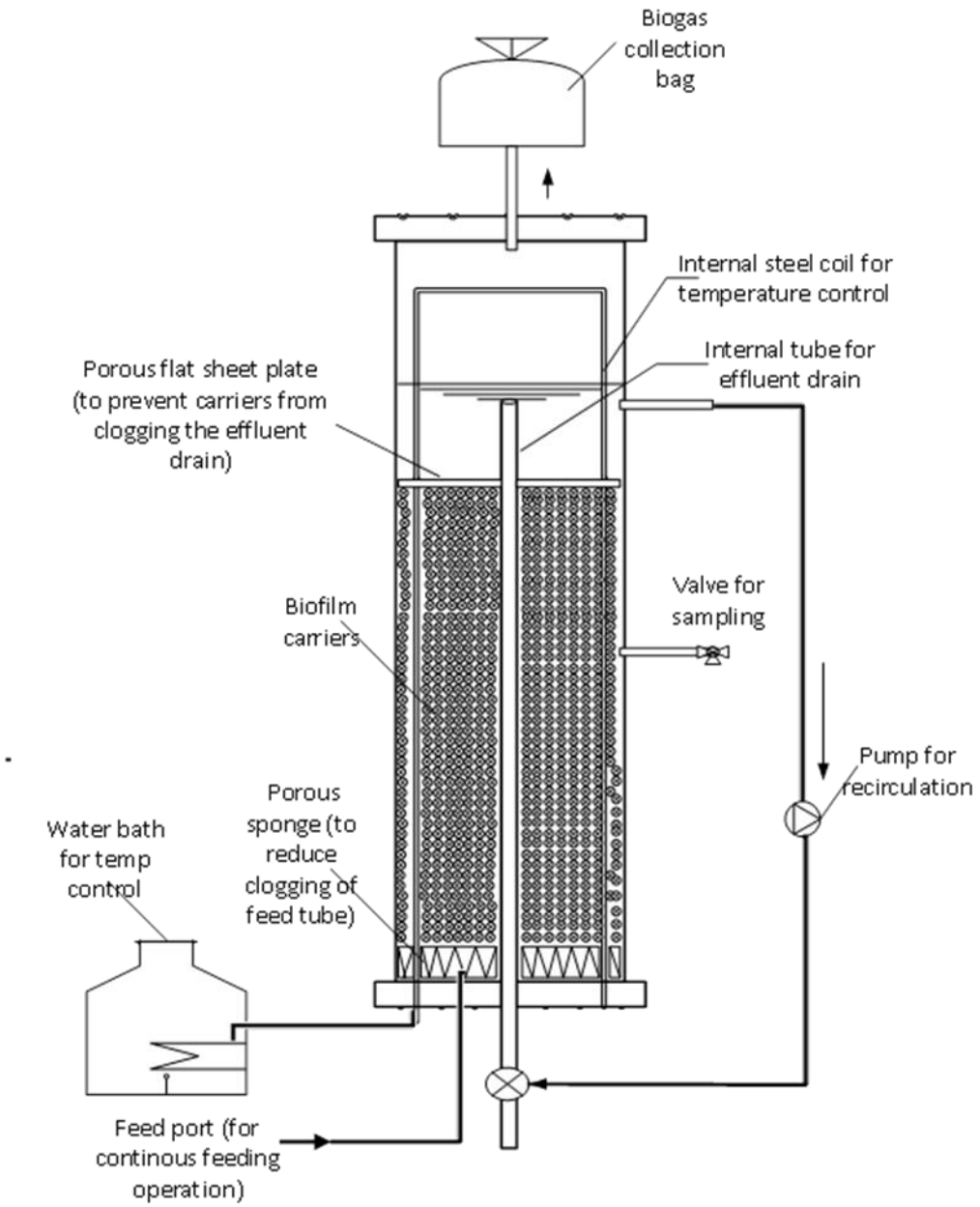

Figure 3-8: Schematic of the AF digester

3.7.4 Upflow Anaerobic Sludge Blanket

A second set of two reactors of identical dimensions but inoculated with granular sludge was also set up to operate as Upflow Anaerobic Sludge Blanket (UASB) reactors. The reactors functioned as an upflow feeding system with an internal tube of 2 cm diameter to enable discharge of effluent at the working level of 50 cm from the bottom of the reactor.

Table 3-5: Digester properties and dimension

Digester properties	Measurement
Height (cm)	56
Diameter (cm)	10
Volume (L)	4.5
Working volume (L)	4
Filter media height (cm)	30
Filter media porosity (%)	85

3.7.5 Coupled DM

For the long-term experiment, a DM was coupled to a pair of anaerobic filter. A second DM was also operated by coupling with a pair of UASB digesters. Each set of reactors provided the effluent to feed one DM unit submerged externally in a 3-L closed vessel. The 3-L vessel was equipped with a float level sensor that activated a peristaltic pump (Watson Marlow, UK) to enable intermittent operation based on the liquid level in the vessel. The cycle was such that the liquid level sensor switched on the pump switched on the pump at the higher liquid level and switches of at the lower liquid level. A pressure sensor (-1 to +6 bar, Hydrotechnik, UK) was placed in the permeate tube. The pressure sensor measured the change in pressure and the signal was converted with the use of a data acquisition device (LabJack, USA) connected to a computer for data capture and saved on the dedicated computer. Permeate was collected in a container placed on a laboratory scale (Adam, UK) which recorded the weight (kg). The complete set-up is as shown in Fig 3-9. The feed was stored in a plastic tank equipped with a stirrer, which was kept in a refrigerator at a temperature of 5 ºC

Figure 3-9: Photo of set-up for long-term experiments

The digesters were operated in a continuous mode, i.e. fed daily with a specific amount of feedstock added and effluent removed to maintain a constant volume in the digesters.

3.8 Calculations

3.8.1 Organic Loading rate

The organic loading rate (OLR) was determined according to equation 3.27

$$OLR = \frac{COD_S V_S}{V_r} \qquad \text{Equation 3.27}$$

Where:

- COD_s is the chemical oxygen demand of substrate daily added to the reactor (g COD L^{-1})
- V_s is the volume of the substrate added per day (L d^{-1})

- V_r is the volume of reactor (L)

3.8.2 Hydraulic Retention Time

The Hydraulic Retention Time (HRT) of the digester is expressed in equation 3.28

$$HRT = \frac{V_{reactor}}{Q}$$ Equation 3.28

Where:

$V_{reactor}$ is the working volume of each reactor (L)

Q is the daily flow of material (substrate added) through the reactor (L day^{-1})

The amount of substrate and digestate was measured in g but for ease of calculation it was assumed that both the substrate and digestate had a specific gravity of 1.0. Therefore, 1 g of substrate and digestate was considered to be equivalent to 1 mL.

3.8.3 Specific Biogas Production

The specific volumetric biogas production was calculated using Equation 3.29. The volume of gas was measured and presented based on standard temperature and pressure.

Specific biogas production = $\frac{V_{biogas}}{OLR \times V_{reactor}}$ (Equation 3.29)

Where:

- V_{biogas} is the volume of biogas produced daily (L day^{-1})
- OLR is the organic loading rate (g COD L^{-1} day^{-1})
- $V_{reactor}$ is the volume of reactor (l)

3.8.4 Specific Methane Production

Specific methane production is calculated according to equation 3.30

Specific methane production = $\frac{V_{CH4}}{OLR \times V_{reactor}}$ (Equation 3.30)

Where:

- V_{CH4} is the volume of methane produced daily (L^{-1} day^{-1})
- OLR is the organic loading rate (g COD L^{-1} day^{-1})
- $V_{reactor}$ is the volume of reactor (L)

3.8.5 Destruction of Chemical Oxygen Demand (COD) or Total Organic Carbon (TOC)

The destruction of COD or TOC was calculated as given in equation 3.31:

$TOC_{removed} = OLR - (Q)(TOC_e)$ (Equation 3.31)

Where:

- $TOC_{removed}$ = TOC removed (g TOC day^{-1})
- TOC_e = TOC in effluent (g TOC day^{-1})

TOC removal rate (R) = $\frac{TOC_{removed}}{OLR}$ %

3.8.6 Membrane flux

Membrane flux was determined based on the weight of the effluent from the DM vessel, which was collected and recorded at 5 minutes interval. The flowrate was determined using equation 3.32 for which the calculation of the flux is given as equation 3.33

$$Q = \frac{W_{i+5} - W_i}{(\rho)\,(t)} \left(\frac{60min}{hr}\right) \quad \text{(Equation 3.32)}$$

$$\text{Flux (J)} = \frac{Q}{A} \quad \text{(Equation 3.33)}$$

Where

- Q = Flowrate ($L\ h^{-1}$)
- W_i = Initial weight (kg)
- W_{i+5} = weight (kg) after set time

- ρ = density of permeate (kg m^{-3}, assumed to be 1000)
- J = Flux (L m^{-2} h^{-1})
- A = Area of the membrane (m^2)

3.8.7 Resistance

The resistance model used was based on Darcy's law and is presented as equation 3.34

$$R_t = \frac{\Delta TMP}{\mu J} \quad \text{(Equation 3.34)}$$

Where

- R_t = Total resistance (m^{-1})
- ΔTMP = change in transmembrane pressure (Pa)
- μ = viscosity of the liquid (Pa s)
- J = instantaneous flux (m^3 m^{-2} s^{-1})

Furthermore, the Total resistance (R_t) can be broken down into Cake Resistance (R_c), gel resistance (R_g) and support material's intrinsic resistance (R_m) as shown in Equation 3.9

$$R_t = R_m + R_g + R_c \quad \text{(Equation 3.9)}$$

These resistances were determined experimentally as follows:

- R_c is the resistance developed during filtration of liquid of known solids concentration
- R_g is the resistance of cleaned material measured using tap water
- R_m is the resistance of virgin, unused material measured using tap water

Chapter 4: Understanding the impact of different operational parameters on the formation and performance of DM

4.1 Introduction

This chapter covers results of batch tests carried out for evaluation of the materials and hydrodynamic conditions suitable for the development and performance of the DM. The tests carried out include the effect of material type and characterisation, total suspended solids concentration, mixing type and intensity and the effect of imposed TMP based on gravity-driven constant head. Also, the possibility of pre-forming DMs with digestate and applying the pre-formed DMs to low TSS wastewater treatment was testes and evaluated.

The aim of this part of the work was to select a suitable material to act as support layer for DM, from three options: nylon, woven polypropylene and non –woven polypropylene. The selection was based on the following parameters

- Solids concentration (expressed as turbidity) of permeate
- Resistance profile of DM

Upon selection, the selected choice was analysed for the effect of

- Solids concentration
- Mixing type
- Mixing intensity (rpm)
- Imposed flux (based on gravity-driven constant head)

The experiment was designed to evaluate the formation characteristics of DM for each of the materials. This involved the filtration of a given volume and concentration of substrate. 4 L vessels were used for the experiment which was conducted by filtering and returning permeate in a continuous loop with the aid of peristaltic pumps. The permeate was collected and weighed to determine the flux as a means of assessing how the membrane blockage and the cake layer formation develop. The substrate used in this

case was a liquid digestate of known solids concentration diluted with tap water to desired target concentration. The TMP profile and flux rates were measured as indicators of performance and the change in permeate turbidity was used as an indication of retention capacity of the cake layer being formed.

4.2 Characterisation of support materials tested

Three intrinsically different support materials, namely nylon mesh, woven polypropylene and non-woven polypropylene mesh (Figure 4-1) of the same pore size of 20 µm, were analysed. At first, a series of characterisation tests, necessary to establish a baseline for all materials was carried out. The intrinsic material resistance of all three fabrics was measured under gravity flow and at a constant head of 1 m with clean tap water as the substrate medium. In addition, the contact angle of the materials was measured using de-ionised water.

Table 4-1: Properties of the support materials

Material	**Contact angle (°)**	**Average instantaneous flux (L m^{-2} h^{-1})**	**Resistance (X $10^{10} m^{-1}$)**	**Permeability (L m^{-2} h^{-1} bar)**
Nylon	113	693	5.18	6931
Woven polypropylene	120	683	5.23	6865
Non-woven Monofilament polypropylene	109	681	5.27	6814

Table 4-1 shows the results of characterisation tests of the new, unused support materials. The values of resistance were very similar when subjected to clean water tests. Nylon has the least resistance of all three with a value of 5.18 X 10^{10} m^{-1} compared to

woven and non-woven polypropylene with resistances of 5.23 X 10^{10} m^{-1} and 5.27 X 10^{10} m^{-1} respectively. Similarly, in terms of permeability, monofilament was the least permeable although only slightly lower than the nylon and multifilament materials. As can be inferred from the contact angle of the materials (Table 4-1), all materials are hydrophobic since the contact angles are above 90º, with the order of hydrophobicity being non-woven woven polypropylene > nylon > woven polypropylene.

Intrinsic resistance values have been obtained for similar materials of different sizes. For instance, the resistance values obtained were similar to those found by Li et al. (2011) who also observed that nylon mesh had least resistance compared to other woven and non-woven materials. Ersahin et al. (2013) found higher resistance values for monofilament and multifilament meshes, of 9.2 X 10^{10} m^{-1} and 8.5 X 10^{10} m^{-1} respectively for materials with a pore size of 10 µm. This was much higher than the resistance values of 3.8 x 10^{7} m^{-1} determined for a dacron mesh of 61 µm pore size by Zhang et al. (2010). Fan and Huang (2002) calculated the R_m for a new 38 µm Dacron mesh as 1.94 X 10^{9} m^{-1}. This was higher than that of 1.84 X 10^{9} m^{-1} for the mesh after use: this different was attributed to the surface hydrophobicity of the new mesh, as dead water regions were observed on the new mesh. Although most membranes are made of hydrophobic materials, as these offer better mechanical, thermal and chemical resistances, this tends to make them foul more rapidly (Stuckey, 2012).

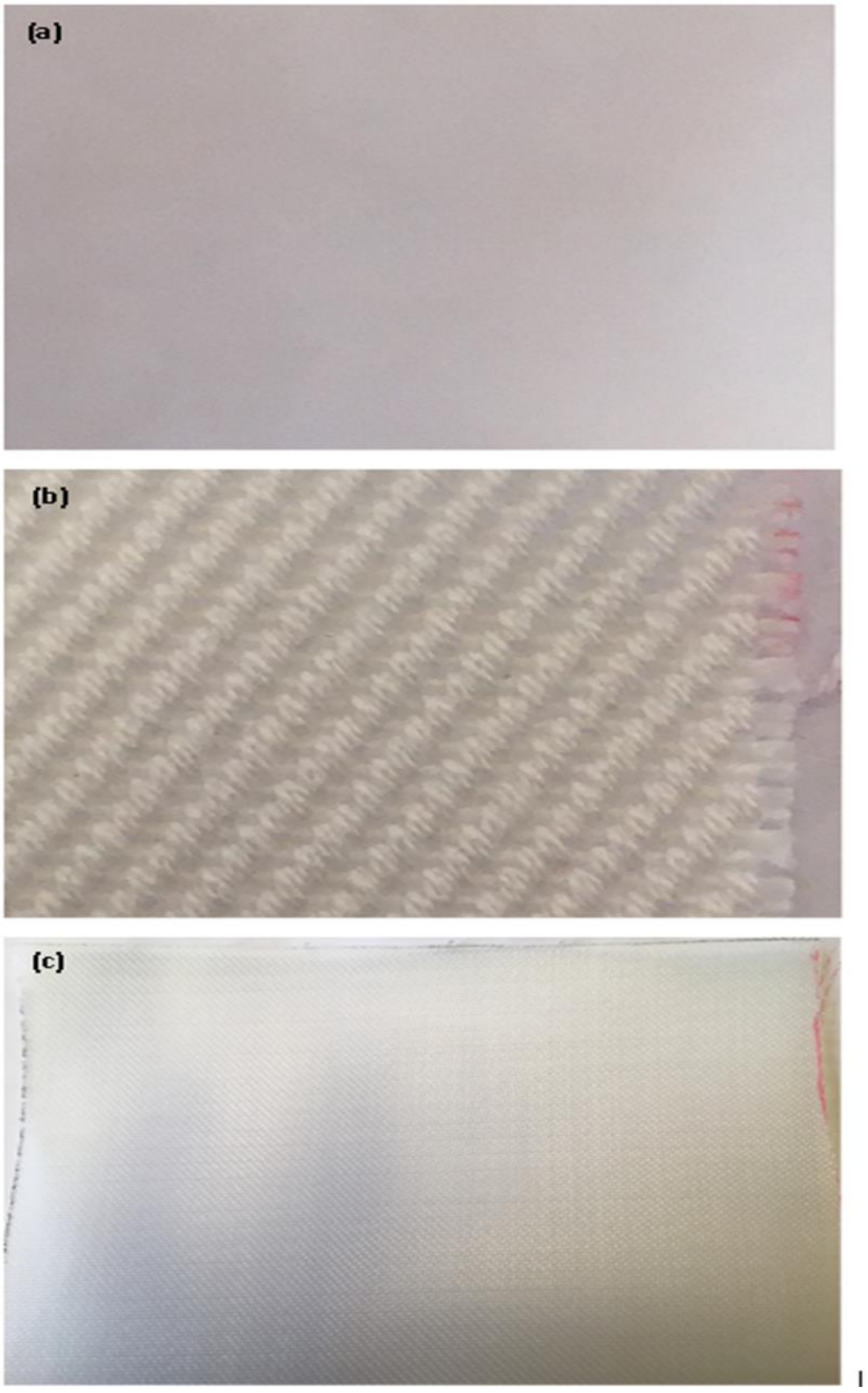

Figure 4-1 : Photos of support materials used (a) nylon mesh (b) woven polypropylene (c) non-woven polypropylene

4.3 Characteristics of the substrate used

The substrate used in the testing was anaerobic digestate from the Millbrook wastewater treatment plant (Southampton, UK). The digestate was passed through a 1 mm pore sieve to remove larger particles before dilution with tap water to the required target concentration. This substrate was chosen in order to mimic the type of biomass that may occur in real experiments at either laboratory or industrial scale. The pH and solids content of the undiluted substrate are shown in Table 4.2.

Table 4-2: Properties of digestate (before dilution) used for the batch test

Parameter	**Value**
pH	7.1±0.3
TS (%)	4.05 ± 0.01
VS (% TS)	69.61 ± 0.14
TSS (g L-1)	36.2 ± 0.99

4.4 Particle Size Distribution

To determine the distribution and range of particle sizes of the digestate, particle size analysis was performed using three different samples from the same batch supplied and used for the tests. The particle size distribution is shown in Fig 4.2 and shows that the majority of particles are in the size range between <1 µm and 1000 µm. with a maximum at around 80 µm. Since the PSD indicated that the majority of the particles were above 20 µm, the digestate was expected mainly to promote the formation of a cake layer rather than entering within the pores of the support materials.

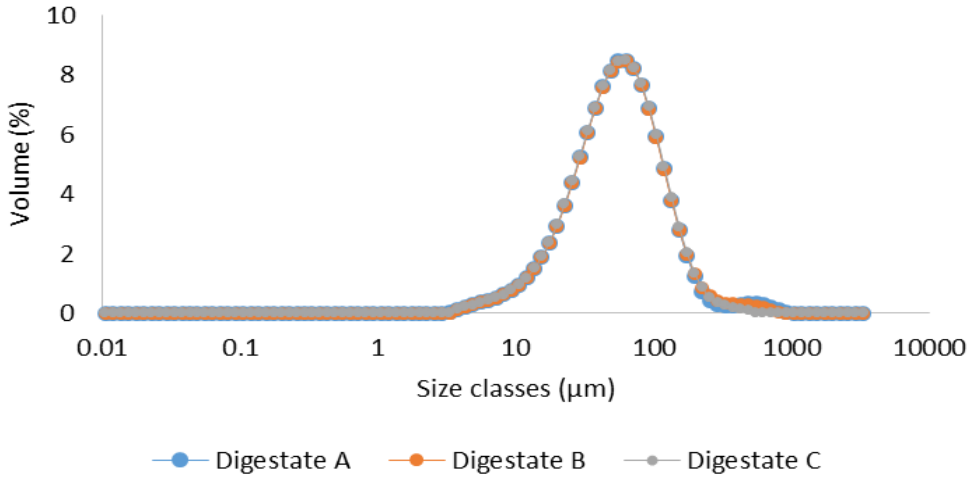

Figure 4-2: Particle size distribution of samples of the three separate samples of digestate used in study

Similar values were obtained and observations made by Martinez-Sosa et al. (2011) for anaerobic digestate obtained from a mesophilic treatment plant, although Jeison et al. (2008) found lower PSD values for anaerobic inoculum. It is important to observe the changes in PSD during the operation of the reactor, as the effect of shear may reduce the size of particles and in effect can cause lower flux (Tardieu et al., 1998). The correlation between pore size and particle size is shown to play a dominant role in the filtration performance of the membranes (Hwang et al., 2008b). The PSD indicated that most of the particles (>70%) were above 20 µm, with a median size of >50 µm. As the support material pore size is 20 µm, the digestate could readily deposit on the surface of the material and would be expected to promote the formation of a cake layer rather than entering within the pores of the support materials. The combination of support material and substrate therefore appears suitable for building a DM.

4.5 Correlation between turbidity and total suspended solids concentration of low-solids permeate

The ability of the DM to retain SS in the tank and produce low-solids effluent was assessed by measuring the turbidity of the permeate. An attempt was made to obtain a correlation between between the measured TSS concentration and the permeate turbidity. This was done by diluting the substrate in tap water to give a range of concentrations. Tests were

carried out in triplicate and the turbidity of the diluted samples was plotted against the corresponding values of TSS concentration, as shown in Figure 4.3. It can be seen that a relationship exists between the two and that turbidity can be used as an approximate indicator of the concentration of TSS. This relationship is wastewater-specific, however, as confirmed by Fuchs et al. (2005) who carried out similar work. The relationship is also only approximate in this case as effluent from the DM system will have a different PSD from dilute digestate, because the larger particles have been filtered out on the DM; and thus its turbidity will not necessarily be similar. Large and small particles in the substrate may be of different types, with different light-scattering properties. Figure 4.3 also appears to show a difference between the relationship for <175 mg TSS L^{-1} and > 175 mg TSS L^{-1}, although the slope is similar in these two ranges. The relationship should therefore be used with caution even for this work.

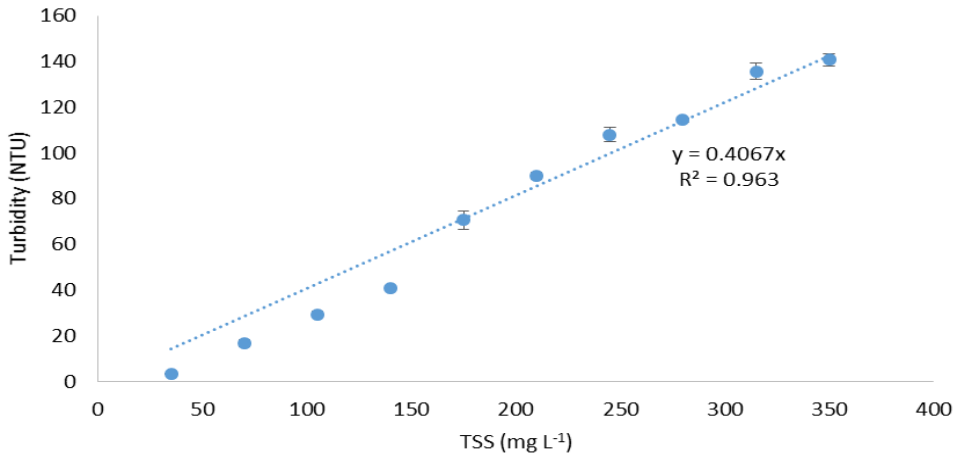

Figure 4-3: Correlation between TSS and Turbidity of permeate (average of triplicate samples per concentration)

4.6 Investigating the impact of material type on DM performance at low TSS concentration

The influence of the three materials on DM formation was investigated by measuring the changes in flow rate, pressure and permeate turbidity during the filtration of anaerobic digestate of known concentration. In this experiment, a low concentration of dilute digestate (1.5 g L^{-1} TSS) was used.

Figure 4-4a shows the flux profiles for the three fabrics tested under a constant pump flow rate set at 10.5 L m^{-2} h^{-1}. Monofilament fabric and nylon had near-identical flux values, which were maintained at 11 L m^{-2} h^{-1} for the period of operation. This compares to a flux of 9.5 L m^{-2} h^{-1} for woven fabric, around 14% lower than both nylon and woven polypropylene.

The process of formation of the DM involves initial pore blocking and subsequent cake layer formation, which is identified by an increase in resistance characterised by changes in suction pressure or TMP as illustrated in Figure 4-4b. The TMP was observed to be stable with only very slight fluctuations for all the materials tested, although woven fabric showed the lowest variability and highest pressure at 0.062 bar, while non-woven fabric had the lowest at around 0.36 bar. The pressure for nylon also remained stable at 0.04 bar without significant changes

The resistance profiles were calculated based on the Darcy equation, assuming a substrate viscosity equivalent to that of water at the given test temperature during filtration. Figure 4-4c shows that resistance for the materials tested remained almost constant, with the non-woven material showing the highest resistance of 2.6 $x10^{12}$ m^{-1} and the other two materials with much lower resistances of around 1.5 $x10^{12}$ m^{-1}.

Figure 4-4d shows the permeate turbidity results during the filtration tests carried out at a constant flux of 10 L m^{-2} h^{-1} and using a tank solids concentration of 1.5 g TSS L^{-1}. The woven and non-woven fabrics took longer than the nylon to achieve steady state values of less than 50 NTU. All reactors achieved less than 10 NTU in the permeate after the 48-hour mark. The 48 hours it took to achieve low values of turbidity in this experiment is significantly shorter than the 10 days reported by Ersahin et al. (2014) while using a mesh of lower pore size which implies the influence of the pore size on time of formation of the DM.

The quality of the permeate, as indicated by its turbidity, identifies the formation stage and filtration phase of the DM. As such, the formation stage appears to have been completed after 30 hours of operation as indicated by a significant decline in permeate turbidity. In real applications, during the formation stage – represented by higher permeate TSS or turbidity – effluent is recycled to improve permeate quality and provide material for DM formation (Fan and Huang, 2002, Kiso et al., 2005).

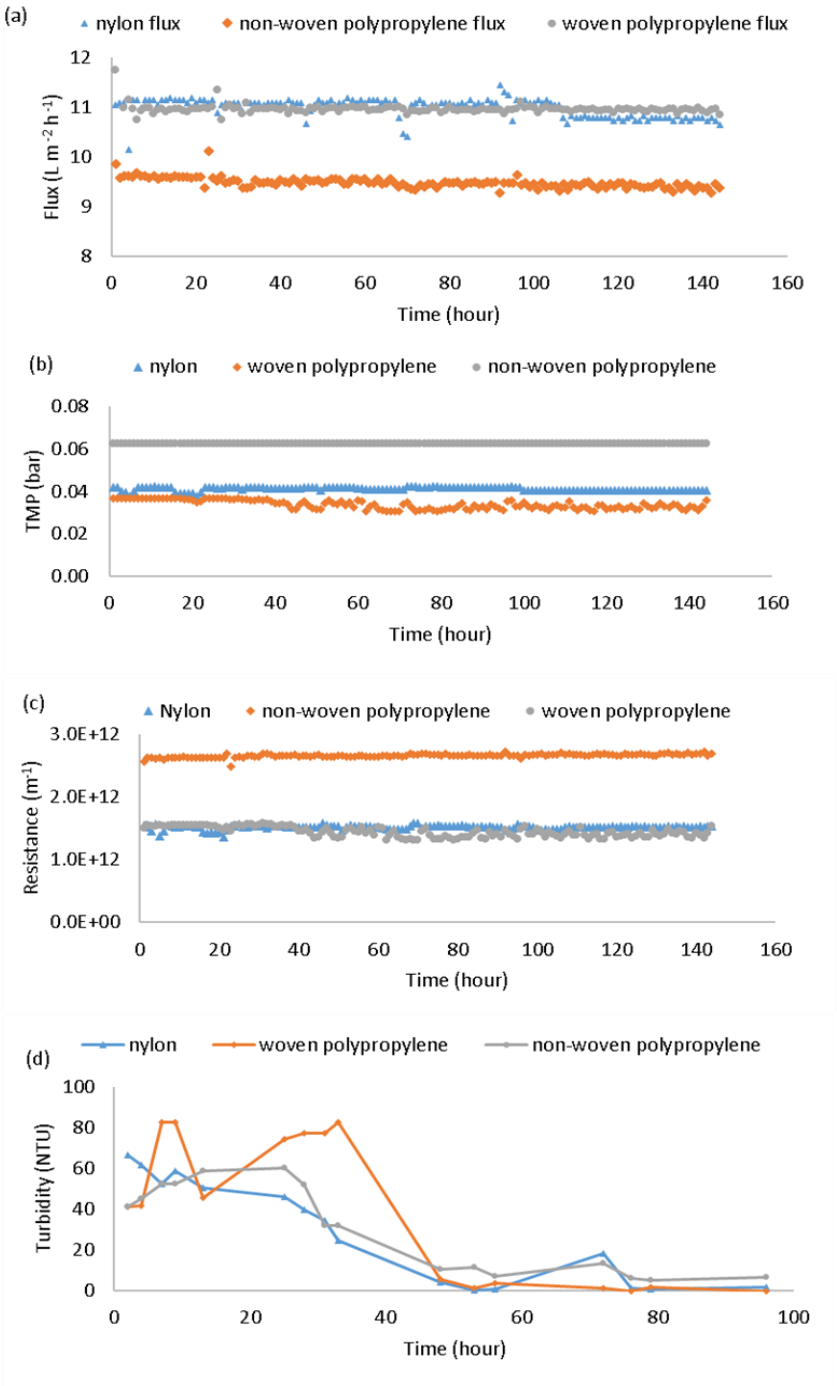

Figure 4-4: Performance of the profile of the nylon, woven and non-woven polypropylene materials tested at a substrate TSS of 1.5 g L^{-1} at pump flowrate of 3 rpm (a) Flux profile (b) TMP profile (c) Calculated total resistance profile of the DM (d) Permeate turbidity

The lower flux achieved with the non-woven polypropylene in comparison to nylon and woven meshes can be attributed to the observable physical structure of this material.

From a purely physical nature, the non-woven material was the toughest, and unlike the woven polypropylene had a very smooth surface making it harder to cut and form in order to fit the DM support and this may be a contributing factor to its increased resistance. Vrijenhoek et al. (2001) observed that the more particles were deposited on 'rough' membranes than on smooth membranes- due to the presence of valleys - although this may result in a more severe flux decline.

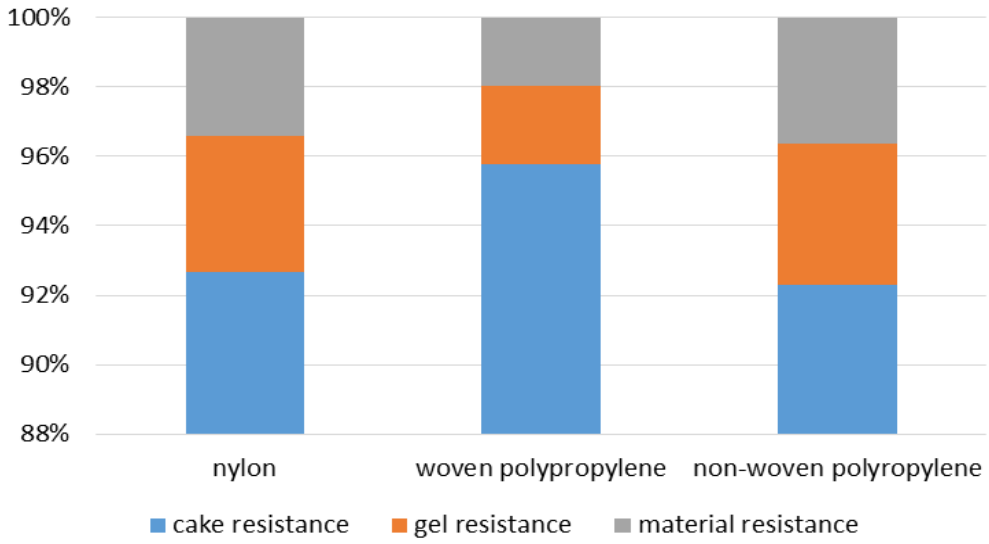

Figure 4-5: Resistance composition of the materials at constant flux of 10 L m^{-2} h^{-1} and 1.5 g TSS L^{-1}

The proportion of the total resistance for the materials were calculated at the end of the run and are presented in Figure 4-5. For all three materials, resistance attributed to the gel and cake formed on the surface where similar at 95%, 97% and 95% for nylon, woven and non-woven polypropylene fabrics. The contribution of material intrinsic resistance to total resistance where in the order of woven < nylon < non-woven. Tardieu et al. (1998) observed that if the flux is lower than the critical flux, as it appears to be in this case, there will be little change in TMP. This does not imply that the cake/biofilm is not being formed, but that the rate of formation is sustainable enough not to cause a significant jump in TMP. A similar observation was made by Cho and Fane (2002) when they were able to sustain flux without intervention and with no apparent changes in TMP for 140 hours (flux of 30 m^{-2} h^{-1}), although the membrane was coupled to receive effluent of biomass concentration of 550 mg L^{-1} supplied by the UASB

The critical importance of the DM process lies in its capacity for rejection of SS in the effluent. Based on the relationship between turbidity and SS**,** removal rates of over 90% were achieved during the DM formation stage, and almost 100% thereafter, while maintaining the same flux; with the difference in flux between the materials being attributable to differences in their individual material properties. The flux for all three materials remained constant throughout the operational period. This can be attributed to the low pump flow rate (pre-set flux) and is an indication that the operational flux was much lower than the critical flux and as such low TMP is required. In addition, given the wastewater low SS concentration of 1.5 g TSS L^{-1} the rate of deposition will be low, resulting in lower consolidation and resistance. Studies by Ersahin et al. (2013) and Satyawali and Balakrishnan (2008) determined critical flux values of 9 L m^{-2} h^{-1} and 3.9 L m^{-2} h^{-1} for woven polypropylene of pore size 10 µm and nylon fabric of 30 µm respectively; although it should be noted that the substrate TSS concentrations used were very much higher in both cases, and gas sparging was used to control cake formation.

In DM operation, gel layer formation precedes formation of the cake layer, which has been shown to dominate resistance by contributing almost 90% of the total DM resistance (Li et al., 2012b). The decrease in permeate turbidity in spite of the low TMP rise is therefore an indication that pore blocking, or gel layer formation is responsible for removal of turbidity. Given that retention of the SS is achieved, it is expected that such operation can be sustained for much longer until the TMP value of 0.2 -0.5 bar usually cited as threshold value of TMP before cleaning is required (Yu et al., 2014, Jeison et al., 2008, Ma et al., 2013a, Xie et al., 2014).

4.7 Assessing the impact of increased feed TSS (5 g L^{-1}) on performance for the three materials tested

To assess the impact of increased TSS concentration on the formation and performance of DM, the experiment from section 4.7 was repeated with an increase in the tank's TSS concentration to 5 g L^{-1}, using the same experimental set-up and conditions.

Flux: The test was carried out and lasted for 167 hours and as can be seen from Figure 4.6a, flux declines rapidly for nylon and non-woven polypropylene in the first few minutes. The initial flux value was halved after 30 minutes of the start of the operation resulting in flux

values of 5 and 4.4 L m^{-2} h^{-1} respectively. For nylon, the decline in continues until 15 hours after the start of the test, when a steady flux of around 2 L m^{-2} h^{-1} is achieved which remained stable for the rest of the test which lasted for 167 hours. For non-woven polypropylene, the flux declined to a steady flux of 0.5 L m^{-2} h^{-1} from 3 hours to 77 hours before further drop to 0.2 L m^{-2} h^{-1} after 78 hours of operation. Thereafter, an attempt to restore flux was carried out by increasing the pump flow rate from 3 rpm to 6 rpm. This resulted in an increase in flux to an average of 1.1 L m^{-2} h^{-1} which lasted for 16 hours before dropping to 0.1 L m^{-2} h^{-1} and consequently the test was terminated after 149 hours. For the woven polypropylene the initial decline took place in two distinct stages: The flux remained around 9 L m^{-2} h^{-1} for the first 6 hours, followed by a sharp drop to 8 L m^{-2} h^{-1}. This was maintained until 18 hours when there was a rapid fall to a minimum of 1 L m^{-2} h^{-1}, which almost immediately recovered to 2 L m^{-2} h^{-1}. This was followed by a long steady decline to 1 L m^{-2} h^{-1} by then another sharp drop to 0.7 L m^{-2} h^{-1} and therefore run was terminated after 150 hours of operation.

TMP: As can be observed in Figure 4.6b, the non-woven polypropylene shows an immediate increase in TMP to 0.03 bar within a few minutes of start of operation. Thereafter, the TMP remained fairly stable at around 0.12 bar until around 30 hours before steadily increasing at a rate of 0.001 bar h^{-1} reaching 0.27 bar and remaining stable for the next 20 hours. The increase in pump speed from 3 to 6 rpm, which resulted in a rapid increase in TMP from 0.27 to 0.36 bar at an average rate of 0.06 bar h^{-1} for 15 hours after which it falls very rapidly to 0.06 bar and stabilises at 0.04 bar until the end of the run. Resistance values for the materials (Figure 4.6c) show that while the resistance for nylon and non-woven materials were generally lower with steady performance values of 1.25 X 10^{12} m^{-1} and 3 X 10^{13} m^{-1}, which were lower than the average of 1.11 X $10^{14}m^{-1}$ for non-woven polypropylene, without accounting for the highly fluctuating performance from hour 78 onwards.

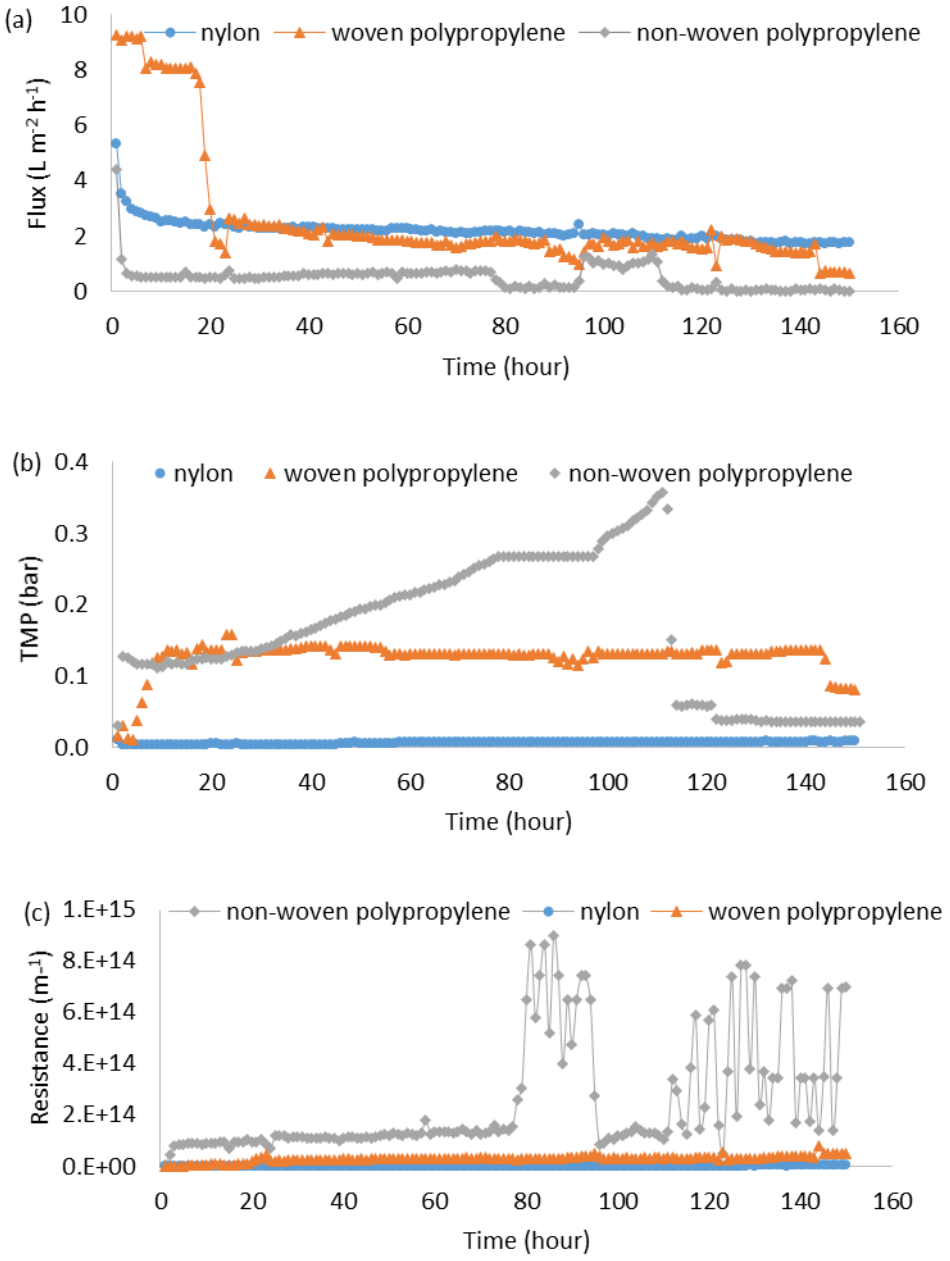

Figure 4-6: Performance of nylon, woven and non-woven polypropylene with TSS of 5g L^{-1} (a) Flux profile (b) TMP during filtration (c) Resistance profile

Figure 4-7 shows the change in permeate turbidity during constant flux filtration of 5 g TSS L^{-1}. Nylon and woven fabrics showed similar permeate turbidity at the formation stage, with a steady decline from the start of the filtration until steady state (0 NTU) after 25 hours which was then maintained throughout the duration of the study. During the DM formation stage permeate turbidity was highest for non-woven compared to nylon

and woven fabrics, but all three materials showed similar permeate turbidities after 20 hours which can be considered as the completion of the formation stage.

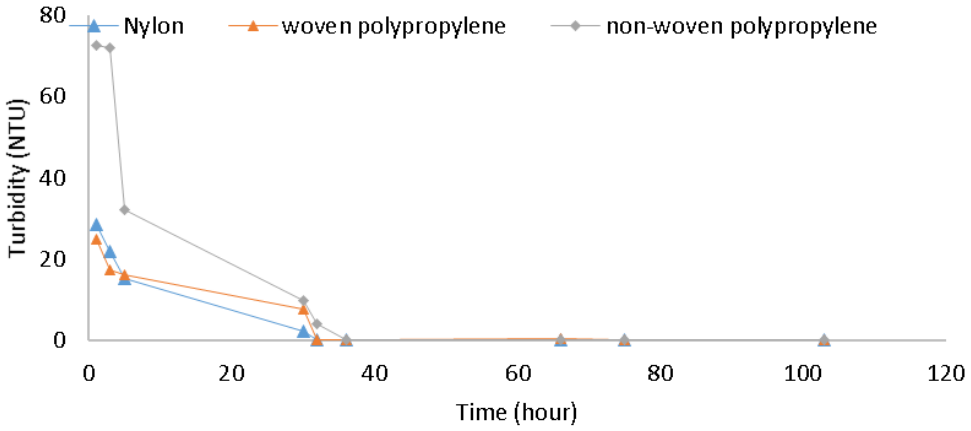

Figure 4-7: Permeate turbidity of nylon, woven and non-woven materials subjected to a flux of 10 L m^{-2} h^{-1} and solids concentration of 5 g TSS L^{-1}

Discussion: The above results show that DM was successfully developed resulting in the reduction of turbidity, indicating retention of TSS by all materials during steady state operation. The nylon fabric offered the highest flux and most stable performance for the duration of the test and it has the advantage of achieving steady flux in a shorter amount of time compared to the other two materials. It also had the highest turbidity removal even though it showed the highest turbidity during the formation stage. Steady state flux values were 20%, 5% and 20% of the initial flux for nylon, woven and non-woven polypropylene respectively. This result is similar to that of Li et al. (2011) who determined the resistance of 90 µm nylon fabric as lower compared to woven and non-woven materials of smaller pore sizes. The gradual increase in TMP for non-woven fabric is indicative of pore blocking or rapid cake formation and given that a TMP of 0.3 bar is usually cited as the upper limit for flat sheet membrane operation, cleaning would have been carried before TMP reached this value. The high TMP values may be due to entrapment of fine particles within the pores of the material, which can be hard to remove (Seo et al., 2007), as visual observation showed much less accumulation of solids on the surface compared to woven and nylon polypropylene materials (Figure 4.8). A similar observation was made by Ersahin et al. (2013) wherein monofilament fabric was found to be ten times more resistant to flux compared to staple (spun) yarn for short term experiments. The nylon and non-woven fabrics reached a TMP of 0.08 bar and 0.2

bar respectively. TMP drop was observed for the woven polypropylene towards the end of the experiment-which coincided with the loss of flux, indicating blockage of the pores. Increased solids concentration has been shown to lead to increased resistance (Flux decrease and TMP increase) as observed by (Chu and Li, 2006) wherein increasing the MLSS caused a loss of flux of around 90%.

Deposition of particles can take place in a few minutes of operation, but retention of particles via removal of turbidity takes longer. Ersahin et al. (2014) and Zhang et al. (2010) observed that it took 10 days and 7 days respectively for the formation of the DM and production of permeate of an acceptable standard (<13NTU), despite having widely different solids concentrations of 7.4 g TSS L^{-1} and 0.25g L^{-1} respectively. Increasing TSS in the reactor in this study resulted in a general fall in turbidity for both woven and non-woven fabric, demonstrating that a significant proportion of fine particles are entrapped in the pores of the material. Although all materials showed excellent retention capacity as shown by the turbidity values and the clarity of the permeate (Figure 4.14), the deciding factor is the resistance profiles of the materials. The non-woven polypropylene mesh had the highest resistance at 5 g TSS L^{-1} TSS and was therefore discontinued.

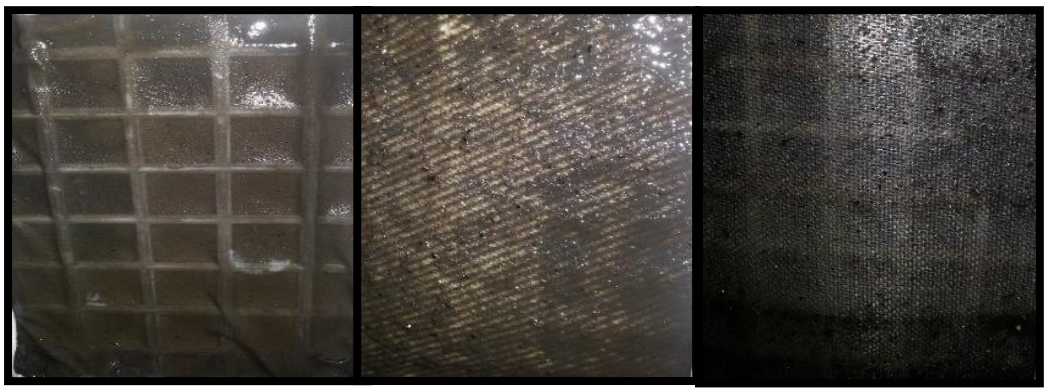

Figure 4-8: Images of support materials showing deposition when subjected to 5 TSS g L^{-1} a) nylon b) woven polypropylene c) non-woven polypropylene

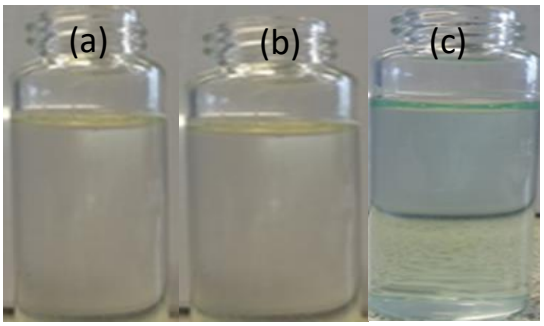

Figure 4-9 : Samples of permeate after filtration of 5 g TSS L^{-1} at 10 L m^{-2} h^{-1} (a) woven polypropylene (b) non-woven polypropylene (c) nylon mesh

4.8 Investigating the effect of constant head/imposed TMP filtration using nylon and woven polypropylene materials only

This test was carried out to provide an understanding of whether constant imposed TMP (under gravity) affects the continuous flux and DM formation.

Filtration tests were conducted using the equipment and techniques described in section 4.3 and 4.7 respectively with flow induced under gravity for both nylon mesh and woven polypropylene. The applied concentration in the tank was kept at 5 g TSS L^{-1} for the tests, which were, carried out under constant head gravity filtration of 1 m and 0.5 m head corresponding to an imposed TMP of 0.1 bar and 0.05 bar respectively. The permeate was recycled in the same manner as previously described in section (4.1), only in this case the filtration pump was replaced and flow was induced under gravity by the head difference.

Filtration fluxes for nylon mesh under constant gravity head of 1 m and 0.5 m are presented in Figure 4.10. For both cases, filtration dropped to 6 L m^{-2} h^{-1} in the first hour and settled at around 2 L m^{-2} h^{-1} after 20 hours of operation with little change thereafter, although some fluctuations were observed which may be attributable to daily 24-hour cyclical temperature changes. The permeate turbidities are presented in Figure 4.16. The permeate turbidity fell

from around 65 NTU for 1 m imposed head and 60 NTU for 0.5 m imposed head to less than 10 NTU, and was as low as 0 NTU after 30 hours of operation.

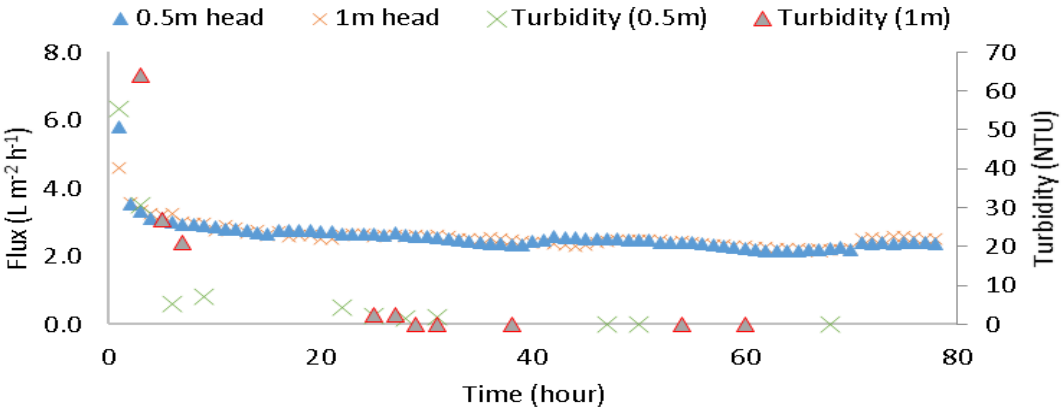

Figure 4-10: Flux and permeate turbidity profile for constant head (TMP) filtration of 5 g L^{-1} TSS filtration using nylon mesh

For the woven polypropylene, the flux started at around 10.5 L m^{-2} h^{-1} for the first hour then quickly dropped to 2 and 1.6 L m^{-2} h^{-1} for 1 m and 0.5 m gravity head respectively (Figure 4-11). The 1 m constant head filtration was discontinued after 30 hours of operation due to return pump failure, even though a stable flux of around 2 L m^{-2} h^{-1} can

be observed. For the 0.5 m constant head, a stable filtration flux of around 1.6 L m^{-2} h^{-1} was maintained for 100 hours without any fluctuations

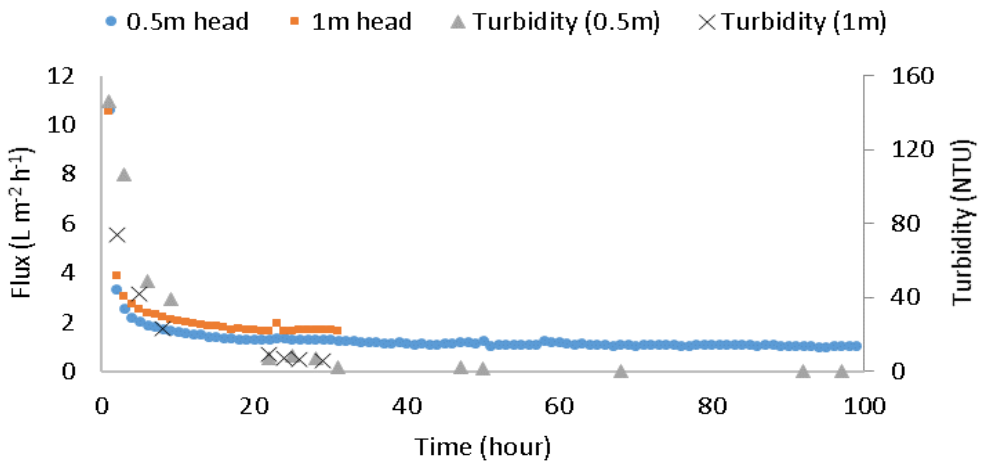

Figure 4-11: Flux and permeate turbidity profile for constant head (TMP) filtration of 5 g L^{-1} TSS filtration using woven mesh

After 30 hours of operation, permeate turbidity (Figure 4-15) showed a drop from 145 NTU and 75 NTU to less than 10 NTU for both 1 m and 0.5 m head respectively. The permeate turbidity remained at 0 NTU for the 0.5m head for the remaining duration of the test.

For both cases, it is observed that doubling the imposed TMP does not translate to a commensurate increase in filtration flux during steady state operation. For the nylon mesh, the flux behaviour is identical irrespective of the imposed TMP; while for the woven mesh an increase in flux of 20% is observed, although this is not conclusive as the filtration at imposed TMP of 1m gravity head was discontinued before the end of the experiment. The time for formation of the DM was not significantly influenced either. A critical factor in selection of TMP during gravity filtration could be the time taken for the DM to form, the achievable flux during steady state and other external engineering factors. Although DM formation occurred more quickly at higher imposed TMP, the process was complete in the first 10-20 hours in both cases and the difference was thus not significant enough to influence the choice of applied TMP. It is worth mentioning that a study by Defrance and Jaffrin (1999), showed that for any given flux, TMP was higher under constant TMP operation compared to under constant flux. This difference in behaviour - attributable to the effect of drag forces during the formation stage of the

DM - warrants careful consideration and thus appears to be a significant limitation when considering the use of constant TMP mode of operation.

4.9 Investigating the differences in performance of nylon and woven polypropylene mesh under constant imposed TMP

To compare the performance of nylon and woven polypropylene to enable selection of a single support material for DM development and use in subsequent filtration experiments.

Further tests to compare nylon and polypropylene as support for DM were done using 5 g TSS L^{-1} with TMP induced via gravity at head of 1 m and 0.5 m using the same experimental set-up as section 4.7

The decline in flux started in the first hour for both materials (Figure 4-12) and values quickly fell to about 2 L m^{-2} h^{-1} and 1 L m^{-2} h^{-1} for nylon and woven polypropylene respectively. The woven polypropylene mesh presented a much more consistent and stable flux, whereas slight fluctuations attributable to the laboratory 24-hour ambient temperature cycle were noticeable for the nylon mesh.

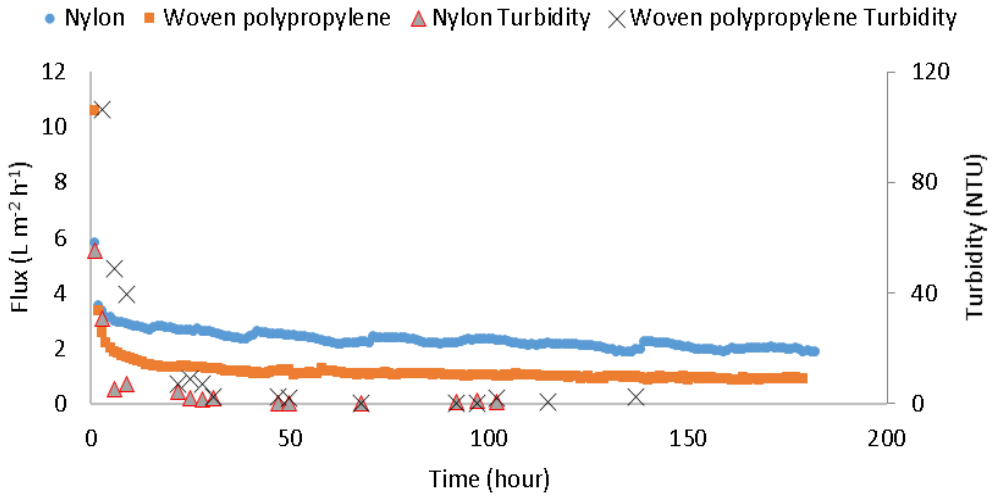

Figure 4-12: Filtration flux and permeate turbidity of nylon and woven polypropylene support materials under constant TMP of 0.5 m gravity head and 5g TSS L^{-1}

Permeate turbidity for the two materials (Figure 4-12) showed similar behaviour with a high of 146 NTU and 55 NTU for woven polypropylene and nylon respectively at the start of the test declining to less than 20 NTU after 10 hours for both materials, but permeate turbidity

measurement was discontinued after 137 hours for nylon. The nylon mesh consistently presented lower turbidity values than the woven polypropylene mesh.

Increasing the induced TMP from 0.5 m to 1 m head gave a slight increase in the filtration flux for both materials (Figure 4.13). The nylon mesh maintained a flux of 2.6 L m^{-2} h^{-1} compared to 1.5 L m^{-2} h^{-1} for woven polypropylene. The permeate turbidity values were similar for both materials (Figure 4.16). Although permeate turbidity was consistently below 20 NTU after the first 10 hours and dropped to less than 10 NTU after 20 hours of operation in both cases, at any given time the nylon mesh consistently provided less turbidity compared to the woven polypropylene mesh.

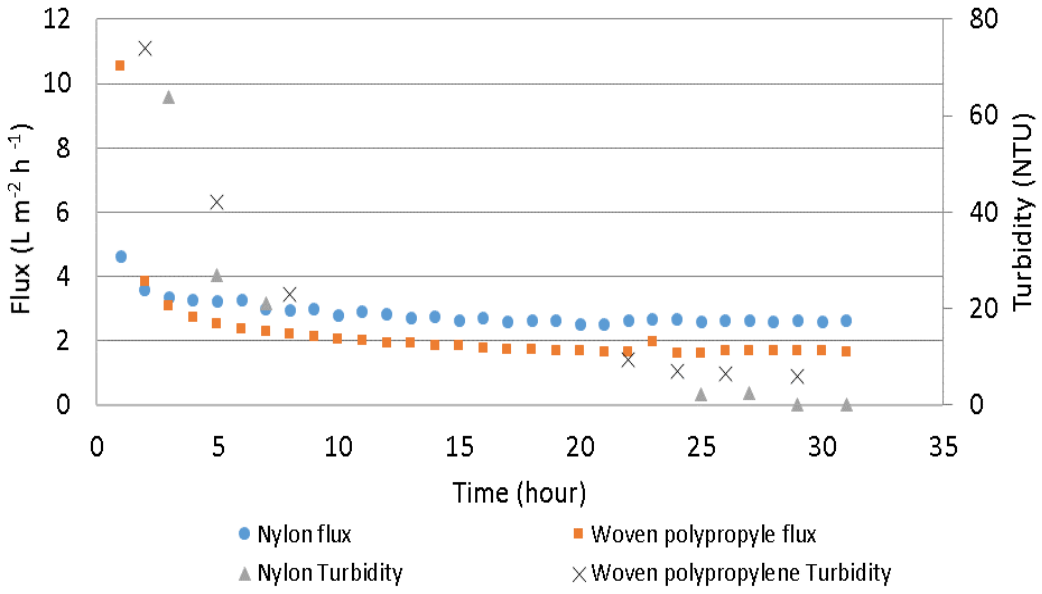

Figure 4-13: Flux and permeate turbidity values for nylon and woven polypropylene support materials under imposed TMP of 1 m head and 5 g TSS L^{-1}

When comparing the nylon and woven polypropylene fabrics based on flux induced by the hydraulic head, the following observations can be made:

- Increase in the imposed TMP does not lead to a commensurate increase in the achievable flux for either nylon or woven polypropylene
- Nylon consistently provided a higher steady-state flux compared to woven polypropylene. Under 1 m head of TMP, nylon sustained flux of 2.6 L m^{-2} h^{-1}compared to 1.6 L m^{-2} h^{-1} for woven polypropylene and at lower TMP of 0.5m

head, steady state flux of 2.2 L m^{-2} h^{-1} and 1 L m^{-2} h^{-1} for nylon and woven polypropylene respectively.

- Although the permeate turbidity values were quite low during steady state filtration, nylon mesh consistently showed a lower permeate turbidity compared to woven polypropylene.

It was therefore concluded that nylon mesh offered the greater potential for use as support material for the DM. It was consequently decided to select the nylon mesh for further tests.

4.10 Investigating the effect of TSS on filtration performance under constant flux of 5 L m^{-2} h^{-1}

To determine the effect of TSS concentration on formation and performance of DM, a constant flux of 5 L m^{-2} h^{-1} was applied to concentrations of 1.5, 3 and 5 g TSS L^{-1}. This trial was done using the nylon mesh, as results in section (4.10) indicated that it was the most suitable support material for this purpose. This stage was therefore necessary to test how much solids concentration it could cope with. An imposed flux of 5 L m^{-2} h^{-1} was chosen for this experiment, on the basis that this might represent a sensible minimum for full-scale operation if an excessive membrane area is to be avoided. This was lower than the flux used in the previous experiment, which aimed to establish performance in a more normal operating range of 10 L m^{-2} h^{-1}

For this experiment, flux was measured but not recorded due to malfunction of the data acquisition software. Figure 4.17a, provides the TMP profile for the test, which shows that there was no significant change in TMP for the lower TSS concentrations of 1.5 g L^{-1} and 3 g L^{-1} both of which remained well below 0.05 bar throughout the test period of 80 hours. For the increased TSS of 5 g L^{-1}, the TMP changes at a constant rate of 0.02 bar h^{-1}, reaching 0.3 bar before dropping to a rate of 0.01 bar h^{-1} and reaching 0.6 bar for the next 25 hours before levelling with relatively little or no change for the final 15 hours of operation. This implies the rapid formation of the DM, with solids being deposited to form the cake layer in the first 20 hours before the consolidation process takes over with reduced TMP rate. There may also be a point at which the cake layer has reached a critical point and as such the maximum deposition is reached.

The permeate turbidity results are shown in Figure 4.18b. Similar permeate turbidity profiles were observed for the 1.5 and 3 g TSS L^{-1} concentrations. In both cases, the turbidity values show a slight increase from the start then a gradual decrease when the DM is fully formed after about 48 hours, after which turbidity values less than 10 NTU are maintained. At 5 g L^{-1} SS concentration, the turbidity profile shows a slight difference as an immediate decline is observed and the DM is formed in the first 20 hours of operation. Although the initial turbidity was higher for the 5 g L^{-1} SS, at 50 NTU compared to 31 NTU and 20 NTU for the 3 g L^{-1} SS and 1.5 g L^{-1} SS respectively, the permeate turbidity following the formation of the DM layer was lowest (less than 10 NTU).

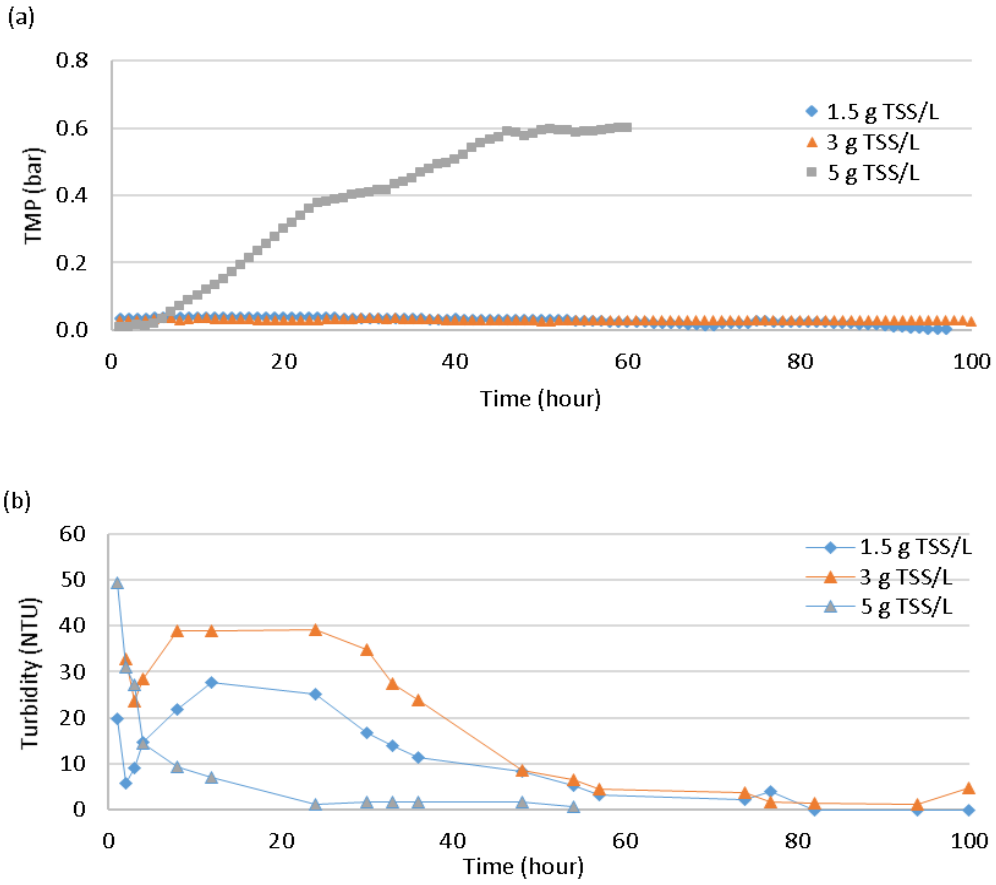

Figure 4-14 (a) TMP profile for constant flux filtration at 5 L m^{-2} h^{-1} for 1.5, 3 and 5 g TSS L^{-1} (b) Permeate turbidity during constant flux filtration at 5 L m^{-2} h^{-1} for 1.5, 3 and 5 g TSS L^{-1}

The lower TMP values for the 1.5 g L^{-1} and 3 g L^{-1} TSS concentrations indicate a much slower consolidation of the DM layer compared to concentration of 5 g TSS L^{-1}. The rise in TMP at

the higher solids concentration shows not only the rapid formation of the DM but also the compression of the cake layer which led to pore blockage. There is a consensus that an increase in TSS concentration results in increase in fouling and cake layer deposition (Cicek et al., 1998, Madaeni et al., 1999, Yigit et al., 2008), but this relationship is not linear as observed by the wide difference in TMP observed in this trial. The reason is that the TMP jump occurs quite rapidly following the occurrence of pore blockage. Although cake consolidation may be reversible, higher concentration of solids means a higher presence of smaller particles capable of blocking the pores of the support material with evidence of rapid rise in TMP. On the other hand, the advantage of a higher TSS concentration is that the cake layer forms earlier and is more comprehensive resulting in lower permeate turbidity compared to lower TSS concentration. Interestingly, the relationship between the TSS concentration and permeate turbidity shows that higher TSS concentration leads to lower turbidity as there is more solids to form the cake layer and intercept more materials. This is slightly different for the lower TSS values, where 3 g TSS L presented higher permeate than 1.5 g TSS L although they do converge after about 48 hours. This could be due to the much thinner gel/biofilm layer being the dominating mechanism as evidenced in the low TMP rise in both cases.

4.11 Assessing the effect of different stirring mechanisms (quiescent stirrer vs agitation) on performance

Background: For submerged and external immersed membrane filtration systems, mixing of the reactor contents can be achieved either by placing a mechanical mixer or agitator inside the reactor or by creating turbulence through recirculation of the biogas produced. An agitator achieves the dual purpose of keeping the contents in suspension and inducing shear. This delays the accumulation of the cake layer on the membrane surface.

For this trial, two tanks were operated sequentially with the digestate split in two parts. The first test was carried out with the stirrer following which the contents and the stirrer were replaced by digestate of same concentration and a purpose-built agitator with four flat sheet wings covering the depth of the DM cassette and rotating on the axis of the stirring rod respectively (Figure 4.15). Each flange of the agitator had a length of 10cm and width of 2 cm. Mixing was carried out at 50 revolutions per minute (rpm) for the stirrer and the agitator. Apart from the change in stirring mechanism employed, the set-up and mode of operation

is as described in section 4.3. Nylon mesh was used as support material and the test lasted for around 100 hours

For both tests the initial flux was set at about 10 L m^{-2} h^{-1} and the TSS in the tank was kept at 5 g TSS L^{-1}. Performance was assessed by measuring and comparing the TMP, flux and permeate turbidity of both systems.

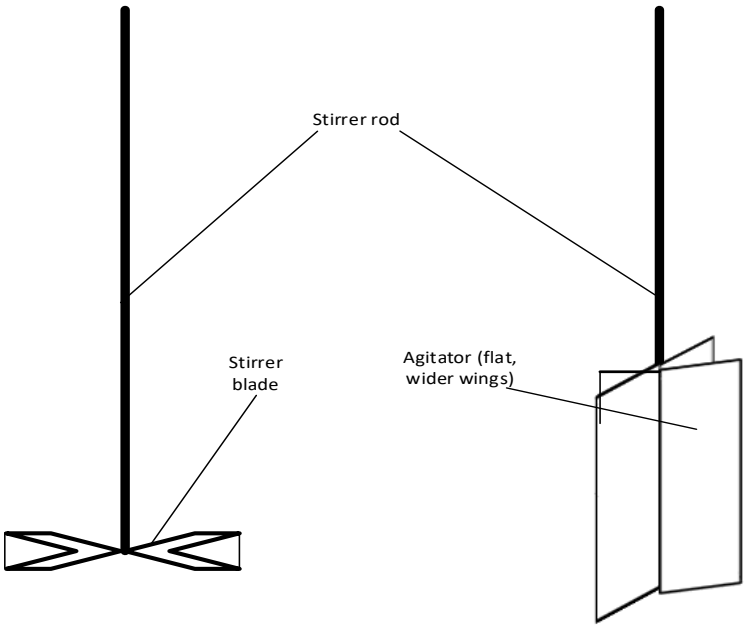

Figure 4-15: The two types of mixers used (a) simple stirrer and b) agitator

For the stirred condition, the TMP rose continuously from around 16 hours and reached 0.9 bar after 34 hours of operation. It then remained stable for the next 12 hours and the test was terminated after a run period of 46 hours due to high TMP. The agitated tank showed a lower TMP and a much gentler rise to 0.1 bar after 8 hours and maintained an average TMP of 0.12 bar until the test was terminated.

Flux: Visual observation showed that the agitator caused more turbulence compared to the quiescent mixing of the stirrer. Figure 4-16a shows the flux profile for both operations. For the stirred tank, the flux was steady at around 10 L m^{-2} h^{-1} for the first 22 hours before steadily declining and ending at 3 L m^{-2} h^{-1} when the test was terminated after 46 hours. The agitated tank maintained a flux of 9 L m^{-2} h^{-1} for around 6 hours from the start of the test before dropping slightly to about 8 L m^{-2} h^{-1} for the next 11 hours. Following this, a sharp decline to

a steady flux averaging around 2 L m^{-2} h^{-1} although with minor fluctuations until it was concluded after 97 hours.

Permeate turbidity: Figure 4-16b shows the permeate turbidity for both conditions of operation. There was a steep decline from 1000 NTU at the start of the filtration to about 42 NTU for the stirred condition after 40 hours of operation and shortly before the test was terminated due to high TMP. In contrast, using an agitator presents permeate of 24 NTU during formation leading to 0 NTU in the effluent during the stable filtration stage.

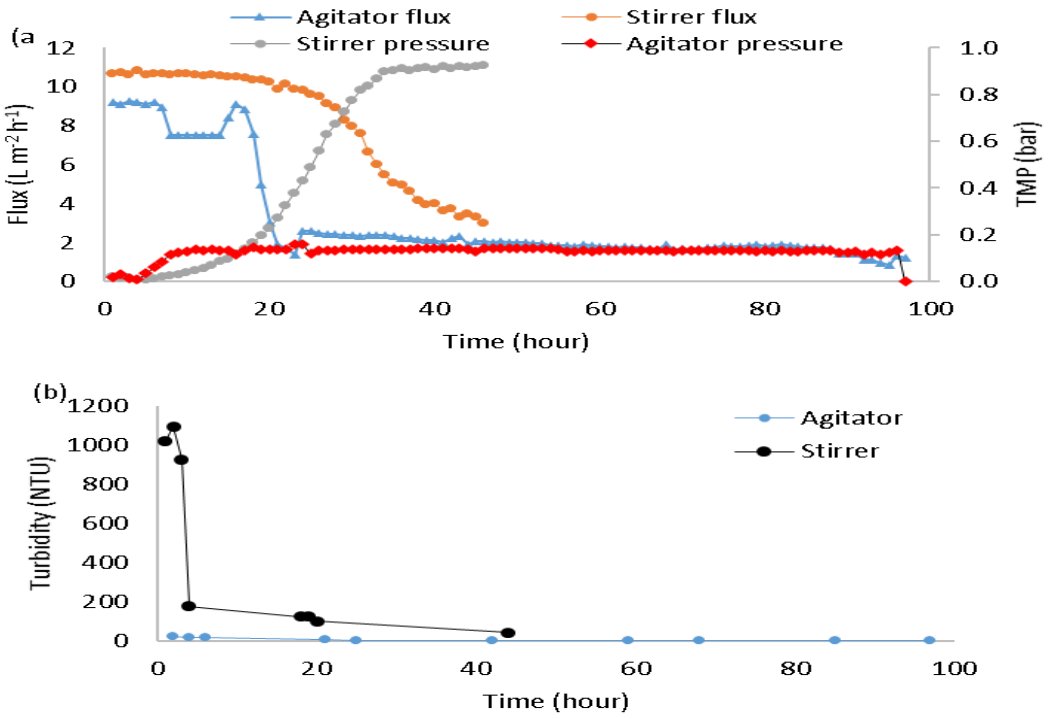

Figure 4-16: Performance of agitator and stirrer at a constant flux of 10 L m^{-2} h^{-1} and 5 g TSS L^{-1} (a) Flux and TMP profile and (b) Permeate turbidity

Discussion: A simple explanation of the above result is that the agitator paddles increase the shear distribution across the membrane surface and cause more back transport of solids thereby prolonging effective filtration and preventing immediate pore blockage of the support material. Even though the stirrer provided particle suspension, the forward drag of suspended matter due to suction was much higher than the back transport caused by the action of the stirrer. This causes increase in TMP and initial permeate turbidity compared to the agitator. This is similar to the results of Elmaleh and Abdelmoumni (1997) who found that a baffle significantly improved flux by a maximum of 50% compared to the flux obtained

without the baffle. Also, Gupta et al. (1995) found that by introducing a helical baffle, the rate of deposition on the membrane surface decreased and an increase in flux of up to 80% was achieved.

4.12 Assessing the effect of TSS on filtration at constant TMP

To assess the effect of TSS concentration on filtration at constant TMP, constant head gravity filtration was carried out at TSS concentrations of 1.5, 3 and 5 g L^{-1} to observe the formation and performance of DM under constant pressure induced by gravity flow. The gravity filtration was carried out at about 1 m head differential, corresponding to 0.9 bar as TMP. The experimental set-up is as described in section 4.12. In this case, the agitator was employed as the mixing mechanism for the test.

All concentrations of TSS showed similar decline in flux (Figure 4-17) that started in the first hour of operation. The lowest flux was at 5 g TSS concentration for which the flux drops to 4.6 L m^{-2} h^{-1} and further declines to 2.5 L m^{-2} h^{-1} which lasted for the rest of the test lasting for 80 hours. The flux for the solids concentration of 1.5g TSS L^{-1} and 3 g TSS L^{-1} declined to 7 and 9.3 L m^{-2} h^{-1} respectively in the first half hour of operation. They both declined at a rate of an average rate of 0.02 L m^{-2} h^{-1} Overall, flux values for 1.5, 3 and 5 g TSS L^{-1} were around 2.5, 2.6 and 2.3 L m^{-2} h^{-1} respectively, representing flux losses of 65%, 72% and 50% relative to the clean flux at start of the test. The slights fluctuations in flux are attributable to ambient conditions as the tests were carried out without temperature control. In the DM formation stage the 5 g TSS L^{-1} had the highest initial permeate turbidity followed by 3 and then 1.5 g TSS L^{-1} (Fig 4.17). In all cases, the permeate turbidity dropped to less than 20 NTU in the first 5 hours, and no turbidity was detected after 25 hours of filtration (0 NTU). The return pump for the test at with 5 g L^{-1} failed at around Hour 78 and filtration was stopped.

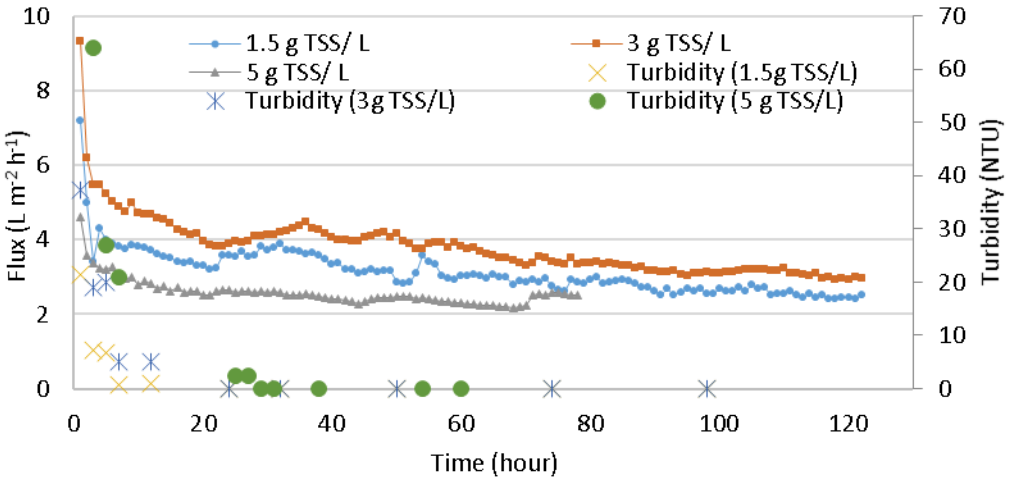

Figure 4-17: Flux and permeate turbidity of nylon mesh filtration under 1 m head constant TMP for TSS concentration of 1.5, 3 and 5 g L^{-1}

Discussion: Kiso et al. (2000) showed that increasing the SS concentration at a given hydraulic head resulted in a drop in flux although the reactor MLSS was high (8g L^{-1}), and aeration was used to control clogging. In all three cases tested here, fluxes were higher than in a study conducted by (Chang et al., 2001) in which flux declined by 95% when using 5 µm non-woven membrane. The slight difference in flux for the three concentrations tested indicate that there is a threshold pressure which when applied, the flux can be maintained irrespective of the concentration of the solids. Turbidity values were comparable to those of less than 5 NTU achieved by Ren et al. (2010) for a 100 µm non-woven filter reactor MLSS of 5 g L^{-1} driven by hydrostatic head although flux was dependent on the HRT.

4.13 Assessing the effect of mixing rates on DM performance

To determine the effect of mixing rates induced by agitator speed on DM performance, two different mixing speeds of 50 rpm and 100 rpm were applied and compared. The mixers used were agitators which had 2 cm flanges on both sides of a 10 cm stem. The rpm of the agitators was adjusted by increasing the voltage supply to the motor for the mixer. The experimental set-up was as described in section 4.3. The TSS concentration in each tank was kept at 5 g L^{-1} and the flux was set at 5 L m^{-2} h^{-1}.

Figures 4.18a & 4.18b show the flux and TMP at an applied initial flux of 5 L m^{-2} h^{-1} and TSS concentration of 5 g L^{-1}. The flux showed similar trends at both mixing speeds. A decline in flux was observed for the lower mix speed after 15 hours of operation. The decline took much longer for the higher mix speed, starting after 25 hours, and showing some fluctuation before stabilising at about 4.5 L m^{-2} h^{-1}, equivalent to a flux loss of 10%. As for the lower mix rate value of 50 rpm, the flux loss was about 35 % after stabilising at 3.5 L m^{-2} h^{-1}, 30 hours into the test. For both cases, some level of fluctuations, attributable to environmental conditions and temperature changes are apparent as the tests were carried out under laboratory ambient conditions.

In terms of resistance, the higher mixing rate showed significantly lower TMP compared to the lower mixing rate of 50 rpm. At 100 rpm, the TMP rose to 0.03 bar in 2 hours; this is considerably below the 0.2 bar reached in 18 hours of operation at 50 rpm.

This behaviour shows that, as in conventional microfiltration, shear promotion via induced turbulence is necessary to maintain flux levels as indicated by the 20% higher flux at higher rpm compared to lower rpm. This should be applied with care, however, as it may be less beneficial to the formation of the cake layer.

Figure 4.18b shows the changes in permeate turbidity over time. It can be seen that permeate turbidity was significantly lower at 50 rpm compared to 100 rpm. This is attributable to the higher mixing rate causing more turbulence in the tank, and thereby preventing the formation of the DM. Similar observations were made by Kiso et al (2000) in which increasing the aeration intensity resulted in higher effluent turbidity.

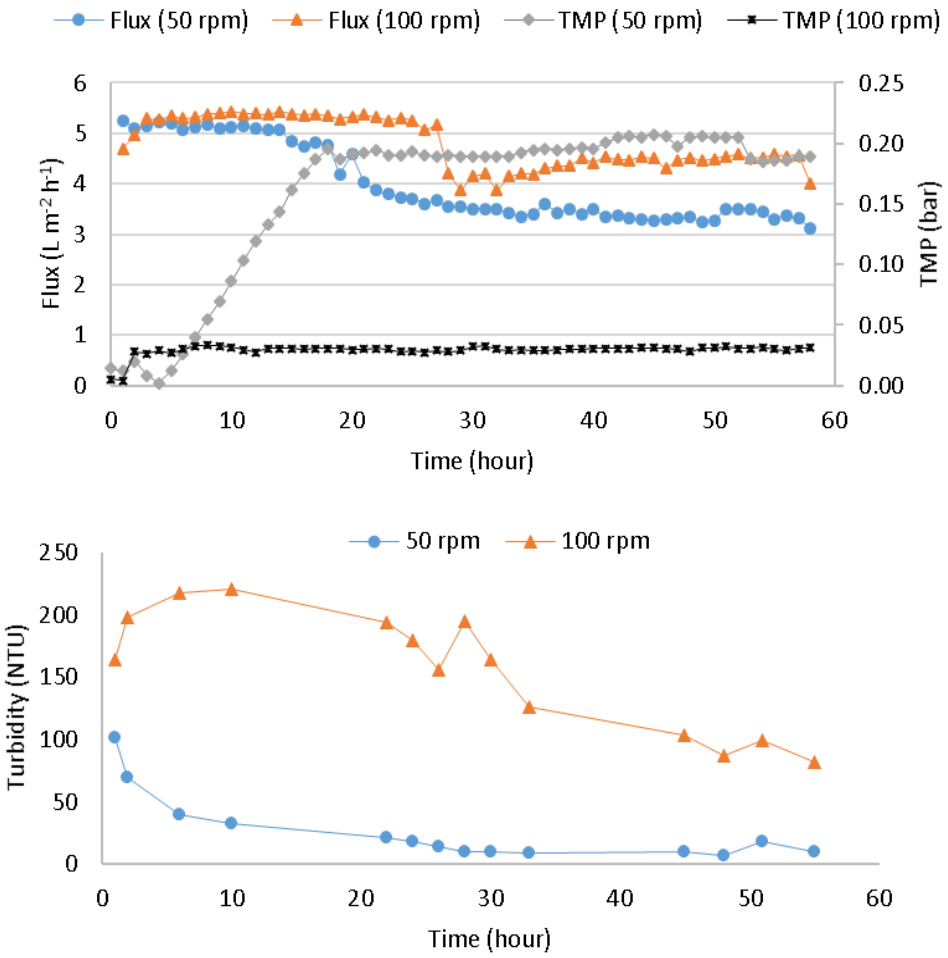

Figure 4-18: Performance of nylon mesh DM under different mixing speed for constant flux of 5 L m^{-2} h^{-1} and solids concentration of 5g TSS L^{-1} (a) Flux and TMP profile for two different mixing rates at 50 and 100 rpm (b) Permeate turbidity

4.14 Investigating the potential for pre-formation of self-forming DM as a filtration option for wastewaters with low TSS

A few studies have been reported showing that the DM can be pre-formed on a support material prior to its application to wastewater treatment, although these were carried out using known chemicals or materials such as powdered activated carbon (PAC), diatomite kaolin and oxides or colloids of Zr and Manganese (Ye et al., 2006, Chu et al., 2008, Yang et al., 2011). Pre-formation usually involves the controlled deposition of such materials or of oxides unto the surface of the support material to create the porous cake layer. The major

attraction of such cases is that the characteristics and properties of the elements are known, and the approach has previously been applied to aerobic systems with very promising results. To apply such a technique to anaerobic systems, it is interesting to test the pre-coating of support materials using the contents of the mixed liquor. In the following trials, anaerobic digestate was applied as the medium for pre-coating the nylon mesh.

To evaluate the potential for pre-forming the DM and assess its use in filtering effluent of very low TSS

For this trial, the test was carried out as follows:

- Build-up of the DM under high solids conditions by filtering 10 g TSS L^{-1} digestate at constant flux rates of 5, 10 and 15 L m^{-2} h^{-1}
- Replace the contents of the batch tank with low solids wastewater of 0.2 g TSS L^{-1}
- Apply design flux rates (5 - 10 - 15 L m^{-2} h^{-1}) to the low TSS wastewater and observe performance of flux, change in pressure and turbidity removal
- The same equipment and techniques as previously described in section 4.3 was employed (constant flux filtration carried out with the aid of a peristaltic pump)

Figure 4.19 shows the pre-formation flux which was set at a value of 5.5 L m^{-2} h^{-1} and lasted for a duration of 1342 minutes (22.4 hours). During this period, the flux was stable (apart from slight fluctuations due to frequency of data capture - logging every 2 minutes).

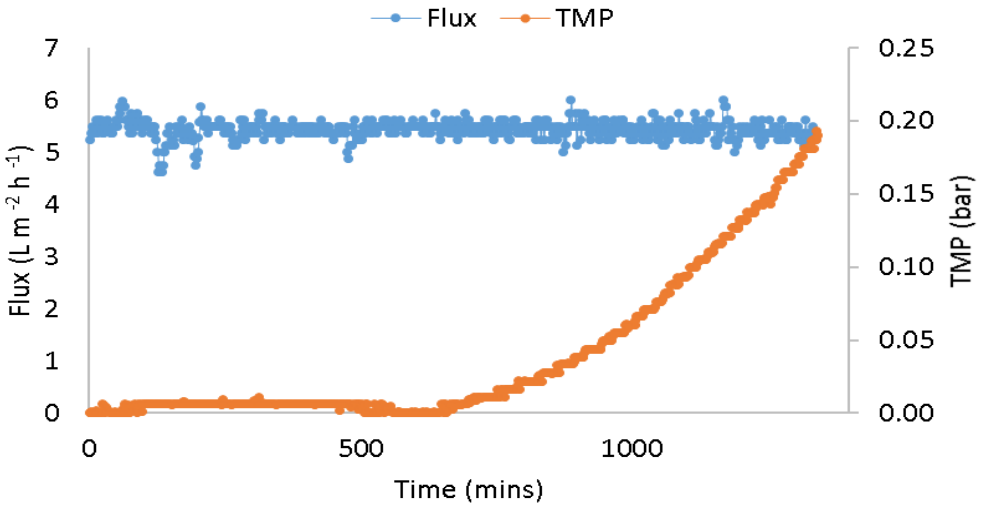

Figure 4-19: Flux and TMP profile for pre-formation using solid concentration of 10 g TSS L^{-1} and constant flux set at 5.5 L m^{-2} h^{-1}

The TMP was stable at around 0.003 bar for 500 minutes from the start before gradually dropping to 0 bar for about 150 minutes. Following this dip, the TMP began to rise steeply and reached 0.17 bar, at which point the test was terminated

Figure 4.20 shows the TMP and flux performance for the flux set at 10 L m^{-2} h^{-1}, which ran for about 130 minutes. Flux was stable at around 10 L m^{-2} h^{-1} (with small fluctuations due to environmental conditions), although a very slight drop is seen shortly before the test ended. TMP remained stable at around 0.04 bar for 60 minutes before decreasing to 0.003 bar about 80 mins from the start. Following this drop, the TMP rose steeply to 0.28 bar in 36 minutes and then fell slightly to 0.24 bar shortly before the end of the test.

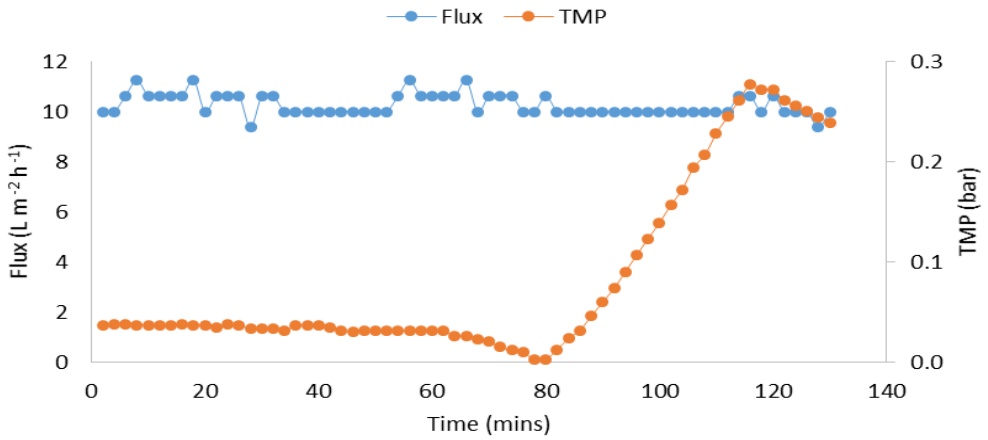

Figure 4-20: Flux and TMP profile for DM pre-formation Flux and pressure profile for pre-formation using solid concentration of 10 g TSS L^{-1} and constant flux set at 10 L m^{-2} h^{-1}

Figure 4.21 shows the performance when the formation flux was set at 15 L m^{-2} h^{-1}, with the trial lasting for about 130 minutes. The imposed flux of 15 L m^{-2} h^{-1} was stable for 120 minutes before a sudden drop, ending at 6 L m^{-2} h^{-1} when the test was discontinued. The TMP rose to 0.06 bar in 44 minutes before dropping slightly to 0.03 bar for 10 mins. Another steeper rise in TMP commenced, reaching 0.29 bar in 60 minutes, after which the test was stopped.

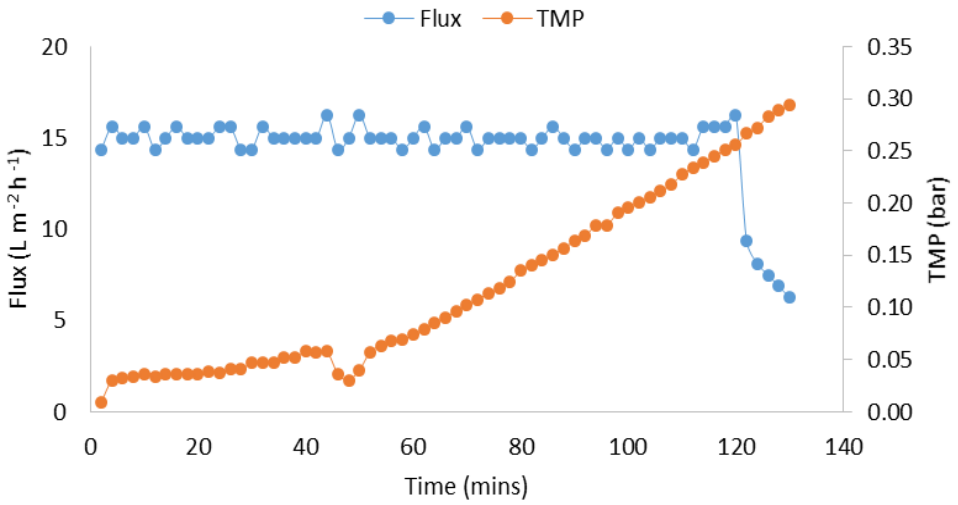

Figure 4-21: Flux and TMP profile for DM pre-formation using solids concentration of 10 g TSS L^{-1} and constant flux set at 15 L m^{-2} h^{-1}

Discussion: It is evident that the imposed flux influences the time taken for cake formation and consolidation. Higher flux results in reduced formation time of the cake layer, given the same TSS concentration. Based on the change in TMP, cake formation/consolidation begins after about 600 mins, 60 mins and less than 5 minutes for imposed flux values of 5, 10 and 15 L m^{-2} h^{-1} respectively. A characteristic observed in all three cases of the pre-formation tests is the TMP slightly dipping before the steep increase, indicative of cake formation/consolidation. Two possible causes can be suggested for this. Firstly, some portion of the cake layer may have fallen off after formation due to the hydrodynamic conditions. Secondly, the evolution of the cake layer across the surface of the membrane is not uniform and as such, during filtration, the membrane surface may become unevenly covered resulting in localised 'clean' flow regions. The flow through these regions occurs at lower resistance hence the decline in TMP. When these spots eventually become covered in cake, a steeper, more consistent rise in TMP is observed. In addition, it is common to see a TMP drop, with concurrent increase in flux, as this in cases where flux is remains relatively stable. In particular, the flux at 5 L m^{-2} h^{-1} had lower consolidation as the TMP rise was up to 0.17 bar, compared to 0.27 bar and 0.30 bar for the 10 and 15 L m^{-2} h^{-1} respectively. In terms of building up a cake layer, it can be seen that reducing the imposed flux increases the formation time of the DM considerably.

4.15 **Testing the filtration performance of pre-formed DM**

The series of pre-formed DM created in the preceding section (section 4.14) were tested to assess their performance.

Upon completion of the formation stage using 10 g TSS L^{-1} as described in section 4.1, the contents of the tanks were replaced by a low TSS sludge concentration of around 0.2 g L^{-1}. The three pre-formed DMs with formation fluxes of 5, 10 and 15 L m^{-2} h^{-1} were tested for performance in terms of flux stability, TMP changes and permeate turbidity. The three trials are as outlined below:

- Trial 1: Formation flux 5 L m^{-2} h^{-1} and filtration flux 5 L m^{-2} h^{-1}
- Trial 2: Formation flux 10 L m^{-2} h^{-1} and filtration flux 5 L m^{-2} h^{-1}
- Trial 3: Formation flux 15 L m^{-2} h^{-1} and filtration flux 5 L m^{-2} h^{-1}

Trial 1: Flux and TMP for the constant filtration flux set at 5.5 L m^{-2} h^{-1} (formation and filtration) are shown in Figure 4-22a. The flux was stable for just over 20 hours before dropping to around 4.2 L m^{-2} h^{-1}. This value was maintained until hour 50 when flux increased to 5.3 L m^{-2} h^{-1}, then remained stable until around 167 hours when it began to drop steeply, falling to below 1 L m^{-2} h^{-1} in less than 30 hours. Similarly, TMP started low at around 0.003 bar for around 50 hours before rising to 0.014 bar, following which it fell back briefly to 0.001 bar. This temporary increase in flux and reduction in TMP may have been due to solids that were not well attached falling off the support material. Following this brief drop, the TMP started gradually to rise and reached about 0.08 bar at around 168 hours from the start of the run. Shortly afterwards it declined, and dropped to 0.012 bar at the end of the trial. Permeate turbidity values (Figure 4-22b) fell from 10 NTU to 2 NTU in 10 hours and further declined to less than 0.5 NTU after 20 hours of operation, then maintained this value for the rest of the test. The fluctuation in flux in the first 50 hours is typical of the formation stage of the DM, pore blocking is the predominant mechanism, followed by cake deposition and growth. As the flux is kept relatively low (5.5 L m^{-2} h^{-1}), the gradual rise in TMP is an indication of the increasing deposition of the cake layer. The drop in both flux and TMP after 160 hours shows is attributable to the cessation of flow due to complete blockage of the DM. Applying a low formation flux of 5 L m^{-2} h^{-1} may have reduced cake layer formation and caused the permeation of small particles to block the pores of the support materials.

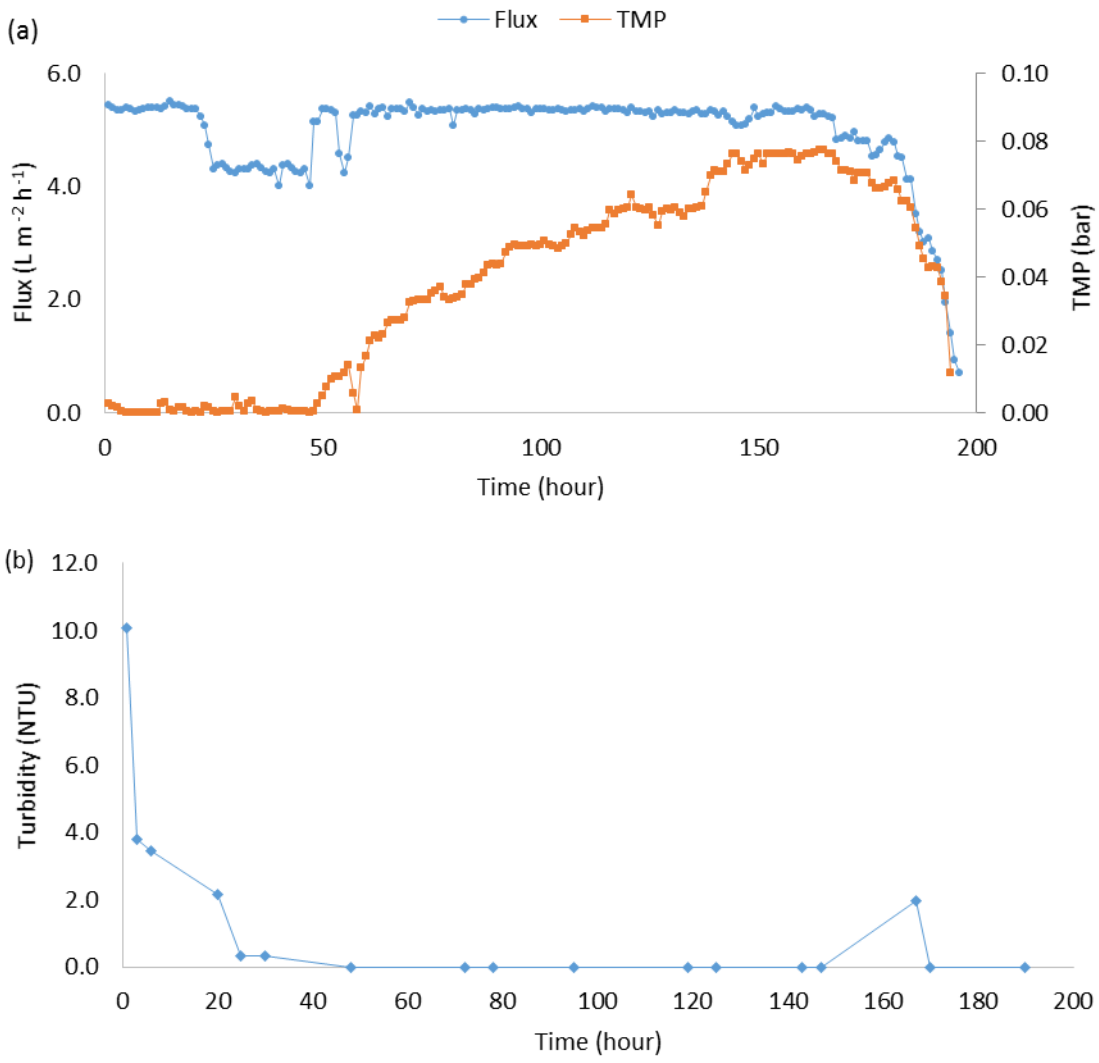

Figure 4-22: Performance of pre-formed DM (formation flux of 5.5 L m^{-2} h^{-1}) subjected to filtration of 0.2 g TSS L^{-1} at an imposed flux of 5.5 L m^{-2} h^{-1} (b) Permeate turbidity

Trial 2: Results for formation flux set at 10 L m^{-2} h^{-1} and operational filtration flux of 5.5 L m^{-2} h^{-1} are shown in Figure 4-23a. The flux remained around 5 L m^{-2} h^{-1} and was very stable for around 167 hours. At this point, the pump rpm was doubled to increase the flow rate. This resulted in a flux of around 10 L m^{-2} h^{-1} for the remainder of the trial without significant change. During DM preformation (10 L m^{-2} h^{-1} flux, 10 g TSS L^{-1} the TMP was around 0.14 bar which was similar to the value in pre-formation. After this, it dropped to 0.001 bar and remained low at around 0.05 bar for 24 hours before starting to rise gently. It reached 0.13 bar at 166 hours and then rose steeply in a 2-step process:

first to 0.22 bar at 189 hours, followed by another TMP jump to 0.25 bar at 191 hours, after which it continued rising until the trial was ended after 212 hours. These jumps in TMP are likely to indicate changes in the consolidation of the cake layer when subjected to increased drag forces (Defrance and Jaffrin (1999), causing the resistance to change. Permeate turbidity (Figure 4-23b) started at 13 NTU and quickly dropped to below 5 NTU in less than an hour of operation then remained at this value for the rest of the trial. This drop in turbidity indicates that the DM has been formed and was fully functional, blocking the suspended solids that could otherwise have been present in the permeate. Interestingly, the drop in turbidity to less than 0.5 NTU (after 50 hours of operation) coincides with the start of the rise in TMP. This gradual rise in TMP is indicative that the cake layer is intercepting particles within a size class, resulting in the narrowing of the DM pores. Increasing the pump rpm in an attempt to double the flux resulted in a much steeper TMP rise within a very short period, indicating rapid consolidation of the cake layer. Similar observations were made by Alibardi et al. (2016), in which the increase in membrane flux was not proportional to the measured TMP when subjecting DM to treatment of synthetic wastewater under ambient conditions. Another possible explanation is that by keeping the flux constant for a long period of filtration, the porosity of the cake layer is established and cake consolidation is gradual. Therefore, an attempt to change the flux increases the drag force of particles in the cake layer causing pore blockage and a sudden rise in TMP is observed.

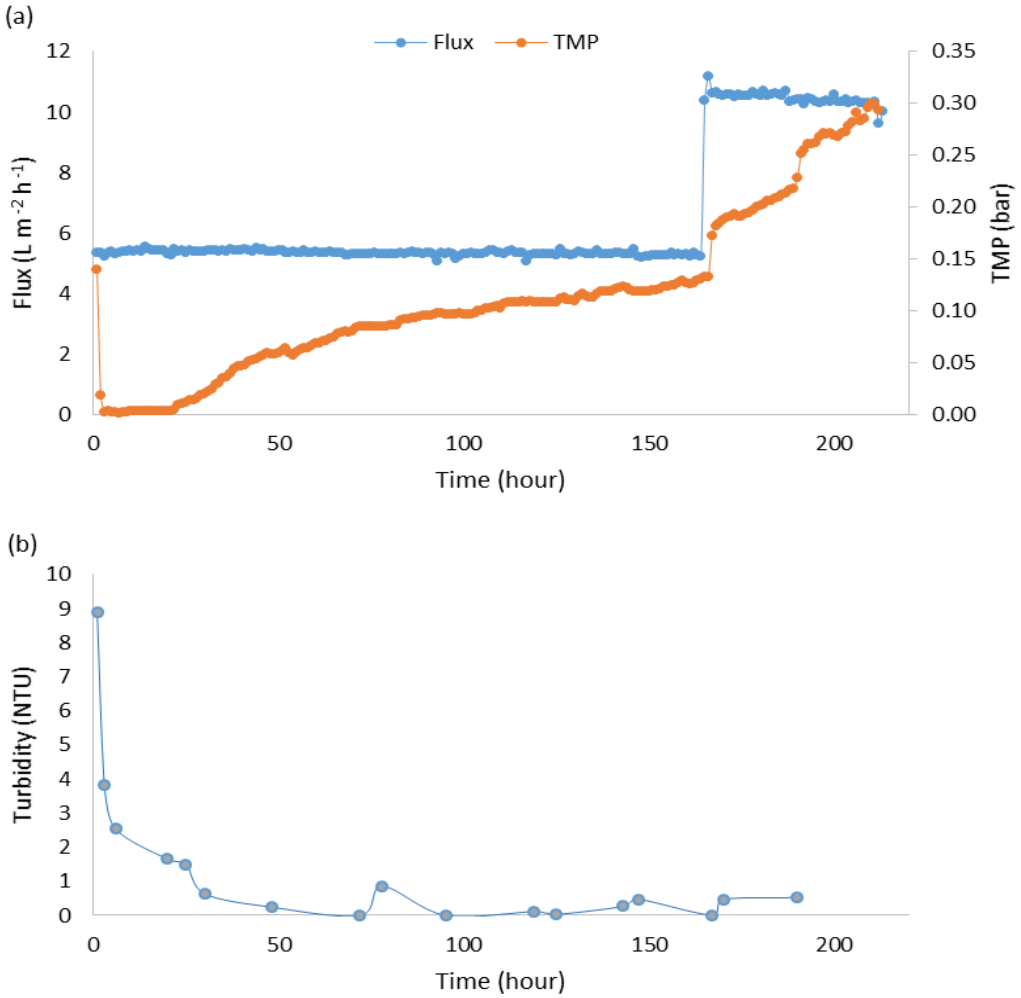

Figure 4-23: Performance of pre-formed DM (formation flux of 10 L m^{-2} h^{-1}) subjected to filtration of 0.2 g TSS L^{-1} at an imposed flux of 5.5 L m^{-2} h^{-1} (b) Permeate turbidity

Trial 3: The pre-formed DM built using 15 L m^{-2} h^{-1} was applied to the filtration of a low solids (0.2 g TSS L^{-1}) wastewater at an operational flux of 5.5 L m^{-2} h^{-1} for over 200 hours, as presented in Figure 4-24a. The flux dropped to around 3.2 L m^{-2} h^{-1} in under 8 hours from the start of operation at low solids. The flux stabilised at just above 3 L m^{-2} h^{-1} until 165 hours when the pump rpm was doubled, resulting in an increase in flux to around 6 L m^{-2} h^{-1} and then to 9 L m^{-2} h^{-1}. This lasted for about 10 hours, before dropping to 6 L m^{-2} h^{-1} with some fluctuations until the end of the trial. TMP rise showed a similar pattern at the start, dropping from 0.15 bar to around 0.1 bar after 5 hours. It stabilised at around 0.1 bar for 160 hours before rising to around 0.18 bar following the increase in pump rpm, stabilising briefly at just over 0.2 bar before rising steeply to 0.28 bar due to the

second increase in pump rpm. Permeate turbidity (Figure 4-24b) fell from around 14 NTU to just under 2 NTU in less than two hours of operation and remained low for the rest of the trial. Although there is a very noticeable loss in flux, the stability of the filtration indicates that the increased flux may have caused the formation of a very uniform and more dense cake layer compared to when the lower pre-formation fluxes of 5 or 10 L m^{-2} h^{-1} was applied, thereby increasing the resistance of the cake layer. This behaviour can be further explained by the increased transportation of particles and deposition on the surface of the support material to form a compact cake layer, shifting the equilibrium between the particle drag and back transport in favour of the former. Similar observations was made by Saleem et al. (2016) in which a high initial flux, even when applied to a low solids concentration, caused a thicker and more resistance cake layer to be formed. This compact layer significantly increases the resistance and if not removed, increase in pump rpm, is not capable of achieving a commensurate increase in operational flux.

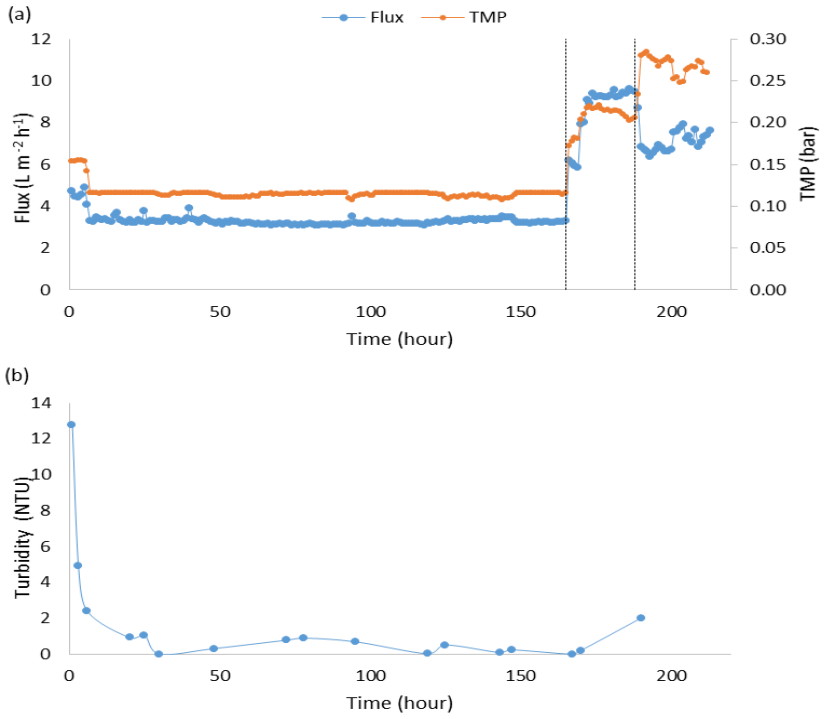

Figure 4-24: Performance of pre-formed DM (formation flux of 15 L m^{-2} h^{-1}) subjected to filtration of 0.2 g TSS L^{-1} at an imposed flux of 5.5 L m^{-2} h^{-1} (b) Permeate turbidity (Vertical dashed line indicate change in pump rpm)

Pre-formation of the DM by filtering solids of a much higher concentration than the working value to build a cake layer was applied as a means of ensuring the rapid formation of the DM. It was observed that a higher imposed formation flux resulted in more rapid deposition of cake layer as seen in the higher TMP values. It took approximately 300 mins, 150 mins and 120 mins to reach 0.2 bar for 5.5 L m^{-2} h^{-1}, 10 L m^{-2} h^{-1}, and 15 L m^{-2} h^{-1} respectively. Following that, filtration fluxes of the same values as the formation flux showed different behaviour. It was observed that the DM formed at higher pre-formation fluxes were not able to (a) maintain the same imposed operational flux as the DMs pre-formed with lower fluxes. It was observed that the best performance was obtained with filtration fluxes that were lower than the formation flux. Formation flux at 10 and 15 L m^{-2} h^{-1} and filtration flux set at 5 L m^{-2} h^{-1} showed more stable performance and a much gentler increase in resistance compared to when both the pre-formation and filtration flux were set at 5 L m^{-2} h^{-1}. This may be due to a more uniform cake layer thickness for the higher flux than the lower flux which can lead to a steeper rise in TMP as the cake layer are more prone to blockage. Attempts at increasing the flux rate during operation led to unstable performance, however, and should be avoided. In all trials involving pre-formation of DMs, permeate turbidity was already very low after 20 hours of operation. This is an indication that the DM can retain the suspended solids and can be used as a polishing stage for effluents discharged from bioreactors from an early stage of the operating cycle after formation, even though other parameters indicated that consolidation of the membrane was still occurring.

4.16 **Conclusion**

Batch tests were carried out to investigate the suitability of support materials for DM support and performance. Results from the tests showed the influence of material type on flux and TMP, under different substrate TSS concentration. This allowed the selection of the most suitable material out of the three options tested, with the nylon mesh offering higher flux and lower permeate turbidity values compared to woven and non-woven polypropylene meshes. Subsequent tests were carried out to evaluate the effect of solids concentration, mixing type and speed and mode of operations on performance. It was observed that under constant flux operation TMP increased considerably beyond certain TSS concentration (3 g TSS L^{-1}).

While operation under constant TMP has its merits, such as production of higher volume of permeate per unit time, the constant flux had a more linear correlation between volume of permeate produced which ensures better operational stability. Further tests on nylon mesh showed that while vigorous agitation certainly improved flux, it reduced the quality of the permeate and this must be considered when designing a system to achieve a specific degree of treatment performance and effluent quality.

A novel way of building the DM by pre-forming with digestate was tested and showed that lower pre-formation flux resulted in more stable performance making it suitable as a post treatment/polishing unit for AD digesters treating wastewater. This is beneficial if used in an environment where low-tech solutions and simplicity of operation is desired, as the DM unit can be easily assembled using fabric and various configurations can be adopted. For example, in developing communities for which conventional membranes may represent a significant cost and for which treatment using MF membranes will be an overkill.

Chapter 5: Integrating Anaerobic Filter Bioreactor with DM in continuous operation

This chapter describes the set-up and testing of anaerobic filters treating simulated wastewaters derived from tomato processing to produce effluent for subsequent testing in a coupled DM system.

The objective of this work was to evaluate the potential of integrating DM to an anaerobic filter treating low solids wastewater of a treatment system for handling simulated wastewater from tomato-juice processing.

5.1.1 Feed wastewater characteristics

The physico-chemical characteristics of the feed tomato juice in concentrated form are shown in Table 5-1. This concentration was diluted to give a working strength of 1 - 4 g L^{-1} COD, depending on the target OLR.

Table 5-1 : Characteristics of concentrated tomato juice used in the study

Properties		**Elemental composition**	
Characteristics	**Values**	**Element**	**Content (%)**
COD (g L^{-1})	55054 (±3637)	Carbon	58.5
SCOD (g L^{-1})	43958 (±3171)	Nitrogen	9.5
TOC (g L^{-1})	20317 (±240)	Hydrogen	2.3
STOC (g L^{-1})	18491 (±214)	Sulphur	0.2
TSS (g L^{-1})	11.5	Oxygen	29.5
TS/VS (g L^{-1})	47/41		
Alkalinity (g $CaCO_3$) L^{-1}	11		
TKN (g N L^{-1})	1.26		

Total Phosphorous ($g\ P\ L^{-1}$)	0.08		

5.1.2 Digester description and operation

Two upflow Anaerobic Filter (AF) bioreactors (Figure 5-1) were set up for the treatment of simulated tomato-processing wastewater. The media used for the AF digester were the K1 plastic wheel type carrier originally developed by Kaldnes Miljoteknolog, Norway The characteristic specific gravity of the carrier is between 0.96 - 0.98 with dimensions of 7mm length by 10 mm diameter and specific surface area of 500 $m^2\ m^{-3}$. The digester was fed in an up flow manner such that the feed was pumped from the bottom of the digester and rises until it reaches the working level and the effluent flows out by the action of an internal pipe, which acts as a siphon to drain the effluent.

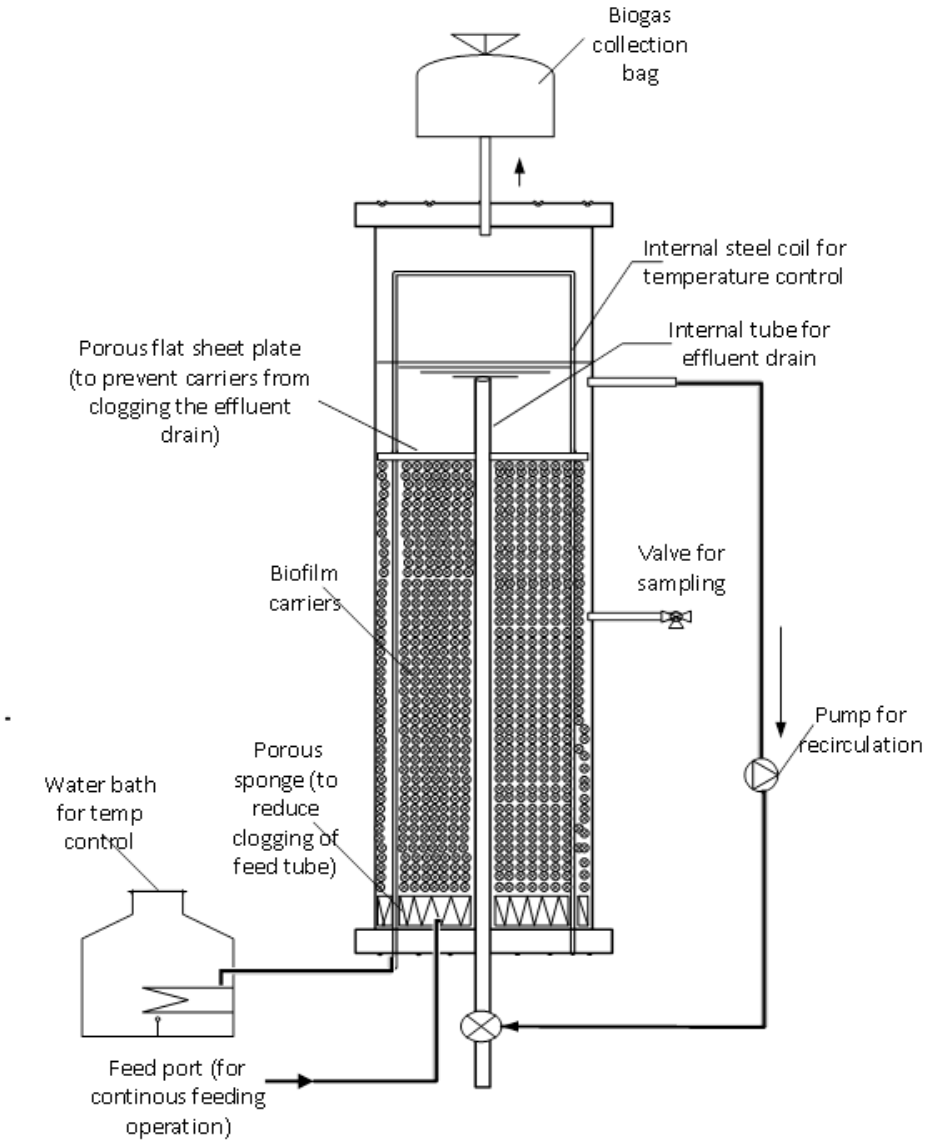

Figure 5-1: Description and set-up of the AF digester

The digesters were filled with carriers up to 50% of their working volume. A porous flat plate was placed at the top of the carrier layer to prevent the carriers from entering and blocking the effluent pipe, and a porous sponge was placed in the bottom to aid distribution of the feed. The first digester was inoculated by diluting 0.5 L digestate (properties as described in section 3.3.3) with 3.5 L tap water. The digester headspace was then purged using Nitrogen gas. Feed was provided through a tube connected to the underside of the digester.

The set-up and operation of the first digester (AF1) is as shown in Figure 5-1. The inoculum was allowed to sit in the digester without feed for 3 days at the set temperature of 30 ºC to enable conditioning and monitor for leaks. The first 10 days involved batch feeding once per

day with 25 mL of concentrated substrate and recirculation of the mixed liquor in the AF reactor at a rate of 2.3 L h^{-1} using a peristaltic pump. This was done in order to promote colonisation of the carriers and to encourage biofilm growth essential for the reduction of solids for the second stage of the process. The volume of concentrated feed was increased to 30 mL and 60 mL after 21 and 36 days respectively reflecting the increase in OLR accordingly. This period in which the digester was batch fed lasted for 60 days in total.

5.1.3 AF1 Start up performance

pH and Total VFA: Figure 5-2a shows the pH and total VFA for the duration of the start. The pH dropped rapidly on the first day due to the lack of buffer and to addition of the substrate. The pH then gradually dropped to 6.5 after the first 15 days of operation, and from day 15 to day 19, around 1 g of urea was added to the feed daily to forestall further drop in pH. This resulted in a gradual increase in pH reaching 7.6 by day 20 before a slight drop to 7.3, after which the value remained stable for the rest of the period.

Monitoring of VFA was started on day 13 shortly before adding the urea to the digester and total VFA concentrations were converted to COD equivalents (according to the following conversion factors: acetic acid - 1.07, propionic acid - 1.51, iso-butyric acid and n-butyric acid - 1.82, isovaleric acid - 2.04, hexanoic acid - 2.21 and heptanoic acid - 2.34). The total VFA rose to 0.6 g COD L^{-1} at day 18 before dropping to <80 mg COD L^{-1} after 25 days of operation. There was a small increase in VFA after the rise in OLR which also appeared in the IA/PA ratio. Monitoring stopped after day 42 but it was clear from the IA/PA ration that the VFA had been successfully removed.

The drop in pH indicates the feedstock's lack of buffering capacity. This led to the accumulation of VFAs and the need for addition of external buffer. The response of the reactor's mixed liquor showed that this was necessary to forestall the gradual acidification of the digester. Addition of urea was discontinued to observe if the biomass would acclimate to the feed.

The Total Alkalinity (TA) at the start was around 1g $CaCO_3$ L^{-1} (Figure 5-2b) and remained between 1-2 g $CaCO_3$ L^{-1} until day 14 when it began to increase sharply to around 5g $CaCO_3$ L^{-1} by day 19 due to the daily addition of urea from day 15-19. TA rose to 5.5 following the increase in OLR but showed a slight decline to around 4.7g $CaCO_3$ L^{-1} by the end of the run.

Partial Alkalinity (PA) showed a similar trend, rising to 3.6 g $CaCO_3$ L^{-1} on day 21 and remained close to this value thereafter. Intermediate Alkalinity (IA) rose to 1.4 g $CaCO_3$ L^{-1} by day 19 and remained steady apart from a brief increase around day 40. The IA/PA ratio peaked at 0.67 on day 13, just before the addition of urea and again at 0.56 on day 40 but otherwise remained below 0.5. These values indicated stable operation in response to the addition of urea.

Total Ammonia Nitrogen (TAN) profile (Figure 5-2c) was broadly similar to that for TA, rising from around 0.2 g N L^{-1}, before day 15 to around 1.1 g N L^{-1} by day 21 but then declined after increase in OLR to around 0.9 g N L^{-1} by day 60. The decline in urea is attributable to the cessation of urea addition and to the uptake of TAN during the formation of biofilm on the carrier in response to the OLR increase.

TSS/VSS: Figure 5-2d shows the concentration of the TSS/VSS sampled from the digester. The TSS of the first day of operation was around 2 g L^{-1} but decreased to 1 g L^{-1} by day 15 maintaining an average of around 1 g L^{-1} until day 43 when the measurement was discontinued. The VSS concentration mimicked the TSS profile at about 1.8 g VSS L^{-1} and ending at an average of 0.7 g VSS L^{-1} by day 43. Since the sampling was carried out in the same location (mid-section) of the digester, the decrease in TSS/VSS may be due to the biomass remaining within the interstices of the carrier and the biofilm formation.

VMP: The volumetric methane production (VMP) profile (Figure 5-2e) shows a steady increase reaching a 0.13 L CH_4 L^{-1} day^{-1} after 15 days and a slight dip to 0.08 L CH_4 L^{-1} day^{-1} on day 19 before rising to 0.19 L CH_4 L^{-1} day^{-1} following a slight increase in OLR from 0.5 to 0.6 on day 19. Average VMP was maintained at 0.18 L CH_4 L^{-1} day^{-1} between day 21 to 32. An increase in OLR from 0.6 to 1.2 g COD L day^{-1} resulted in an increase in VMP to 0.34 with an average of 0.32 L CH_4 L^{-1} day^{-1} maintained for the remainder of the operational period.

Biogas Composition: Measurement of biogas composition started at day 7 with CH_4 and CO_2 composition of 48% and 21% respectively (Figure 5-2f) with the remaining attributable to the N_2 gas used to purge the headspace at the start. Biogas fluctuated between 45-55% CH4 until day 19 when it rises to 80% on days 20-21. This was due to the consumption of accumulated VFA (0.6 g COD L-1). CH4 falls to around 60% from day 24-29 then maintained an average of 51% from day 30 onwards- with no visible change associated with OLR increase on day 35.

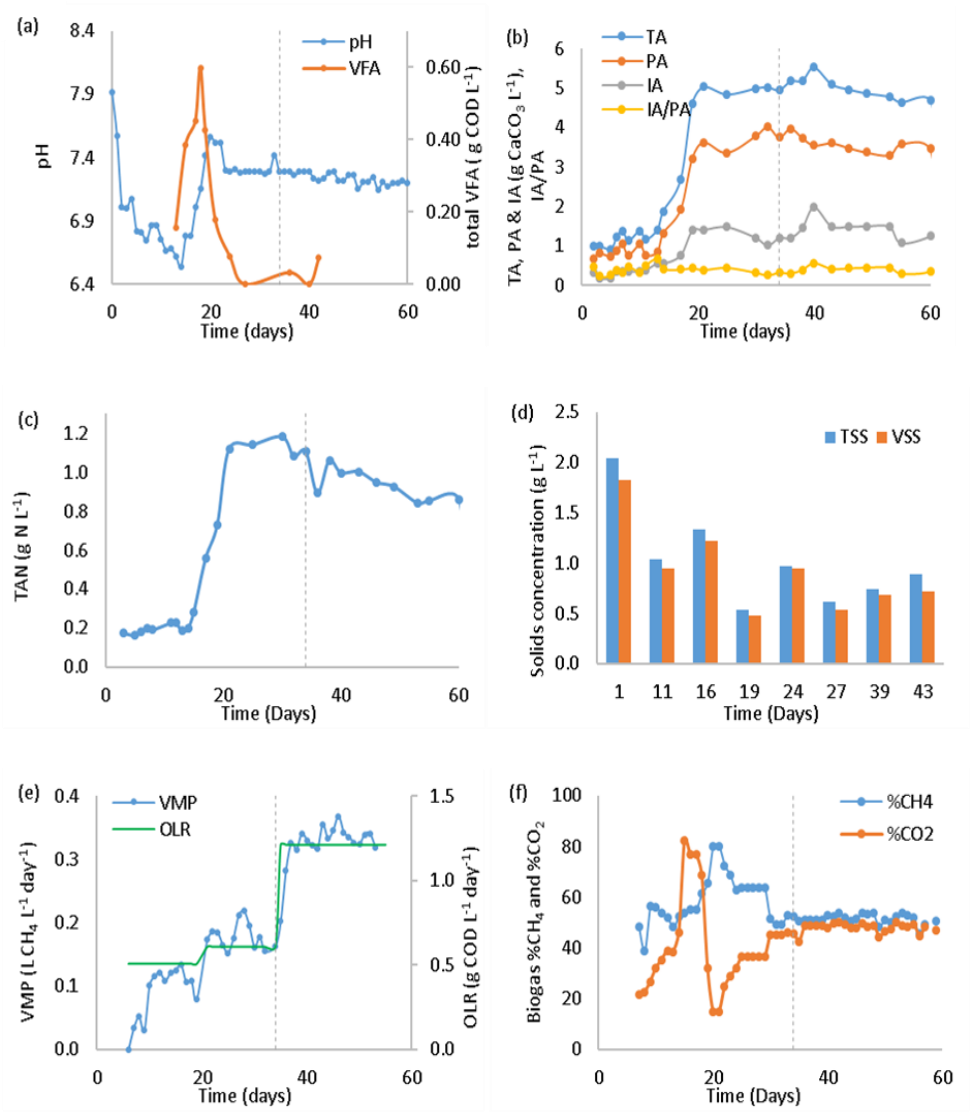

Figure 5-2: Start-up performance of AF1 on tomato wastewater with vertical dash line indicating change in OLR (a) effluent pH (b) Alkalinity profile and IA/PA ration (c) TAN (d) Digester TSS/VSS concentration (e) Volumetric methane production (VMP) (f) Biogas composition

5.1.4 AF2 start up performance

The second digester (AF2) with same dimension and properties as AF1 was set up in a similar manner as AF1 but in this case 1 L digestate was diluted to make up 4 L with tap water and sealed and the headspace was purged with Nitrogen gas. The inoculum was allowed to sit for 2 days before batch feeding with 60 mL of concentrated tomato juice once per day. The

content of the digester was recirculated at 2.5 L h^{-1} with the aid of a peristaltic pump. Batch feeding of AF2 lasted 25 days, maintaining the same OLR and temperature which was set at 30 ºC throughout the operational period.

5.1.4.1 pH

The pH profile for AF2 is shown in Figure 5.3a and it can be observed that the pH drops from 7.6 to around 6.5 on day 5 before slightly increasing to 6.9 on day 7 following the addition of 1 g urea and then fluctuates between 6.6 and maintains an average of 6.8 for the remainder of the trial, reaching 7.01 on day 25. The TAN was measured from day 7 and was around 0.4 g N L^{-1} following addition of urea and was very stable for the rest of the trial.

TA values measured from day 4 was fairly stable at around 1.9 g $CaCO_3$ L^{-1} and slightly decreased to 1.8 g $CaCO_3$ L^{-1} on day 10 before increasing to 2.3 g $CaCO_3$ L^{-1} from day 17 to day 24. PA was around 1.5 g $CaCO_3$ L^{-1} on day 7 and decreased to 0.9 g $CaCO_3$ L^{-1} on day 10 before recovering back to 1.5 g $CaCO_3$ L^{-1} by day 13 and increasing to 1.6 on day 24. IA behaved slightly different from PA increasing from 0.4 g $CaCO_3$ L^{-1} on day 7 to 0.9 g $CaCO_3$ L^{-1} on day 10 before reducing to an average of 0.6 g $CaCO_3$ L^{-1} until day 25.

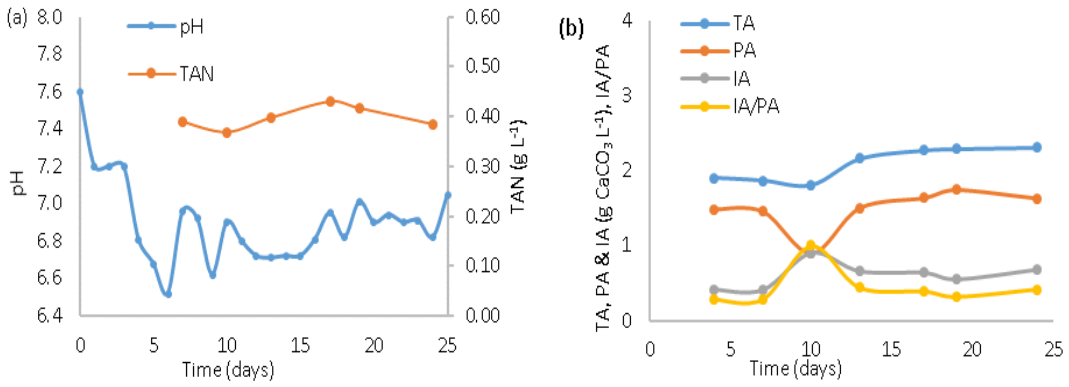

Figure 5-3:AF2 start -up performance (a) pH and TAN (b) Alkalinity and IA/PA ratio

From the above results for AF1 and AF2 it appeared that the start-up strategies adopted were successful and the reactors shown acclimatisation to the conditions and feedstock.

5.2 Mixing of the contents of AF1 and AF2

Following the initial start-up of AF1 and AF2 (with operational periods of 60 and 25 days respectively), the digesters were opened, and contents of both digesters were mixed together. Unused K1 biofilm carriers and fresh digestate was added to the contents of the digester, mixed together and split into two equal portions by weight before returning one portion each to digester AF1 and AF2. This was carried out in order to harmonise the contents of AF1 and AF2 and increase the potential biofilm capacity, with the plan to operate the digesters in an identical manner. The digesters were batch fed and monitored to evaluate performance and observe any differences. The same batch feeding procedure as described previously although 50 mL concentrated tomato juice was used. This lasted for 38 days without recirculation of the mixed liquor.

5.2.1 Results of mixed trial

5.2.1.1 pH

The pH profile (Figure 5-4a) shows a steady decline in pH from around 7.5 on day 1 for both digesters to 6.7 on day 10 before slightly increasing to around 7.1 and 6.8 for AF1 and AF2 on day 14 and maintaining an average pH of 6.9 until day 37.

TAN: The TAN profile shows similar behaviour for both digesters starting at around 0.6 g N L^{-1} for both digesters before declining to 0.43 g N L^{-1}on day 9 before slightly increasing to an average of 0.52 g N L^{-1} and 0.48 g N L^{-1} respectively for the rest of the trial.

5.2.1.2 Alkalinity

On day 1, TA was around 3.5 and 3.1 g $CaCO_3$ L^{-1} (Figure 5-4c) for AF1 and AF2 respectively. AF2 decreased to a low of 2.2 g $CaCO_3$ L^{-1} on day 10 while AF1 had its lowest value of 2.5 g $CaCO_3$ L^{-1} on day 11. Thereafter, both digesters showed a slow but steady increase in TA and reached a peak of 3.5 and 3.1 g $CaCO_3$ L^{-1} on day 25 for AF1 and AF2 respectively. Although a drop in The TA for to 2.4 for AF1 and 2.1 g $CaCO_3$ L^{-1} for AF2 is observed on day 36 which is the end of the trial. PA shows similar profile starting at 2.6 g $CaCO_3$ L^{-1} for AF1 and 2.4 g $CaCO_3$ L^{-1} for AF2, then decreasing to a low of 1.8 g $CaCO_3$ L^{-1} on day 11 for AF1 and 1.5 g $CaCO_3$ L^{-1} on day 10 for AF2. Both digesters recovered some PA, maintaining an average of 2.3 g $CaCO_3$ L^{-1} and 2.2 g $CaCO_3$ L^{-1} for the rest of the trial and ending at around 1.8 g $CaCO_3$ L^{-1} on day 36.

There was a marked difference in IA at the start with values of 0.88 g $CaCO_3$ L^{-1} and 0.64 g $CaCO_3$ L^{-1} for AF1 and AF2 respectively, and average values of 0.85 and 0.76 for AF1 and AF2 respectively. Just like the TA and PA, the IA dropped to 0.62 and 0.46 g $CaCO_3$ L^{-1} on day 36. Both digesters show stable IA/PA ratios of 0.3 at the start and was maintained below 0.5 throughout this period indicating that the digesters were stable throughout this period without any adverse effect.

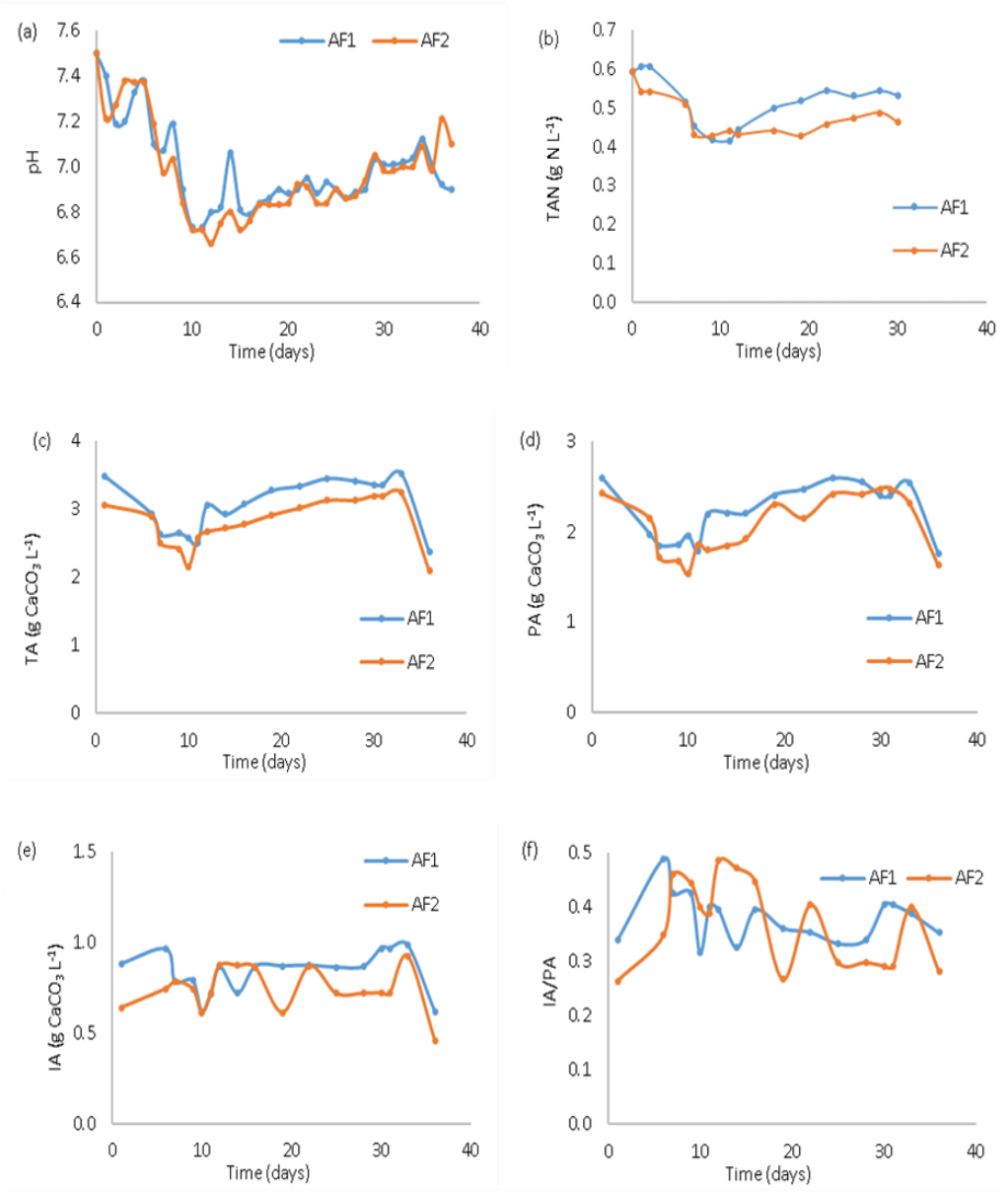

Figure 5-4 Second trial start up performance (a) pH (b) TAN (c) Total Alkalinity (d) Partial Alkalinity (e) Intermediate Alkalinity (f) IA/PA ratio

Biogas production, composition, VMP and SMP: Measurement of biogas composition started on day 3. Both digesters showed identical biogas composition profiles (Figure 5-5 a and b), the CH_4 content started low at 22% on day 3. And by day 10 had increased to 59% for AF1 and AF2 respectively. Both digesters were able to maintain an average CH_4 content of 52% for the rest of the trial period. CO_2 values were also similar, averaging 42% for AF1 and 43% for AF2. The total biogas composition, presumably contained other atmospheric gases as the sum of CH_4 and CO_2 were always slightly below 100%

VMP values were identical for both digesters, starting at 0.1 and 0.03 L CH_4 L^{-1} day^{-1} and reaching 0.3 L CH_4 L^{-1} day^{-1} by day 9. Except for slight fluctuations, VMP values remained above 0.3 L CH_4 L^{-1} day^{-1} until day 29 when AF1 dropped to 0.1 L CH_4 L^{-1} day^{-1} on day 29 before recovering and a second drop followed for both digesters on day 34 resulting in VMP values of 0.03 and 0.1 L CH_4 L^{-1} day^{-1} for AF1 and AF2 respectively.

SMP of both digesters show similar profile starting although AF1 was slightly higher at the start with a value of 0.064 L CH_4 g^{-1} COD_{added} compared to 0.028 L CH_4 g^{-1} COD_{added} for AF2.

Both digesters showed an increase in SMP and had average values of 0.26 L CH_4 g^{-1} COD_{added} for the rest of the trial period.

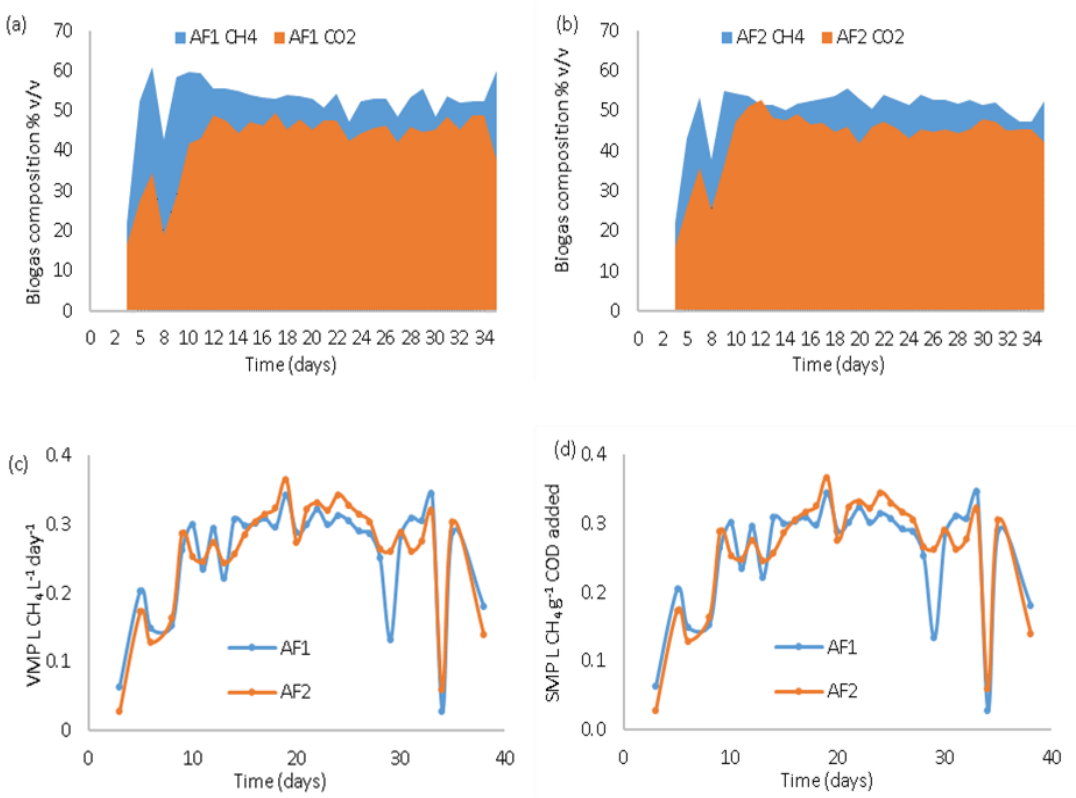

Figure 5-5: Start-up performance of AF1 and AF2 (a) Biogas composition for AF1 (b) Biogas composition for AF2 (c) VMP (d) SMP

5.2.2 Discussion on start -up strategy and performance

The batch feed start-up strategy was adopted to encourage acclimatisation of the new substrate and encourage biofilm growth particularly in the early stages of digester operation. It was also envisaged that introducing continuous feeding with dilute wastewater of equal strength could cause the wash out of essential nutrients and alkalinity, leading to digester instability. Escudié et al. (2011) showed that recycling improved the biomass resistance to environmental changes and that longer contact time favours biofilm growth . In fact, even though the batch feeding was adopted, and the feed recycled during this period, it was obvious that this was not enough to forestall the decline of the digester as evidenced by drop in pH, VFA accumulation and IA/PA increase. It was therefore decided to supplement the feed with ammonia-in the form of urea addition. This resulted in the recovery of pH, and

subsequent consumption of VFA. While this inevitably led to the increase in TAN, it was not enough to cause inhibition as it was below 1.5 g N L^{-1} quoted as the lower limit at which ammonia concentration could cause inhibition of the AD process (McCarty and McKinney, 1961), and therefore biogas production was relatively stable and responded well to the increase in OLR. Generation of alkalinity from urea addition is based on the reaction of ammonia N with CO_2 from the AD process resulting in the generation of ammonium bicarbonate and improved system alkalinity. Khanal (2011) describes the chemical reaction (Equation 5-1a and b).

$$RCHNH_2COOH + 2H_2O \rightarrow RCOOH + NH_3 + CO_2 + 2H_2 \qquad \text{Equation 5-1a}$$

$$NH_3 + H_2O + CO_2 \rightarrow NH_4^+ + HCO_3^- \qquad \text{Equation 5-1b}$$

5.2.3 Conclusion

This demonstrated the feasibility of supplementing the feed with ammonia N to enable stable performance of the digester. The attraction is that tomato wastewater can be co-digested with such wastes that are naturally high in organic N, to provide much needed buffer, thereby reducing the costs and implications of adding inorganic sources of buffer such as bicarbonates. It was also shown that the strategy adopted enhanced biomass attachment and biofilm growth necessary for the acclimation of the biomass to the substrate.

This trial was carried out without external buffer addition for alkalinity, but urea was added for N supplementation and to enhance alkalinity through conversion of the ammonia with the CO_2 from the anaerobic process causing an increase in the bicarbonate alkalinity. This could also prevent acidification and lead to a stabilisation of the anaerobic process (Boncz et al., 2012, Janke et al., 2016).

5.3 Start up: Continuous operation

The AF digesters were fed by making a dilution of concentrated juice (initially 150 mL, and increasing according to target OLR) made up to 10 L with tap water, which was stored in a fridge at 5 ^{o}C. Continuous feeding involved the supply of around 2.6 L of diluted tomato juice throughout the day at a flow rate of 0.11 L h^{-1}. The concentrate was diluted to a specific COD in order to achieve the target OLR. The temperature of the digesters was maintained at around 30 ± 2 ^{o}C throughout all experimental phases.

The start-up and operation of the integrated AF-DM process is as presented in Table 5-2.

Table 5-2: Experimental phases and properties for AF digesters

Phase	Duration (days)	COD (g L^{-1})	HRT (d)	OLR	Feed type/Flow
Phase 1	58	1	1	1	Continuous feed
Phase 2	41	2	1	2	Continuous feed
Phase 3	52	3	1	3	Continuous feed
Phase 4	47	4	1	4	Continuous feed

The feed was simulated by diluting with tap water to target concentration. Urea was added to supplement Nitrogen and it was envisaged that this would also increase the much-needed alkalinity. The mechanism as suggested as (Van Haandel, 2005) is based on the enzymatic hydrolysis of urea to provide CO_2 and ammonia. Each mol of urea adding 2 eq. of alkalinity leading to the increase in pH. (Boncz et al., 2012) showed that the dosing of urea for increasing alkalinity in the treatment of vinasse (pH = 4.3), helped increase and maintain pH.

The digesters were operated for 198 days with phases based on increasing OLR as shown in Table 5-2 and performance parameters monitored include daily pH, daily biogas production and composition, alkalinity, TAN, effluent COD/TOC, VMP, SMP and TOC removal rates.

5.4 **pH**

At the start of the continuous run in phase 1 (Figure 5-7a), the pH dropped quite rapidly from 7.2 to 6.5 over 4 days for both digesters. To forestall any deterioration of the performance due to falling pH, urea (30 mL of 68 g L^{-1} concentration) was added to the digesters on day 4, which helped to improve the pH to 6.8 and 7 for AF1 and AF2 respectively. For the rest of this phase, urea was added to the feed at 0.2g L^{-1}. The pH stabilised above 6.8 and trended upwards for the rest of phase 1.

For the second phase of the experiment from day 58 to day 97, the OLR was increased to 2 g COD L^{-1} d^{-1}, but the same amount of urea added to the feed with no major change in the pH following this increase showing that the digesters were able to cope with increased loading

Phase 3 started on day 99 with an increase in OLR to 3 g COD L^{-1} d^{-1} by increasing the influent feed COD to 3 g L^{-1}. The immediate response following this change in feed concentration was a drop in pH to 6.6 for both digesters on day 99, but this was soon followed by a recovery of the pH rising to 6.9 on day 105. This was maintained and remained above 6.8 until day 110 when a sudden drop to pH 6.5 was observed for both digesters. At this point, the feeding was skipped for one day to aid recovery. To restart feeding, the concentration of urea was increased to 0.25 g L^{-1} for both digesters. The pH had recovered to around 6.7 for AF1 and AF2 before feeding commenced again. This was maintained around 6.8 for several days and increased to 7 from day 133 to 141. The average pH in this period was 6.84 and 6.85 for AF1 and AF2 respectively.

The fourth and final phase (day 142 to 198) , when the influent COD was increased to 4 g L^{-1}, which corresponded to an OLR of 4 g COD L^{-1} day^{-1}. The pH decreased slightly to 6.7 and 6.8 for AF1 and AF2 respectively before increasing to 6.9. The pH for AF1 dropped to 6.5 on day 156 and the feeding was stopped for one day to prevent acidification of the reactor. This helped in restoring the pH to 6.9 after 2 days and between 6.7 and 6.9 for several days. On the other hand, AF2 remained stable between pH 6.7 and 6.9. On day 171 of the trial, the pH

dropped to around 6.5 for both reactors. The influent concentration of both digesters was reduced to 2 g COD L and a consequent OLR of 2 g COD L^{-1} day^{-1} for two consecutive days from day 172 to 174 to prevent overload of the reactor. This reduction in OLR led to an increase in pH to around 6.9 after one day. Based on this recovery of the pH, the feed concentration was resumed to 4 g COD L^{-1} and resulted in stable pH profile for the rest of the trial, even reaching 6.9 for both digesters at the end of the run.

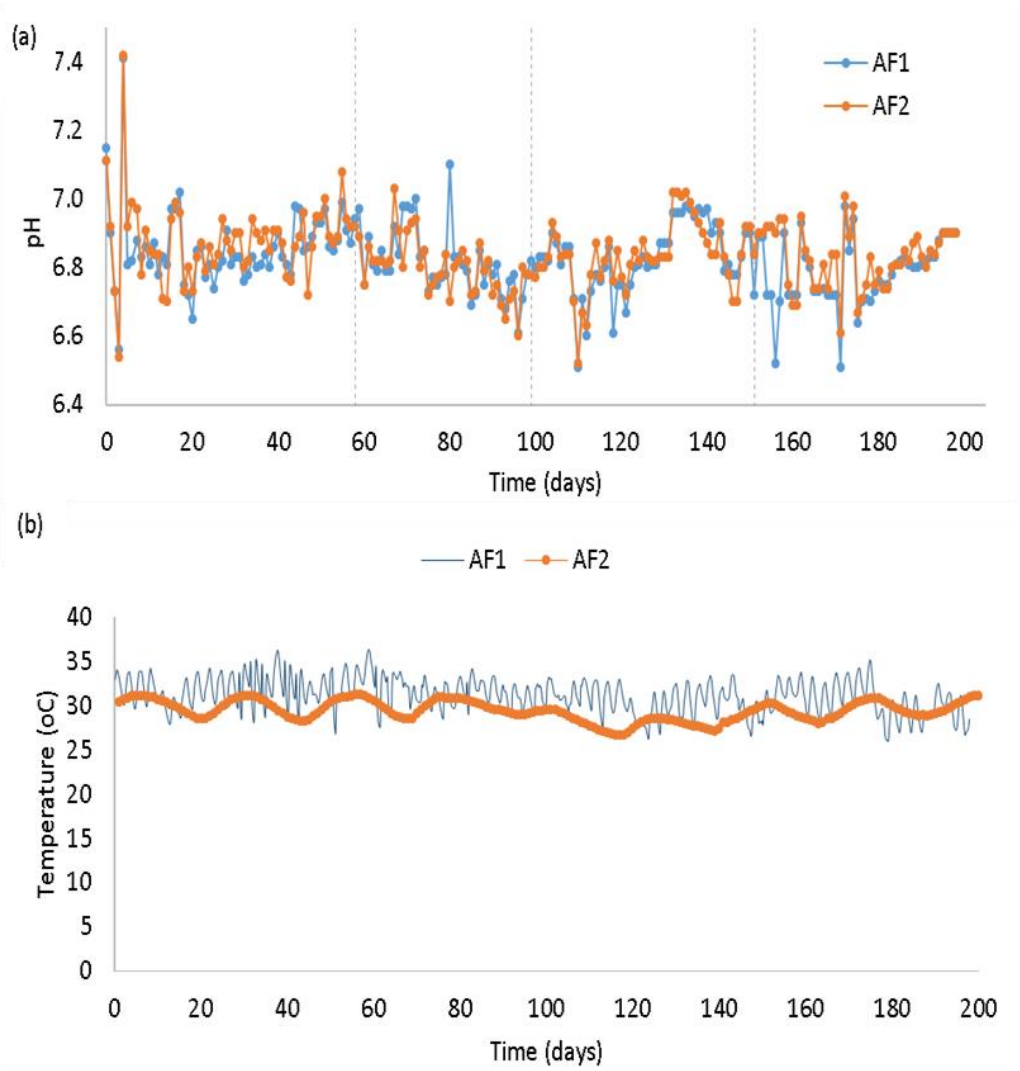

Figure 5-6: (a) pH profile of the digesters for the duration of the trial (dashed vertical line represents the end of each phase) (b) Operational temperature of the digesters set at 30 °C

5.4.1 Discussion on management of pH

Fixed film digesters such as anaerobic filters are characterised by their requirement for a long start-up period for acclimation and development of a robust biofilm, and as such require careful management of conditions in which the pH plays a critical role. The daily addition of urea (46% NH_3-N) was carried out in order to increase the ammonia N content of the digester and its subsequent hydrolysis to free ammonia by the action of the formed bicarbonate resulting in the reduction of acidity. It is evident that the addition of urea was able to achieve this and, save for the occasional drop in pH which mostly resulted from change in influent concentration and increase in OLR, the digesters were able to cope with this strategy.

5.4.2 Alkalinity

The total alkalinity (TA) in the digesters is presented in Figure 5-8a. As can be seen, the alkalinity was 2.3 and 2.1 g $CaCO_3$ L^{-1} at the start of the trial and quickly dropped to 0.5 $CaCO_3$ L^{-1} on day 9. To increase the alkalinity in the digesters, urea was added directly to the digester in soluble form, and subsequently 0.2 g L^{-1} urea was added daily to the substrate. This resulted in an increase in the total alkalinity to 1 g $CaCO_3$ L^{-1} and 0.8 g $CaCO_3$ L^{-1} for AF1 and AF2 respectively. In this manner, alkalinity was maintained in the digesters with minimal deviations from the average of 0.8 g $CaCO_3$ L^{-1} from day 25 to day 87.

Despite the increase in the feed concentration from 1 g COD L^{-1} to 2 g COD L^{-1} on day 58, the alkalinity was not significantly affected although it rose to 1.3 g $CaCO_3$ L^{-1} and quickly returned to 0.9 g $CaCO_3$ L^{-1} in both digesters. On day 112, the total alkalinity rises significantly to 1.4 and 1.5 g $CaCO_3$ L^{-1} for AF1 and AF2 respectively following the cessation of feeding due to low pH in the digesters. Resumption of continuous feed improved the alkalinity to 1 g $CaCO_3$ L^{-1} and subsequently reaching a high of 1.7 g $CaCO_3$ L^{-1} and 1.6 g $CaCO_3$ L^{-1} for AF1 and AF2 respectively on day 162. Alkalinity readings showed a rather fluctuating trend between days 159 and 202 with values ranging between a low of 0.9 g $CaCO_3$ L^{-1} and a high of 1.6 g $CaCO_3$ L^{-1} for both digesters.

The PA of both digesters (Figure 5-8b) behaved in a similar manner to the TA with stable values around 0.6 g $CaCO_3$ L^{-1} for both digesters in phase 1 and phase 2. Phase 3 showed a gentle increase in PA rising to 1.0 and 1.2 g $CaCO_3$ L^{-1} for AF1 and AF2 respectively due to the

increased ammonia N concentration. There was a fluctuating trend in PA for during phase 4 due to breaks in feeding and lowering of the OLR in some instances.

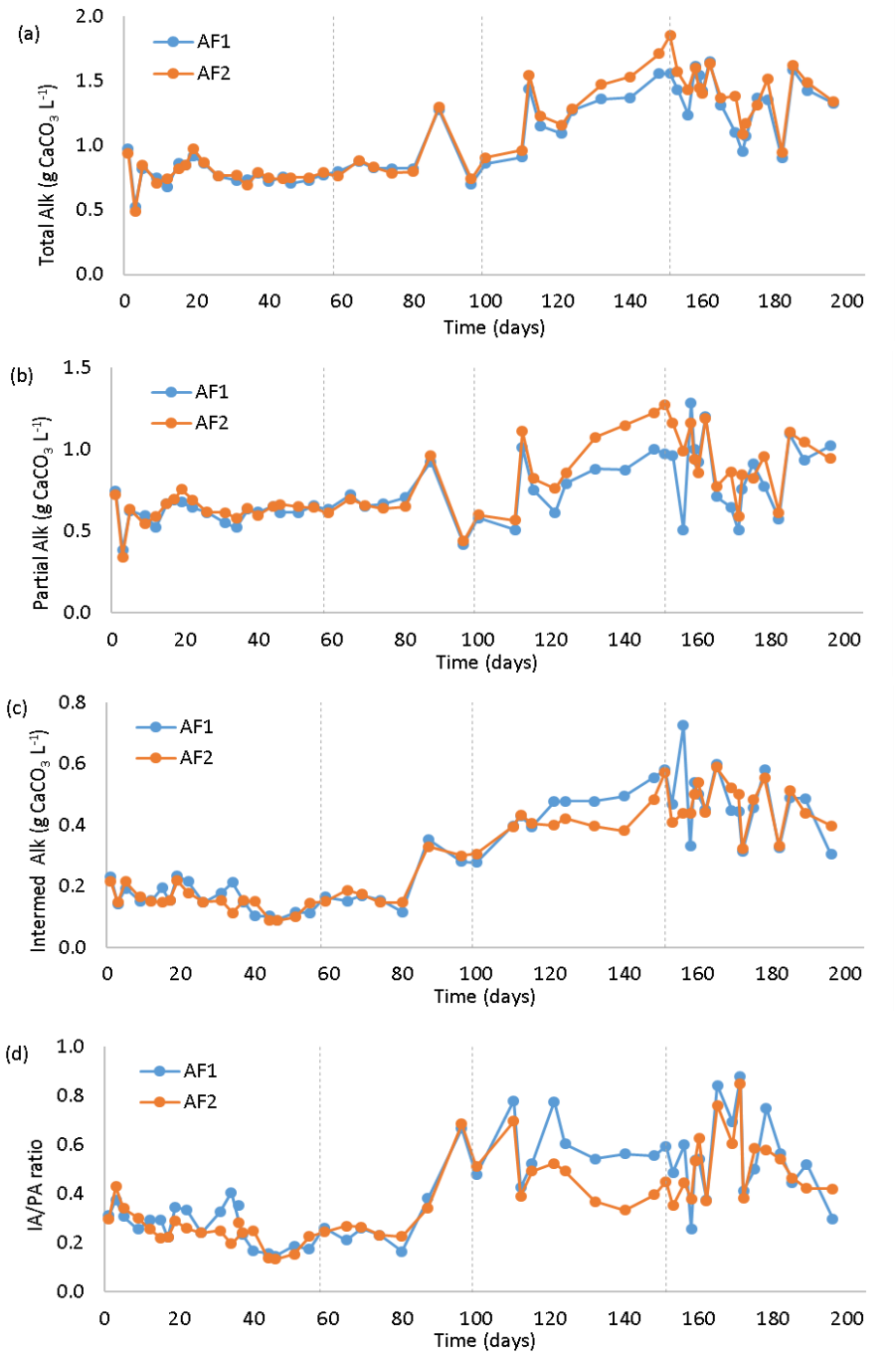

Figure 5-7: Alkalinity measurements (a) Total Alkalinity (b) Partial Alkalinity (c) Intermediate Alkalinity (d) IA/PA ratio

IA of the digesters (Figure 5-8c) was relatively stable for most of phases 1 and 2 averaging around 0.2 g $CaCO_3$ L^{-1} until day 87 when it rose and maintained average of 0.4 g $CaCO_3$ L^{-1} for phase 3. Phase 4 witnessed a fluctuating trend ranging from 0.3 to 0.7 g $CaCO_3$ L^{-1} until the end of the trial.

Figure 5-8d shows the IA/PA ratio which remains below 0.4 for the first 80 days before sharply rising to 0.8, and fluctuating between 0.4 and 0.8 between days 151 to 198 due to the digesters' struggle to cope with increased OLR.

A drop in alkalinity (TA, PA, IA) following the start of the continuous feeding operation is due to the gradual washout of the inherent alkalinity in the digestate without adequate replacement of the buffer from the feed. Addition of urea slightly increased the ammonia concentration in the feed and resulted in increased alkalinity, which stabilised the digesters particularly in the first 100 days, as the digester was able to cope with the OLR. In addition, the increase in ammonia due to the addition of urea enhanced the neutralisation of the acidity generated in the reactor and helped in maintaining an equilibrium between the rate of acidity generation and its neutralisation. Subsequent increase in OLR showed an increase in the alkalinity due to the more ammonia being available and its reaction with the CO_2 produced to increase the bicarbonate alkalinity. For the increased OLR period of between 120 to 202 days, which resulted in increased alkalinity to over 1 g $CaCO_3$ L^{-1} which is within the minimum range of 1.0 -1.5 g $CaCO_3$ L^{-1} for methane-forming bacteria as suggested by Gerardi (2003). Similar observation was made by León-Becerril et al. (2016) for AF digester treating cold meat industry wastewater at 37 ^{o}C in which the alkalinity was maintained at 0.75 g $CaCO_3$ L^{-1} even at a high OLR of 3.5 g COD L^{-1} day^{-1} without significantly affecting the reactor performance. The fluctuating alkalinity trend observed when the OLR was increased particularly from day 160 and 202 can be attributed to an imbalance between the reaction of the increased ammonia accumulation and the increase time lag for gas equilibrium of converting the CO_2 to bicarbonate made it difficult to keep the alkalinity stable (Ward et al., 2008).

IA/PA ratio is a quick and relatively simple method of determining the buffering capacity of the digesters and can signal the accumulation of the VFA. Studies by Ripley et al. (1986) suggested that the ideal ratio for digesters was between the range of 0.2 to 0.4, although (Martín et al., 2010) observed a slightly higher value depending on feed characteristics and operational conditions, without significant effect on overall digester health. On the days in

which the ratio climbed above the 0.6 mark –see days 110, day 121 (AF1), day 171 attempts were made to forestall the increase in IA/PA ratio by either pausing the feed for a few hours or reducing the OLR through applying a more dilute feed (OLR = 2 g COD L^{-1} day^{-1}). This showed intermittent recovery of the digester as indicated by the immediate reduction in the IA/PA ratio following such interventions, although this strategy was not sufficient to guarantee the reduction in IA/PA and any attempt to re-establish the OLR at 4 g COD L^{-1} day^{-1} resulted in higher IA/PA ratios. This indicates that the digesters are almost at their limit of tolerance, and if optimum performance is desired, and then it is necessary either to reduce the strength of the feed or, increase HRT

5.5 COD/TOC removal

The organic content removal rates were measured and analysed throughout the duration of the trial. It should be noted that for the first 25 days, the influent and effluent TCOD was measured to determine the rate of substrate degradation. Starting from day 28, this was replaced by measuring the soluble TOC of both feed and effluent. The TOC can be determined much more quickly, does not require the use and disposal of toxic reagents and possesses higher accuracy since human error is significantly less.

The feed COD could be converted to TOC concentration because samples of the concentrate were tested for both COD and TOC to establish the relationship between the two, which should not be affected by the degree of dilution. As a check, spot samples from different days were also tested: the data are presented in Figure 5-9 and show a strong correlation (n = 11, R^2 = 0.99, p = 1.96 X 10^-19). A similar approach was used for the soluble feed concentration (Figure 5-9b) and again there is a strong correlation (n = 17, R^2 = 0.99, p = 1.7 X 10^-19). The effluent soluble strength, despite fewer samples, could also be reliably tested in the same manner as the samples were centrifuged and filtered to remove any suspended and particulate matter and the results (Figure 6-4f) show a strong correlation (n = 5, R^2 = 0.97, p = 0.002) between the COD and TOC. Data from the analysis of the effluent total COD/TOC (Figure 6-4 d) showed a weaker correlation (R^2 = 0.69, n = 4, p =0.16). This can be attributed the presence of particulates in the samples, and not all the degradable fraction may already be degraded prior to testing. The TOC analysis involved the use of an autosampler for loading the sample, which could allow the settling of the particulates in the sample prior to analysis. For this reason, the correlation between feed total COD and feed

total STOC was applied to convert the effluent total COD to effluent soluble TOC. This relationship was applied when converting the effluent samples in the first 25 days which were tested for COD before switching to TOC in subsequent analysis.

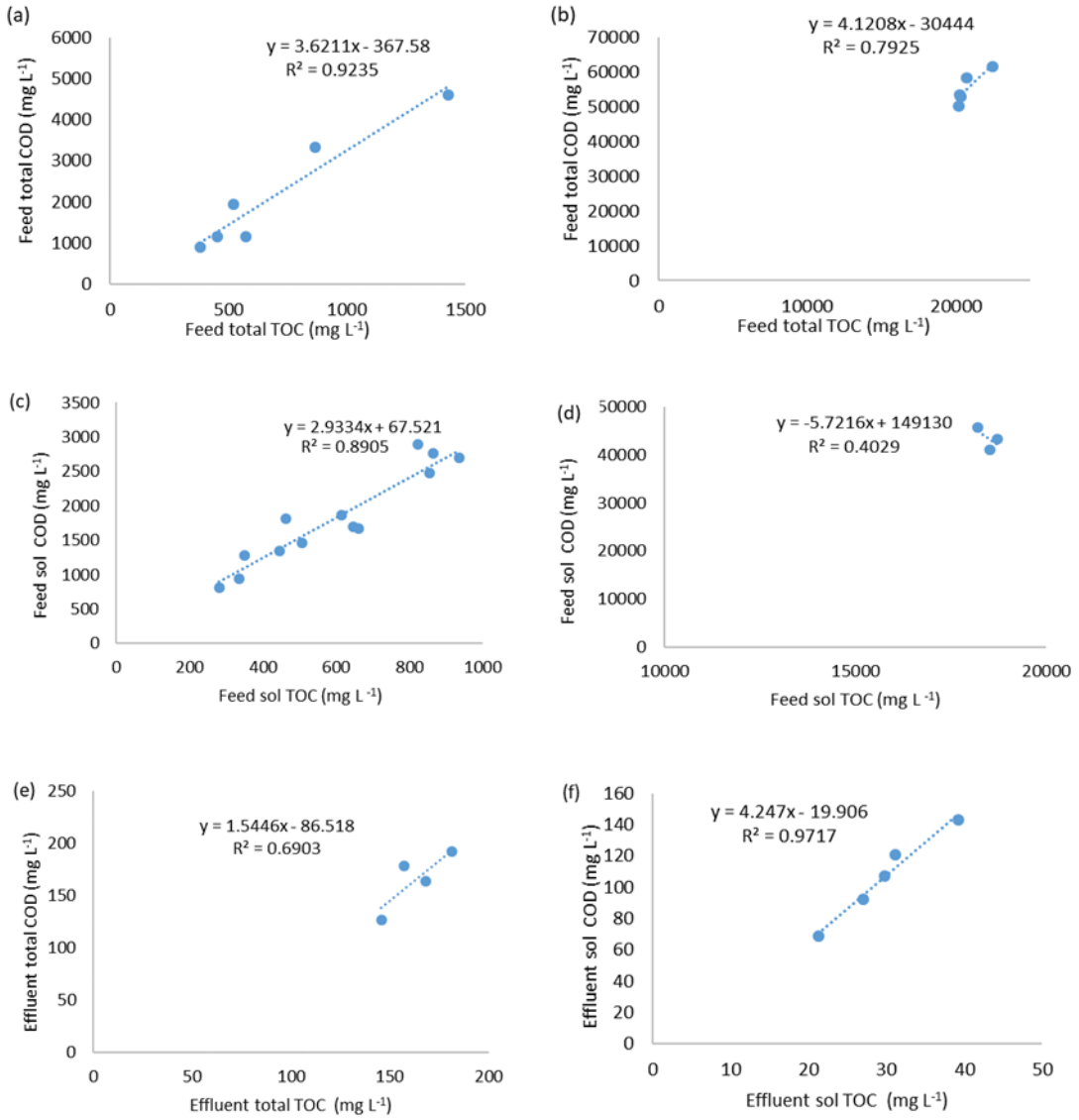

Figure 5-8: Plot of COD against TOC for tomato juice (a) Total feed –dilute (b) Total feed – concentrate (c) Soluble feed –dilute (d) soluble feed –concentrate (e) Total effluent (f) Soluble effluent

Organic matter removal: The concentration of influent and effluent and rate of degradation is presented in Fig 5-10a and b. At the start of the trial in phase 1, the target was to feed with influent TOC at around 350 mg TOC L^{-1} to meet the OLR of 1 g COD L^{-1} day^{-1}. This was difficult because of the concentrated form of the tomato juice and the degree of suspended material.

The target influent TOC was thus initially higher than planned, but was adjusted after 15 days to reflect the target OLR more closely. Effluent TOC was around 188 and 221 mg TOC L^{-1} on day 1 for AF1 and AF2 respectively, but quickly declined to an average of around 67 mg TOC L^{-1} for both digesters.

The influent TOC was doubled for phase 2 with average of 606 mg TOC L^{-1} and the effluent TOC was even lower than 30 mg TOC L^{-1} for both digesters showing that the biofilm was coping quite well with increase in OLR.

Phase 3 started on day 90 with increase in influent TOC to around 840 mg TOC L^{-1} corresponding to OLR of 3 g COD L^{-1} day^{-1}, although there was drop a one-off drop when half of the influent TOC was used on day 141 but this was soon rectified. Phase 3 saw an increase in effluent TOC which began on day 105 with values of 165 and 213 mg TOC L^{-1} for AF1 and AF2 respectively. Average effluent TOC during this phase was much higher than the previous phases and was around 135 and 99 mg TOC L^{-1} for AF1 and AF2 respectively. This trend continued in Phase 4 when the influent TOC was increased to around 1200 mg TOC L^{-1}. From day 150, the effluent TOC increased significantly for AF1 to 231 mg TOC L^{-1} while AF2 was much lower at 111 mg TOC L^{-1}. Despite fluctuating performance, the average effluent TOC was around 130 mg TOC L^{-1} for both digesters taking into account that there were a total of 3 days during which the OLR was halved by reducing the influent TOC concentration.

TOC removal rates at the start of phase 1 rose from over 50% for AF1 and 40% for A2 on day 1 but rose to around 80% by day 3 and subsequently maintained an average removal rate of 80% on day 3 and averaging over 80% during phase 1. The removal rate increased in phase 2 reaching an average of over 90% for both digesters before slightly dropping in phase 3 and phase 4 to just over 85% although occasionally lower removal rates were also observed. Phase 4 removal rates were also influenced by periods in which the OLR was reduced and which witnessed slightly higher removal rates.

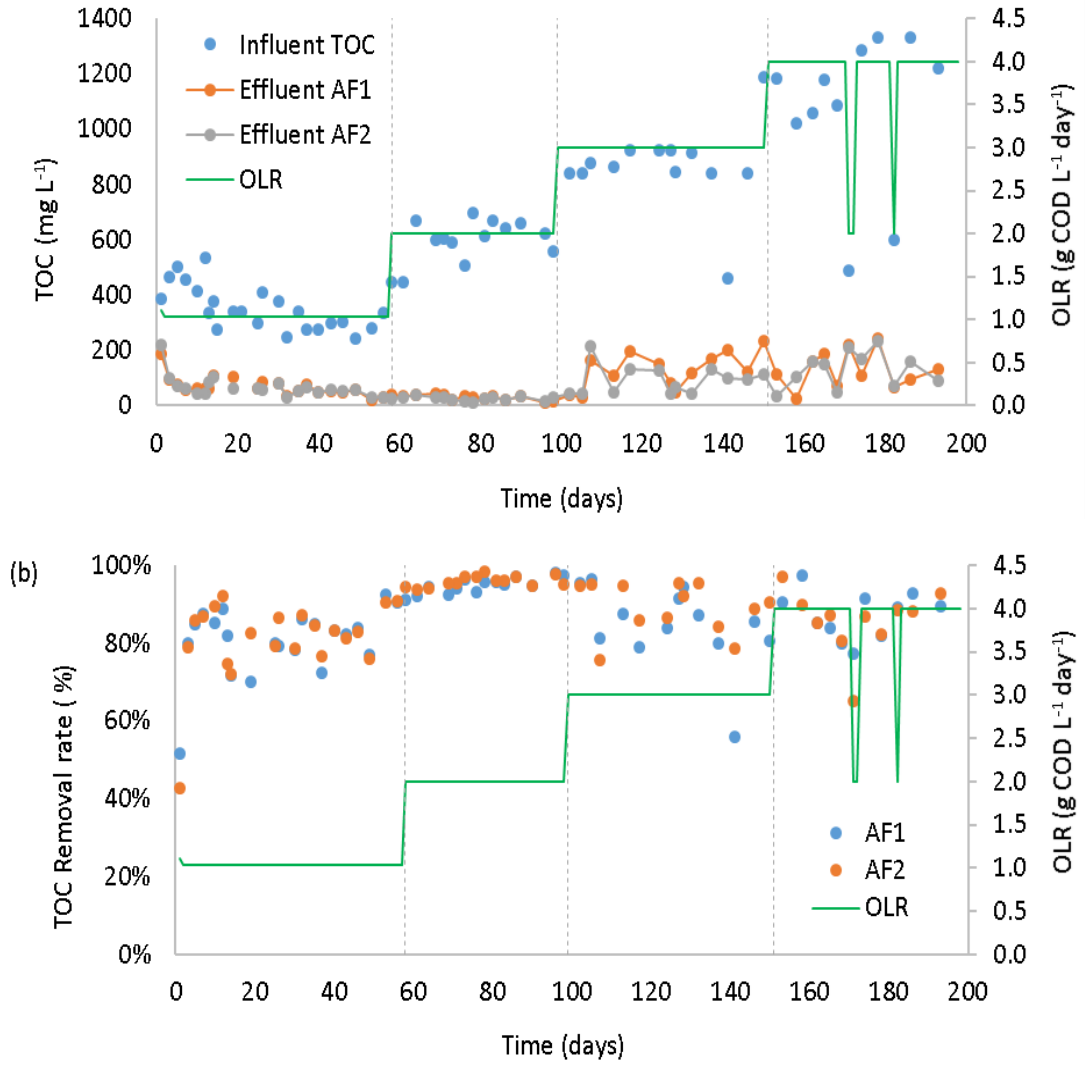

Figure 5-9: TOC removal during long term operation of AF1 and AF2 treating tomato wastewaters at 30 ºC (a) TOC values for influent, effluent and OLR (b) Removal rate of AF1 and AF2 (vertical dashed line signifies change in OLR)

Similar performances for AF were observed by (Cresson et al., 2006, Cresson et al., 2008), due to the initial washout of planktonic and unattached biomass giving way to the growth of more robust and attached biomass necessary for biofilm development. The effluent from digesters and AF typically does not meet wastewater discharge standards, necessitating the need for post treatment at additional cost (Chernicharo, 2006).

5.6 Biogas production

The biogas composition during operation is presented in Figure 5-11. The methane content of the biogas starts from a low of 66% and 64 % for AF1 and AF2 respectively then increases to an average of about 70% CH4 with a slightly decreasing trend towards the end of phase 4 for both digesters. CO_2 fraction of the biogas averaged around 22% with the rest being other atmospheric gases present in the headspace. The feed temperature was kept at 5 ºC to reduce the level of degradation: this leads to an increased dissolution of atmospheric air into the feed and the digesters; hence, the presence of some residual gases coming out of liquid feed solution and into the digester headspace operated at a digester temperature of 30 ºC.

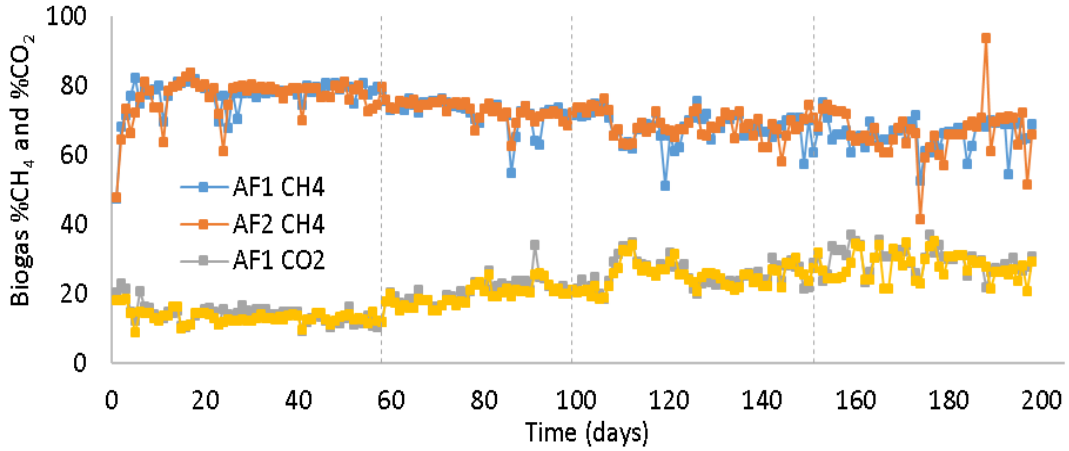

Figure 5-10: Biogas composition of AF digesters treating tomato wastewater at 30 ºC

5.7 Specific methane production

The SMP for the digesters is presented in Figure 5-12. There appears to be a fluctuating trend and the average SMP for both digesters was around 0.07 L CH4 g TOC added for the entire trial. The first 20 days showed more fluctuation as the changes in anabolic/catabolic activities expected due to the evolution of the biomass, gradual attachment of biomass to the carriers and loss of suspended and unattached biomass with the effluent. The relatively short HRT of 24 hours favours the removal of unattached biomass and promotes only the robust biomass capable of attachment and growth of the biofilm. Similar observations were made by

(Cresson et al., 2008) in which a fast washout (short HRT) resulted in increased attached biofilm compared to slower effluent removal (longer HRT).

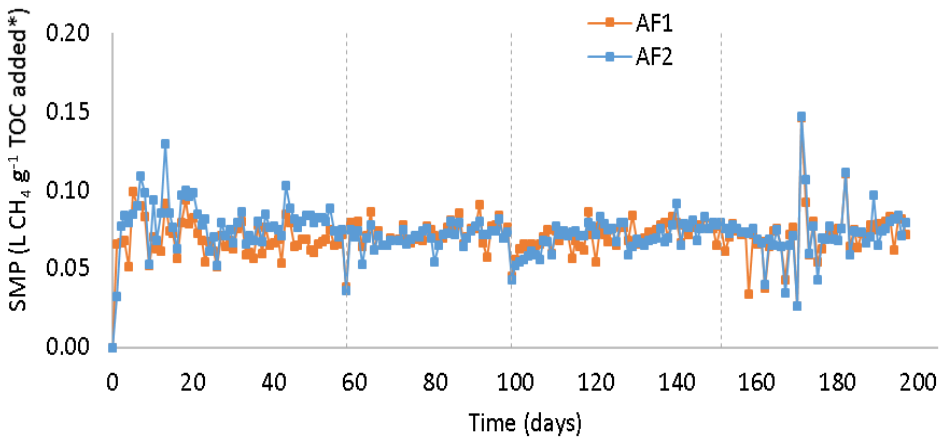

Figure 5-11: Specific methane production of the AF digesters treating tomato wastewater under increasing OLR

Volumetric Methane Production (VMP): VMP readings throughout the trial are presented in Figure 5-13. The VMP at the start (phase1) was around 0 for day 1 but increased to 0.2 L CH_4 L^{-1} day^{-1} and was stable for the rest of phase 1 which lasted for 58 days. There was a doubling of the VMP immediately following the start of phase 2 commensurate to the increase in OLR to 2 g COD L^{-1} day^{-1} with an average VMP of 0.4 L CH_4 L^{-1} day^{-1}. Similar trends were observed for phase 3 and phase 4 for both digesters. A more fluctuating trend was observed in phase 4 when increased OLR led to performance issues. Attempts were made in some instances, particularly on day 171 and 182, to cope with this by temporarily reducing the OLR from 4 g COD L^{-1} day^{-1} to 2 g COD L^{-1} day^{-1} and this is reflected in the drop in VMP in both cases.

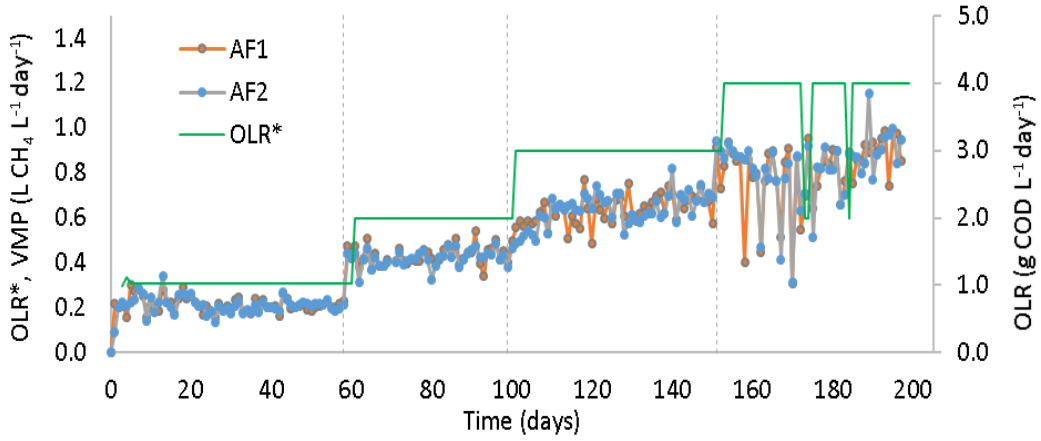

Figure 5-12: VMP for digesters AF1 and AF2 treating tomato wastewater at 30 ºC

5.8 Self-forming Dynamic Membrane Performance

This section focuses on the performance of the DM treating the effluent from the operations of the AF1 and AF2 described in section 5.3.

DM performance: Long-term operation of the DM was conducted and assessed based on modes as described in Table 5-4.

For the mode 1 operation, the DM was continuously filtering the effluent from the two digesters at the same time, without relaxation. A change in filtration to mode 2 was necessary because of the chance of overflowing observed in instances when the DM is blocked, leading to the backflow of permeate into the headspace of the digesters. To forestall this occurrence, an intermittent mode of operation controlled by a float switch connected to the peristaltic pump. Intermittent operation is widely applied in conventional membrane filtration processes (Hong et al., 2002, Zsirai et al., 2012, Chen et al., 2016, Dong et al., 2016) and aids in the alleviation of fouling and cake consolidation.

Table 5-3: Details of SFDM operational modes

Operation	Mode	Imposed Flux	Period (day)	Duration (days)	Number of cleaning episodes
1	Continuous	25-27	0-11	11 days	0
2	Intermittent operated by level float switch	40-44	30-201	167	3

5.8.1 AF-DM Operational Mode 1

This mode of operation was carried out for 11 days and performance of the DM was evaluated in three ways: the flux measurement, the TMP reading and the permeate turbidity. The TMP readings are presented in Figure 5-14a. At the start of the filtration, the pressure rose to 0.1 bar within the first hour and stabilised at 0.6 bar after 2 hours. The TMP maintained an average of 0.6 bar throughout the test period with very little change. The flux readings as presented in Figure 5-14b shows hourly flux for the first 24-hours. Although the flux was originally set at around 30 L m^{-2} h^{-1}, it quickly dropped to 25 L m^{-2} h^{-1} within a few minutes of the start and maintained this level for about 10 hours after which an attempt was made to increase the flux to compensate for the flow level in the DM tank. This resulted in an increase back to 27 L m^{-2} h^{-1} but this only lasted for about 11 hours before falling back to an average of 24 L m^{-2} h^{-1}. Permeate turbidity (Figure 5-14c) values for the first three days of operation were over 60 NTU but declined sharply afterwards to around 12 NTU and remained below 15 NTU daily for the remaining 8 days.

Discussion: Increase in TMP within an hour of the start of operation indicates rapid formation of the DM. This rapid formation may be attributed to the DM being formed by the higher concentration of solids being washed out from the AF following the start of the continuous operation. This can aid in the formation of the DM but at the expense of increased TMP and reduced flux. During operation, the TMP was very stable implying that a uniform cake layer had been formed and was able to retain the solids from the effluent of the digesters. Although the high imposed flux and lack of shear resulted in high TMP, it was possible to have a stable DM

The initial plan was to have a process such that the DM continuous filters the effluent produced directly from the digesters AF1 and AF2. This led to some issues and a need sometimes to manually adjust the rpm of the pump to compensate for the imbalance- caused by either the flux being lower than the produced permeate or set flux being higher than produced effluent, leading to sub-optimal operation.

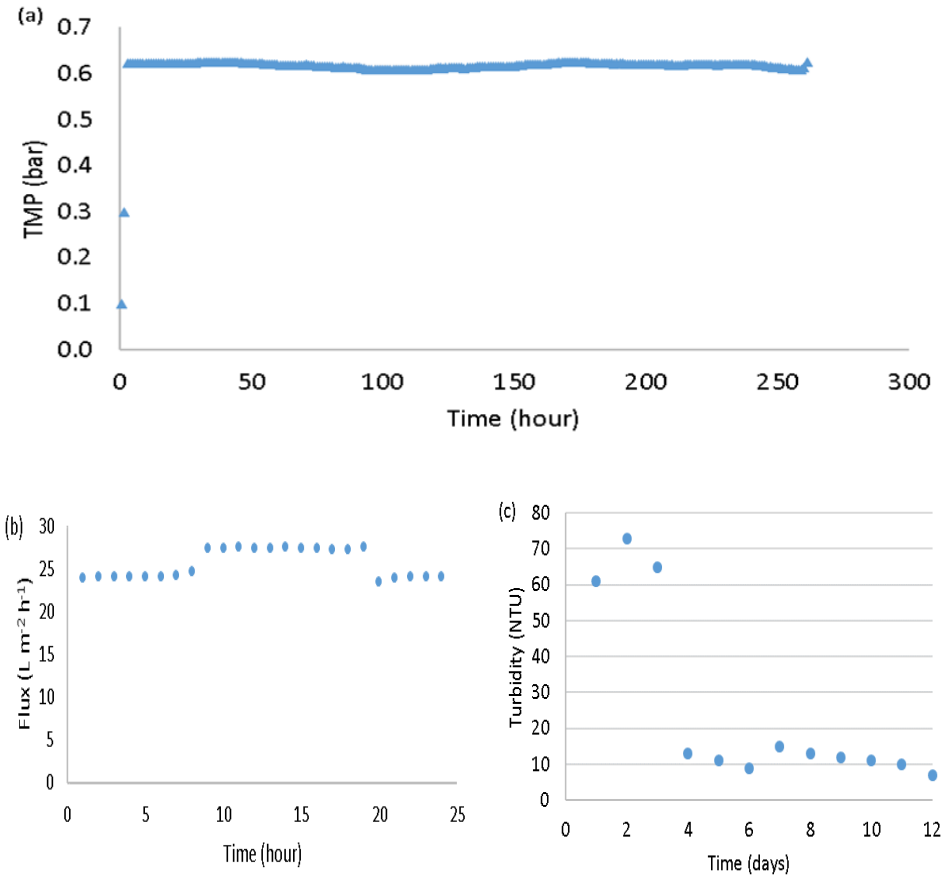

Figure 5-13: Performance of DM under constant filtration (a) Average hourly TMP values (b) average hourly flux profile for the first 24 hours of operation -with imposed flux of 30 L m^{-2} h^{-1} (c) Daily permeate turbidity for the 12 days of operation .

The relatively quick formation of the DM is observable as the TMP rises shortly after the filtration commenced. This was contributed by the TSS from the initial washout at the start of the operation. Gradual deposition of the suspended solids from the effluent resulted in the rise in TMP until an equilibrium is reached in which there is little change in the TMP. A sudden increase in TMP coincided with a significant loss of flux indicating that the pores are partially blocked and the effluent is unable to permeate through the cake layer. Because of

this rise in TMP, removal of the biofilm/cake layer and cleaning of the support mesh was done. Cleaning was carried out by running under flowing tap water and gently brushing off the cake/biofilm layer shown in Figure 5-15. The analysis of total resistance (Figure 5-16) showed that the resistance due to cake filtration contributed 81% of the total resistance, while gel resistance and clean membrane (intrinsic) resistance were 18% and 0.3% respectively. The implication of the gel layer resistance is that cleaning with water is capable of removing much of the cake layer and recovery of at least 80% of the clean material flux. It also presents evidence that some of the particles remain in the interstices of the pores and are not removed completely through regular cleaning with water.

Figure 5-14: Photo of cake layer formed during continuous operational flux of around 30 L m^{-2} h^{-1} at the end of the continuous operation cycle prior to cleaning with tap water.

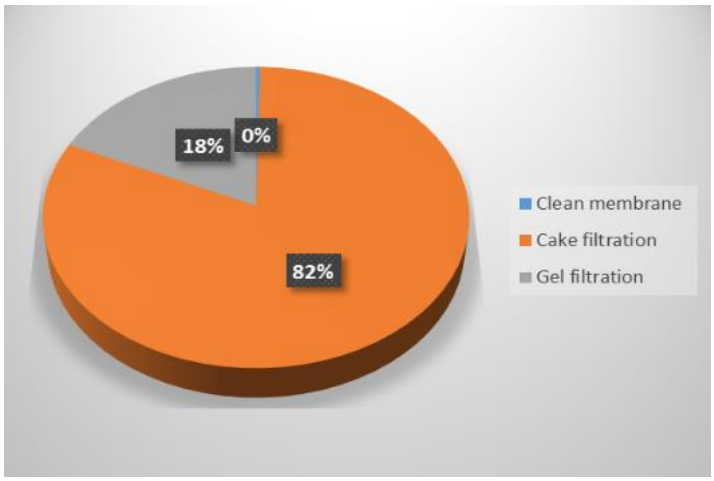

Figure 5-15: Resistance composition for the DM

5.8.2 AF-DM Operational Mode 2

Mode 2 started on day 12 of the operation and involved the introduction of a float switch to control the operation of the peristaltic pump providing suction for the DM. This resulted in an intermittent operation whereby the pump switched on when the liquid reaches a high level and switches off at a lower level. Based on the operational process, the pump rpm was set up to provide a flux of around 25 L m^{-2} h^{-1}

The performance of the DM during this mode of operation based on TMP and flux is presented in Figure 5-17a. It should be noted that the DM was not cleaned in between switching from mode 1 to mode 2. The flux was originally set up at an rpm to correspond to around 25 L m^{-2} h^{-1} but as can be seen from Figure 6.12a, it occasionally fell slightly to between around 19 and 23 L m^{-2} h^{-1} and averaged around 19 L m^{-2} h^{-1} throughout. The occasional drop preceding either a cleaning episode or due to operational stoppage is noticeable.

The evolution of the TMP starts from around 0.02 bar and remained level for around 8 days before a sudden rise to 0.05 bar followed by fluctuating TMP for 3 days and falling back to 0.03 bar on day 13. Day 34 saw the first cleaning episode carried out, although no significant increase in TMP preceded this episode. The TMP then begins to rise gently until day 88 when it reached 0.06 bar at which point, the second cleaning episode was carried out by removing the DM module from the tank. Cleaning lasted for about 10 minutes before resuming

operation, with the TMP starting at around 0.01 bar. It then increased gently and reached 0.06 bar around 86 days after the start.

At this point the second cleaning operation was carried out, and the TMP dropped back to around 0.02 bar on day 86. There was very little change for some time followed by rise in TMP and the occasional jump in TMP on days 112 and 127 when the TMP reached around 0.06 bar although there was no intervention. This implies that there is a point where the cake layer begins to fall off after reaching a threshold.

Days 144-157 experienced a haphazard performance where the TMP behaved rather erratically, and it was decided to clean the DM for the third time on day 159. After this the TMP began to rise, reaching 0.05 bar after 14 days before falling and staying at around 0.02 bar for the remainder of the trial. In addition, the falling temperature in this period (Figure 6.12b) may have increased the viscosity of the liquid medium thereby causing an increase in TMP.

Permeate turbidity (Figure 5.16b) shows that the DM can improve the effluent quality irrespective of loading rate. The turbidity of the effluent from the digesters was measured in a few cases and ranged from 100 to 370 NTU due to the increasing organic loading from the digesters. The permeate turbidity remained below or around 20 NTU for the first 70 days before increasing slightly in the days preceding the second cleaning episode. Following that the permeate turbidity peaked between days 106 and 122, due to the DM being formed in the period after the cleaning episode. The permeate turbidity fluctuated slightly but remained largely below 40 NTU from day 122 until the end although there were a few episodes where the permeate turbidity spiked.

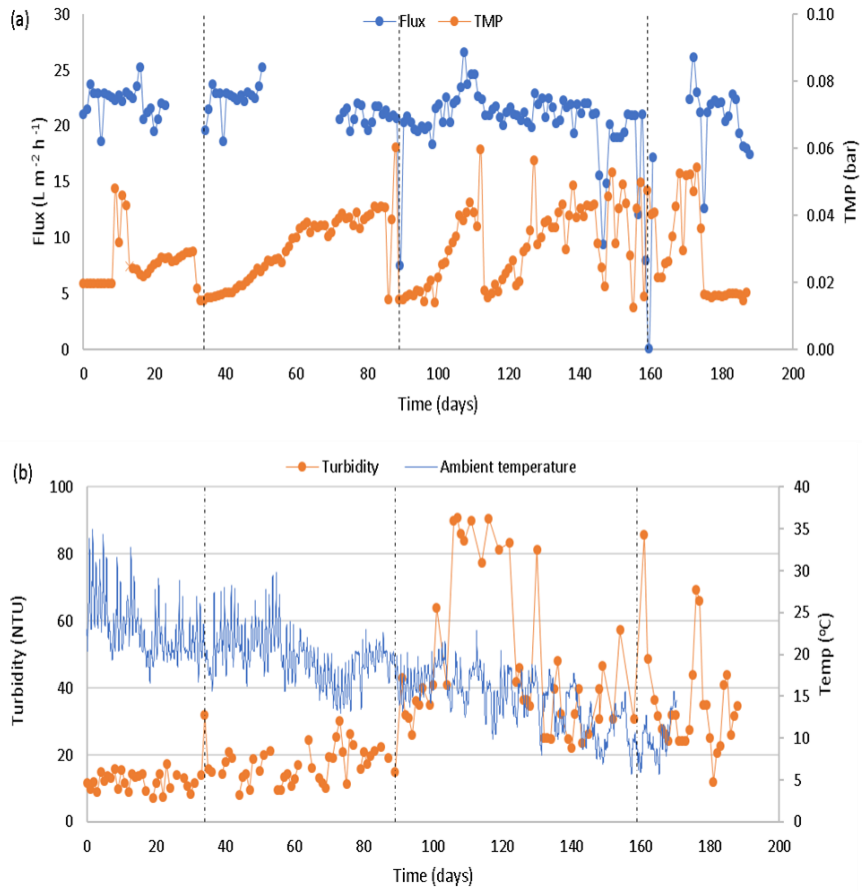

Figure 5-16: Long term performance of the DM treating the effluent from AF digesters under ambient temperature conditions (a) Daily average TMP and flux profile (b) Permeate turbidity and ambient temperature readings (Dashed vertical lines represent periods between cleaning episodes)

These periods coincided with fluctuating TMP and may indicate some patches or uneven cake formation. Similar observations were made by Citulski et al. (2009) in which intermittent increases in the feed organic load resulted in spikes in turbidity and increased reversible fouling although irreversible fouling was not much affected. The number of cleaning episodes were less frequent than reported by Sahinkaya et al. (2017) which required 10 cleaning episodes over a 63-day period. This can be attributed to the intermittent operation adopted in this study as the flux were similar

5.8.3 Comparison of continuous operation (Mode 1) and intermittent operation (mode 2):

It is evident that the continuous mode offered higher TMP (0.6 bar) compared to the intermittent operation (less than 0.06 bar), even under similar net flux, due to the higher consolidation and compression of the cake layer expected in continuous operation compared to intermittent operation. This is in agreement with Liang et al. (2012) who found that the critical flux was up to 20% higher when intermittent operation was introduced compared to under continuous operation for a SFDM. Similar observations were made by (Wu et al., 2008) in which they observed that the application of a relaxation period alleviated the rise in TMP and therefore resulted in longer interval between cleaning episodes.

5.8.4 Effect of Temperature on DM performance.

The effect of temperature on the DM performance (effluent turbidity) can be seen in Figure 5-16b. For the first 100 days the temperature ranged from 15-32 ˚C with evident diurnal temperature variations. The DM flux was maintained around 20 L m^{-2} h^{-1} during this period although a gradual TMP rise is observed. For the later wintery months, where the temperature dropped below 20 ˚C (day 100), a more frequent and steep rise in TMP becomes evident.

This can be partially explained by changes in physical phenomena such as increased mixed liquor viscosity and deflocculation of biomass which is evidenced in the increased permeate turbidity (greater than 80 NTU) following the cleaning episode at day 86. It is also evident, however, that gel layer formation became more pronounced at lower temperatures, possibly due to increased production of EPS and SMP. This agrees with several studies showing a positive correlation between membrane fouling and lower temperature operation (van den Brink et al., 2011, Ma et al., 2013b)

Following the second cleaning episode the permeate turbidity increased significantly, although the rise in OLR from 2 to 3 g COD L^{-1} d^{-1} may also have been a contributing factor as a result of higher EPS and soluble microbial products concentrations coupled with the inherent limitations of the cake layer in blocking low molecular weight soluble products.

This is expected as EPS and SMP have been shown to have a characteristic size below 2000 nm (Ramesh et al., 2006) resulting in increased turbidity in the permeate. The lack of

temperature control implies that the filtration is subjected to ambient variations and the effect is evident particularly when the temperature drop corresponds to a fluctuation in permeate turbidity values as seen in Figure 5-16b after day 100.

5.8.5 Particle Size Analysis of the GD-DM

Particle size distributions for the effluent from AF1 and AF2 and the permeate from the DM at steady state (day 144, 24 NTU) are presented in Figure 5-18. The particle size distribution were similar for both mixed effluent (AF1+ AF2) and the DM permeate (range between 0.5 µm and 1000 µm), although the median particle size was much lower for the permeate than the effluent with values of 10 µm and 94 µm respectively. In addition, 70% of the total particle volume in the mixed effluent were in the range of 30 to 500 µm, while 68% of the particles in the DM permeate were less than 20 µm. These indicate that the larger particles were intercepted by the formed cake layer rather than passing through the support material. This is in agreement with a study by which analysed the PSD of the cake layer and bulk sludge liquor of a submerged AnMBR treating thermochemical pulping whitewater, with 3% of the total particle volume in the bulk sludge having less than 5 µm compared to 18% in the cake layer. Similar observations were also made by (Lin et al., 2010) when treating kraft pulp mill evaporator condensate using a flat sheet microfiltration membrane resulting in a shift from a particle size predominantly larger than 10 µm (and less than 200 to particle sizes less than 100 µm in the cake layer tested.

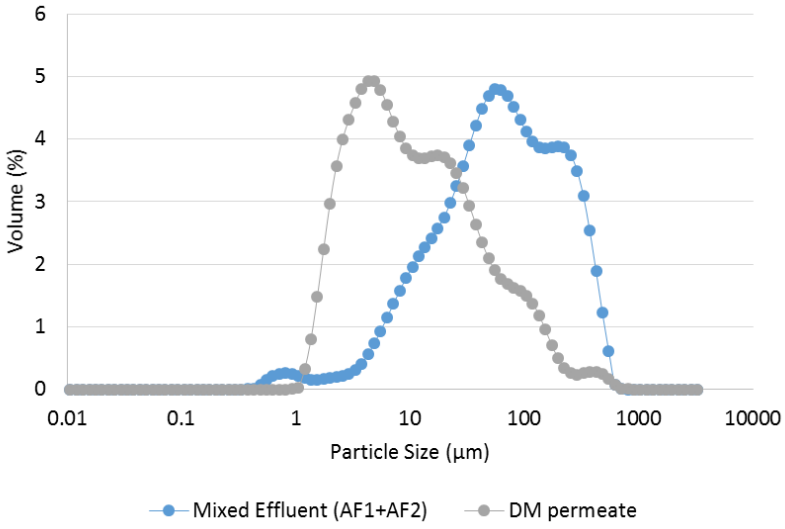

Figure 5-17: Comparison of particle size distribution of the effluent from the AF digesters and the DM permeate under steady state operation (day 144)

5.8.6 Effects of cleaning episodes

For the 187-day operation of the continuous DM filtration, a total of 3 cleaning episodes were carried out. Table 5-5 shows the resistances shortly (one day) before and following cleaning (one day after). Resistance on day one of the operation was about 4.2 X 10^{11} m^{-1}. On day 34, cleaning was carried out prematurely as the turbidity was higher than usual, but as can be seen, there was not much difference in the resistance values. The second DM cleaning episode carried out on day 89 saw the resistance drop from 7.1 X 10^{11} m^{-1} to 2.6 X 10^{11} m^{-1} (63%), while the final cleaning episode saw the resistance increase significantly prior to cleaning (1.4 X 10^{11} m^{-1}), primarily due to blockage of the pores (cessation of flow). Although cleaning ensured that 63% of resistance (compared to pre-cleaning) was removed, it is clear that successive cleaning episodes were not able to restore the resistance to values seen at the start of the trial. The increase in residual resistance due to imperfect cleaning had some benefits, however, as it could aid in the quicker formation of DM following each successive cleaning cycle. The use of low cost fabrics as such as nylon mesh that can be washed by simple physical methods as it may make this type of treatment affordable and accessible in applications where high cost and complexity would not be suitable.

Table 5-4: Resistance values before and after cleaning episodes of DM treating effluent from AF digesters.

Day	Total Resistance (m^{-1})
0	4.2 X 10^{11}
34	2.7 X 10^{11}
35	2.6 X 10^{11}
89	7.1 X 10^{11}
90	2.6 X 10^{11}
159	1.2 X 10^{14}

160	6.5 X 10 ^{11}

5.8.7 SEM analysis of AF-DM cake layer

Further examination of the DM was carried out by SEM and the results are presented in Figure 5-19. The cleaned nylon mesh shows that most of the cake layer is removed using tap water and lightly brushing off, although this does not completely rid the support material of some deposits, as some particles are still visibly attached to the strands of the nylon mesh. The evolution of the DM formation was tested by subjecting a cleaned mesh to filtration for about five hours. The image as captured in Figure 5-19b shows the support material being partially blinded by solids although the strands of the nylon mesh are still visible. Figure 5-19c shows the complete formation of the DM with the cake layer visible, with solids and microbial cells present. A closer magnification of the surface (5000X) as shown in Figure 5-19d with clusters of microbial products (including microbes) present. This is an indication that in addition to provision of a physical barrier present, the DM also has the potential to act as a biofilm. This is in agreement with Smith et al. (2015), who showed that the presence of biofilm rich in methanogenic archaea further enhanced treatment performance.

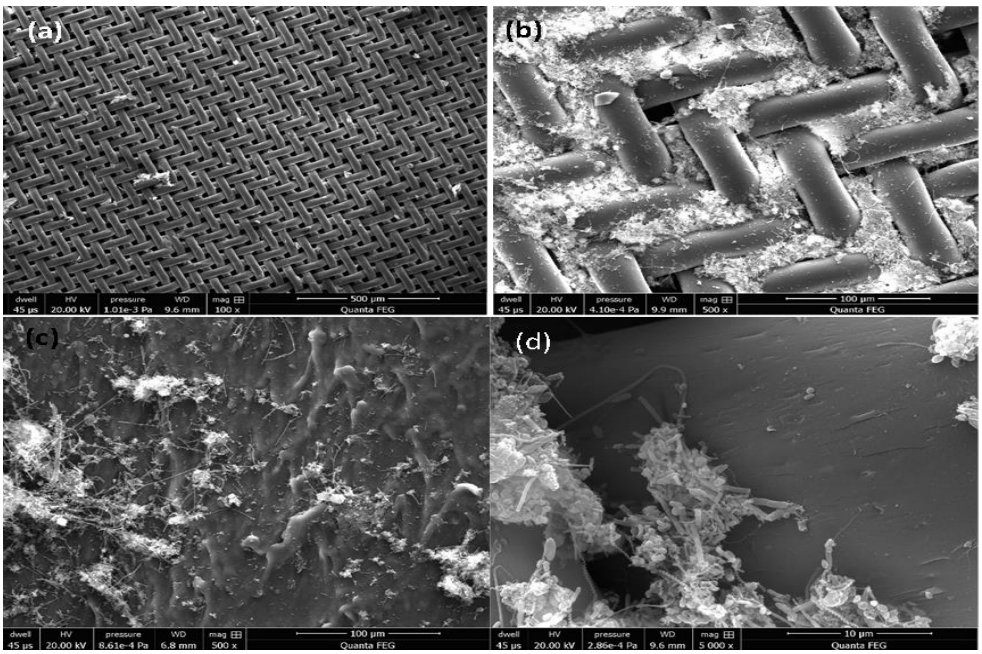

Figure 5-18: SEM images of nylon mesh DM (a) Cleaned nylon mesh (tap water and brush) (b) partially formed DM formed on nylon mesh (day) (c) Formed DM showing

cake layer (day 85) (d) high magnified section of the cake layer showing presence of microbes (day 85)

Chapter 6: Integrating Anaerobic Granular Digesters with DM (GD-DM) in continuous operation

Granular biomass is widely applied in anaerobic digestion, as an improvement to the use of more suspended and flocculant biomass for certain types of effluent. Most granular biomass is incorporated within UASB or EGSB and operated within defined hydrodynamic conditions to prevent washout. In this section, the performance of DM treating effluent from digesters inoculated with granular biomass was tested.

Anaerobic Filters have been applied effectively for the treatment of wastewaters of different strength with the limitations being HRT and OLR for low strength and high strength wastewaters respectively (Rajinikanth et al., 2009). While performance is subject to the feed characteristics and operational conditions, it is widely recommended that a post treatment should be carried out in order to meet discharge standards (Karadag et al., 2015, Rajinikanth et al., 2009). The main objectives of this approach are as follows:

- To evaluate the ability of the DM to polish the effluent produced by the AF treating tomato wastewaters.
- To evaluate the effect of cleaning and re-use of the nylon material as a support for DM
- To assess the long-term performance of DM in response to increased OLR

The complete setup of the integrated UAF-DM is as shown in Figure 6-1. Effluent from AF1 and AF2 was collected in an external PVC tank of total volume 3L and working volume of 2.5L, in which the DM cassette was located. Permeate was withdrawn through the DM with the aid of a peristaltic pump that was controlled by a simple float switch which switched the pump on and off depending on the liquid level inside the DM tank. This enabled an intermittent operation of the pump with the target of reducing the build-up of the cake resistance since there was no shear inducement due to mixing or gas bubbles. TMP and flux were measured and logged and temperature was maintained at 30 ± 2^{o}C for the entire duration of the trial, and permeate from the DM was also collected, weighed and logged every 5 minutes.

The complete set-up of the integrated Anaerobic Granular Digester –Dynamic Membrane is as shown in Figure 6.2. The digesters are set up in the same manner as the AF digesters

described in section 5.3, with the biofilm carrier replaced by granular biomass obtained from a wastewater treatment plant for processing pulp and paper wastewater (Kent, UK). Two identical digesters (GD1 and GD2) were set up and connected to a vessel to receive the effluent from the treated wastewaters. This effluent was then collected in an external PVC in the same manner as the AF-DM set up described in section 6.2. A pressure transducer was placed in the line of the DM tube and permeate from the DM was also collected, weighed and logged every 5 minutes. The diluted feed, chosen to mimic wastewater from a typical tomato processing factory, was placed in a refrigerator at 5 °C to prevent degradation.

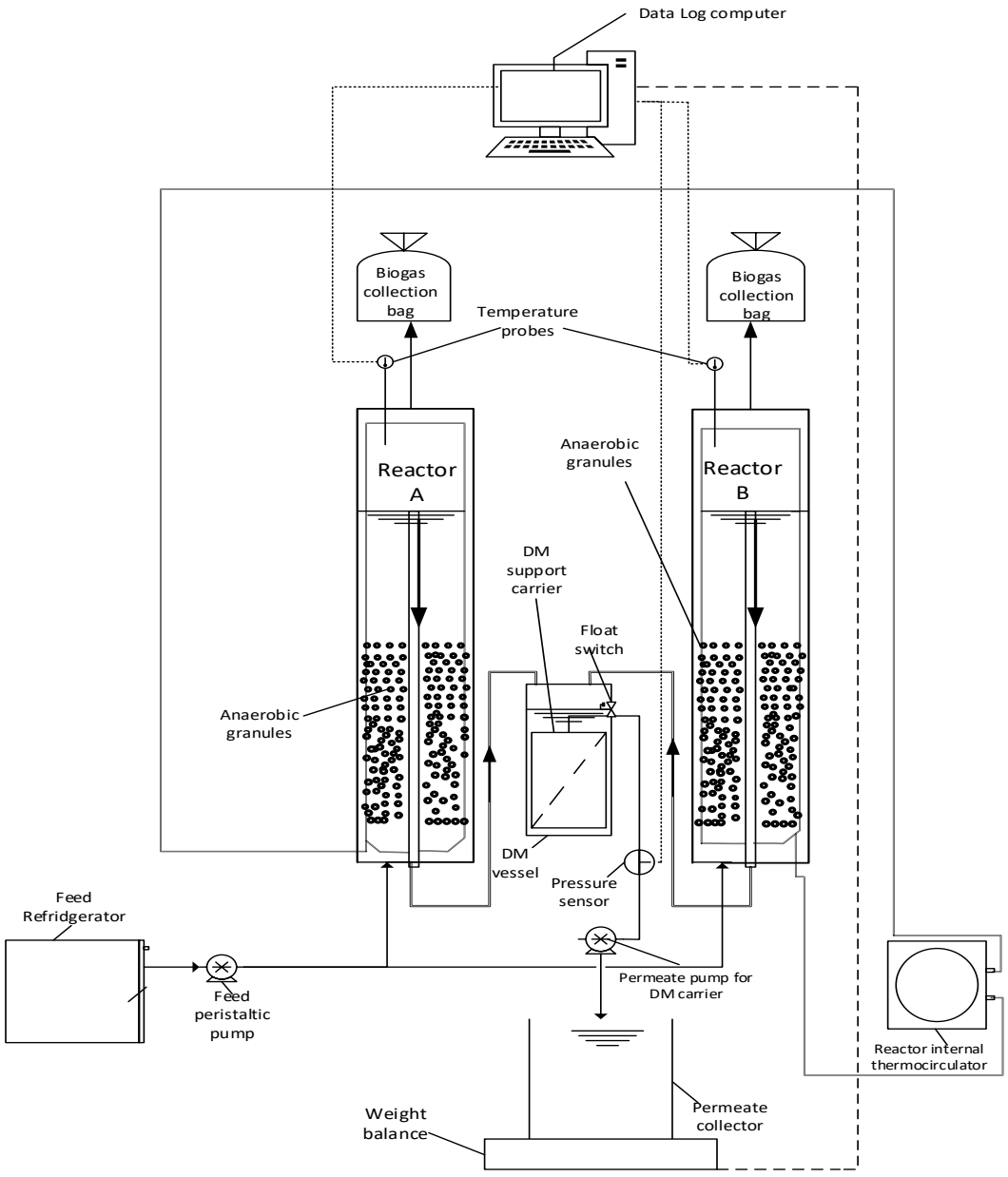

Figure 6-1: The integrated GD-DM for treatment of tomato-processing wastewater

6.1 **Start-up**

Inoculum: The inoculum used was anaerobic granular digestate obtained from a wastewater treatment plant for processing pulp and paper wastewater (Smurfit Kappa, Kent, UK). The anaerobic granules were first rinsed under running tap water to remove fines. 1.3 g of digestate (TS = 145 ± 0.2 g L^{-1}, VS = 116 g L^{-1}) was mixed with 4 L of diluted feed (TCOD = 0.5 g L^{-1}), and the headspace was sparged with N_2 gas. The same feed as prepared and as described in section 5.3.1 was used in this trial.

This was allowed to remain for 3 days before recirculation of the contents for 7 days and the commencement of continuous feeding. The OLR was adjusted based on the feed TCOD concentration and is summarised as shown in Table 6.1. The digesters were fed in an upflow configuration such that the effluent drained from the top and was collected in the DM tank from which a peristaltic pump controlled by a float switch provided intermittent suction. This mode of operation resulted in an average flux of 23 L m^{-2} h^{-1}

Table 6-1: Operational phases for the granular digesters for treatment of tomato-based wastewaters

Phase	**Duration (days)**	**COD (g L^{-1})**	**HRT (d)**	**OLR**	**Feed type/Flow**
Phase 1	36	1	1	1	Continuous feed
Phase 2	36	3	1	3	Continuous feed
Phase 3	24	4	1	4	Continuous feed

6.1.1 pH

At the start of the continuous run in phase 1 the pH dropped slightly (Figure 6-3), from 7.2 to 6.9 over 5 days for both digesters. Based on the observations described in section 6.2, the feed was supplemented with urea at a concentration of 0.2 g L^{-1} and the pH stabilised around 7.2 for both digesters for the rest of phase 1. For the second phase of the experiment from day 34 to day 70, the OLR was increased to 3 g COD L^{-1} day^{-1} by increasing the feed concentration to 3 g COD L^{-1}. The pH dropped to 6.9 during this period, although it increased

slightly towards the end of the phase before dropping back to around 6.8 for the rest of the trial.

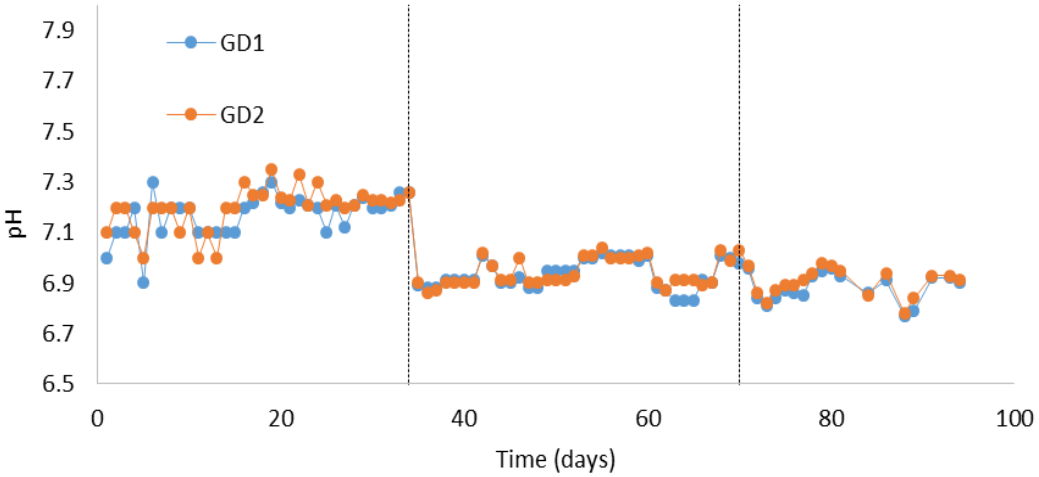

Figure 6-2: pH profile for granular digesters treating tomato wastewater at 30 °C (Vertical dashed lines indicate change in OLR)

6.2 Alkalinity

The TA of the digesters is presented in Figure 6-4a and shows that the alkalinity had dropped to 0.5 g $CaCO_3$ L^{-1} after 5 days but began to increase and reached above 1.5 g $CaCO_3$ L^{-1} by day 28. Increase in OLR from 1 g COD L^{-1} day^{-1} to 3 g COD L^{-1} day^{-1} on day 34 resulted in a decrease in total alkalinity to around 1.2 g $CaCO_3$ L^{-1} for both digesters. The alkalinity stabilised at around 1.4 g $CaCO_3$ L^{-1} for the rest of the trial without showing any change due to increase in feed concentration on day 70.

The PA of both digesters (Figure 6-4b) behaved in a similar manner to the TA, starting around 0.3 g $CaCO_3$ L^{-1} for both digesters in and steadily rising to around 1.3 g $CaCO_3$ L^{-1} by day 33. The change in OLR caused the PA to drop to around 0.7 g $CaCO_3$ L^{-1} shortly before rising to 1.2 g $CaCO_3$ L^{-1} by day 42. PA for both digesters remained around 1 g $CaCO_3$ L^{-1} for the rest of the trial.

IA of the digesters (Figure 6-4c) started at around 0.2 g $CaCO_3$ L^{-1} and increased to 0.5 g $CaCO_3$ L^{-1} after 28 days before dropping slightly at the increase in OLR, and stabilised around 0.4 g $CaCO_3$ L^{-1} until the end of the trial.

IA/PA ratios of the digesters are presented in Figure 6-4d, showing values below 0.6 on day 5 and trending downwards to steady values of around 0.4 throughout the trial.

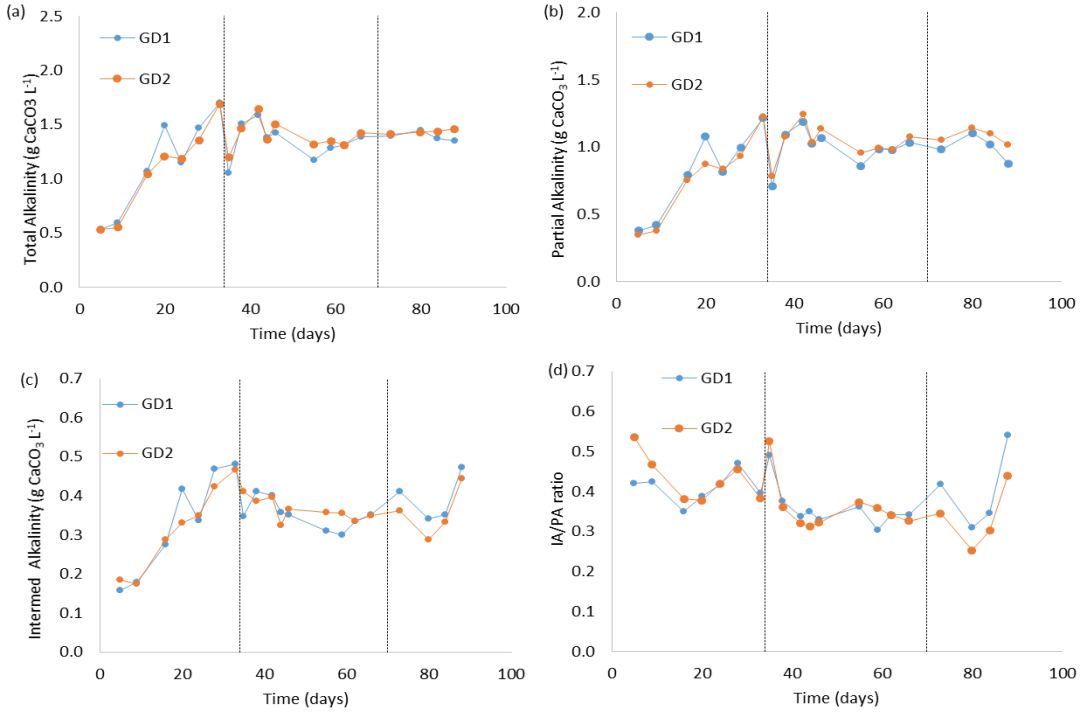

Figure 6-3: Alkalinity profile for granular digesters treating tomato wastewater at 30 °C (a) Total alkalinity (b) Partial alkalinity (c) Intermediate alkalinity (d) IA/PA ratio (Vertical dashed lines indicate change in OLR)

6.3 TAN

TAN concentrations during operation of the digesters are presented in Figure 6-5. TAN increased from around 0.2 g N L^{-1} to over 0.3 g N L^{-1} on day 35, after which it remained stable before dropping briefly to just under 0.2 g N L^{-1} on day 56. It recovered back to just over 0.2 g N L^{-1} by day 80.

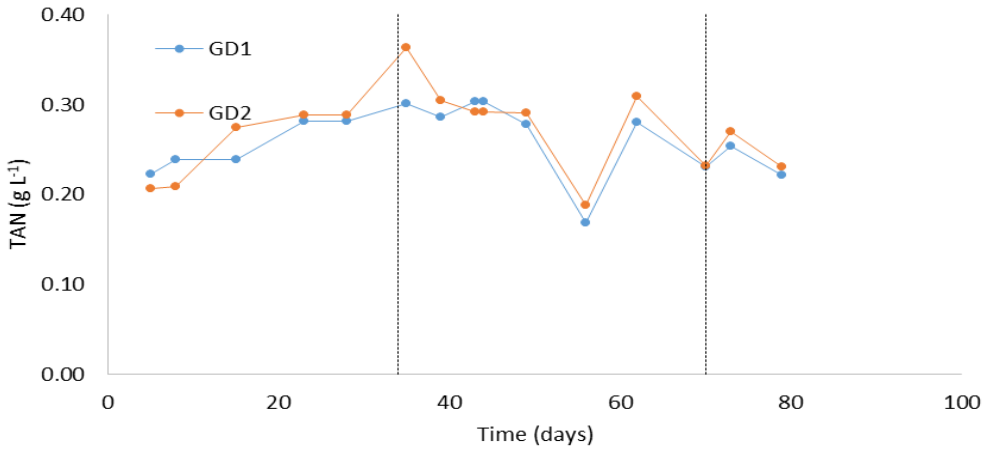

Figure 6-4: TAN profile of granular digesters treating tomato wastewater at 30 ^{O}C (Vertical dashed lines indicate change in OLR)

6.4 TOC removal

The organic degradation as represented by changes in TOC is presented in Figure 6-6. Influent TOC for phase 1 started at around 200 mg L^{-1}, slightly lower than the target OLR of 1 g COD L^{-1}, before increasing to around 700 mg TOC L^{-1} by day 33. During this period, effluent TOC averaged 25 g L^{-1}. The influent TOC was increased on day 34, with values of around 917 by day 52 equivalent to OLR of about 3 g COD L^{-1}, with the effluent TOC for both digesters averaging less than 30 mg L^{-1}. Influent TOC concentration was increased for phase 3 to around 1.4 g L^{-1} and effluent TOC during this phase remained below 60 mg L^{-1}.

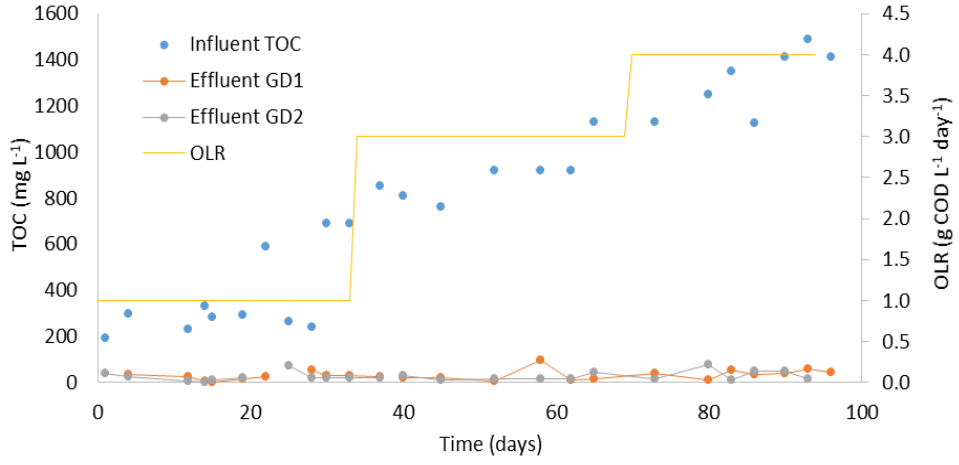

Figure 6-5: Influent and effluent TOC profile for granular digesters treating tomato wastewater at 30 ^{o}C

6.5 Biogas composition and volumetric methane production

Biogas composition is presented in Figure 6-7a. Average CH_4 content was 72% for GD1 and GD2 while CO_2 content averaged 21% for both digesters, with the rest being residual atmospheric gases and water vapour. Biogas composition was similar throughout the phases of the trial. Volumetric methane production (Figure 6-7b) was also similar for both digesters with phase 1 starting at around 0.2 L CH_4 L^{-1} day^{-1}. VMP increased to around 0.6 L CH_4 L^{-1} day^{-1} for phase 2 and subsequently averaged around 0.9 L CH_4 L^{-1} day^{-1} for phase 3. In terms of SMP (Figure 6-7c), the digesters averaged around 0.07 L CH_4 g TOC $_{added}^{-1}$: this is without taking into account the unusually high values on days 11, 15 and 21, which are likely caused by operational/pumping issues.

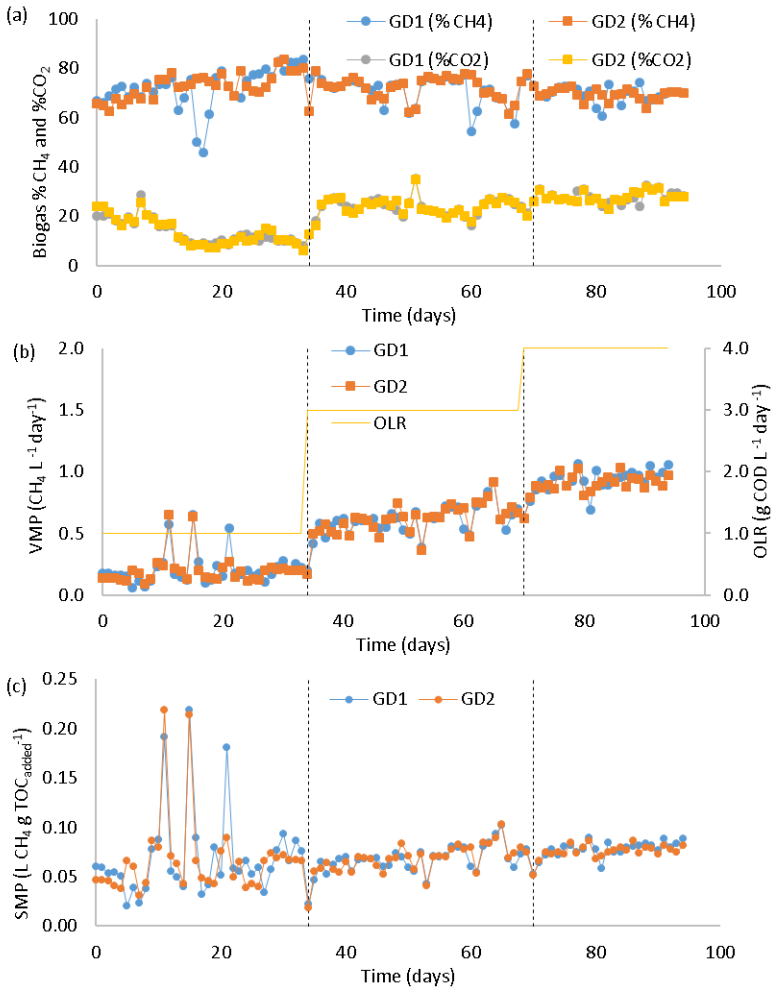

Figure 6-6: Biogas production for granular digesters treating tomato wastewater at 30 °C (a) Biogas composition (b) Volumetric methane production (c) specific methane production (Vertical dashed line indicate change in OLR)

6.6 Performance of GD-DM

As can be seen from Figure 6-8a, the flux started around 16 L m^{-2} h^{-1} but was changed to 20 L m^{-2} h^{-1} by increasing the pump rpm. The flux dropped to around 12 L m^{-2} h^{-1} between days 12 to 14 due to operational problems before increasing to 18 L m^{-2} h^{-1}. The average flux was around 16 L m^{-2} h^{-1} until day 44 when failure of the float level pump caused some brief operational setbacks, and this was taken as a chance to clean the DM. Operation continued on day 46 with flux returning to 17 L m^{-2} h^{-1}. Flux data for days 47 -55 were missing due to a computer error but there was no apparent reason to suggest that the flux was significantly different in this period as daily operation was maintained as usual. On day 56, operation had to be paused for several hours due to an unplanned power cut in the lab, before operation was resumed and flux was increased to 26 L m^{-2} h^{-1} by increasing the pump rpm. A slow decline in flux followed and by day 75 it had dropped to around 7 L m^{-2} h^{-1}, at which point the DM was cleaned. The flux resumed at around 20 L m^{-2} h^{-1} for a few days before falling back to around 17 L m^{-2} h^{-1} for the rest of the trial.

TMP rose to 0.04 bar in just under one day before stabilising at around 0.06 bar from day to day 35 when it increased slightly to 0.07 bar. Cleaning was carried out on day 44, following which the TMP dropped to 0.3 bar before increasing to 0.07 bar. From day 55 onwards, TMP began to trend downwards reaching 0.02 on day 74. As the flux was also low, this prompted the second cleaning episode as it signalled pore blockage. This resulted in gradual increase in TMP from day 76 until day 86 when the trial was ended. Decreasing TMP in long term DM operation was also reported by Cai et al. (2018). They observed that when operating a DM, driven by water head loss- treating synthetic wastewater, at an SRT of 40 days, the TMP started to decline 20 days after start of operation and only trended upwards after around 45 days, although aeration could have contributed to the TMP decline.

Permeate quality as indicated by daily turbidity values (Figure 6.8b) shows a fall in turbidity after 2 days from around 90 NTU to below 20 NTU. Slight increases were observed prior to and following the two cleaning episodes. The period between the two cleaning episodes saw a slight increase in turbidity from an average of 14 NTU to 29 NTU which may be due in part to increased loading as well as accumulation of some irreversible fouling on the surface of the DM that may not be easily removed by simply cleaning with tap water and brush. During this period, laboratory ambient temperatures were also automatically recorded for the first

55 days of operation before the laboratory computer malfunctioned. Diurnal temperature changes and environmental factors are evident as the ambient temperature readings fluctuated between 8 and 19 ºC. The impact of temperature changes on the DM were not quite evident as the flux was not affected. This is a marked difference from what we expect in conventional membranes due to the correlation of lower temperature and increased viscosity. An explanation to why this is so may be due to the cake layer acting as an additional physical barrier and the predominant contributor to the total resistance of the DM.

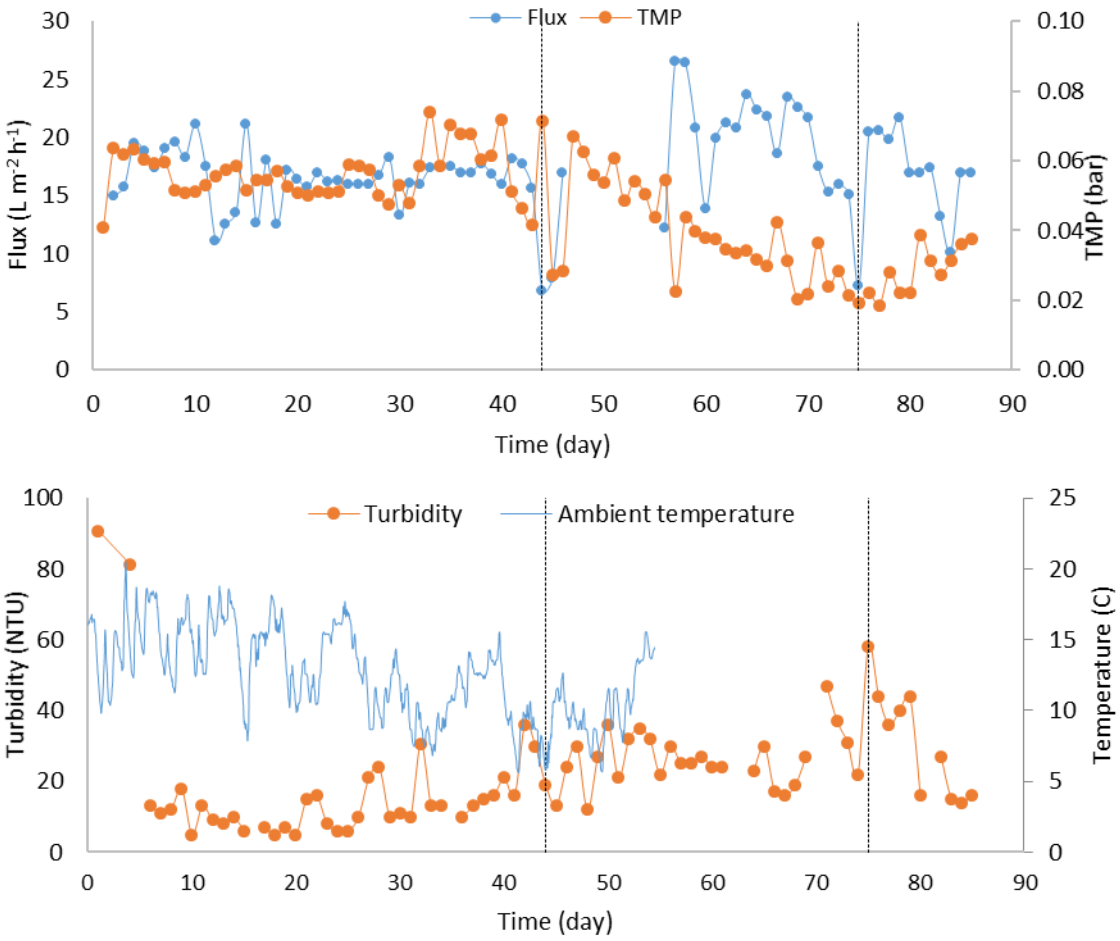

Figure 6-7: DM performance for treating effluent from granular digesters (a) Flux and TMP profile (b) Permeate turbidity. (Vertical dashed lines indicate cleaning episodes)

6.6.1 Particle Size Analysis of the GD-DM

Particle size distribution for the mixed effluent from GD1 and GD2 was compared to the permeate and is as shown in Figure 6.9. The mixed effluent had particles ranging between 4 and 600 µm while the DM permeate had a range of 0.04 and 230 µm. Similarly, median size for the DM permeate was much lower (11 µm) compared to that of effluent from the granular digesters (95 µm). This shows that much of the larger particles (>10 µm) were intercepted by the cake layer, although a portion of particles with sizes smaller than 10 µm were able to pass through the DM. In addition, there appears to be the presence of organic colloidal matter, widely regarded as belonging to size classes less than 10 µm (Lead and Wilkinson, 2006) and these may have a higher impact on the light-scattering properties when measuring permeate turbidities. This is particularly interesting as tomatoes-processing wastewaters characteristically possess a higher concentration of colloidal and particulate COD (Gohil and Nakhla, 2006) and further confirms the observation made in batch tests done in this study (see section 4.5) stating that the use of turbidity as a strict measure of retention capability of the DM should be treated with caution. In order to assess performance, turbidity removal should also be assessed based on the relative difference between influent and effluent turbidity rather than strictly absolute effluent turbidity values.

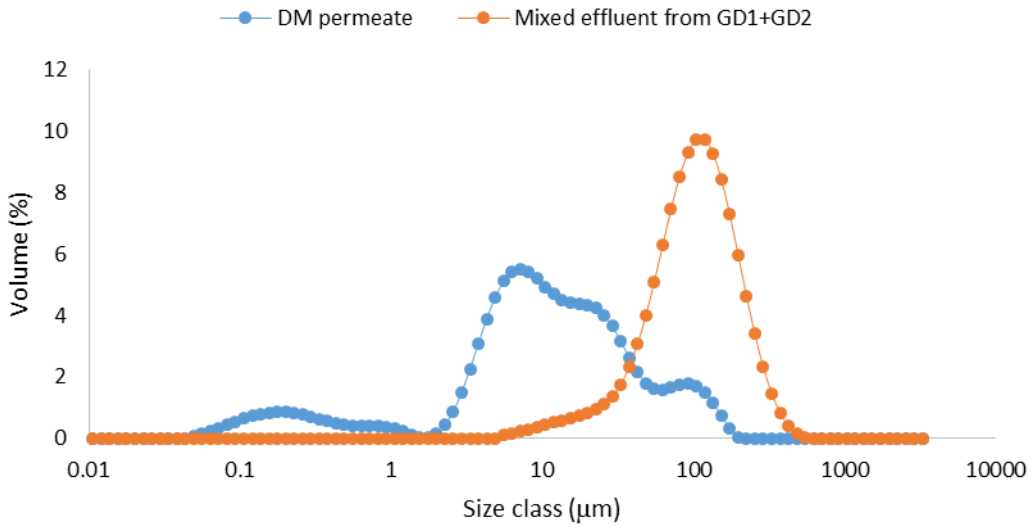

Figure 6-8: Particle size distribution of effluent from digesters treating tomato wastewater and DM permeate

6.6.2 **SEM analysis of GD-DM cake layer**

SEM micrographs of the DM surface area are presented in Figure 6-10. The cleaned nylon support shows that although most of the materials have been removed, there is some material trapped on the surface of the membrane and are not as easily removed using brush and tap water. This is expected given the nature of the nylon materials- formed of weaves and ridges. This could benefit the DM performance as they could easily help in the re-formation of the DM in a shorter period compared to a new material. It is also noticeable that cake formation (Figure 6-23a and 6-23b) was quite dense and may be uneven in some parts of the support materials, hence the slightly fluctuating performance in the later days of the DM operation. A magnified look at the DM surface (Figure 6-23d) shows the presence of a dense web of short filamentous microbes on the surface of the DM- a clear indication that not only does the DM act as a physical barrier, but also acts as a biofilm. Several studies have suggested the presence of microbial products such as EPS on the surface of membranes (He et al., 2005, Gao et al., 2010).

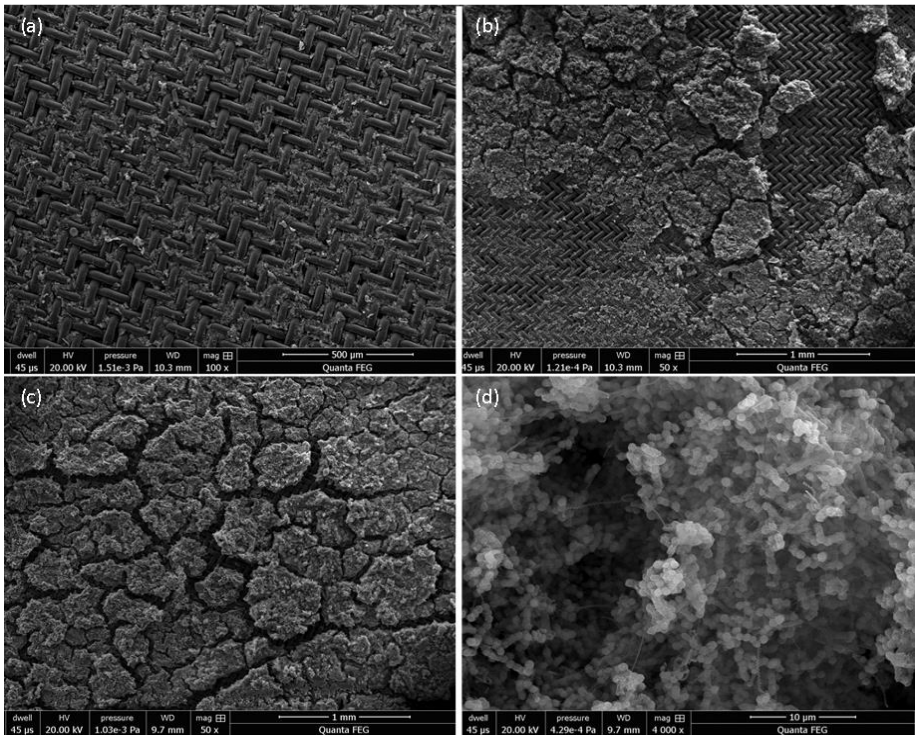

Figure 6-9: SEM photos of GD-DM surface treating effluent from granular digesters (a) cleaned nylon support (b) portion of nylon support showing patchy cake formation day 44 (c) well-formed cake layer (day 86) (d) closer image showing presence of microbes on cake layer.

6.7 Discussion

Treatment of tomato-processing wastewaters was trialled in an integrated set up of a pair of granular digesters coupled to an external DM. For the main anaerobic granular digesters, selecting a short start-up period during which daily recirculation of digester mixed liquor was done for the first 10 days was sufficient to aid start-up, even at a short HRT of 1 day. This start-up period was significantly shorter than the 4 weeks reported by Gohil and Nakhla (2006) when treating tomato wastewater using a UASB, although the first week involved the use of synthetic wastewater to aid acclimation. The digesters were able to cope with a jump in OLR from 1 to 3 g COD L^{-1} day^{-1}, as the SMP was kept relatively stable at around 0.07 L-CH_4 g-TOC_{added} $^{-1}$, and CH_4 fraction of biogas averaged 72% throughout the trial. Similar feeding and operational start-up strategies were applied by (Najafpour et al., 2006). It has been shown that recirculation of mixed liquor significantly improved the start-up performance of anaerobic digesters as it helps with acclimation of the biomass to the substrate. Although granular digesters are capable of handling much higher OLRs (depending on substrate and operational characteristics) than those applied in this trial, careful monitoring of the performance when handling increased loading rates is essential. This is because of the nutrient limitation and alkaline deficiency in tomato wastewaters (Xu et al., 2006),which necessitated supplementation with urea. Supplementation of the feed with urea was done to overcome this limitation and TAN concentration ranged between 0.2 and 0.3 g L^{-1}, which has also been shown to help in increasing alkalinity (Van Haandel, 2005). IA/PA ratio, adopted as an indicator for digester stability, proved useful in confirming that supplementation with urea was able to improve digester stability. This is in agreement with a study by Li et al. (2014), in which they found that the IA/PA ratio was the optimal indicator for anaerobic digesters treating feed with low ammonia concentration. In terms of DM performance, selection of an imposed flux of 25 L m^{-2} h^{-1} resulted in an operational flux range between 16 and 20 L m^{-2} h^{-1}, and corresponding TMP between 0.02 and 0.08 bar. The flux obtained in this study was consistently higher than 2.6 L m^{-2} h^{-1} reported by (Ersahin et al., 2014) in a submerged AnDMBR and similar to the 15-20 L m^{-2} h^{-1} obtained by (Alibardi et al., 2016) in an external AnDMBR. Fluctuations in flux/TMP, are typical of DMs, and are attributable to the constant changes in particle deposition and consolidation during operation. The dominant fouling mechanism, which could be either pore blocking or cake formation, or a combination of the two, influences the level of flux achievable. Although it is expected that

pore blocking will dominate in the early stage of filtration, as shown by the difference in the imposed flux and the operational flux , the small flocs could still be transported through the cake layer. As filtration proceeds, the cake layer became the more dominant mode of filtration, hence the rise in TMP- the cake layer contributing over 60% of the total resistance. Similar changes in flux or TMP were observed by Yang et al. (2017) and (Saleem et al., 2016) when operating DM coupled to anaerobic bioreactors. In this study, the change in OLR appears to have affected the DM formed, resulting in fluctuating filtration performance (flux and TMP changes). Cleaning was done a few days later, although the flux achieved in this study was much higher than the 8.2 L m^{-2} h^{-1} obtained by Iaquinta et al. (2009) for nanofiltration of biologically pre-treated tomato wastewater . This demonstrates that changes in organic loading can be detrimental to the stability of the DM and should be avoided, where possible.

In addition, supplementation with urea provided increased nutrient and alkalinity and had a positive operational effect in that a shorter HRT of 24 hours could be achieved. This is much shorter than the HRT of 2.8 days adopted for a UASB- aerobic system in a study carried out by (Gohil and Nakhla, 2006), who applied a UASB- aerobic system for treatment of tomato processing wastewaters. UASB start up took 4 weeks, followed by synthetic wastewater feeding, and subsequently tomato wastewater feeding. To address the alkalinity deficiency, they employed recycling of the UASB effluent –decreasing the bicarbonate alkalinity requirements by 75%.

Chapter 7: Comparison of integrated systems (AF-DM and GD-DM) for the treatment of industrial wastewaters containing low solids.

This chapter focuses on the evaluation and comparison of the two integrated systems namely the Anaerobic Filter + Dynamic Membrane (AF-DM) and the Granular Digester + Dynamic Membrane (GD-DM). The main difference between the two systems is the type of biomass in the main digester, with the AF containing carriers to promote the growth of flocculant biomass to form biofilm and the GD inoculated with granular biomass. Detailed descriptions are presented in sections 5.3 and 6.2.

7.1 Filtration performance

The initial flux in both system was set at 25 L m^{-2} h^{-1}, and all other operational features (support material size, DM vessel, pump type) were identical. Average flux of the AF-DM was consistently higher than the GD-DM (19 L m^{-2} h^{-1} compared 16 L m^{-2} h^{-1}), with the exception of the last 20 days of the trial, during in which the identical flux performance was observed. This period coincided with the highest OLR (4 g COD L^{-1} day^{-1}) trialled for both systems, and may due to increase in soluble products on the DM. It is worth mentioning that the GD-DM trial was started later, 126 days into the trial of AF-DM, which lasted for 188 days. Flux/TMP data for the first 10 days of the AF-DM trial are not included due to the different operational mode employed in this period. As can be seen from Figure 7-1a, the AF-DM maintained a higher flux compared to the GD-DM. This may be due to extensive conditioning that must have occurred during the formation of the cake layer for the AF-DM. In addition, it is apparent that the morphology of the biomass affected the cake layer: whereas the flocculant biomass and biofilm present in the effluent could readily form a very thin gel-like layer on the surface of the GD-DM, the granular biomass resulted in a denser cake formation leading to higher resistance. This is also evident when considering the TMP values of both cases during the trial (Figure 7-1b). The AF-DM consistently operated at a lower TMP range (0.01-0.06 bar), in a steady rise with long periods between required cleaning (days 44, 99 169) compared to the GD-DM which operated within a higher TMP range (0.02- 0.07 bar). This in contrast to a study by Li et al. (2012a), who found that granules provided a lower fouling

propensity compared to sludge flocs in an integrated granular and mesh filter system, although the study was done using aerobic granules. TMP of the GD-DM began to decline from day 47 following a cleaning episode. This may be attributable to some portion of the cake layer falling off due to forces acting on the surface of the membrane, which translated into increased but unstable flux for the rest of the trial.

Figure 7-1: Comparison of performance of AF-DM and GF-DM integrated systems (a) Flux (b) TMP (c) Turbidity of permeate (d) Ambient temperature

This decline in TMP for both systems coincided with the highest OLR (4g COD L^{-1} day^{-1}) and suggests that the loss of some portion of the cake layer may be beneficial to the DM by keeping the TMP reasonably low, since increased deposition leads to consolidation of the cake layer and sudden rise in TMP. Figure 7-1c shows the daily permeate turbidity values for the two systems with permeate turbidity of the AF-DM was higher (between 20 to 50 NTU) than the GD-DM (around 10 to 30 NTU). This difference can be traced back to the morphology of the cake layers of the DM formed by different biomass types. A comparison of the cake layer formed under each system using SEM is shown in Figure 7-2. It can be seen that the cake morphology and distribution were different in both cases. For the AF-DM (Fig 7-2a), the cake layer appeared like a biofilm layer and was more gel-like. The GF-DM appeared to be clusters of dense, cake-like layer on the nylon mesh. This was also confirmed by the higher magnification (4000X) (Figure 7-2c and 7-2d) of the cake layer itself which showed the difference in the distribution of the contents of the cake layer, with the AF-DM cake layer showing clusters of microbes, interspersed by microbial products while the GF-DM showed a denser web of microbes.

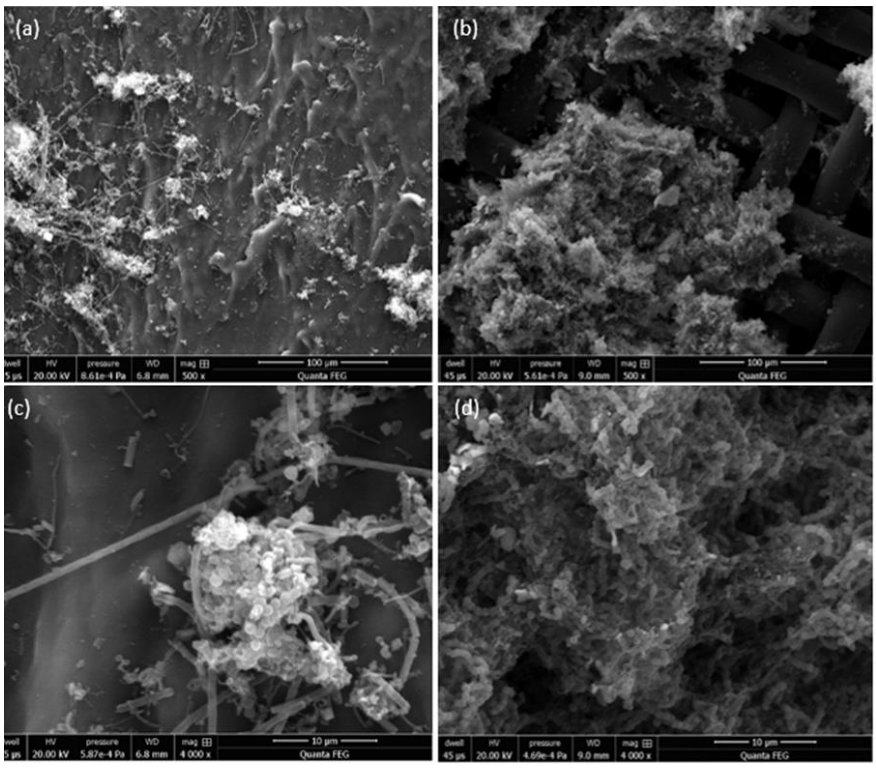

Figure 7-2:SEM photos of formed cake layer on nylon support for (a) AF-DM (b) cake layer GD-DM (c) magnified -4000X close up of cake layer in AF-DM (d) magnified 4000X close up of cake layer formed under GD-DM

These differences underlie the differences in performance of the DM formed under the two systems. A dense cake layer was more like to result from the deposition of the degranulated biomass from the granular digesters feeding the GF-DM, whereas the expected contents of the AF-DM are likely to be predominated by microbial flocs and detached biofilms from the anaerobic filters

7.2 Particle size analysis – Comparison of feed and permeate PSD of both integrated systems

The particle size distributions of effluent from the 4 individual reactors were analysed and are presented in Figure 7-3. The two granular digesters GF-A and GF-B show very similar PSD profiles, with median particle sizes of 94 µm and 103 µm respectively and similar particle size ranges between 4 µm and 650 µm. For the anaerobic filter digesters (AF-A and AF-B), the individual digesters presented markedly different effluent PSD profiles with AF-A and AF-B presenting median sizes of 63 µm and 290 µm respectively and size ranges of 0.4 and 790 µm for AF-A and 0.4 µm and 1970 µm for AF-B. These differences are based on the predominating contents of the effluent and the digester type: detached pieces of biofilm and microbial flocs are more likely to be released in effluents from biofilm reactors such as anaerobic filters, which is markedly different from the more consistent granulated biomass in the effluent of granular digesters.

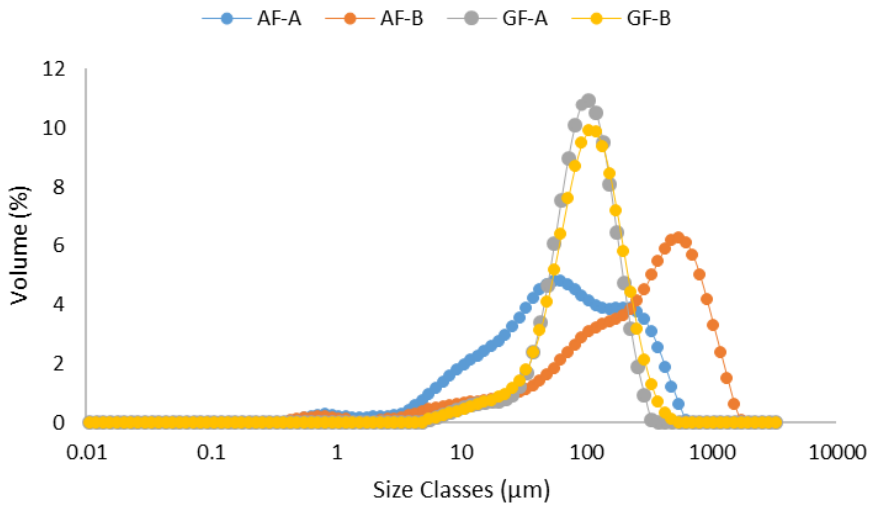

Figure 7-3: Particle size distribution of effluent from the digesters- AF and GD used as feed for the DM

A comparison of the permeate generated from each system is presented in Figure 7-4. The median sizes were quite similar for AF-DM and GD-DM at around 11 µm and 10 µm respectively, although there appears to be a smaller peak between size 0.1 and 1 µm for the GD-DM permeate which is not present in the AF-DM permeate, and the AF-DM presented a wider range of particle sizes. The smaller peak observed for the GD-DM can be attributed to the degranulation of the anaerobic granules, leading to the migration of a distinct portion of the biomass as opposed to the particles present in the feed. Despite the variation in the PSD of the feed to the DM, this similarity in PSD profile for both systems is an indication that the cake layer was able to intercept a significant proportion of the particles, which will have passed through the 20 µm support material. As the effluent from the AF-DM will more likely contain the broken biofilm from the support carriers, a rather wider range of formed cells can be visible in the permeate of the AF-DM whereas the granular nature of the biomass of the GD-DM presents a rather distinct and narrow range.

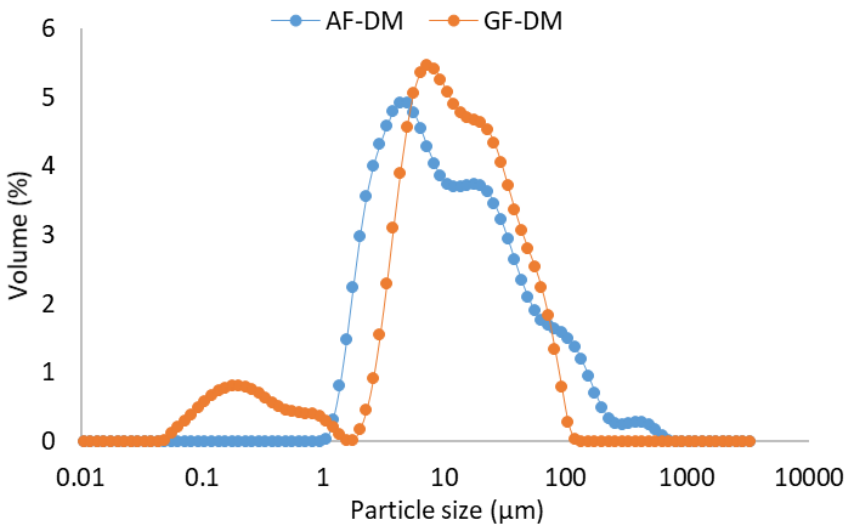

Figure 7-4: Particle size distribution of permeate from the integrated systems (AF-DM and GD-DM)

7.3 **Conclusion**

Chapters 5 & 6 shows that integrating DM with anaerobic digesters offers the chance to handle challenging wastewaters. In the first part, results show that given adequate ammonia supplementation with urea, the digesters can cope with the simulated tomato wastewater. For the DM, wastewaters with high suspended and colloidal matter can be treated at reasonable flux averaging 20 L m^{-2} h^{-1} and the DM is capable of retention of solids as indicated by the lower permeate turbidity of less than 40 NTU. The influence of digester performance treating tomato-based wastewaters show that the granular digesters offer the benefit of quicker start up and acclimation, compared to the anaerobic biofilm reactors. Having acclimated, both systems were similar in terms of SMP with average of 0.07 L CH_4 g TOC_{added}^{-1}. In terms of biogas composition, AF showed a decreasing trend in CH_4 composition (from 77% to 65%) as the OLR was increased, which was not noticeable in the granular digesters as they maintained an average of 70% CH_4 throughout the phases. The granular digesters were able to deal with the highest OLR tested (4 g COD L^{-1} day^{-1}), whereas the AF digesters struggled to cope. This difference is mainly due to the more concentrated biomass granules in the granular digesters compared to the disperse nature of the biofilm, able to cope with the increased loading compared to the biofilm.

The combination of anaerobic treatment and filtration process in a single integrated system offers advantages common to each separate unit, thereby improving the overall efficiency of the treatment process. The increased performance of the anaerobic digester in terms of degradation of organic matter prolongs the stability of the DM unit. In such cases, special tanks can be dedicated to conditioning pre-formed DMs, which can be readily deployed when required. A major benefit of this integrated system is the ease with which the system can be decoupled into separate unit for maintenance or operational purposes.

These integrated systems can be deployed for small-scale treatment of industrial wastewaters derived from soft-drink processing, breweries and other fruit juice and vegetable production processes. A major limitation is the quality of permeate which is higher than conventional settler treatment systems. However, there is need to consider other factors associated with conventional secondary treatment - the relatively large footprint required for clarification tanks, the consideration for operational parameters (surface overflow rates, sludge scrapers) compared to filters. The successful application of secondary

clarifies depend on the use of coagulation agents particularly when handling wastewaters high in TSS (Fuchs and Staudinger, 1999), such as tomato-based wastewaters . The effluent from clarifiers can be influenced by complications due to abnormal biological activities, which can cause bulking and foaming and reduces the settleability of the sludge, making clarification, harder to achieve (Lim and Bai, 2003). Given that the DM presented in this study were able to remove up to 80% of feed turbidity, it is perhaps more feasible to introduce the DMs in series for further clarification of residual turbidity.

Chapter 8: Conclusions and Future Work

The overall aim of this research was to investigate the potential for a low-cost anaerobic integrated system for the treatment of industrial wastewaters with low solids contents. In order to achieve this, it was important to evaluate the potential for application of DM as a low cost option for filtering solids and how this can be integrated with functional anaerobic bioreactors. A series of trials were devised and tested to understand the effect of some specific operational conditions on the cake formation and performance of the DM. These investigations showed the influence of material type on cake formation and performance. The three different support materials tested were capable of enabling cake formation, as evidenced in either declining flux, rising TMP and declining permeate turbidity. Nylon mesh, due to its intrinsic characteristics offered the most promising application in terms of stable flux and lower resistance and better retention capacity compared to woven and non-woven polypropylene.

Increase in feed TSS led to increased resistance and lower flux, although this relationship is dependent on the initial imposed flux and does not appear to be linear. To maintain stable flux performance, the concentration of TSS should be kept low (1.5 g L^{-1}), although an extended time period is required to achieve cake formation. To reduce the cake formation time, the feed TSS can be to 5 g L^{-1} but can result in also in a significant rise in TMP and an unreliable performance material. At lower flux (5 L m^{-2} h^{-1}), further confirmation using nylon mesh suggests that there appears to be a critical TSS threshold (greater than 3 g L^{-1}) beyond which a significant rise in TMP becomes apparent. Increase in TSS resulted in lower flux but a shorter DM formation period and while this may be positive, there appears to be a critical point beyond which high TSS caused significant flux loss irrespective of imposed flux.

Selection of the constant flux filtration (as opposed to water level head filtration mode) was more suitable for the long- term operation of the DM, as the use of the pump allows setting of a suitable flux without having to overcome the rapid consolidation of cake layer caused by imposed TMP. The effect of the filtration mode applied (constant head gravity vs constant flux using pump) showed that for the constant head filtration, formation time were quite similar for the TSS tested (1.5, 3 and 5 g L^{-1}), and this difference was also reflected in the filtration flux obtained, although all three cases tended to trend downloads with increase in operational time. Increasing the constant head differential did not make any difference at

any given feed TSS concentration as the steady state flux remained the same in all cases. Therefore, constant flux operation offers better operational performance, as the flux can be more carefully selected rather than be subject to the effect of height limitation which might restrict the ability to achieve the desired TMP necessary for a given flux.

To optimise operational conditions favourable for cake formation, careful selection of operational parameters including TSS, initial imposed flux, filtration mode and mixing strategies. Initial imposed flux and feed TSS should be kept below 1.5 g-TSS L^{-1} to prevent cake consolidation and increased resistance. In addition, short-term batch trials on influence of different materials and their influence on cake formation should be a pre-requisite before deployment in large-scale applications.

It is evident that pre-formation of DM can be achieved using concentrated (high TSS) digestate to build the DM before deploying to treatment of low solids wastewater such as typically expected from functional AD systems. This offers a potential for 'offline' DM conditioning before subsequent deployment to online operations. Although low formation flux resulted in longer DM formation time, it offers a more stable filtration performance at similar permeate turbidity compared to when higher filtration fluxes are used to pre-form the DM. It is also important to avoid changes in flux (increase in rpm) during steady state operation of pre-formed DM as this results in unstable flux and rise in TMP. Consequently, it is better to use a lower pre-formation flux (5 L m^{-2} h^{-1}) and to maintain the same level of flux for stable performance.

A single unit DM can function as a low-cost medium for polishing the effluents produced by several units of digesters, provided regular monitoring and maintenance is carried out.

Anaerobic Filters (with plastic carriers and inoculated with flocculant anaerobic biomass) were shown to be able to treat tomato-based wastewaters at mesophilic conditions despite the challenges of low alkalinity, provided sufficient time is allowed for acclimation of the biomass. Acclimation was achieved through extended batch feeding of very low volume but concentrated feed, which aided biomass attachment, and growth of the biofilm. Long-term (198 days) performance of the AF showed that it was able to cope with increasing OLR concentration from 1 to 4 g COD L^{-1} day^{-1} although a few episodes of increasing IA/PA ratios were observed particularly at the highest OLR of 4 g COD L^{-1} day^{-1}. One-day interruptions in

feeding were sufficient to allow consumption of the accumulated VFA, and gradual performance recovery.

The introduction of intermittent filtration to allow for slower cake consolidation was an effective way to maintain flux and to enhance better control of the process. . In this manner, TMP was kept low (less than 0.06 bar) with steady increases between cleaning intervals. Restoration of flux can be achieved through simple cleaning, by taking the DM 'offline' and placing under running water while brushing off with a soft brush. TSS removal (as characterised by permeate turbidity averaging less than 20 NTU in the first 100 days (compared to AF effluent/feed tank turbidity ranging between 100 to 370 NTU), can be achieved with temperature control and lower increments in OLR. Nylon mesh can be used as a low-cost, low maintenance support material for DM application as the cleaning of the nylon mesh can be carried out in a quick and easy way using only tap water and brush and successive re-use of same mesh could even enhance quicker DM formation.

It is important to test the integrated system using a granular biomass- different from the biofilm and carriers employed in the AF digesters. Anaerobic granules can be used as biomass in UASB-type digester under the similar conditions (mesophilic temperature and OLR). This was able to treat the tomato-based wastewaters with limited acclimation time, for which even though overall the period of this trial was shorter (around 100 days) giving credence that there was little need for the long acclimation period required to build up the biofilm in the AF-type digesters. For this reason and given time constraint, it was decided to increase the OLR directly from 1 to 3 g COD L^{-1} day^{-1}, without any observed drop in performance: IA/PA was maintained below 0.4 for the pair of digesters and average SMP of 0.07 CH_4 g TOC_{added}^{-1}. When coupled with the DM, operating at a high flux averaging 16 L m^{-2} h^{-1} was achievable although at higher TMP compared to the AF-DM.

The influence of biomass type on DM formation and performance show that granular biomass tended to form dense cake than flocculant biomass and resulted in slightly lower operational flux even though similar imposed flux was applied to the AF-DM. This denser cake also ensured better retention capability than the AF-DM as the ensured that the permeate turbidity was generally better than the AF-DM even at the highest OLR tested. Similar to the AF-DM, the influence of changing ambient temperature was not pronounced in the operation of the DM; it might be that conditioning of the cake layer on the DM was

dominated by physical rather than biological activity even though SEM observation showed the presence of microbial archaea in the cake layer in both systems.

Compared to anaerobic flocculant or biofilm biomass, granular biomass should be selected to aid quicker start up, although this may be influenced by availability as flocculant biomass are more readily available and there are several carriers that aid formation of biofilms

Overall, this study was able to show that both systems were capable of handling tomato-based wastewaters, given sufficient acclimation and careful monitoring of daily operation. Results obtained from operation of the integrated prove that the systems are replicable as one pair of digesters was operated per reactor type, with identical performance indices. Filtration performance of the DM were shown to be affected by operational parameters and biomass characteristics. The GF-DM performed better than AF-DM in terms of the quality of permeate produced, although it consistently had lower flux. It also required shorter acclimation. This can translate to better savings and quicker start up. Given that flocculant biomass is more readily available, acclimation strategies need to be optimised. Acidification of anaerobic bioreactors treating alkaline-deficient industrial wastewaters can be managed by applying urea to provide 'indirect' alkalinity supplementation during operation. The attraction of this form of supplementation shows the feasibility for co-digestion of low alkalinity wastewaters with ammonia-rich wastewaters or effluents, saving costs associated with chemical addition.

8.1 Future work

Future research needed to advance the application of DM in the AD- wastewater treatment process could aim to address the following:

- It is worth investigating the design of DMs to operate in series in order to overcome some of the limitations found in this study. Operation of 2 or more DMs in series could ensure better permeate quality capable of meeting discharge standards without recourse to other treatment options.
- The impact of module design on DM formation and performance -with a view to standardising and optimisation of DM carriers. Given the ability to mimic standard microfiltration processes, it will help to improve design options that could fit specific

reactor process configurations. These design options could mimic configurations used for conventional membranes such as tubular and plate and frame options.

- To study microbial activity of the DM and its function not only as a physical separation but also as a form of biofilm that could also enhance beneficial biological degradation of organic substrates. Microbial studies could be conducted to finger print the community and compare the activities of the activity of the biofilm to the biomass in the bioreactors.
- Research into pilot scale applications particularly in developing societies where cost and footprint is a major concern could improve the process performance in real wastewater treatment systems. This could lead to small-scale industrial applications particularly to recover and treat wastewaters, which could then be applied to other processes that do not require the same quality expected of microfiltration membrane systems.

REFERENCES

AHMED, Z., CHO, J., LIM, B.-R., SONG, K.-G. & AHN, K.-H. 2007. Effects of sludge retention time on membrane fouling and microbial community structure in a membrane bioreactor. *Journal of Membrane Science,* 287**,** 211-218.

AKRAM, A. & STUCKEY, D. C. 2008. BIOMASS ACCLIMATISATION AND ADAPTATION DURING START-UP OF A SUBMERGED ANAEROBIC MEMBRANE BIOREACTOR (SAMBR). *Environmental Technology,* 29**,** 1053-1065.

AL-MALACK, M. H. & ANDERSON, G. K. 1996. Formation of dynamic membranes with crossflow microfiltration. *Journal of Membrane Science,* 112**,** 287-296.

ALAVI MOGHADDAM, M., SATOH, H. & MINO, T. 2002. Effect of important operational parameters on performance of coarse pore filtration activated sludge process. *Water science and technology,* 46**,** 229-236.

ALIBARDI, L., BERNAVA, N., COSSU, R. & SPAGNI, A. 2016. Anaerobic dynamic membrane bioreactor for wastewater treatment at ambient temperature. *Chemical Engineering Journal,* 284**,** 130-138.

ALTMAN, M., SEMIAT, R. & HASSON, D. 1999. Removal of organic foulants from feed waters by dynamic membranes. *Desalination,* 125**,** 65-75.

ALVAREZ-VAZQUEZ, H., JEFFERSON, B. & JUDD, S. J. 2004. Membrane bioreactors vs conventional biological treatment of landfill leachate: a brief review. *Journal of Chemical Technology & Biotechnology,* 79**,** 1043-1049.

AN, Y., WANG, Z., WU, Z., YANG, D. & ZHOU, Q. 2009. Characterization of membrane foulants in an anaerobic non-woven fabric membrane bioreactor for municipal wastewater treatment. *Chemical Engineering Journal,* 155**,** 709-715.

APHA 2005. *Standard Methods for the Examination of Water and Wastewater*, American Technical Publisher.

BADANI, Z., AIT-AMAR, H., SI-SALAH, A., BRIK, M. & FUCHS, W. 2005. Treatment of textile waste water by membrane bioreactor and reuse. *Desalination,* 185**,** 411-417.

BARRETT, D. M., GARCIA, E. & WAYNE, J. E. 1998. Textural modification of processing tomatoes. *Critical Reviews in Food Science and Nutrition,* 38**,** 173-258.

BATSTONE, D. J. & KELLER, J. 2001. Variation of bulk properties of anaerobic granules with wastewater type. *Water Research,* 35**,** 1723-1729.

BEAUBIEN, A., BÂTY, M., JEANNOT, F., FRANCOEUR, E. & MANEM, J. 1996. Design and operation of anaerobic membrane bioreactors: development of a filtration testing strategy. *Journal of Membrane Science,* 109**,** 173-184.

BÖHM, L., DREWS, A., PRIESKE, H., BÉRUBÉ, P. R. & KRAUME, M. 2012. The importance of fluid dynamics for MBR fouling mitigation. *Bioresource Technology,* 122**,** 50-61.

BONCZ, M. A., FORMAGINI, E. L., SANTOS LDA, S., MARQUES, R. D. & PAULO, P. L. 2012. Application of urea dosing for alkalinity supply during anaerobic digestion of vinasse. *Water Sci Technol,* 66**,** 2453-60.

BOUHABILA, E. H., BEN AÏM, R. & BUISSON, H. 1998. Microfiltration of activated sludge using submerged membrane with air bubbling (application to wastewater treatment). *Desalination,* 118**,** 315-322.

BOURGEOUS, K. N., DARBY, J. L. & TCHOBANOGLOUS, G. 2001. Ultrafiltration of wastewater: effects of particles, mode of operation, and backwash effectiveness. *Water Research,* 35**,** 77-90.

BROECKMANN, A., BUSCH, J., WINTGENS, T. & MARQUARDT, W. 2006. Modeling of pore blocking and cake layer formation in membrane filtration for wastewater treatment. *Desalination,* 189**,** 97-109.

BUONOMENNA, M. G. & BAE, J. 2015. Membrane processes and renewable energies. *Renewable and Sustainable Energy Reviews,* 43**,** 1343-1398.

CAI, B., YE, H. & YU, L. 2000. Preparation and separation performance of a dynamically formed MnO2 membrane. *Desalination,* 128**,** 247-256.

CAI, D., HUANG, J., LIU, G., LI, M., YU, Y. & MENG, F. 2018. Effect of support material pore size on the filtration behavior of dynamic membrane bioreactor. *Bioresource Technology,* 255**,** 359-363.

CARRÈRE, H., BLASZKOWA, F. & DE BALMANN, H. R. 2002. Modelling the microfiltration of lactic acid fermentation broths and comparison of operating modes. *Desalination,* 145**,** 201-206.

CHANG, I.-S., GANDER, M., JEFFERSON, B. & JUDD, S. 2001. Low-cost membranes for use in a submerged MBR. *Process Safety and Environmental Protection,* 79**,** 183-188.

CHEN, C. & CHIANG, B. 1998. Formation and characteristics of zirconium ultrafiltration dynamic membranes of various pore sizes. *Journal of membrane science,* 143**,** 65-73.

CHEN, H., CHANG, S., GUO, Q., HONG, Y. & WU, P. 2016. Brewery wastewater treatment using an anaerobic membrane bioreactor. *Biochemical Engineering Journal,* 105**,** 321-331.

CHEN, V., FANE, A. G., MADAENI, S. & WENTEN, I. G. 1997. Particle deposition during membrane filtration of colloids: transition between concentration polarization and cake formation. *Journal of Membrane Science,* 125**,** 109-122.

CHERNICHARO, C. A. L. 2006. Post-Treatment Options for the Anaerobic Treatment of Domestic Wastewater. *Reviews in Environmental Science and Bio/Technology,* 5**,** 73-92.

CHO, B. D. & FANE, A. G. 2002. Fouling transients in nominally sub-critical flux operation of a membrane bioreactor. *Journal of Membrane Science,* 209**,** 391-403.

CHU, H.-Q., CAO, D.-W., JIN, W. & DONG, B.-Z. 2008. Characteristics of bio-diatomite dynamic membrane process for municipal wastewater treatment. *Journal of Membrane Science,* 325**,** 271-276.

CHU, H., ZHANG, Y., ZHOU, X., ZHAO, Y., DONG, B. & ZHANG, H. 2014. Dynamic membrane bioreactor for wastewater treatment: Operation, critical flux, and dynamic membrane structure. *Journal of Membrane Science,* 450**,** 265-271.

CHU, L.-B., YANG, F.-L. & ZHANG, X.-W. 2005. Anaerobic treatment of domestic wastewater in a membrane-coupled expended granular sludge bed (EGSB) reactor under moderate to low temperature. *Process Biochemistry,* 40**,** 1063-1070.

CHU, L. & LI, S. 2006. Filtration capability and operational characteristics of dynamic membrane bioreactor for municipal wastewater treatment. *Separation and Purification Technology,* 51**,** 173-179.

CHUANG, S.-H., CHANG, W.-C., CHANG, M.-C. & HU, K.-L. 2011. Filtration performances of a novel submerged nonwoven filter for particle separation. *Desalination,* 279**,** 163-169.

CICEK, N., WINNEN, H., SUIDAN, M. T., WRENN, B. E., URBAIN, V. & MANEM, J. 1998. Effectiveness of the membrane bioreactor in the biodegradation of high molecular weight compounds. *Water Research,* 32**,** 1553-1563.

CITULSKI, J. A., FARAHBAKHSH, K. & KENT, F. C. 2009. Effects of total suspended solids loading on short-term fouling in the treatment of secondary effluent by an immersed ultrafiltration pilot system. *Water Environ Res,* 81**,** 2427-36.

CRESSON, R., CARRÈRE, H., DELGENÈS, J. P. & BERNET, N. 2006. Biofilm formation during the start-up period of an anaerobic biofilm reactor—Impact of nutrient complementation. *Biochemical Engineering Journal,* 30**,** 55-62.

CRESSON, R., ESCUDIÉ, R., STEYER, J.-P., DELGENÈS, J.-P. & BERNET, N. 2008. Competition between planktonic and fixed microorganisms during the start-up of methanogenic biofilm reactors. *Water Research,* 42**,** 792-800.

DECLOUX, M. & TATOUD, L. 2000. Importance of the control mode in ultrafiltration: case of raw cane sugar remelt. *Journal of Food Engineering,* 44**,** 119-126.

DEFRANCE, L. & JAFFRIN, M. Y. 1999. Comparison between filtrations at fixed transmembrane pressure and fixed permeate flux: application to a membrane bioreactor used for wastewater treatment. *Journal of Membrane Science,* 152**,** 203-210.

DERELI, R. K., ERSAHIN, M. E., OZGUN, H., OZTURK, I., JEISON, D., VAN DER ZEE, F. & VAN LIER, J. B. 2012. Potentials of anaerobic membrane bioreactors to overcome treatment limitations induced by industrial wastewaters. *Bioresource Technology,* 122**,** 160-170.

DONG, Q., PARKER, W. & DAGNEW, M. 2016. Long term performance of membranes in an anaerobic membrane bioreactor treating municipal wastewater. *Chemosphere,* 144**,** 249-56.

DREWS, A. 2010. Membrane fouling in membrane bioreactors—Characterisation, contradictions, cause and cures. *Journal of Membrane Science,* 363**,** 1-28.

EC. 2018. *European Commission* [Online]. Available: http://ec.europa.eu/environment/water/reuse.htm [Accessed].

ELMALEH, S. & ABDELMOUMNI, L. 1997. Cross-flow filtration of an anaerobic methanogenic suspension. *Journal of Membrane Science,* 131**,** 261-274.

ERSAHIN, M. E., OZGUN, H., DERELI, R. K., OZTURK, I., ROEST, K. & VAN LIER, J. B. 2012. A review on dynamic membrane filtration: Materials, applications and future perspectives. *Bioresource Technology,* 122**,** 196-206.

ERSAHIN, M. E., OZGUN, H., TAO, Y. & VAN LIER, J. B. 2014. Applicability of dynamic membrane technology in anaerobic membrane bioreactors. *Water Research,* 48**,** 420-429.

ERSAHIN, M. E., OZGUN, H. & VAN LIER, J. B. 2013. Effect of support material properties on dynamic membrane filtration performance. *Separation Science and Technology,* 48**,** 2263-2269.

ERSAHIN, M. E., TAO, Y., OZGUN, H., GIMENEZ, J. B., SPANJERS, H. & VAN LIER, J. B. 2017. Impact of anaerobic dynamic membrane bioreactor configuration on treatment and filterability performance. *Journal of Membrane Science,* 526**,** 387-394.

ESCUDIÉ, R., CRESSON, R., DELGENÈS, J.-P. & BERNET, N. 2011. Control of start-up and operation of anaerobic biofilm reactors: An overview of 15 years of research. *Water Research,* 45**,** 1-10.

ESPINASSE, B., BACCHIN, P. & AIMAR, P. 2008. Filtration method characterizing the reversibility of colloidal fouling layers at a membrane surface: Analysis through critical flux and osmotic pressure. *Journal of Colloid and Interface Science,* 320**,** 483-490.

FAN, B. & HUANG, X. 2002. Characteristics of a Self-Forming Dynamic Membrane Coupled with a Bioreactor for Municipal Wastewater Treatment. *Environmental Science & Technology,* 36**,** 5245-5251.

FAN, F. & ZHOU, H. 2007. Interrelated Effects of Aeration and Mixed Liquor Fractions on Membrane Fouling for Submerged Membrane Bioreactor Processes in Wastewater Treatment. *Environmental Science & Technology,* 41**,** 2523-2528.

FANE, A. G., FELL, C. J. D. & SUKI, A. 1983. The effect of ph and ionic environment on the ultrafiltration of protein solutions with retentive membranes. *Journal of Membrane Science,* 16**,** 195-210.

FARIZOGLU, B. & UZUNER, S. 2011. The investigation of dairy industry wastewater treatment in a biological high performance membrane system. *Biochemical Engineering Journal,* 57**,** 46-54.

FIELD, R. W. & PEARCE, G. K. 2011. Critical, sustainable and threshold fluxes for membrane filtration with water industry applications. *Advances in Colloid and Interface Science,* 164**,** 38-44.

FIELD, R. W., WU, D., HOWELL, J. A. & GUPTA, B. B. 1995. Critical flux concept for microfiltration fouling. *Journal of Membrane Science,* 100**,** 259-272.

FOLEY, G. 2006. A review of factors affecting filter cake properties in dead-end microfiltration of microbial suspensions. *Journal of Membrane Science,* 274**,** 38-46.

FUCHS, A. & STAUDINGER, G. 1999. Characterising the clarification of the supernatant of activated sludges. *Water Research,* 33**,** 2527-2534.

FUCHS, W., BINDER, H., MAVRIAS, G. & BRAUN, R. 2003. Anaerobic treatment of wastewater with high organic content using a stirred tank reactor coupled with a membrane filtration unit. *Water Research,* 37**,** 902-908.

FUCHS, W., RESCH, C., KERNSTOCK, M., MAYER, M., SCHOEBERL, P. & BRAUN, R. 2005. Influence of operational conditions on the performance of a mesh filter activated sludge process. *Water Research,* 39**,** 803-810.

GALIB, M., ELBESHBISHY, E., REID, R., HUSSAIN, A. & LEE, H.-S. 2016. Energy-positive food wastewater treatment using an anaerobic membrane bioreactor (AnMBR). *Journal of Environmental Management,* 182**,** 477-485.

GAO, D.-W., ZHANG, T., TANG, C.-Y. Y., WU, W.-M., WONG, C.-Y., LEE, Y. H., YEH, D. H. & CRIDDLE, C. S. 2010. Membrane fouling in an anaerobic membrane bioreactor: Differences in relative abundance of bacterial species in the membrane foulant layer and in suspension. *Journal of Membrane Science,* 364**,** 331-338.

GERARDI, M. H. 2003. *The microbiology of anaerobic digesters*, John Wiley & Sons.

GHYOOT, W. R. & VERSTRAETE, W. H. 1997. Coupling Membrane Filtration to Anaerobic Primary Sludge Digestion. *Environmental Technology,* 18**,** 569-580.

GIL, J. A., TÚA, L., RUEDA, A., MONTAÑO, B., RODRÍGUEZ, M. & PRATS, D. 2010. Monitoring and analysis of the energy cost of an MBR. *Desalination,* 250**,** 997-1001.

GOHIL, A. & NAKHLA, G. 2006. Treatment of tomato processing wastewater by an upflow anaerobic sludge blanket–anoxic–aerobic system. *Bioresource Technology,* 97**,** 2141-2152.

GOULD, W. A. 1992. CHAPTER 9 - Tomato Juice Manufacture. *In:* GOULD, W. A. (ed.) *Tomato Production, Processing and Technology.* Woodhead Publishing.

GROVES, G. R., BUCKLEY, C. A., COX, J. M., KIRK, A., MACMILLAN, C. D. & SIMPSON, M. J. 1983. Dynamic membrane ultrafiltration and hyperfiltration for the treatment of industrial effluents for water reuse. *Desalination,* 47**,** 305-312.

GUAN, D., DAI, J., WATANABE, Y. & CHEN, G. 2018. Changes in the physical properties of the dynamic layer and its correlation with permeate quality in a self-forming dynamic membrane bioreactor. *Water Research,* 140**,** 67-76.

GUPTA, B. B., HOWELL, J. A., WU, D. & FIELD, R. W. 1995. Engineering of Membrane Processes II Environmental ApplicationsA helical baffle for cross-flow microfiltration. *Journal of Membrane Science,* 102**,** 31-42.

HAI, F. I., YAMAMOTO, K. & LEE, C.-H. 2013. *Membrane Biological Reactors Theory, Modeling, Design, Management and Applications to Wastewater Reuse,* London, GBR, IWA Publishing.

HE, Y., XU, P., LI, C. & ZHANG, B. 2005. High-concentration food wastewater treatment by an anaerobic membrane bioreactor. *Water Research,* 39**,** 4110-4118.

HERMIA, J. 1982. CONSTANT PRESSURE BLOCKING FILTRATION LAWS - APPLICATION TOPOWER-LAW NON-NEWTONIAN FLUIDS. *TRANS INST CHEM ENG,* V 60**,** 183-187.

HERNANDEZ, A. E., BELALCAZAR, L. C., RODRIGUEZ, M. S. & GIRALDO, E. 2002. Retention of granular sludge at high hydraulic loading rates in an anaerobic membrane bioreactor with immersed filtration. *Water Sci Technol,* 45**,** 169-74.

HO, J., KHANAL, S. & SUNG, S. 2007. Anaerobic membrane bioreactor for treatment of synthetic municipal wastewater at ambient temperature. *Water Science & Technology,* 55**,** 79-86.

HONG, S. P., BAE, T. H., TAK, T. M., HONG, S. & RANDALL, A. 2002. Fouling control in activated sludge submerged hollow fiber membrane bioreactors. *Desalination,* 143**,** 219-228.

HOWELL, J. A. 1995. Sub-critical flux operation of microfiltration. *Journal of Membrane Science,* 107**,** 165-171.

HSU, K.-C. 2008. Evaluation of processing qualities of tomato juice induced by thermal and pressure processing. *LWT - Food Science and Technology,* 41**,** 450-459.

HU, A. Y. & STUCKEY, D. C. 2006. Treatment of dilute wastewaters using a novel submerged anaerobic membrane bioreactor. *Journal of environmental engineering,* 132**,** 190-198.

HU, Y., WANG, X. C., NGO, H. H., SUN, Q. & YANG, Y. 2018. Anaerobic dynamic membrane bioreactor (AnDMBR) for wastewater treatment: A review. *Bioresource Technology,* 247**,** 1107-1118.

HU, Y., WANG, X. C., SUN, Q., NGO, H. H., YU, Z., TANG, J. & ZHANG, Q. 2017. Characterization of a hybrid powdered activated carbon-dynamic membrane bioreactor (PAC-DMBR) process with high flux by gravity flow: Operational performance and sludge properties. *Bioresource Technology,* 223**,** 65-73.

HWANG, B.-K., LEE, W.-N., YEON, K.-M., PARK, P.-K., LEE, C.-H., CHANG, I.-S., DREWS, A. & KRAUME, M. 2008a. Correlating TMP Increases with Microbial Characteristics in the

Bio-Cake on the Membrane Surface in a Membrane Bioreactor. *Environmental Science & Technology,* 42**,** 3963-3968.

HWANG, K.-J., LIAO, C.-Y. & TUNG, K.-L. 2008b. Effect of membrane pore size on the particle fouling in membrane filtration. *Desalination,* 234**,** 16-23.

IAQUINTA, M., STOLLER, M. & MERLI, C. 2006. Development of synthetic wastewater from the tomato industry for membrane processing purposes. *Desalination,* 200**,** 739-741.

IAQUINTA, M., STOLLER, M. & MERLI, C. 2009. Optimization of a nanofiltration membrane process for tomato industry wastewater effluent treatment. *Desalination,* 245**,** 314-320.

IORHEMEN, O. T., HAMZA, R. A. & TAY, J. H. 2017. Membrane fouling control in membrane bioreactors (MBRs) using granular materials. *Bioresource Technology,* 240**,** 9-24.

IVERSEN, V., MEHREZ, R., HORNG, R. Y., CHEN, C. H., MENG, F., DREWS, A., LESJEAN, B., ERNST, M., JEKEL, M. & KRAUME, M. 2009. Fouling mitigation through flocculants and adsorbents addition in membrane bioreactors: Comparing lab and pilot studies. *Journal of Membrane Science,* 345**,** 21-30.

JABBARI, S.-S., JAFARI, S. M., DEHNAD, D. & SHAHIDI, S.-A. 2018. Changes in lycopene content and quality of tomato juice during thermal processing by a nanofluid heating medium. *Journal of Food Engineering,* 230**,** 1-7.

JANKE, L., LEITE, A. F., BATISTA, K., SILVA, W., NIKOLAUSZ, M., NELLES, M. & STINNER, W. 2016. Enhancing biogas production from vinasse in sugarcane biorefineries: Effects of urea and trace elements supplementation on process performance and stability. *Bioresource Technology,* 217**,** 10-20.

JEISON, D., DÍAZ, I. & VAN LIER, J. B. 2008. Anaerobic membrane bioreactors: Are membranes really necessary? *Electronic Journal of Biotechnology,* 11**,** 1-2.

JEISON, D., TELKAMP, P. & VAN LIER, J. B. 2009. Thermophilic Sidestream Anaerobic Membrane Bioreactors: The Shear Rate Dilemma. *Water Environment Research,* 81**,** 2372-2380.

JEISON, D. & VAN LIER, J. B. 2007. Cake formation and consolidation: Main factors governing the applicable flux in anaerobic submerged membrane bioreactors (AnSMBR) treating acidified wastewaters. *Separation and Purification Technology,* 56**,** 71-78.

JI, J., QIU, J., WONG, F.-S. & LI, Y. 2008. Enhancement of filterability in MBR achieved by improvement of supernatant and floc characteristics via filter aids addition. *Water Research,* 42**,** 3611-3622.

JIN, B., WILÉN, B.-M. & LANT, P. 2003. A comprehensive insight into floc characteristics and their impact on compressibility and settleability of activated sludge. *Chemical Engineering Journal,* 95**,** 221-234.

JIN, B., WILÉN, B.-M. & LANT, P. 2004. Impacts of morphological, physical and chemical properties of sludge flocs on dewaterability of activated sludge. *Chemical Engineering Journal,* 98**,** 115-126.

JOHNSON, J. S., KRAUS, K. A., FLEMING, S. M., COCHRAN, H. D. & PERONA, J. J. 1968. Hyperfiltration studies XIV Porous tubes precoated with filteraids as supports for dynamically formed membranes. *Desalination,* 5**,** 359-369.

JOHNSON, J. S., MINTURN, R. E. & WADIA, P. H. 1972. Hyperfiltration. XXI. Dynamically formed hydrous Zr(IV) oxide-polyacrylate membranes. *Journal of Electroanalytical Chemistry and Interfacial Electrochemistry,* 37**,** 267-281.

JUDD, S. 2010. *MBR Book, The : Principles and Applications of Membrane Bioreactors for Water and Wastewater Treatment*, Butterworth-Heinemann.

JUNG, Y.-J., KISO, Y., KWON, K.-H., KAMIMOTO, Y. & MIN, K.-S. 2015. Biological removal characteristics of phenol with filtration bio-reactor. *Desalination and Water Treatment,* 53**,** 3096-3103.

KARADAG, D., KÖROĞLU, O. E., OZKAYA, B. & CAKMAKCI, M. 2015. A review on anaerobic biofilm reactors for the treatment of dairy industry wastewater. *Process Biochemistry,* 50**,** 262-271.

KATAYON, S., MEGAT MOHD NOOR, M. J., AHMAD, J., ABDUL GHANI, L. A., NAGAOKA, H. & AYA, H. 2004. Effects of mixed liquor suspended solid concentrations on membrane

bioreactor efficiency for treatment of food industry wastewater. *Desalination,* 167**,** 153-158.

KHAING, T.-H., LI, J., LI, Y., WAI, N. & WONG, F.-S. 2010. Feasibility study on petrochemical wastewater treatment and reuse using a novel submerged membrane distillation bioreactor. *Separation and Purification Technology,* 74**,** 138-143.

KIM, K.-J., CHEN, V. & FANE, A. G. 1993a. Ultrafiltration of colloidal silver particles: flux, rejection, and fouling. *Journal of colloid and interface science,* 155**,** 347-359.

KIM, K., CHEN, V. & FANE, A. 1993b. Some factors determining protein aggregation during ultrafiltration. *Biotechnology and bioengineering,* 42**,** 260-265.

KISO, Y., JUNG, Y.-J., ICHINARI, T., PARK, M., KITAO, T., NISHIMURA, K. & MIN, K.-S. 2000. Wastewater treatment performance of a filtration bio-reactor equipped with a mesh as a filter material. *Water Research,* 34**,** 4143-4150.

KISO, Y., JUNG, Y.-J., PARK, M.-S., WANG, W., SHIMASE, M., YAMADA, T. & MIN, K.-S. 2005. Coupling of sequencing batch reactor and mesh filtration: Operational parameters and wastewater treatment performance. *Water Research,* 39**,** 4887-4898.

KUBERKAR, V. T. & DAVIS, R. H. 2000. Modeling of fouling reduction by secondary membranes. *Journal of Membrane Science,* 168**,** 243-258.

KWON, D. Y. & VIGNESWARAN, S. 1998. Influence of particle size and surface charge on critical flux of crossflow microfiltration. *Water Science and Technology,* 38**,** 481-488.

LE-CLECH, P., CHEN, V. & FANE, T. A. G. 2006. Fouling in membrane bioreactors used in wastewater treatment. *Journal of Membrane Science,* 284**,** 17-53.

LE CLECH, P., JEFFERSON, B., CHANG, I. S. & JUDD, S. J. 2003. Critical flux determination by the flux-step method in a submerged membrane bioreactor. *Journal of Membrane Science,* 227**,** 81-93.

LEAD, J. R. & WILKINSON, K. J. 2006. Aquatic colloids and nanoparticles: current knowledge and future trends. *Environmental Chemistry,* 3**,** 159-171.

LEE, J., AHN, W.-Y. & LEE, C.-H. 2001. Comparison of the filtration characteristics between attached and suspended growth microorganisms in submerged membrane bioreactor. *Water Research,* 35**,** 2435-2445.

LEÓN-BECERRIL, E., GARCÍA-CAMACHO, J. E., DEL REAL-OLVERA, J. & LÓPEZ-LÓPEZ, A. 2016. Performance of an upflow anaerobic filter in the treatment of cold meat industry wastewater. *Process Safety and Environmental Protection,* 102**,** 385-391.

LETTINGA, G. 1995. Anaerobic digestion and wastewater treatment systems. *Antonie van Leeuwenhoek,* 67**,** 3-28.

LETTINGA, G., REBAC, S. & ZEEMAN, G. 2001. Challenge of psychrophilic anaerobic wastewater treatment. *TRENDS in Biotechnology,* 19**,** 363-370.

LEVINE, A. D., TCHOBANOGLOUS, G. & ASANO, T. 1985. Characterization of the Size Distribution of Contaminants in Wastewater: Treatment and Reuse Implications. *Journal (Water Pollution Control Federation),* 57**,** 805-816.

LEVINE, A. D., TCHOBANOGLOUS, G. & ASANO, T. 1991. Size distributions of particulate contaminants in wastewater and their impact on treatability. *Water Research,* 25**,** 911-922.

LEW, B., TARRE, S., BELIAVSKI, M., DOSORETZ, C. & GREEN, M. 2009. Anaerobic membrane bioreactor (AnMBR) for domestic wastewater treatment. *Desalination,* 243**,** 251-257.

LI, L., HE, Q., WEI, Y., HE, Q. & PENG, X. 2014. Early warning indicators for monitoring the process failure of anaerobic digestion system of food waste. *Bioresource Technology,* 171**,** 491-494.

LI, N., HE, L., LU, Y.-Z., ZENG, R. J. & SHENG, G.-P. 2017. Robust performance of a novel anaerobic biofilm membrane bioreactor with mesh filter and carbon fiber (ABMBR) for low to high strength wastewater treatment. *Chemical Engineering Journal,* 313**,** 56-64.

LI, W.-W., SHENG, G.-P., WANG, Y.-K., LIU, X.-W., XU, J. & YU, H.-Q. 2011. Filtration behaviors and biocake formation mechanism of mesh filters used in membrane bioreactors. *Separation and Purification Technology,* 81**,** 472-479.

LI, W.-W., WANG, Y.-K., SHENG, G.-P., GUI, Y.-X., YU, L., XIE, T.-Q. & YU, H.-Q. 2012a. Integration of aerobic granular sludge and mesh filter membrane bioreactor for cost-effective wastewater treatment. *Bioresource Technology,* 122**,** 22-26.

LI, W.-W., WANG, Y.-K., XU, J., TONG, Y.-R., ZHAO, L., PENG, H., SHENG, G.-P. & YU, H.-Q. 2012b. A dead-end filtration method to rapidly and quantitatively evaluate the fouling resistance of nylon mesh for membrane bioreactors. *Separation and Purification Technology,* 89**,** 107-111.

LIANG, S., ZHAO, T., ZHANG, J., SUN, F., LIU, C. & SONG, L. 2012. Determination of fouling-related critical flux in self-forming dynamic membrane bioreactors: Interference of membrane compressibility. *Journal of Membrane Science,* 390-391**,** 113-120.

LIAO, B.-Q., KRAEMER, J. T. & BAGLEY, D. M. 2006. Anaerobic Membrane Bioreactors: Applications and Research Directions. *Critical Reviews in Environmental Science and Technology,* 36**,** 489-530.

LIM, A. L. & BAI, R. 2003. Membrane fouling and cleaning in microfiltration of activated sludge wastewater. *Journal of Membrane Science,* 216**,** 279-290.

LIN, H., GAO, W., MENG, F., LIAO, B.-Q., LEUNG, K.-T., ZHAO, L., CHEN, J. & HONG, H. 2012. Membrane Bioreactors for Industrial Wastewater Treatment: A Critical Review. *Critical Reviews in Environmental Science and Technology,* 42**,** 677-740.

LIN, H. J., XIE, K., MAHENDRAN, B., BAGLEY, D. M., LEUNG, K. T., LISS, S. N. & LIAO, B. Q. 2010. Factors affecting sludge cake formation in a submerged anaerobic membrane bioreactor. *Journal of Membrane Science,* 361**,** 126-134.

LIU, H., YANG, C., PU, W. & ZHANG, J. 2009. Formation mechanism and structure of dynamic membrane in the dynamic membrane bioreactor. *Chemical Engineering Journal,* 148**,** 290-295.

LODERER, C., WORLE, A. & FUCHS, W. 2012. Influence of different mesh filter module configurations on effluent quality and long-term filtration performance. *Environ Sci Technol,* 46**,** 3844-50.

MA, J., WANG, Z., ZOU, X., FENG, J. & WU, Z. 2013a. Microbial communities in an anaerobic dynamic membrane bioreactor (AnDMBR) for municipal wastewater treatment: Comparison of bulk sludge and cake layer. *Process Biochemistry,* 48**,** 510-516.

MA, Z., WEN, X., ZHAO, F., XIA, Y., HUANG, X., WAITE, D. & GUAN, J. 2013b. Effect of temperature variation on membrane fouling and microbial community structure in membrane bioreactor. *Bioresource Technology,* 133**,** 462-468.

MADAENI, S. S., FANE, A. G. & WILEY, D. E. 1999. Factors influencing critical flux in membrane filtration of activated sludge. *Journal of chemical technology and biotechnology,* 74**,** 539-543.

MARCINKOWSKY, A. E., KRAUS, K. A., PHILLIPS, H. O., JOHNSON, J. S. & SHOR, A. J. 1966. Hyperfiltration Studies. IV. Salt Rejection by Dynamically Formed Hydrous Oxide Membranes1. *Journal of the American Chemical Society,* 88**,** 5744-5746.

MARSHALL, A., MUNRO, P. & TRAGARDH, G. 1996. Design and development of a cross-flow membrane rig to compare constant pressure and constant flux operation in ultrafiltration and microfiltration. *Food and bioproducts processing: transactions of the Institution of Chemical Engineers, Part C*.

MARTIN, I., PIDOU, M., SOARES, A., JUDD, S. & JEFFERSON, B. 2011. Modelling the energy demands of aerobic and anaerobic membrane bioreactors for wastewater treatment. *Environmental Technology,* 32**,** 921-932.

MARTÍN, M. A., DE LA RUBIA, M. A., MARTÍN, A., BORJA, R., MONTALVO, S. & SÁNCHEZ, E. 2010. Kinetic evaluation of the psychrophylic anaerobic digestion of synthetic domestic sewage using an upflow filter. *Bioresource Technology,* 101**,** 131-137.

MARTINEZ-SOSA, D., HELMREICH, B., NETTER, T., PARIS, S., BISCHOF, F. & HORN, H. 2011. Anaerobic submerged membrane bioreactor (AnSMBR) for municipal wastewater treatment under mesophilic and psychrophilic temperature conditions. *Bioresource Technology,* 102**,** 10377-10385.

MCADAM, E., JUDD, S. J., GILDEMEISTER, R., DREWS, A. & KRAUME, M. 2005. Critical analysis of submerged membrane sequencing batch reactor operating conditions. *Water Research,* 39**,** 4011-4019.

MCCARTY, P. L. & MCKINNEY, R. E. 1961. Salt Toxicity in Anaerobic Digestion. *Journal (Water Pollution Control Federation),* 33**,** 399-415.

MENDRET, J., GUIGUI, C., SCHMITZ, P. & CABASSUD, C. 2009. In situ dynamic characterisation of fouling under different pressure conditions during dead-end filtration: Compressibility properties of particle cakes. *Journal of Membrane Science,* 333**,** 20-29.

MENG, F., CHAE, S.-R., DREWS, A., KRAUME, M., SHIN, H.-S. & YANG, F. 2009. Recent advances in membrane bioreactors (MBRs): Membrane fouling and membrane material. *Water Research,* 43**,** 1489-1512.

MENG, F., ZHANG, H., YANG, F. & LIU, L. 2007. Characterization of Cake Layer in Submerged Membrane Bioreactor. *Environmental Science & Technology,* 41**,** 4065-4070.

MENG, F., ZHANG, H., YANG, F., ZHANG, S., LI, Y. & ZHANG, X. 2006. Identification of activated sludge properties affecting membrane fouling in submerged membrane bioreactors. *Separation and Purification Technology,* 51**,** 95-103.

METCALF & EDDY, I., G. TCHOBANOGLOUS, H.D. STENSEL, R. TSUCHIHAHASHI, F. BURTON 2013. *Wastewater engineering: treatment and resource recovery*, McGraw-Hill Higher Education.

MILLER, D. J., KASEMSET, S., PAUL, D. R. & FREEMAN, B. D. 2014. Comparison of membrane fouling at constant flux and constant transmembrane pressure conditions. *Journal of Membrane Science,* 454**,** 505-515.

NAJAFPOUR, G. D., ZINATIZADEH, A. A. L., MOHAMED, A. R., HASNAIN ISA, M. & NASROLLAHZADEH, H. 2006. High-rate anaerobic digestion of palm oil mill effluent in an upflow anaerobic sludge-fixed film bioreactor. *Process Biochemistry,* 41**,** 370-379.

NAKAMURA, K., ORIME, T. & MATSUMOTO, K. 2012. Response of zeta potential to cake formation and pore blocking during the microfiltration of latex particles. *Journal of Membrane Science,* 401-402**,** 274-281.

NAKAO, S.-I., NOMURA, T., KIMURA, S. & WATANABE, A. 1986. FORMATION AND CHARACTERISTICS OF INORGANIC DYNAMIC MEMBRANES FOR ULTRAFILTRATION. *Journal of Chemical Engineering of Japan,* 19**,** 221-226.

NOOR, M. J. M. M., AHMADUN, F. R., MOHAMED, T. A., MUYIBI, S. A. & PESCOD, M. 2002. Performance of flexible membrane using kaolin dynamic membrane in treating domestic wastewater. *Desalination,* 147**,** 263-268.

NOVAK, J. T., SADLER, M. E. & MURTHY, S. N. 2003. Mechanisms of floc destruction during anaerobic and aerobic digestion and the effect on conditioning and dewatering of biosolids. *Water Research,* 37**,** 3136-3144.

OECD/IEA 2016. Water Energy Nexus. *In:* PRIDDLE, R. (ed.).

ÖRMECI, B. & VESILIND, P. A. 2000. Development of an improved synthetic sludge: a possible surrogate for studying activated sludge dewatering characteristics. *Water Research,* 34**,** 1069-1078.

OZGUN, H., GIMENEZ, J. B., ERSAHIN, M. E., TAO, Y., SPANJERS, H. & VAN LIER, J. B. 2015. Impact of membrane addition for effluent extraction on the performance and sludge characteristics of upflow anaerobic sludge blanket reactors treating municipal wastewater. *Journal of Membrane Science,* 479**,** 95-104.

PACHECO-RUIZ, S., HEAVEN, S. & BANKS, C. J. 2017. Effect of mean cell residence time on transmembrane flux, mixed-liquor characteristics and overall performance of a submerged anaerobic membrane bioreactor. *Environ Technol,* 38**,** 1263-1274.

PARK, M. S., KISO, Y., JUNG, Y. J., SIMASE, M., WANG, W. H., KITAO, T. & MIN, K. S. 2004. Sludge thickening performance of mesh filtration process. *Water Sci Technol,* 50**,** 125-33.

PILLAY, V. & BUCKLEY, C. 1992. Cake formation in cross-flow microfiltration systems. *Water Science & Technology,* 25**,** 149-162.

PILLAY, V., TOWNSEND, B. & BUCKLEY, C. 1994. Improving the performance of anaerobic digesters at wastewater treatment works: The coupled cross-flow microfiltration/digester process. *Water science and technology,* 30**,** 329-337.

PING CHU, H. & LI, X. Y. 2005. Membrane fouling in a membrane bioreactor (MBR): sludge cake formation and fouling characteristics. *Biotechnology and bioengineering,* 90**,** 323-331.

QUEK, P. J., YEAP, T. S. & NG, H. Y. 2017. Applicability of upflow anaerobic sludge blanket and dynamic membrane-coupled process for the treatment of municipal wastewater. *Applied Microbiology and Biotechnology,* 101**,** 6531-6540.

RAJINIKANTH, R., GANESH, R., ESCUDIE, R., MEHROTRA, I., KUMAR, P., THANIKAL, J. V. & TORRIJOS, M. 2009. High rate anaerobic filter with floating supports for the treatment of effluents from small-scale agro-food industries. *Desalination and Water Treatment,* 4**,** 183-190.

RAMESH, A., LEE, D.-J. & HONG, S. G. 2006. Soluble microbial products (SMP) and soluble extracellular polymeric substances (EPS) from wastewater sludge. *Applied Microbiology and Biotechnology,* 73**,** 219-225.

RAMESH, A., LEE, D. J. & LAI, J. Y. 2007. Membrane biofouling by extracellular polymeric substances or soluble microbial products from membrane bioreactor sludge. *Applied Microbiology and Biotechnology,* 74**,** 699-707.

RAPER, E., STEPHENSON, T., ANDERSON, D. R., FISHER, R. & SOARES, A. 2018. Industrial wastewater treatment through bioaugmentation. *Process Safety and Environmental Protection,* 118**,** 178-187.

REN, X., SHON, H., JANG, N., LEE, Y. G., BAE, M., LEE, J., CHO, K. & KIM, I. S. 2010. Novel membrane bioreactor (MBR) coupled with a nonwoven fabric filter for household wastewater treatment. *Water research,* 44**,** 751-760.

RIPLEY, L. E., BOYLE, W. C. & CONVERSE, J. C. 1986. Improved Alkalimetric Monitoring for Anaerobic Digestion of High-Strength Wastes. *Journal (Water Pollution Control Federation),* 58**,** 406-411.

SABAGHIAN, M., MEHRNIA, M. R., ESMAIELI, M. & NOURMOHAMMADI, D. 2018. Influence of static mixer on the formation and performance of dynamic membrane in a dynamic membrane bioreactor. *Separation and Purification Technology,* 206**,** 324-334.

SAHINKAYA, E., YURTSEVER, A. & ÇINAR, Ö. 2017. Treatment of textile industry wastewater using dynamic membrane bioreactor: Impact of intermittent aeration on process performance. *Separation and Purification Technology,* 174**,** 445-454.

SALEEM, M., ALIBARDI, L., LAVAGNOLO, M. C., COSSU, R. & SPAGNI, A. 2016. Effect of filtration flux on the development and operation of a dynamic membrane for anaerobic wastewater treatment. *Journal of Environmental Management,* 180**,** 459-465.

SATOH, H. & MINO, T. 2002. Effect of important operational parameters on performance of coarse pore filtration activated sludge process. *Water Science & Technology,* 46**,** 229-236.

SATYAWALI, Y. & BALAKRISHNAN, M. 2008. Treatment of distillery effluent in a membrane bioreactor (MBR) equipped with mesh filter. *Separation and Purification Technology,* 63**,** 278-286.

SCHREINEMACHERS, P., SIMMONS, E. B. & WOPEREIS, M. C. S. 2018. Tapping the economic and nutritional power of vegetables. *Global Food Security,* 16**,** 36-45.

SEO, G., MOON, B., LEE, T., LIM, T. & KIM, I. 2003. Non-woven fabric filter separation activated sludge reactor for domestic wastewater reclamation. *Water science and technology,* 47**,** 133-138.

SEO, G., MOON, B., PARK, Y. & KIM, S. 2007. Filtration characteristics of immersed coarse pore filters in an activated sludge system for domestic wastewater reclamation. *Water Science & Technology,* 55**,** 51-58.

SHARIATI, F. P., MEHRNIA, M. R., SALMASI, B. M., HERAN, M., WISNIEWSKI, C. & SARRAFZADEH, M. H. 2010. Membrane bioreactor for treatment of pharmaceutical wastewater containing acetaminophen. *Desalination,* 250**,** 798-800.

SMITH, A. L., SKERLOS, S. J. & RASKIN, L. 2015. Membrane biofilm development improves COD removal in anaerobic membrane bioreactor wastewater treatment. *Microbial biotechnology,* 8**,** 883-894.

SMITH, A. L., STADLER, L. B., LOVE, N. G., SKERLOS, S. J. & RASKIN, L. 2012. Perspectives on anaerobic membrane bioreactor treatment of domestic wastewater: A critical review. *Bioresource Technology,* 122**,** 149-159.

SONG, L. 1998. Flux decline in crossflow microfiltration and ultrafiltration: mechanisms and modeling of membrane fouling. *Journal of Membrane Science,* 139**,** 183-200.

STAZI, V. & TOMEI, M. C. 2018. Enhancing anaerobic treatment of domestic wastewater: State of the art, innovative technologies and future perspectives. *Science of The Total Environment,* 635**,** 78-91.

STEPHENSON, T. 2000. *Membrane bioreactors for wastewater treatment*, IWA publishing.

STUCKEY, D. C. 2012. Recent developments in anaerobic membrane reactors. *Bioresource Technology,* 122**,** 137-148.

TARDIEU, E., GRASMICK, A., GEAUGEY, V. & MANEM, J. 1998. Hydrodynamic control of bioparticle deposition in a MBR applied to wastewater treatment. *Journal of Membrane Science,* 147**,** 1-12.

TCHOBANOGLOUS, G., BURTON, F. L., STENSEL, H. D., METCALF & EDDY 2003. *Wastewater Engineering: Treatment and Reuse*, McGraw-Hill Education.

TOMEI, M. C., RITA, S. & MININNI, G. 2011. Performance of sequential anaerobic/aerobic digestion applied to municipal sewage sludge. *Journal of Environmental Management,* 92**,** 1867-1873.

VAN 'T OEVER, R. 2005. MBR focus: is submerged best? *Filtration & Separation,* 42**,** 24-27.

VAN DEN BRINK, P., SATPRADIT, O.-A., VAN BENTEM, A., ZWIJNENBURG, A., TEMMINK, H. & VAN LOOSDRECHT, M. 2011. Effect of temperature shocks on membrane fouling in membrane bioreactors. *Water Research,* 45**,** 4491-4500.

VAN HAANDEL, A. 2005. Integrated energy production and reduction of the environmental impact at alcohol distillery plants. *Water Science and Technology,* 52**,** 49-57.

VRIJENHOEK, E. M., HONG, S. & ELIMELECH, M. 2001. Influence of membrane surface properties on initial rate of colloidal fouling of reverse osmosis and nanofiltration membranes. *Journal of Membrane Science,* 188**,** 115-128.

VYAS, H. K., BENNETT, R. J. & MARSHALL, A. D. 2002. Performance of crossflow microfiltration during constant transmembrane pressure and constant flux operations. *International Dairy Journal,* 12**,** 473-479.

WAKEMAN, R. J. 1994. Visualization of Cake Formation in Cross-Flow Microfiltration. *Chemical Engineering Research & Design,* 72**,** 530-540.

WAKEMAN, R. J. & WILLIAMS, C. J. 2002. Additional techniques to improve microfiltration. *Separation and Purification Technology,* 26**,** 3-18.

WALKER, M., ZHANG, Y., HEAVEN, S. & BANKS, C. 2009. Potential errors in the quantitative evaluation of biogas production in anaerobic digestion processes. *Bioresource Technology,* 100**,** 6339-6346.

WANG, C.-C., YANG, F.-L., LIU, L.-F., FU, Z.-M. & XUE, Y. 2009. Hydrophilic and antibacterial properties of polyvinyl alcohol/4-vinylpyridine graft polymer modified polypropylene non-woven fabric membranes. *Journal of Membrane Science,* 345**,** 223-232.

WANG, J.-Y., LIU, M.-C., LEE, C.-J. & CHOU, K.-S. 1999. Formation of dextran-Zr dynamic membrane and study on concentration of protein hemoglobin solution. *Journal of Membrane Science,* 162**,** 45-55.

WANG, W., JUNG, Y.-J., KISO, Y., YAMADA, T. & MIN, K.-S. 2006. Excess sludge reduction performance of an aerobic SBR process equipped with a submerged mesh filter unit. *Process Biochemistry,* 41**,** 745-751.

WANG, X.-M., LI, X.-Y. & HUANG, X. 2007. Membrane fouling in a submerged membrane bioreactor (SMBR): Characterisation of the sludge cake and its high filtration resistance. *Separation and Purification Technology,* 52**,** 439-445.

WARD, A. J., HOBBS, P. J., HOLLIMAN, P. J. & JONES, D. L. 2008. Optimisation of the anaerobic digestion of agricultural resources. *Bioresource Technology,* 99**,** 7928-7940.

WU, J., LE-CLECH, P., STUETZ, R. M., FANE, A. G. & CHEN, V. 2008. Effects of relaxation and backwashing conditions on fouling in membrane bioreactor. *Journal of Membrane Science,* 324**,** 26-32.

WU, Y., HUANG, X., WEN, X. & CHEN, F. 2005. Function of dynamic membrane in self-forming dynamic membrane coupled bioreactor. *Water Science and Technology,* 51**,** 107-114.

XIE, Z., WANG, Z., WANG, Q., ZHU, C. & WU, Z. 2014. An anaerobic dynamic membrane bioreactor (AnDMBR) for landfill leachate treatment: Performance and microbial community identification. *Bioresource Technology,* 161**,** 29-39.

XU, Z., NAKHLA, G. & PATEL, J. 2006. Characterization and modeling of nutrient-deficient tomato-processing wastewater treatment using an anaerobic/aerobic system. *Chemosphere,* 65**,** 1171-1181.

YANG, J., JI, X., LU, L., MA, H., CHEN, Y., GUO, J. & FANG, F. 2017. Performance of an anaerobic membrane bioreactor in which granular sludge and dynamic filtration are integrated. *Biofouling,* 33**,** 36-44.

YANG, T., MA, Z.-F. & YANG, Q.-Y. 2011. Formation and performance of Kaolin/MnO2 bi-layer composite dynamic membrane for oily wastewater treatment: Effect of solution conditions. *Desalination,* 270**,** 50-56.

YE, M., ZHANG, H., WEI, Q., LEI, H., YANG, F. & ZHANG, X. 2006. Study on the suitable thickness of a PAC-precoated dynamic membrane coupled with a bioreactor for municipal wastewater treatment. *Desalination,* 194**,** 108-120.

YE, Y., LE CLECH, P., CHEN, V., FANE, A. G. & JEFFERSON, B. 2005. Fouling mechanisms of alginate solutions as model extracellular polymeric substances. *Desalination,* 175**,** 7-20.

YIGIT, N. O., HARMAN, I., CIVELEKOGLU, G., KOSEOGLU, H., CICEK, N. & KITIS, M. 2008. Membrane fouling in a pilot-scale submerged membrane bioreactor operated under various conditions. *Desalination,* 231**,** 124-132.

YU, H., WANG, Q., WANG, Z., SAHINKAYA, E., LI, Y., MA, J. & WU, Z. 2014. Start-Up of an Anaerobic Dynamic Membrane Digester for Waste Activated Sludge Digestion: Temporal Variations in Microbial Communities. *PLoS ONE,* 9**,** e93710.

ZHANG, J., CHUA, H. C., ZHOU, J. & FANE, A. G. 2006. Factors affecting the membrane performance in submerged membrane bioreactors. *Journal of Membrane Science,* 284**,** 54-66.

ZHANG, X., WANG, Z., WU, Z., LU, F., TONG, J. & ZANG, L. 2010. Formation of dynamic membrane in an anaerobic membrane bioreactor for municipal wastewater treatment. *Chemical Engineering Journal,* 165**,** 175-183.

ZHANG, X., WANG, Z., WU, Z., WEI, T., LU, F., TONG, J. & MAI, S. 2011. Membrane fouling in an anaerobic dynamic membrane bioreactor (AnDMBR) for municipal wastewater

treatment: Characteristics of membrane foulants and bulk sludge. *Process Biochemistry,* 46**,** 1538-1544.

ZSIRAI, T., BUZATU, P., AERTS, P. & JUDD, S. 2012. Efficacy of relaxation, backflushing, chemical cleaning and clogging removal for an immersed hollow fibre membrane bioreactor. *Water Research,* 46**,** 4499-4507.